UNIVERSIDADE FEDERAL DE MINAS GERAIS
INSTITUTO DE CIÊNCIAS BIOLÓGICAS
Departamento de Botânica
Programa de Pós-Graduação em Biologia Vegetal

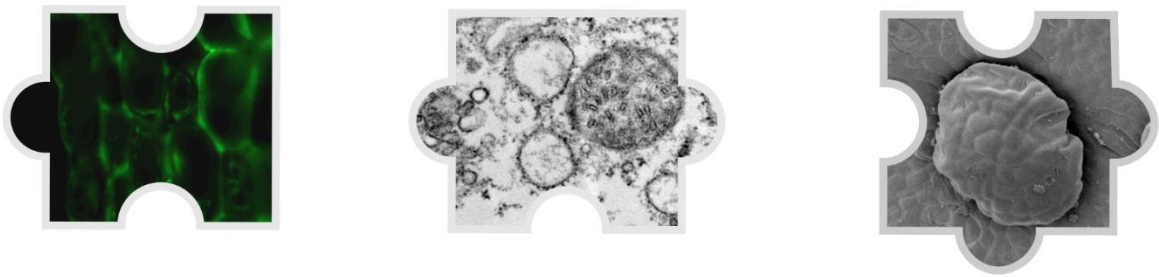

The super-host *Mimosa gemmulata* Barneby (Fabaceae) and the implications of the life cycles of *Lopesia* spp. (Cecidomyiidae) on gall developmental processes

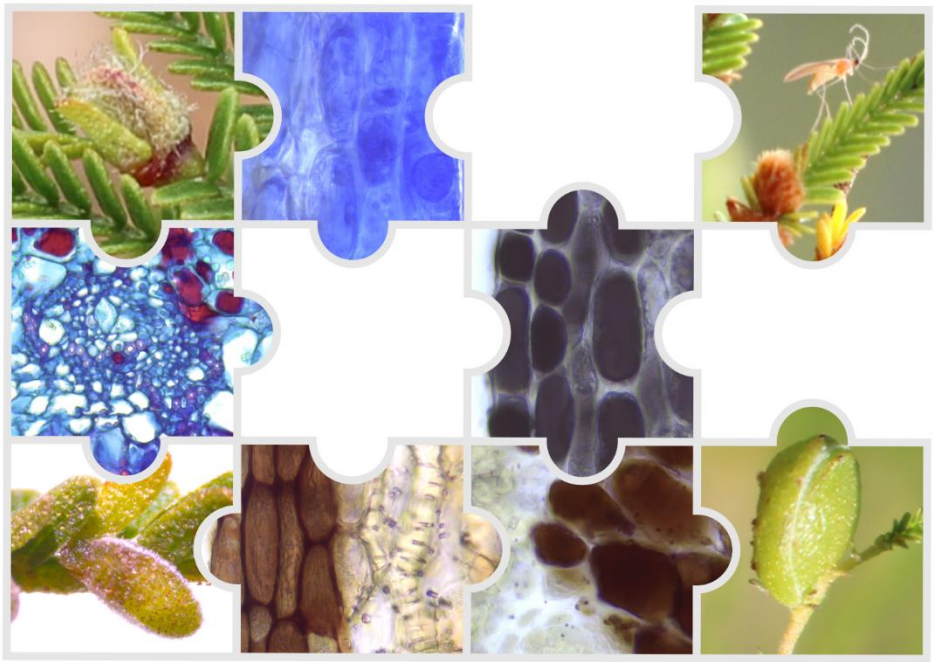

Elaine Cotrim Costa

Belo Horizonte – MG
2021

UNIVERSIDADE FEDERAL DE MINAS GERAIS
INSTITUTO DE CIÊNCIAS BIOLÓGICAS
Departamento de Botânica
Programa de Pós-Graduação em Biologia Vegetal

PPGBV UFMG

UFMG

ELAINE COTRIM COSTA

THE SUPER-HOST *MIMOSA GEMMULATA* BARNEBY (FABACEAE) AND THE IMPLICATIONS OF THE LIFE CYCLES OF *LOPESIA* SPP. (CECIDOMYIIDAE) ON GALL DEVELOPMENTAL PROCESSES

Tese apresentada ao Programa de Pós-Graduação em Biologia Vegetal do Departamento de Botânica do Instituto de Ciências Biológicas da Universidade Federal de Minas Gerais, como requisito parcial à obtenção do título de Doutora em Biologia Vegetal.

Área de concentração: Morfologia, Sistemática e Diversidade Vegetal

Orientadora: Profa. Dra. Rosy Mary dos Santos Isaias
Universidade Federal de Minas Gerais

Coorientador: Prof. Dr. Denis Coelho de Oliveira
Universidade Federal de Uberlândia

BELO HORIZONTE – MG
2021

043 Costa, Elaine Cotrim.
The super-host *Mimosa gemmulata* Barneby (Fabaceae) and the implications of the life cycles of *Lopesia* spp. (Cecidomyiidae) on gall developmental processes [manuscrito] / Elaine Cotrim Costa. – 2021.

174 f. : il. ; 29,5 cm.

Orientadora: Profa. Dra. Rosy Mary dos Santos Isaias. Coorientador: Prof. Dr. Denis Coelho de Oliveira.
Tese (doutorado) – Universidade Federal de Minas Gerais, Instituto de Ciências Biológicas. Programa de Pós-Graduação em Biologia Vegetal.

1. Anatomia vegetal. 2. Fabaceae. 3. Mimosa. 4. Mosquitos de galhas. 5. Fenologia vegetal. 6. Senescência Celular. I. Isaias, Rosy Mary dos Santos. II. Oliveira, Denis Coelho de. III. Universidade Federal de Minas Gerais. Instituto de Ciências Biológicas. IV. Título.

CDU: 581

Ficha catalográfica elaborada pela bibliotecária Rosilene Moreira Coelho de Sá – CRB 6 – 2726

UNIVERSIDADE FEDERAL DE MINAS GERAIS
INSTITUTO DE CIÊNCIAS BIOLÓGICAS
COLEGIADO DO CURSO DE PÓS-GRADUAÇÃO EM BIOLOGIA VEGETAL

FOLHA DE APROVAÇÃO

"**The super-host *Mimosa gemmulata* Barneby (Fabaceae) and the implications of the life cycles of *Lopesia* spp. (Cecidomyiidae) on gall developmental processes**"

Tese defendida por ELAINE COTRIM COSTA em 27 de agosto de 2021 e aprovada pela Banca Examinadora constituída pelos professores:

Dra. Rosy Mary dos Santos Isaias (UFMG)

Dr. Bruno Garcia Ferreira (UFRJ)

Dr. Geraldo Luiz Gonçalves Soares (UFRGS)

Dra. Lubia María Guedes (Universidade de Concepción -Chile)

Dr. Fernando Henrique Aguiar Vale (UFMG)

Belo Horizonte, 27 de agosto de 2021.

Documento assinado eletronicamente por **Lubia María Guedes García**, **Usuário Externo**, em 27/08/2021, às 19:20, conforme horário oficial de Brasília, com fundamento no art. 5º do Decreto nº 10.543, de 13 de novembro de 2020.

Documento assinado eletronicamente por **Bruno Garcia Ferreira**, **Usuário Externo**, em 27/08/2021, às 19:20, conforme horário oficial de Brasília, com fundamento no art. 5º do Decreto nº 10.543, de 13 de novembro de 2020.

Documento assinado eletronicamente por **Geraldo Luiz Gonçalves Soares**, **Usuário Externo**, em 27/08/2021, às 19:21, conforme horário oficial de Brasília, com fundamento no art. 5º do Decreto nº 10.543, de 13 de novembro de 2020.

Documento assinado eletronicamente por **Fernando Henrique Aguiar Vale**, **Professor do Magistério Superior**, em 27/08/2021, às 19:24, conforme horário oficial de Brasília, com fundamento no art. 5º do Decreto nº 10.543, de 13 de novembro de 2020.

Documento assinado eletronicamente por **Rosy Mary dos Santos Isaias**, **Professora do Magistério Superior**, em 27/08/2021, às 19:24, conforme horário oficial de Brasília, com fundamento no art. 5º do Decreto nº 10.543, de 13 de novembro de 2020.

A autenticidade deste documento pode ser conferida no site https://sei.ufmg.br/sei/controlador_externo.php?acao=documento_conferir&id_orgao_acesso_externo=0, informando o código verificador **0920068** e o código CRC **BF5B5842**.

DEDICATÓRIA

Aos meus pais, Alnoir e Luide

AGRADECIMENTOS

A Deus e à minha intercessora, Nossa Senhora Aparecida, pela força e suporte espiritual nos momentos difíceis, pelas alegrias, conquistas e por guiarem meus caminhos e encontros durante esta jornada acadêmica.

À minha orientadora, prof. Dra. Rosy Mary dos Santos Isaias, agradeço pelo nosso encontro nos primórdios da minha graduação e, por desde então, acreditar e incentivar o meu potencial. Gratidão por sua orientação perspicaz, profissional e empolgante. Obrigada por me mostrar que podemos ser produtivas com leveza, diversão e comemorando à vida! Agradeço ainda pela sua amizade. Você não é só uma inspiração como professora, orientadora e pesquisadora, mas como mulher, mãe e amiga.

Ao meu co-orientador, prof. Dr. Denis Coelho de Oliveira, por acreditar no meu potencial, pelos incentivos, discussões, ideias e empolgação no decorrer desta tese. Admiro sua alegria, humildade, profissionalismo e o modo como sempre estimula seus alunos a crescerem. Agradeço, ainda, pela amizade e boas risadas.

Aos meus amados pais, Alnoir Costa e Luide Costa, por viverem esse sonho comigo, vibrando com as minhas alegrias e sempre dando apoio e palavras de sabedoria nos momentos necessários. Ao meu irmão Flávio Costa e a minha irmã-cunhada Kellyane Costa por sempre me apoiarem e estarem presentes nos momentos difíceis e alegres. Aos meus sobrinhos, Maicon, Kauã e Enzo, por serem fonte de força, luta, esperança e amor! Eu amo vocês!

Ao Programa de Pós-graduação em Biologia Vegetal da UFMG pela oportunidade de obter o título de doutora. Aos professores pelos ensinamentos compartilhados. Aos coordenadores da Pós-graduação e a secretária Denise Marcia Figueiredo Monteiro pela prontidão e suporte prestado nesta jornada.

À Coordenação de Aperfeiçoamento de Pessoal de Nível Superior (CAPES) pela concessão da bolsa de doutorado.

Aos professores Dr. Marcel França, Dr. Geraldo Soares e Dr. Narciso Aguilera pelas sugestões e contribuições valiosas ao segundo capítulo desta tese, no momento da qualificação do doutorado.

Aos professores Dr. José Pires Lemos, Dr. Mario Cozzuol, Dr. Renê Carneiro, e Dr. Vitor Martini pela colaboração nos trabalhos da tese com análises estatísticas, novas ideias, redação dos manuscritos e troca de aprendizado.

Às alunas de iniciação científica, Dayse Ferreira e Mariana Freitas, pela ajuda e troca de conhecimento no laboratório. À Aline Souza-Silva, Jorge Ferreira Silva e meu irmão Flávio Costa pela ajuda nas coletas de campo e amizade de sempre. Nem as medidas de *predawn* durante as madrugadas frias nos desanimava. Gratidão, pessoal!

Às professoras Dra. Valéria Cid Maia e a Dra. Sheila Carvalho-Fernandes pelas identificações dos Cecidomyiidae galhadores e hospitalidade durante a minha visita técnica no Museu Nacional da Universidade Federal do Rio de Janeiro. Agradeço imensamente à querida professora Dra. Lúcia Helena Sampaio da Silva pela hospedagem e boas risadas pelo Rio de Janeiro.

Ao prof. Dr. Paul Hanson pela identificação dos parasitoides.

Aos professores integrantes da minha banca de doutorado, Dr. Bruno Ferreira, Dra. Jarcilene Almeida-Cortez, Dr. Geraldo Soares, Dra. Gracielle Bragança, Dra. Lúbia Guedes, Dr. Fernando Vale, Dra. Valéria Cid Maia e Dr. Vinícius Kuster por aceitarem ler e contribuir com esta tese.

Ao Wagner Afonso Rocha, por todo auxílio e ensinamentos no laboratório e pela companhia e conversas descontraídas durante os cafezinhos e almoços na UFMG.

Ao prof. Dr. Fernando Vale (Fernandinho) por todos os ensinamentos acadêmicos e pessoais, admiro demais a sua forma de lecionar. Obrigada pelos bons papos no laboratório e fora da academia.

À família grupo galhas, Ana Flávia Melo, Bruno Ferreira, Gracielle Bragança, Igor Arriola, Mariana Freitas, Nina Jorge, Ravena Malheiros, Reisila Mendes e Renê Carneiro pela boa convivência, parcerias, ensinamentos, apoio e momentos de descontração dentro e fora da UFMG. Gratidão pelas valiosas contribuições em cada capítulo desta tese, especialmente, durante as reuniões virtuais semanais nesse período de pandemia da COVID-19 até o fechamento do texto. Tem um pouco de cada um de vocês nesta tese!

À Graci e a Ravena pela amizade, companheirismo, apoio, desabafos, alegrias e viagens incríveis desde o início desta jornada. Vocês são luz na minha vida!

Aos demais colegas do laboratório de Anatomia Vegetal, Aryanne Evellyn, André Rodrigues, Dayse Kelly, Flávia Gomes, Francisco Abreu, Gabriella Bertollo, Michele Gomes e Thaís de Paula, pela troca de conhecimento, boa convivência e risadas.

Aos amigos de outros laboratórios e para além da UFMG, Daniela Boanares, Pedro Mafia, Danielle Alvarenga, Stéphani Vasconcelos, Vagner Bellaver, Daniele Cury, Daniele Pianetti, Humberto Almeida, Letícia Cunha, Tiago Vilas Boas e Ione Salim, por tornarem os meus dias mais leves, alegres e descontraídos.

Ao Arthur Rocha, por todo companheirismo, paciência, incentivo, carinho e amor tão importantes na reta final do meu doutorado. A você, gratidão!

Por fim, a todos vocês e àqueles que de alguma forma contribuíram para esta tese, a minha eterna gratidão!

PREFÁCIO

As galhas entraram na minha vida acadêmica durante o meu terceiro período da graduação na UNEB-Caetité, despertando muitas curiosidades e me levando para caminhos que antes eu nem sonhara em ir. Em 2011, tive meu primeiro contato prático com as galhas quando fiz uma visita técnica ao laboratório de Anatomia Vegetal-UFMG com a profa. Dra. Rosy Isaias. Essa experiência prática e a convivência com o grupo galhas fizeram com que eu me apaixonasse ainda mais por essa temática científica. Ao retornar para a Bahia, cheia de ideias e muito material para leitura, comecei um levantamento de plantas hospedeiras e suas galhas na Serra Geral de Caetité e, foi aí que conheci a super-hospedeira *Mimosa gemmulata* Barneby (Fabaceae). Suas galhas bivalvas lanceoladas nas cores verde e marrom, abundantes e semelhantes, induzidas na raquíola me chamaram a atenção. Inicialmente, pensei que fossem fases diferentes de desenvolvimento de uma mesma galha, até sugiro essa hipótese no meu primeiro artigo de levantamento de galhas. No entanto, com observações de campo, percebi que as galhas bivalvas lanceoladas marrons e verdes se tratavam de galhas distintas. Por serem abundantes em *M. gemmulata*, durante o meu mestrado na UNEB-Paulo Afonso sob orientação da profa. Dra. Juliana Santos-Silva, coorientação da profa. Dra. Rosy Isaias e colaboração do prof. Dr. Renê Carneiro, estudei em um dos capítulos o desenvolvimento da galha bivalva marrom. Neste trabalho, vimos que as alterações anatômicas em cada estágio de desenvolvimento estavam associadas às diferentes fases do indutor *Lopesia* sp. (Cecidomyiidae), identificado pela Dra. Sheila Carvalho-Fernandes com quem desenvolvi uma parceria desde a graduação.

Ao pensar em ingressar no doutorado, tive dúvidas se seguiria com uma carreira na Botânica ou na Ecologia, mas tinha duas certezas: fazer doutorado em Minas Gerais e meus orientadores, profa. Dra. Rosy Isaias e prof. Dr. Dênis Oliveira. Depois de muito pensar e trocar ideias sobre esses dois mundos científicos, optei pela Botânica e em consonância com meus orientadores, escolhemos *M. gemmulata* e suas galhas associadas como modelo de estudo, tendo em vista que os fenólicos, diversos em *Mimosa,* seriam a linha mestra da tese. No entanto, devido aos empecilhos logísticos e laboratoriais que se agravaram com a pandemia do COVID-19, a tese teve que ser reformulada. Assim, vimos a oportunidade de aprofundar os estudos do desenvolvimento de galhas semelhantes induzidas em um mesmo sítio de indução por espécies congenéricas, mas com diferentes ciclos de vida. Duas importantes descobertas guiaram essa nova ideia. O primeiro texto

desenvolvido para a tese, que no final tornou-se o segundo capítulo, mostra que o sincronismo fenológico de *M. gemmulata* com os ciclos de vida distintos dos indutores das quatro galhas bivalvas (lenticular, globoide e as duas lanceoladas, a verde e a marrom) é importante para a indução dessas galhas na raquíola. Além disso, um outro suporte para as comparações no desenvolvimento das galhas bivalvas, foi a identificação dos indutores das outras três galhas bivalvas como também pertencentes à *Lopesia* (Cecidomyiidae) pelas profa. Dra. Valéria Cid Maia e profa. Dra. Sheila Carvalho-Fernandes. E assim, nasceu esta tese composta de seis capítulos: "The super-host *Mimosa gemmulata* Barneby (Fabaceae) and the implications of the life cycles of *Lopesia* spp. (Cecidomyiidae) on gall developmental processes". O primeiro capítulo é uma revisão das espécies de *Mimosa* hospedeiras de galhas submetido à Biota Neotropica. O segundo capítulo aborda o sincronismo fenológico de *M. gemmulata* com o ciclo de vida dos insetos galhadores, publicado na Tropical Ecology. O terceiro capítulo evidencia o investimento estrutural e nutricional nos tecidos das quatro galhas bivalvas relacionado com os diferentes ciclos de vida de *Lopesia*, publicado na Frontiers in Plant Science. O quarto capítulo trata dos padrões anatômicos das galhas bivalvas e está submetido à Flora. O quinto capítulo demonstra que os sítios de acúmulo de auxinas e citocininas estão relacionados às dinâmicas celulares durante o desenvolvimento das galhas bivalvas, formatado segundo à Australian Journal of Botany. Por fim, o sexto capítulo, submetido à Protoplasma, aborda o impacto de relações tri-tróficas nos padrões citológicos e histoquímicos das galhas bivalvas globoides. O amadurecimento desses capítulos ocorreu durante as reuniões semanais virtuais do Grupo Galhas desde o início da pandemia do COVID-19. Essas reuniões, regadas a leituras e sugestões críticas, discussões cientificas, políticas, culturais, boas risadas e apoio humano, foram fundamentais para impulsionar e estimular a escrita desta tese em um momento crítico para o mundo. Assim, concluo esses quatro anos e meio de doutorado por onde as galhas me levaram e que começou a ser sonhado na graduação.

RESUMO

O gênero *Mimosa* L. (Fabaceae) tem 21 espécies hospedeiras, nas quais 35 morfoespécies de galhas são reportadas na flora brasileira. *Mimosa gemmulata* Barneby destaca-se como uma super-hospedeira com seis morfoespécies de galhas, sendo quatro galhas bivalvas: as lenticulares (GL), as lanceoladas marrons (GLM), as lanceoladas verdes (GLV) e as globoides (GG). De modo peculiar, em *M. gemmulata,* essas quatro galhas bivalvas são induzidas na raquíola por quatro espécies de *Lopesia* Rübsaamen 1908 (Cecidomyiidae). Os estudos fenológicos, anatômicos, citométricos, histoquímicos e imunocitoquímicos revelam diferenças entre as galhas bivalvas em *M. gemmulata.* Tais diferenças estão relacionadas à duração dos ciclos de vida de cada espécie de *Lopesia* e, consequentemente, de sua galha. *Mimosa gemmulata* tem brotamento foliar contínuo que suporta os ciclos de vida multivoltinos das quatro *Lopesia* spp., que possuem assincronismo entre os períodos de indução, evitando sobreposição. As GL têm ciclo de vida de dois meses, as GLV e as GLM de três meses e as GG de quatro meses. Essa variação de 1 a 2 meses no ciclo de vida entre as galhas influencia diretamente o maior acúmulo de recursos estruturais e nutricionais nas paredes celulares e no protoplasma dos tecidos da GG em comparação às outras três galhas. Durante o desenvolvimento das galhas bivalvas, os tipos de tricomas foliares de *M. gemmulata* são conservados, mas seu tamanho, número de células e distribuição são variáveis em cada galha. As células parenquimáticas da raquíola recrutadas para o desenvolvimento das galhas são rediferenciadas em células de armazenamento, esclerenquimáticas e vasculares nas quatro galhas bivalvas, mas o maior potencial de respostas em todas as linhagens celulares é estimulado na GG. Nestas galhas, as células nutritivas típicas têm origem mista, a partir de células epidérmicas e parenquimáticas. Os sítios de detecção temporal e espacial de citocininas e auxinas determinam os padrões de divisão e alongamento de todas as linhagens celulares durante a ontogênese de cada galha bivalva. A maior dinâmica celular e tecidual em resposta ao acúmulo de hormônios também é relacionada ao maior ciclo de vida de *Lopesia* sp. associada a GG. No sistema *M. gemmulata-Lopesia* sp. associada a GG, a entrada do ectoparasitoide *Torymus* sp. e do endoparasitoide Platygastridae impacta o comportamento alimentar da larva indutora, resultando no processo de senescência precoce da galha. Assim, concluímos que as diferenças das galhas bivalvas associadas a *M. gemmulata* são determinadas pelo tempo que cada espécie de *Lopesia* estimula o desenvolvimento de sua galha, com maior potencial de respostas na GG, cujo ciclo de vida é mais longo.

Palavras-chave: anatomia, citologia, fenologia, histoquímica, interação planta-inseto, longevidade da galha, senescência precoce.

ABSTRACT

The genus *Mimosa* L. (Fabaceae) has 21 host species, in which 35 gall morphospecies are reported for the Brazilian flora. *Mimosa gemmulata* Barneby stands out as a super-host of six gall morphospecies, of which four are bivalve-shaped: the lenticular (LG), the green lanceolate (GLG), the brown lanceolate (BLG) and the globoid (GG) galls. Peculiarly, on *M. gemmulata*, the four bivalve-shaped galls are induced on the pinna-rachis by four species of *Lopesia* Rübsaamen 1908 (Cecidomyiidae). Phenological, anatomical, cytometric, histochemical and immunocytochemical studies reveal that differences among the bivalve-shaped galls associated with *M. gemmulata* relate to the lifespans of the *Lopesia* spp., and consequently, to their galls. The constant leaf flushing in *M. gemmulata* supports the asynchrony of the multivoltine life cycles of *Lopesia* spp. and the non-overlapping of gall induction periods. The LG life cycle lasts two months, the GLM and the GLV life cycles last three months, and the GG life cycle lasts four months. This variation of 1 to 2 months in the gall lifespans determines the highest structural and nutritional support in the cell walls and protoplasm of the GG tissues, when compared to the other galls. During the development of the bivalve-shaped galls, the types of leaf trichomes of *M. gemmulata* are conserved, but their size, cell number and distribution are differently altered in each gall. The parenchyma cells recruited from the pinna-rachis redifferentiate into the storage, sclerenchyma cells, and vascular cells of the four bivalve-shaped galls, but the highest stimuli-induced responses in all host plant cell lineages occur in the GG. In this gall, the typical nutritive tissue has mixed origin, from epidermal and parenchyma cells. The sites of spatial and temporal detection of auxins and cytokinins determine the patterns of cell division and elongation during the ontogenesis of each bivalve-shaped gall. The highest cell and tissue dynamics in responses to plant hormones is related to the longest life cycle of the *Lopesia* sp. associated to the GG. The entrance of the ectoparasitoid *Torymus* sp. and the endoparasitoid Platygastridae in *M. gemmulata*-*Lopesia* GG system impacts the feeding behavior of the gall-inducing *Lopesia* larvae, resulting in precocious gall senescence. Thus, we conclude that the differences among the bivalve-shaped galls associated with *M. gemmulata* are determined by the time that each *Lopesia* sp. stimulates the development of its specific gall, with the highest potential of responses in the GG, which has the longest lifespan.

Keywords: anatomy, cytology, gall lifespan, histochemistry, plant-insect interaction, phenology, precocious senescence.

SUMÁRIO

Introdução geral 18

Capítulo 1 - *Mimosa* L. (Fabaceae) in Brazil: what do we know about the host species and their galls?..... 24

Abstract..... 25

Resumo..... 26

Introduction..... 27

Material and methods..... 27

Results and discussion..... 28

Distribution, endemism, and conservation status..... 28

Ecological traits 30

The patterns of galls 31

Gall-inducing insects and associated insect guilds..... 32

Anatomical traits..... 33

Chemical traits..... 34

Conclusion..... 34

Acknowledgements..... 35

References..... 35

Anexos..... 41

Capítulo 2 - How galling herbivores share a single super-host plant during their phenological cycle: the case of *Mimosa gemmulata* Barneby (Fabaceae)..... 53

Abstract 54

Introduction 54

Material and methods 55

Study area..... 55

Super-host plant phenology 56

Life cycles of the galls..... 56

Water potential measurements..... 56

Data analysis..... 56

Results 58

General features of the galls 58
Life cycles of the galls..... 58
Phenology of the super-host plant 58
Relationship between the induction of the leaf gall morphotypes and leaf flushing 60
Gall morphotypes abundance versus abiotic and physiological factors..... 61
Discussion 61
Univoltinism versus multivoltinism 62
Temporal strategies of multivoltine galling insects 63
Seasonal abundance of insect galls and climatic factors, water potential, and plant phenology 64
Conclusions 64
Acknowledgements 65
References 65

Capítulo 3 - Structural and nutritional peculiarities related to lifespan differences on four *Lopesia* induced bivalve-shaped galls on the single super-host *Mimosa gemmulata* 68
Abstract..... 69
Introduction..... 69
Material and methods..... 70
The Lifespans of Lopesia *Galls on* M. gemmulata..... 70
Structural analysis 70
Histometric analysis 70
Histochemical analysis 71
Immunocytochemical analysis..... 71
Results..... 71
Non-galled Pinna-Rachis Profile (Control) 71
Profiles of Lopesia *Galls*..... 71
Structural Profiles 71
Histometric Profiles 71
Histochemical Profiles 75
Immunocytochemical Profiles 75

Discussion 75
Structural Peculiarities in the Lopesia *Galls* 75
Nutritional Profiles in the Protoplasm of the Lopesia *Galls* …..... 79
Nutritional Profiles in Cell Walls of Lopesia *Galls*…..... 79
Conclusion 79
Acknowledgements 80
References 80

Capítulo 4 - The ontogenesis of four *Lopesia* Rübsaamen (Cecidomyiidae) galls on the super-host *Mimosa gemmulata* Barneby (Fabaceae) reveals peculiar anatomical traits 82
Highlights..... 83
Abstract..... 84
Introduction..... 85
Material and methods..... 86
Sampling and collection 86
Light microscopy analysis 86
Scanning electron microscopy analysis 87
Results 87
Non-galled Pinna-rachis (NGP) and Pinnula 87
General aspects of the four Lopesia *gall*..... 88
Lenticular bivalve-shaped galls (LG)..... 88
Green lanceolate bivalve-shaped galls (GLG)..... 90
Brown lanceolate bivalve-shaped galls (BLG)…..... 91
Globoid bivalve-shaped galls (GG)……..... 92
Discussion 93
Diversity of cell lineages in the development of the Lopesia *galls* 94
Anatomical features related to the structural-functional traits of Lopesia *galls*…….. 97
Conclusion 100
Acknowledgements 102
References 102
Anexos 109

Capítulo 5 - Cytokinins and auxins influence distinct dynamics of cell growth along the life cycle of three *Lopesia* bivalve-shaped galls on *Mimosa gemmulata* (Fabaceae)..... 122
Summary text for the Table of Contents..... 124
Abstract..... 124
Introduction..... 125
Material and methods..... 126
Sampling and collection 126
Histochemical analyses of phytohormones..... 127
Cytometric analyses 128
Statistical analyses..... 129
Results 129
Non-galled pinna-rachis..... 129
Lopesia *galls*..... 130
Histochemical analyses of the galls…..... 130
LG 130
GLG 130
GG 131
Cytometric analyses..... 131
LG 131
GLG 132
GG 133
Principal-component analysis (PCA) 133
Discussion 134
Influence of CKs and IAA in the bivalve-shaped galls..... 134
Key factors that determine the bivalve-shaped galls..... 138
Acknowledgements 139
References 139
Anexos 146

Capítulo 6 - Parasitoid impairment on the galling *Lopesia* activity reflects on the cytological and histochemical profiles of the globoid bivalve-shaped gall on *Mimosa gemmulata* 161
Abstract 163
Introduction 164
Material and methods 165
Sample design 165
Structural analyses 165
Cytological analyses 165
Histochemical analyses 165
Results 166
Cytological profiles 166
Galls with non-parasitized Lopesia *larva* 166
Galls with ectoparasitized Lopesia *larva* 166
Galls with endoparasitized Lopesia *larva* 167
Histochemical profiles 167
Galls with non-parasitized Lopesia *larva* 167
Galls with ecto- and endoparasitized Lopesia *larvae* 167
Discussion 168
Cytological traits 168
Histochemical traits 169
Final considerations 170
Acknowledgements 171
References 171
Anexos 176
Considerações finais 186

INTRODUÇÃO GERAL

Mimosa L. (Fabaceae) é um gênero amplamente distribuído no Brasil, com cerca de 374 espécies, e altas taxas de endemismo (Simon e Proença 2000; Dutra et al. 2020). Dentre as espécies de *Mimosa*, 21 são reportadas como hospedeiras de galhas nos domínios fitogeográficos brasileiros Caatinga, Cerrado, Mata Atlântica, Pantanal e Pampa (Julião et al. 2002; Nogueira et al. 2016; Maia e Mascarenhas 2017; Brito et al. 2018). As galhas podem ser definidas como estruturas derivadas do desenvolvimento anormal dos tecidos da planta hospedeira (Mani 1964; Shorthouse 2005). Elas possuem padrões anatômicos, citológicos, fisiológicos e químicos muitas vezes únicos, quando comparados aos seus órgãos de origem (Meyer e Maresquelle 1983; Mani 1964; Oliveira et al. 2016), sendo as galhas consideradas novos órgãos vegetais (Shorhouse et al. 2005). Essa interação ecológica entre os organismos galhadores, principalmente insetos e, suas plantas hospedeiras que resultam em galhas são, na maioria dos casos, espécie-específica (Mani 1964; Carneiro et al. 2009). Por causa da especificidade da interação, galhas são ferramentas úteis na conservação ambiental (Santana e Isaias 2014), das suas plantas hospedeiras e seus insetos galhadores (Maia 2019, 2021). Neste panorama, esta tese está dividida em seis capítulos e, se inicia com uma revisão bibliográfica sobre a distribuição, endemismo, estado de conservação e atributos ecológicos, anatômicos e químicos das espécies de *Mimosa* hospedeiras de galhas, suas galhas e seus galhadores bem como fauna associada. Nossa perspectiva é apontar lacunas do conhecimento na Flora Brasileira e direcionar a escolha de sistemas planta hospedeira-organismo galhador interessantes para estudos de caso em ecologia, anatomia e química de importância para a conservação ambiental.

No gênero *Mimosa* algumas espécies são consideradas super-hospedeiras. Essas são espécies hospedeiras em que diversas espécies de galhadores se associam para induzir suas galhas, sendo, portanto, importantes para a riqueza de insetos galhadores (Isaias et al. 2013; Grandez-Rios et al. 2020). *Mimosa gemmulata* Barneby destaca-se como uma super-hospedeira, associada a até seis morfoespécies de insetos galhadores em ambientes de Caatinga e de Cerrado no Brasil (Costa et al. 2014, 2021b; Nogueira et al. 2016). Dentre as galhas de *M. gemmulata*, uma é fusiforme e induzida em caules por uma espécie não determinada de Lepidoptera (Costa et al. 2021b). As outras cinco galhas são induzidas na raquíola por cinco espécies congenéricas de *Lopesia* Rübsaamen 1908 (Diptera: Cecidomyiidae) ainda não descritas para a ciência, sendo uma galha clavada e as outras

quatro galhas bivalvas: uma lenticular, uma globoide e duas lanceoladas, as quais são distinguidas pela coloração, verde e marrom. Em espécies super-hospedeiras, as estratégias de sincronismo entre as fenofases da planta e os ciclos de vida dos insetos galhadores são cruciais para o aporte nutricional para as galhas e para o sucesso dos galhadores (Castro et al. 2012; Oliveira et al. 2013, 2016). Além disso, a fenologia da planta hospedeira está sujeita à interferência de fatores climáticos, tais como precipitação e temperatura, os quais influenciam nas estratégias de sincronismo (Oliveira et al. 2013). Sendo assim, o segundo capítulo visa demonstrar quais as estratégias que permitem a associação dos seis diferentes galhadores à uma mesma planta hospedeira, *M. gemmulata*.

Em galhas induzidas em folhas ou folíolos, como é o caso das galhas bivalvas em *M. gemmulata*, há uma tendência de sincronismo com o período de brotação, já que órgãos jovens são sítios com alta qualidade de recursos nutricionais (Oliveira et al. 2016). Metabólitos primários como proteínas, lipídios, açúcares redutores e amido, detectados por análises histoquímicas no protoplasma de células de reserva e nutritivas, têm sido relacionados à manutenção da galha e a nutrição do galhador (Bronner 1992; Oliveira et al. 2011; Bragança et al. 2017). Recentemente, xiloglucanos, detectados por imunocitoquímica nas paredes celulares de galhas, têm sido relacionados não só a funções estruturais, mas também à função de reserva nutricional para o galhador quando detectados em células nutritivas (Bragança et al. 2020; Ferreira et al. 2020). Dessa forma, o terceiro capítulo visa demonstrar o padrão de organização dos tecidos de reserva e nutritivos das quatro galhas bivalvas e seus recursos nutricionais armazenados, tanto nas paredes celulares, quanto no protoplasma, relacionando-os aos ciclos de vida das espécies de *Lopesia*.

O entendimento dos ciclos de vida das galhas associadas a *M. gemmulata* permite a definição dos seus estágios de indução, crescimento e desenvolvimento, maturação e senescência (Costa et al. 2021b). A delimitação destes estágios permite o estudo comparativo do desenvolvimento das galhas bivalvas e suas especificidades anatômicas, apresentado no quarto capítulo. O desenvolvimento e, consequentemente, a forma final da galha são determinados pelo sítio de indução na planta hospedeira, o *taxon* do organismo galhador e seu modo de alimentação (Meyer e Maresquelle, 1983; Rohfritsch, 1992; Ferreira et al. 2019; Miller e Raman 2019). Além disso, a determinação da forma está relacionada à dinâmica de hiperplasia, da hipertrofia celular e dos diferentes padrões de alongamento durante o desenvolvimento das galhas, processos estes mediados pelo

acúmulo e histolocalização de citocininas e auxinas (Bedetti et al. 2014, 2017, 2018). O estudo comparativo das galhas bivalvas lenticulares, lanceoladas e globoides, apresentado no quinto capítulo, demonstra a detecção dos sítios de acúmulo de citocininas e auxinas sobrepostos aos sítios de hiperplasia e hipertrofia celular, respectivamente, influenciando os padrões de alongamento celular e seu papel na determinação da forma final de cada galha.

Além do envolvimento dos dois níveis tróficos, planta hospedeira e inseto galhador, diversas relações tróficas podem ser estabelecidas e associadas às galhas (Luz et al. 2020). O acompanhamento de diferentes galhas na natureza permite evidenciar a entrada de outros níveis tróficos no sistema, como os parasitoides, que impactam o comportamento alimentar e os estímulos do indutor, levando a mudanças estruturais, citológicas e histoquímicas (Rezende et al. 2019). Tal impacto altera os padrões de desenvolvimento das galhas, objetivo abordado no sexto capítulo, o qual visa elucidar o impacto de relações tri-tróficas envolvendo parasitoides nos tecidos das galhas bivalvas globoides em *M. gemmulata*.

Esta tese, cujo principal modelo de estudo é *M. gemmulata* e suas quatro galhas bivalvas induzidas na raquíola por quatro espécies de *Lopesia*, tem como eixo central a hipótese de que o tempo no qual a morfogênese da planta hospedeira é manipulada por galhadores congenéricos, mas com ciclos de vida distintos, será determinante para as peculiaridades espécie-específicas de cada galha. Os objetivos de cada capítulo são (1) investigar o estado da arte das espécies de *Mimosa* hospedeiras de galhas no Brasil (Costa et al. 2021a, Biota Neotropica; submetido); (2) elucidar as estratégias temporais e sazonais de sincronismo entre as fenofases de *M. gemmulata* e os ciclos de vida dos galhadores, bem como de assincronismo durante os períodos de indução das galhas (Costa et al. 2021b); (3) estabelecer a relação entre o investimento estrutural e nutricional tanto nas paredes celulares quanto no protoplasma das células de cada galha bivalva com os seus ciclos de vida (Costa et al. 2021c); (4) determinar a origem e os destinos das linhagens celulares durante os estágios de desenvolvimento das quatro galhas bivalvas (Costa et al. 2021d, Flora; submetido); (5) relacionar a dinâmica temporal de auxinas e citocininas ao estabelecimento dos padrões de divisão e alongamento celular durante o desenvolvimento das galhas bivalvas lenticulares, lanceoladas verdes e globoides (Formatado para Australian Journal of Botany); e (6) determinar as alterações nos perfis citológicos e histoquímicos nos tecidos de armazenamento e nutritivo da galha bivalva

globoide devido à influência dos ecto- e endoparasitoides no comportamento alimentar da larva de *Lopesia* (Costa et al. 2021e, Protoplasma; submetido).

Referências Bibliográficas

Bedetti CS, Modolo LV, Isaias RMS (2014) The role of phenolics in the control of auxin in galls of *Piptadenia gonoacantha* (Mart.) MacBr (Fabaceae: Mimosoideae). Biochemical Systematics and Ecology 55: 53–59.

Bedetti CS, Bragança GP, Modolo LV, Isaias RMS (2017) Influence of auxin and phenolic accumulation on the patterns of cell differentiation in distinct gall morphotypes on *Piptadenia gonoacantha* (Fabaceae). Australian Journal of Botany 65(5): 411–420.

Bedetti CS, Jorge NC, Trigueiro F, Bragança GP, Modolo LV, Isaias, RMS (2018) Detection of cytokinins and auxin in plant tissues using histochemistry and immunocytochemistry. Biotechnic & Histochemistry 93(2): 1–6.

Bragança GP, Oliveira DC, Isaias RMS (2017) Compartmentalization of metabolites and enzymatic mediation in nutritive cells of Cecidomyiidae galls on *Piper arboreum* Aubl. (Piperaceae). J. Plant Tiss 6: 11–22.

Bragança GPP, Alencar CF, Freitas MSC, Isaias RMS (2020). Hemicelluloses and associated compounds determine gall functional traits. Plant Biology 22: 981–991.

Brito GP, Costa EC, Carvalho-Fernandes SP, Santos-Silva J (2018) Riqueza de galhas de insetos em áreas de Caatinga com diferentes graus de antropização do estado da Bahia, Brasil. Iheringia. Série Zoologia 108: e2018003.

Bronner R (1992) The role of nutritive cells in the nutrition of cynipids and cecidomyiids. In: Shorthouse, J.D., Rohfritsch, O. (Eds), Biology of insect induced-galls. Oxford University Press, Oxford, pp. 118–140.

Castro AC, Oliveira DC, Moreira ASFP, Lemos-Filho JP, Isaias RMS (2012). Source–sink relationship and photosynthesis in the horn-shaped gall and its host plant *Copaifera langsdorffii* Desf. (Fabaceae). South African Journal of Botany 83: 121–126.

Costa EC, Carvalho-Fernandes SP, Santos-Silva J (2014) Galhas de insetos em uma área de transição caatinga-cerrado no Nordeste do Brasil. Sitientibus Série Ciências Biológicas 14: 1–9.

Costa EC, Oliveira DC, Isaias RMS (2021a) *Mimosa* L. (Fabaceae) in Brazil: what do we know about the host species and their galls? Biota Neotropica. Submitted.

Costa EC, Martini VC, Souza-Silva A, Lemos-Filho JP, Oliveira DC, Isaias RMS (2021b) How galling herbivores share a single super-host plant during their phenological cycle: the case of *Mimosa gemmulata* Barneby (Fabaceae). Tropical Ecology 1–14.

Costa EC, Oliveira DC, Ferreira DKL, Isaias RMS (2021c) Structural and nutritional peculiarities related to lifespan differences on four *Lopesia* induced bivalve-shaped galls on the single super-host *Mimosa gemmulata*. Frontiers in Plant Science 12: 1–13.

Costa EC, Freitas, MSC, Carneiro RGS, Oliveira DC, Isaias RMS (2021d) The ontogenesis of four *Lopesia* Rübsaamen (Cecidomyiidae) galls on the super-host *Mimosa gemmulata* Barneby (Fabaceae) reveals peculiar anatomical traits. Flora. Submitted.

Costa EC, Oliveira DC, Isaias RMS (2021e). Parasitoid impairment on the galling *Lopesia* activity reflects on the cytological and histochemical profiles of the globoid bivalve-shaped gall on *Mimosa gemmulata.* Protoplasma. Submitted.

Dutra VF, Morales M, Jordão LSB, Borges LM, Silveira FS, Simon MF, Santos-Silva J, Nascimento JGA, Ribas ODS (2020) *Mimosa* in Flora do Brasil 2020. Jardim Botânico do Rio de Janeiro. Available in: <http://reflora.jbrj.gov.br/reflora/floradobrasil/FB18823>. (last access on 03/May/2021).

Ferreira BG, Álvarez R, Bragança GP, Alvarenga DR, Hidalgo NP, Isaias RMS (2019) Feeding and other gall facets: patterns and determinants in gall structure. Botanical Review 85: 78–106.

Ferreira B G, Bragança GP, Isaias RM (2020). Cytological attributes of storage tissues in nematode and eriophyid galls: pectin and hemicellulose functional insights. Protoplasma 257(1): 229–244.

Grandez-Rios J M, Pizango CG, Araújo WS (2020). Insights into Super-host plant species of galling insects in the Neotropical region. The Open Biology Journal, 8(1): 66–73.

Julião GR, Amaral MEC, Fernandes GW (2002) Galhas de insetos e suas plantas hospedeiras no Pantanal Sul Mato-grossense. Naturalia 27(1): 47–74.

Maia VC (2019) Insect galls on Myrtaceae: richness and distribution in brazilian restingas. Biota Neotropica.19(1): e20180526.

Maia VC (2021) Geographic distribution of eight Neotropical species of Cecidomyiidae (Diptera, Insecta) Brazilian Journal of Animal and Environmental Research 4(1): 1374–1383.

Maia VC, Mascarenhas B (2017) Insect galls of the Parque Nacional do Itatiaia (Southeast Region, Brazil). Academia Brasileira de Ciências 89: 505–575.

Meyer J, Maresquelle HJ (1983) Anatomie des galles. (Gebrüder Borntraeger, Berlin, Germany)

Miller III DG, RamanA (2019). Host–plant relations of gall-inducing insects. Annals of the Entomological Society of America 112: 1–19.

Nogueira RM, Costa EC, Carvalho-Fernandes SP, Santos-Silva J (2016) Insect galls from Serra Geral, Caetité, BA, Brazil. Biota Neotropica 16(1): e20150035.

Oliveira DC, Carneiro RGS, Magalhães TA, Isaias RMS (2011) Cytological and histochemical gradients on two *Copaifera langsdorffii* Desf. (Fabaceae) Cecidomyiidae gall systems. Protoplasma 248: 829–837.

Oliveira DC, Mendonça MS, Moreira ASFP, Lemos-Filho JP, Isaias RMS (2013) Water stress and phenological synchronism between *Copaifera langsdorffii* (Fabaceae) and multiple galling insects: formation of seasonal patterns. Journal of Plant Interactions 8: 225–233.

Oliveira DC, Isaias RMS, Fernandes GW, Ferreira BG, Carneiro RGS, Fuzaro, L (2016) Manipulation of host plant cells and tissues by gall-inducing insects and adaptive strategies used by different feeding guilds. Journal of Insect Physiology 84: 103–113.

Rezende UC, Cardoso JCF, Kuster VC, Gonçalves LA, Oliveira DC (2019) How the activity of natural enemies changes the structure and metabolism of the nutritive tissue in galls? Evidence from the *Palaeomystella oligophaga* (Lepidoptera)-*Macairea radula* (Metastomataceae) system. Protoplasma 256(3): 669–677.

Rohfritsch O (1992) Patterns in gall development. In 'Biology of insect-induced galls'. (Eds JD Shorthouse, O Rohfritsch) pp. 60–86. (Oxford University Press: New York)

Rübsaamen EH (1908) Beiträge zur Kenntnis aussereuropäischer Zoocecidien. III. Beitrag: Gallen aus Brasilien und Peru. Marcellia 7: 15–79.

Simon MF, Proença C (2000) Phytogeographic patterns of *Mimosa* (Mimosoideae, Leguminosae) in the Cerrado biome of Brazil: an indicator genus of high-altitude centers of endemism? Biological Conservation 96(3): 279–296.

Chapter 1

Mimosa L. (Fabaceae) in Brazil: what do we know about the host species and their galls?

Submitted to Biota Neotropica

Mimosa L. (Fabaceae) in Brazil: what do we know about the host species and their galls?

Elaine C. Costa[1], Denis C. Oliveira[2], Rosy M.S. Isaias[1, *]

[1]Departamento de Botânica, Instituto de Ciências Biológicas, Universidade Federal de Minas Gerais, Avenida Antônio Carlos, 6627, Pampulha, Belo Horizonte, Minas Gerais Zip code: 31270-901, Brazil.

[2]Instituto de Biologia, Universidade Federal de Uberlândia, Campus Umuarama, Rua Ceará s/n, Uberlândia, Minas Gerais, Zip code: 38402-018, Brazil.

[*]Corresponding author: rosy@icb.ufmg.br

***Abstract*:** *Mimosa* L. is a genus widely distributed in Brazil, and their species are reported as hosts of galling insects in different phytogeographic domains. We used literature and herbarium data to review the state-of-the-art of the *Mimosa* spp. and their galls with focus in the distribution, endemism, and conservation status, as well as the associated gall-inducing insects. In addition, we provide ecological, anatomical, and chemical traits of the host species and the galls. Our perspective is to direct possible case studies to understand the choice or by-chance occurrence of host species-galling insect systems in the Brazilian flora. Twenty-one *Mimosa* spp. are reported as hosts of 35 gall morphospecies, and some of them are non-endemic with wide (5) or restrict (4) distribution in the Brazilian phytogeographic domains. The other species are endemic to *Caatinga* and *Cerrado* (3), or exclusive of *Caatinga* (3), *Cerrado* (n = 3), Atlantic Forest (2), and *Pampa* (n = 1). The endemism can extend to their associated gall inducers, whose species belong to the Coleoptera, Diptera and Lepidoptera orders, but the mostly are unknown to science. The host species have deciduous, semideciduous or perennial phenological strategies, which can influence the life cycles of the insects. Some of the anatomical traits of *Mimosa* are variable, and the types of trichomes, for instance, are abundant among the galls. The diversity of secondary metabolites in the *Mimosa* is an important chemical trait that may be involved in the dynamics of gall development, in the expression of the red gall color, and in the chemical defense. Thus, the *Mimosa* spp. and their galls are potential models for ecological, anatomical, chemical, and physiological approaches. We highlight as potential models of study the super-hosts: *M. gemmulata*, *M. incana*, *M. melanocarpa*, and *M. tenuiflora*, which respond to the stimuli of species of different gall-inducers. In addition, the host plant-galling insect systems endemic to the *Caatinga*, *Cerrado* or Atlantic Forest are pointed out as interesting case studies in the Brazilian flora.

***Keywords**: Atlantic forest; Caatinga; Cerrado; endemism; insect galls.*

***Mimosa* L. (Fabaceae) no Brasil: o que sabemos sobre as espécies hospedeiras e suas galhas?**

***Resumo*:** *Mimosa* L. é um gênero amplamente distribuído no Brasil e suas espécies são reportadas como hospedeiras de insetos galhadores em diferentes biomas. Usamos dados da literatura e de herbários para revisar o estado da arte das *Mimosa* spp. e suas galhas com foco na distribuição, endemismo e estado de conservação, como também dos seus insetos indutores de galhas associados. Além disso, fornecemos dados de atributos ecológicas, anatômicas e químicas das espécies hospedeiras e das galhas. Nossa perspectiva é direcionar possíveis estudos de caso para entender a escolha ou ocorrência por acaso de sistemas espécie hospedeira-inseto galhador na flora brasileira. Vinte e uma *Mimosa* spp. são reportadas como hospedeiras de 35 morfoespécies de galhas, sendo algumas delas não endêmicas com ampla (n = 5) ou restrita (n = 4) distribuição nos domínios fitogeográficos brasileiros. As demais espécies são endêmicas da Caatinga e Cerrado (n = 3), ou exclusivas dos biomas Caatinga (n = 3), Cerrado (n = 3), Mata Atlântica (n = 2) e Pampa (n = 1). O endemismo pode se estender aos seus indutores de galhas associados, cujas espécies pertencem às ordens Coleoptera, Diptera e Lepidoptera, mas a maioria é desconhecida da ciência. As espécies hospedeiras possuem estratégias fenológicas decíduas, semidecíduas ou perenes, que podem influenciar os ciclos de vida dos insetos. Alguns atributos anatômicos em *Mimosa* são variáveis, e os tipos de tricomas, por exemplo, são abundantes entre as galhas. A diversidade de metabólitos secundários em *Mimosa* é um importante atributo químico que pode estar envolvido na dinâmica de desenvolvimento da galha, na expressão da cor vermelha da galha e na defesa química. Assim, as *Mimosa* spp. e suas galhas são modelos potenciais para abordagens ecológicas, anatômicas, químicas e fisiológicas. Destacamos como modelos potenciais de estudo as super-hospedeiras: *M. gemmulata*, *M. incana*, *M. melanocarpa* e *M. tenuiflora*, que respondem a estímulos de diferentes indutores de galhas. Além disso, os sistemas de plantas hospedeiras-insetos galhadores endêmicos dos biomas Caatinga, Cerrado ou Mata Atlântica são apontados como estudos de caso interessantes na flora brasileira.

***Palavras-chave**: Floresta Atlântica; Caatinga; Cerrado; endemismo; galhas de insetos.*

Introduction

Mimosa is a monophyletic genus of Fabaceae, which is the plant family with the greatest richness of host species of gall-inducing insects in the world (Mani 1964, Raman 2007, Santos-Silva & Araújo 2020). *Mimosa* comprises approximately 600 species (Simon et al. 2011, Jordão et al. 2020) widely distributed in tropical and subtropical regions (Barneby 1991), and in Brazil has the most diversified flora with ca. 374 species, and a high proportion of endemic *taxa* (Dutra & Garcia, 2014, Dutra et al. 2020). The most diversification of the genus occurs in the Central Brazil, especially the *Cerrado* ecoregion, although other ecoregions, such as *Caatinga*, are also well represented by their number of species (Barneby 1991, Simon & Proença 2000, Santos-Silva et al. 2015). The species of *Mimosa* are reported as hosts of galling insects in inventories in the *Caatinga* (Carvalho-Fernandes et al. 2012, Brito et al. 2018), *Cerrado* (Costa et al. 2014, Nogueira et al. 2016), Atlantic Forest (Mendonça-Júnior et al. 2014, Maia & Mascarenhas, 2017), and *Pantanal* (Julião et al. 2002) of Brazil. Several ecological, anatomical, and chemical traits may favor the *Mimosa* geographic distribution, and the choice of *Mimosa* spp. for the galling insects in Brazil. The *Mimosa* has diverse life forms including trees, shrubs, and herbs (Simon et al. 2009). The perennial, semi-deciduous, and deciduous phenological strategies are adaptive to the climatic conditions of the environments where *Mimosa* spp. occur (Lima & Rodal, 2010, Silva et al. 2017b, Holanda et al. 2019), and may host galls on their vegetative and reproductive organs (Mani 1964).

The *Mimosa* spp. potentialities may determine the anatomical and the chemical profiles of their associated galls. For instance, one of the main anatomical traits of the *Mimosa* spp. that is also reflected in gall anatomy is the great diversity of trichomes, which may occur in different organs and/or may be diverse on the same organ surface (Barneby 1991, Santos-Silva et al. 2013, Jordão et al. 2020). Regarding the chemical profiles, *Mimosa* has a high diversity of secondary metabolites, with tryptophan-derivative alkaloids, terpenoids (diterpenes and triterpenes), saponins, phenolic acids, lignins, and flavonoids (De Moraes et al. 1990, Monção et al. 2019, Bezerra et al. 2021). Some classes of these secondary metabolites have been histolocalized in galls, where they work out in the protection of galling organisms, in the scavenging of oxidative stress molecules, and in gall development (Isaias et al. 2015, Kuster et al. 2019).

Currently, we provide a state-of-the-art overview of the *Mimosa* spp. and their galls in Brazilian flora with the focus in the distribution, endemism, and conservation status, as well as in their associated gall inducers with attention to local and general threats to biodiversity. The knowledge on the ecological, anatomical, and chemical traits of the *Mimosa* spp. and their galls may direct potential study cases on understanding the choice or by-chance occurrence of the host plant-galling herbivore systems in Brazilian flora.

Materials and methods

The distribution of the *Mimosa* spp. and their galls in Brazilian flora were carried out based on secondary data available in inventories of diversity and richness of galls, published in scientific articles (n = 80), books (n = 2), thesis (n = 1), and dissertation (n = 1) from 1988 to 2020. The data were accessed on the *Portal de Periódicos da Coordenação de Aperfeiçoamento de Pessoal de Nível Superior* (Capes), Scientific Electronic Library Online (SciELO), Scopus, Springer Science, and Google Scholar, using the keywords: “gall occurrence”, “gall inventory”, “gall survey”, “gall diversity”, “gall richness”, and “gall in Brazil”. As a second step, we consulted the

*species*Link network (SPLink 2021) to access the herbarium data on *Mimosa* spp. hosting galls in Brazil. We opened the search form and inserted the keyword gall on "any field", and the *Mimosa* on the "Scientific name" field. In the search only within records, we scored the options "with geographic coordinates", and the "not suspect coordinate quality". After obtaining the current list of the host *Mimosa* spp. in Brazil, we returned to data base and searched for the keywords: "anatomy of *Mimosa**", "leaf anatomy of *Mimosa**", "chemical composition of *Mimosa**", "phenology of *Mimosa**" (* = species epithets). This second search resulted in articles (n = 87), theses (n = 3), dissertations (n = 7), and reports (n = 4), which were analyzed and sorted out one by one.

The botanical names were updated and the conservation status of all plant species, as well as the data on plant distribution, and endemism were verified, using the *Flora do Brasil* site (Reflora 2020). In addition, the conservation status according to the red-list of the International Union for Conservation of Nature (IUCN 2021) was verified. Based on the high specificity of the gall-inducing insects to their host plants, galling species associated exclusively with endemic plants were proposed as endemic (Maia 2019). Similarly, gall-inducing insects associated exclusively with threatened plants were proposed as threatened. The distribution map of the *Mimosa* spp. and their galls in Brazil was made with QGIS version 3.10.5 (QGIS.org 2020), utilizing the database of the *Instituto Brasileiro de Geografia e Estatistica* (Brazilian Institute of Geography and Statistics). The maps of each species of *Mimosa* and their associated galls in the Brazilian phytogeographic domains were obtained from the *Flora do Brasil* site (Reflora 2020; modified by the authors).

Results and discussion

1. Distribution, endemism, and conservation status

The *Mimosa* genus comprises 374 species in Brazil (Dutra et al. 2020), among which 21 species are reported as hosts of galling insects (Tables 1 and 2, Figure 1). Five *Mimosa* spp. have a wide distribution in the geographic regions of Brazil, and are non-endemic, but the records of their galls up to the moment are local (Figure 2 A-E). This circumstance may be a consequence of the non-recording of the galls due to the methodology of the inventories, or to the local distribution of the gall-inducers. *Mimosa candollei* and *M. sensitiva* occur in the Amazon Forest, *Caatinga*, *Cerrado*, Atlantic Forest, and *Pantanal* in all states of Brazil, with exception of some states in the Southeast region. The globoid bud galls associated with *M. candollei* (Maia & Mascarenhas 2017), and the galls on *M. sensitiva* (Table 2) are reported in the Atlantic Forest of Rio de Janeiro State (Figures 2A-B). The distribution of *M. bimucronata* covers the *Caatinga*, *Cerrado*, Atlantic Forest, *Pampa*, and *Pantanal* of several states in the Northeast, Midwest, Southeast, and South Brazil (Figure C). Nevertheless, the records of the fusiform bud galls induced by *Contarinia* sp. (Cecidomyiidae) are restricted to the Atlantic Forest of Rio de Janeiro State (Oliveira & Maia 2005). *Mimosa somnians* occurs in the Amazon Forest, *Caatinga*, *Cerrado* and *Pantanal* with distribution in several states of the Brazilian phytogeographic domains (Figure 2D), but the fusiform stem galls induced by Cecidomyiidae are restricted to the *Cerrado* of Bahia State (Costa 2016). The distribution of *M. polycarpa* covers the *Cerrado* and *Pantanal* of some states in the North, Midwest, Southeast, and South Brazil (Figure 2E). The associated globoid leaf galls induced by Cecidomyiidae are reported only in the *Cerrado* (Coelho et al. 2013) of Minas Gerais State, while the other globoid stem galls induced by Coleoptera are reported in the *Pantanal* of Mato Grosso do Sul State (Julião et al. 2002).

Four *Mimosa* spp. have restricted phytogeographic distribution and are non-endemic (Figures 2F-I). The distribution of *M. gemmulata* covers the *Caatinga* and *Cerrado* of some states in the Northeast, Midwest, and Southeast Brazil (Figure 2F). The four bivalve-shaped galls, and the clavate galls induced by distinct *Lopesia* spp., as well as the fusiform stem galls induced by Lepidoptera have been recorded in the *Cerrado* of Bahia State (Costa et al. 2014, 2021a, Costa 2016, Nogueira et al. 2016, Silva et al. 2018). The distribution of *M. tenuiflora* covers the *Caatinga* of the Northeast, and the North of Minas Gerais State (Figure 2G). The bivalve-shaped galls induced by *Lopesia pernambucensis* has been recorded in four states: Ceará (Table 2), Sergipe (Carvalho-Fernandes et al. 2012), Bahia (Brito et al. 2018), and Pernambuco (Santos et al. 2011). The other bivalve-shaped galls induced by *L. mimosae* have been recorded only in two states: Bahia (Maia et al. 2010, Nogueira et al. 2018), and Pernambuco (Santos et al. 2011). In addition, the fusiform and the globoid stem galls induced by Curculionidae (Brito et al. 2018), and by Cecidomyiidae (Carvalho-Fernandes et al. 2012), respectively, are reported only in Bahia State. *Mimosa incana* covers the Atlantic Forest and *Pampa* of the Southeast and South Brazil (Figure 2H), and their associated fusiform stem and globoid leaf galls are recorded only in the Atlantic Forest of Rio Grande do Sul State (Mendonça-Júnior et al. 2014). *Mimosa tweedieana* occurs in the Atlantic Forest and its distribution is small and restricted to Rio Grande do Sul State (Figure 2I). Nevertheless, the globoid stem galls associated with *M. tweedieana* are reported in the *Pantanal* of Mato Grosso do Sul State (Ascendino & Maia 2018). This host species may be a misidentification, because no record has been reported to another state in Brazil (Dutra et al. 2020).

The *Mimosa* spp. and their associated gall-inducing insects with a restricted distribution and endemism occur mainly in the *Caatinga*, *Cerrado*, and Atlantic Forest (Figures 3-4). *Mimosa hypoglauca*, *M. coruscocaesia*, and *M. verrucosa* are endemic to the *Caatinga* and *Cerrado*. The distribution of *M. hypoglauca* covers Bahia, Góias, Minas Gerais, and Piauí states (Figure 3A), and their associated fusiform leaf galls are reported only in the *Cerrado* of Bahia State (Costa 2016). The distribution of *M. coruscocaesia* is restricted to Bahia and Minas Gerais states (Figure 3B), and the leaflet bivalve-shaped galls are reported for the *Cerrado* in Bahia state (Santos-Silva 2013). The distribution of *M. verrucosa* covers Bahia, Ceará, Goiás, Maranhão, Pernambuco, and Piauí states, and their associated galls are reported for the *Caatinga* in Bahia State (Figure 3C).

Mimosa caesalpiniifolia, *M. pseudosepiaria* and *M. ophthalmocentra* are endemic to the *Caatinga* (Figures 3D-F). *Mimosa caesalpiniifolia* occurs in Alagoas, Ceará, Maranhão, Paraíba, Pernambuco, Piauí, and Rio Grande do Norte states (Figure 3D), and the associated galls induced by *Schizomyia mimosae* are reported for Ceará state (Gagné & Jaschhof 2017). The distribution of *M. pseudosepiaria* is restricted to Bahia, Pernambuco, and Piauí states (Figure 3E), and the associated asymmetrical stem galls induced by Cecidomyiidae are reported for Alagoas state (Carvalho-Fernandes et al. 2012). *Mimosa ophthalmocentra* occurs in Bahia, Ceará, Minas Gerais, Paraíba, Pernambuco, and Rio Grande do Norte states (Figure 3F), and the associated bivalve-shaped galls induced by Cecidomyiidae are reported for Bahia state (Costa 2016).

Mimosa melanocarpa, *M. sericantha* and *M. spixiana* are endemic to the *Cerrado* (Figures 3D-F). The distribution of *M. melanocarpa* covers Bahia, Goiás, Mato Grosso, Mato Grosso do Sul, and Minas Gerais states (Figure 3G). The fusiform stem and the globoid bud galls induced by distinct Cecidomyiidae species are recorded in Rio de Janeiro state (Maia & Mascarenhas 2017). The distribution of *M. sericantha* covers Bahia, Goiás, Maranhão, Minas Gerais, Piauí, and Tocantins states (Figure 3H), while the distribution of *M. spixiana* is restricted

to Tocantins and Minas Gerais states (Figure 3I). However, the associated bivalve-shaped galls in *M. sericantha* and *M. spixiana* are recorded only in Tocantins state (Santos-Silva 2013).

Mimosa scabrella and *M. itatiaiensis* are endemic to the Atlantic Forest (Figures 4A-B). The distribution of *M. scabrella* covers Minas Gerais, Rio de Janeiro, and São Paulo states, and all of the states in South Brazil (Figure 4A). The associated asymmetrical leaf galls induced by Cecidomyiidae are reported only in Rio Grande do Sul state (Toma & Mendonça-Júnior 2013). The distribution of *M. itatiaiensis* is restricted to Minas Gerais and Rio de Janeiro states with possible occurrences in São Paulo state (Figure 4B), and their globoid bud galls are reported for Rio de Janeiro state (Maia & Mascarenhas 2017). *Mimosa cerifera* is only known from one locality in Rio Grande do Sul state in the *Pampa* (Silveira et al. 2019), where associated galls are also reported (Figure 4C).

According to the red list of IUCN, *M. bimucronata, M. gemmulata, M. itatiaiensis, M. ophthalmocentra, M. sericantha,* and *M. tenuiflora* belong to the Least Concern (LC) category, which is the category of *M. caesalpiniifolia* in the Reflora list. A taxon is at the Least Concerned category when it has been evaluated against the red list criteria and does not qualify for Critically Endangered, Endangered, Vulnerable or Near Threatened (IUCN 2021). The conservation status of the other species is included in the category of data deficient (DD), and was not evaluated by the two lists. A taxon in this category may be well studied, and its biology well known, but appropriate data on its abundance and/or distribution to make a direct, or indirect, assessment of its risk of extinction are lacking (IUCN 2021). Despite the conservation status, many species are endemic to the *Caatinga, Cerrado,* and Atlantic Forest, where most of the *Mimosa* spp. hosting galls occur. The endemism can extend to their associated gall inducers, whose species are mostly unknown to science. In addition, the *Cerrado* and the Atlantic Forest are considered hotspots of biological diversity in the world (Colombo & Joly 2010, Ribeiro et al. 2011, Sano et al. 2019), and the *Caatinga* is an exclusively Brazilian biome (Silva et al. 2017a). The biological diversity can also be enhanced by the occurrence of the super-host species, *M. melanocarpa* and *M. incana* in the Atlantic Forest, *M. gemmulata* in the *Cerrado,* and *M. tenuiflora* in the *Caatinga*, which support several species of galling herbivores in brazilian phytogeographic domains. For these reasons, the conservation of the environments where the host plant-galling insect systems involving endemic or super-host species must be considered.

2. Ecological traits

Most of the *Mimosa* spp. are shrubs (n = 9), the life-form reported for *M. cerifera, M. coruscocaesia, M. gemmulata, M. incana, M. itatiaiensis, M. pseudosepiaria, M. polycarpa, M. tweedieana,* and *M. verrucosa*. The subshrub / shrub life-forms (5) comprise the species: *M. hypoglauca, M. melanocarpa, M. sensitiva, M. spixiana* and *M. somnians,* and the shrub / tree (4) life-form have been reported for *M. bimucronata, M. caesalpiniifolia, M. ophthalmocentra,* and *M. sericantha*. The tree life-form comprises *M. scabrella,* and *M. tenuiflora* (n = 2), and herbs / subshrubs comprise just for *M. candollei* (1).

The synchrony between the host plant phenology and the gall induction depends on the capacity of the young host tissues to respond to the gall-inducing stimuli (Weis et al. 1988). The phenological synchronism with host young tissues is determinant to the quality and quantity of resources for the gall-inducing insects, being vital

for their survival (Yukawa & Akimoto 2006, Yukawa 2000). The vegetative phenological patterns of seven species out of the 21 *Mimosa* spp. are reported. *Mimosa tenuiflora* and *M. verrucosa* are deciduous species in *Caatinga* environments (Lima & Rodal 2010, Silva et al. 2017b). Commonly, the deciduous species have a small window of opportunity for the synchrony of the gall-inducing insects, because the leaf sprouting occurs at a specific time throughout the year (Oliveira et al. 2016) and it is probable that the associated gall inducers on *M. tenuiflora* and *M. verrucosa* have univoltine life cycles. In the semi-deciduous *M. gemmulata*, the multivoltine life cycles of five associated *Lopesia* inducers have been demonstrated (Costa et al. 2021a). The success of the multivoltine life cycles is due to the occurrence of leaf sprouting throughout the year, which promotes windows of opportunity for gall induction. In addition, the phenological strategy of asynchronism of the periods of gall inductions among the five *Lopesia* spp. prevents their overlapping (Costa et al. 2021a). In the *M. scabrella* perennial species (Carpanezzi et al. 1988), the induction site may be available throughout the year, and consequently the synchronism with univoltine or multivoltine gall-inducing insects may occur. The deciduous or semi-deciduous habits of *M. caesalpiniifolia, M. bimucronata*, and *M. ophthalmocentra*, which depend on the environmental conditions where the plants occur (Carvalho 2004, Lima & Rodal 2010, Holanda et al. 2019), may relate to univoltine or multivoltine life cycles for their associated gall-inducing insects.

Several hypotheses that involve ecophysiological processes in responses to abiotic and biotic stimuli are proposed for gall color diversity. The galls on *Mimosa* spp. can be brown (16), green (n5), red (2), orange (1), and yellow (1). Despite the galls usually present low chlorophyll content and low photosynthetic activity, the green galls are related to the chlorophyll in the parenchyma cells (Carneiro et al. 2014, Rezende et al. 2018, Martini et al. 2020). The breakdown, mobilization, and recycling of the chlorophylls for the other plant organs occur in different green plant tissues during leaf senescence and in ripening fruits (Buchanan-Wollaston et al. 2003, Guyer et al. 2014). This ecophysiological process may be involved in the color change from green to brown along gall senescence, which is reported for *M. gemmulata, M. melanocarpa, M. sericantha,* and *M. tenuiflora* galls. In some galls, the color change from red to green is related to the reduction of total anthocyanin content in green galls, due to the decrease in galling stimuli, and its premature death by the interference of parasitoids and inquilines (Dias et al. 2013). The red galls may also be related to the accumulation of anthocyanins to protect the gall inducers against natural enemies (Inbar et al. 2010), or to the protection of the gall tissues (Bonfim et al. 2019). The anthocyanin accumulation in gall tissues may be a photoprotective strategy, maintaining tissue vitality in regions exposed to high light conditions as the *Cerrado* environment (Bonfim et al. 2019). In this respect, the bivalve-shaped galls on *M. ophthalmocentra* (Figures 3F, 5H-I) can be an excellent model to test the hypotheses about the function of the red galls in the *Caatinga* environment. Thus, the *Mimosa* galls are good study models to highlight the cause and effect of the colors.

3. The patterns of galls

A total of 35 gall morphospecies associated with 21 *Mimosa* spp. with variable shapes, and induction organs are reported in the consulted literature (Table 1, Figures 5-6). The galls are mainly bivalve-shaped (10), followed by the globoid (9), and the fusiform (9) morphotypes. One gall is clavate, and two galls are asymmetrical structures. The shapes of the three gall systems are not reported because they are herbarium data, and the three-dimensional observation of the structure is not possible. It is the first time that the bivalve-shaped morphotype is

reported as one of the main gall morphotypes, and its development seems to be related to the feeding site of the gall inducer, the pinna-rachis of the compound leaves of *Mimosa*. The bivalve-shaped galls are induced mainly in the pinna-rachis (6), but also occur in buds (2) or inflorescences (2), and are reported for *M. gemmulata, M. tenuiflora, M. spixiana,* and *M. sericantha*. The globoid galls are induced on buds (3), leaves (3), and stems (3) of *Mimosa* spp., and may be induced by several *taxa* on several host plant *taxa* in different biomes in Brazil. The globoid is the most common gall morphotype reported in the literature (Julião et al. 2002, Santos et al. 2011, Ascendino & Maia 2018), followed by the fusiform galls, which occur on stems of *Mimosa* (7) and are less frequent on buds or leaves. The fusiform galls may be induced by Diptera, Coleoptera or Lepidoptera, and are common in stems, petioles, and in extralaminar position of leaves, where they generally occur in midribs (Isaias et al. 2013). Fusiform galls induced by Cecidomyiidae species are reported on the stems of *M. hypoglauca*, *M. melanocarpa*, *M. scabrella,* and *M. somnians*. *Mimosa gemmulata* hosts fusiform stem galls induced by Lepidoptera, and *M. tenuiflora* also hosts stem fusiform galls, but induced by Coleoptera-Curculionidae.

4. Gall-inducing insects and associated insect guilds

The six orders of insects that evolved the galling habit are the Coleoptera, Diptera, Hemiptera, Hymenoptera, Lepidoptera, and Thysanoptera (Mani 1964, Ferreira et al. 2019). The gall-inducers associated with *Mimosa* spp. belong to three of these orders, and only about 69% were determined (22). The Cecidomyiidae is the main family of gall-inducers in the world associated with different plant *taxa* (Raman 2007, Gagné & Jaschhof 2017, Maia 2021), as is true for *Mimosa*, which hosts 18 Diptera-Cecidomyiidae, i.e., about 82% of the gall inducers. The Coleoptera (2) and the Lepidoptera (2) comprise about 9%, each, of the gall inducers associated with *Mimosa* spp. The genera of nine and the species of three gall-inducing Cecidomyiidae are known to science. One undetermined *Contarinia* sp. induces fusiform galls on the buds of *M. bimucronata* (Oliveira & Maia 2005). The *Lopesia pernambucensis* Maia, 2010, and the *L. mimosae* Maia, 2010 induce bivalve-shaped galls on *M. tenuiflora* (Maia et al. 2010). In addition, five different undetermined *Lopesia* spp. induce galls on *M. gemmulata* pinna-rachis, four are bivalve-shaped, and one is clavate (Costa et al. 2021a, b). The *Schizomyia mimosae* Tavares 1925 induces gall on *M. caesalpiniifolia* (Gagné & Jaschhof 2017).

The galls are differentiated microhabitats for gall-inducing organisms and for many associated insect guilds, because of their nutrient richness (Luz et al. 2019) and protective tissues (Mani 1964, Stone & Schönrogge 2003). These associated guilds can be divided into organisms that interact primarily with gall structure and can interact secondarily with the inducer, which can be inquilines, cecidophages, and successors. The other groups of organisms are those that interact directly with the inducer, which can be predators, parasitoids, symbionts, and kleptoparasites (Luz et al. 2019). Insect guilds associated with galls are reported on *M. ophthalmocentra,* and on two super-hosts, *M. gemmulata* and *M. melanocarpa.* The Hymenoptera parasitoids are reported on the bivalve-shaped galls induced by Cecidomyiidae on the *M. ophthalmocentra* leaflets (Costa 2016). In *M. melanocarpa,* Hemiptera inquilines are reported on the Lepidoptera-induced stem fusiform galls, while Hymenoptera parasitoids are reported on the Cecidomyiidae-induced leaf globoid galls (Maia & Mascarenhas 2017). Hymenoptera parasitoids are associated with six galls on *M. gemmulata*, but only two of these parasitoids were identified at genus level: *Eupelmus* sp. (Eupelmidae) parasitize the lenticular bivalve-shaped, the green lanceolate bivalve-shaped, and the brown lanceolate bivalve-shaped galls, *Torymus* sp. (Torymidae) parasitize the *Lopesia* larvae of

the clavate and globoid bivalve-shaped gall morphotypes (Nogueira et al. 2016, Costa et al. 2021a). In the guild of successors, Collembola can be found in the brown lanceolate bivalve-shaped galls (Costa et al. 2014). The entry of the associated insect guilds can result in changes in the morphological, anatomical, cytological, and histochemical traits of the galls (Brooks & Shorthouse 1998, Stone & Schönrogge 2003, Rezende et al. 2019, 2021). Thus, the two super-hosts, *M. melanocarpa* and *M. gemmulata*, indicate potential gall systems for ecological, structural, and chemical studies involving host-plant, gall-inducing, and associated insect guilds.

5. *Anatomical traits*

Leaf anatomical traits are reported in five *Mimosa* spp.: *M. caesalpiniifolia*, *M. bimucronata*, *M. gemmulata*, *M. hypoglauca*, and *M. tenuiflora* (Table 3). The leaflets of *M. caesalpiniifolia* and *M. hypoglauca*, as well as the pinnulae of *M. gemmulata* and *M. tenuiflora* are amphistomatic, with generally paracitic (*M. caesalpiniifolia* and *M. tenuiflora*) or anisocytic (*M. gemmulata*) stomata. The epidermis is uniseriate in all the five *Mimosa* spp., and mucilaginous epidermal cells occur in *M. tenuiflora* and *M. caesalpiniifolia* (Mattos-Filho 1971, Barros 2010). In *Lopesia* galls on *M. tenuiflora*, the epidermis is uniseriate, but the mucilaginous epidermal cells are not observed. In addition, the trichome typology is varied and has been studied in seventeen species (Table 4) with high importance for understanding the taxonomy of the genus *Mimosa* (Simon et al. 2011, Santos-Silva et al. 2013, Jordão et al. 2020). This diversity is also evidenced in the galls, for among the 32 galls, 23 have trichomes covering the structure (Table 1, Figures 5-6). The diversity and overdifferentiation of the trichomes covering the galls may be determined by the epidermal potentialities in the sites of gall development (Amorim et al. 2017, Arriola & Isaias 2021), like leaflets, pinnula, and pinna-rachis of the host *Mimosa* spp.. In *M. caesalpiniifolia* trichomes, as well as cuticles, and mucilaginous epidermal cells are involved in the foliar water uptake in the *Caatinga* environment, improving the leaf water status (Holanda et al. 2019). The diversity of trichome types and the water uptake process can be explored in the development of leaf galls, mainly, in xeric environments, such as those of the *Caatinga* and the *Cerrado*, where most of the species of *Mimosa* occur.

The mesophyll is dorsiventral in the five *Mimosa* spp. studied up to the moment, with variations of 1-4-layered palisade parenchyma, and 1-6-layered spongy parenchyma (Table 3). Peculiarly, in the palisade and spongy parenchyma of *M. hypoglauca* brachysclereids are diffusely distributed (Mendes et al. 2021), while in the palisade and spongy parenchyma of *M. tenuiflora* and *M. gemmulata*, crystalliferous inclusions occur (Barros 2010, Costa et al. 2018, Nogueira et al. 2018). The ground tissue system of the galls induced by *Lopesia* spp. on *M. tenuiflora* and *M. gemmulata* pinna-rachis is altered from the pinnula dorsiventral arrangement toward the homogenous parenchyma (Nogueira et al. 2018, Costa et al. 2021b). The new structural-functional trait may help to avoid desiccation, as large cells, with diminutive intercellular spaces may efficiently accumulate water, which may help the galls to tolerate the hydric stress of the *Caatinga* (Nogueira et al. 2018). The tissue compartments of the galls also accumulate energetic resources as proteins, lipids, and carbohydrates for the feeding of *Lopesia* larvae, and maintenance of gall structure (Nogueira et al. 2018, Costa et al. 2021b). The calcium oxalate crystals accumulate in the homogenous parenchyma cells of young galls on *M. gemmulata*, which are indicative of the high metabolic activity of young cells during the development of the gall, and can also protect the gall inducer against natural enemies (Costa et al. 2018).

The vascular bundles have collateral arrangement as a common anatomical trait in the five *Mimosa* spp. (Table 3), which is a conservative trait in the galls on *M. tenuiflora*, and *M. gemmulata* (Nogueira et al. 2018, Costa et al. 2018, 2021b). Peculiarly, the collateral vascular bundles are surrounded by pericyclic fibers with crystalliferous inclusions in *M. caesalpiniifolia*, *M. bimucronata*, *M. gemmulata*, and *M. tenuiflora*, while the laticifers are peculiar anatomical traits in the phloem region in *M. caesalpiniifolia*.

6. Chemical traits

The main chemical traits of the *Mimosa* genus relate to the secondary metabolites, including the tryptophan-derivative alkaloids, terpenoids (diterpenes and triterpenes), saponins, phenolic acids, lignans, and flavonoids (De Moraes et al. 1990, Monção et al. 2015, 2019, Bezerra et al. 2021). The chemical composition of the secondary metabolites of eight *Mimosa* hosting galls has been studied, and the other fourteen species have no data in the consulted literature (Table 5). Alkaloids, phenolic compounds, flavonoids, and terpenoids have been reported for *M. bimucronata*, *M. scabrella*, and *M. tenuiflora*, while flavonoids, phenolic compounds, and terpenoids have been reported for *Mimosa caesalpiniifolia*, and *M. gemmulata*. For *M. verrucosa* has been reported for flavonoids and phenolic compounds, while for *M. ophthalmocentra* and *M. somnians* only alkaloids have been reported. In the host plant-galling insect interactions, the phenolic compounds, flavonoids, terpenoids, and alkaloids have been mainly associated with the protection of galling organisms against natural enemies (Stone & Schönrogge 2003), and with the scavenging of oxidative stressing molecules in gall tissues (Isaias et al. 2015). In addition, the phenolic compounds and flavonoids associated with auxins are related to gall development (Bedetti et al. 2017, 2018, Kuster et al. 2019). The several chemical traits in the host *Mimosa* spp., mainly of flavonoid profile, indicate the genus as an excellent group to deepen the understanding of the dynamics and function of the secondary metabolites in the development, and adaptability of galls in the diverse environments where *Mimosa* occurs. In *M. tenuiflora*, the accumulation of phenolic compounds may be associated with the stress of high insolation and low pluviosity of the *Caatinga* environment, in addition these secondary metabolites may adjust the microenvironment of the gall favoring the gall inducing *Lopesia* (Nogueira et al. 2018). The terpenes and alkaloids that are common in *M. tenuiflora* (Bezerra et al. 2021), and in the galls may enhance the potential chemical protection (Nogueira et al. 2018).

Conclusion

The review of the *Mimosa* spp. and their associated galling-insects demonstrates that their host plant-gall inducer systems have a great potential for future studies involving ecological, anatomical, chemical and physiological aspects. Such potential is supported by the high degree of endemism of the *Mimosa* spp., together with their different phenological strategies, and diversity of anatomical and chemical traits. Special attention can be directed to the super-host species, *M. gemmulata*, *M. tenuiflora*, *M. incana* and *M. melanocarpa*, which respond to the stimuli of different galling insects. In addition, the conservation of environments such as the *Caatinga*, *Cerrado* and Atlantic Forest, where the endemic species of *Mimosa* and those with restricted distribution occur, also imply in the conservation of the gall inducers and the associated guild, which are mostly unknown to science.

Acknowledgments

We thank the Neotropical Gall Group for the reading and critical suggestions on the manuscript. We also thank *Coordenação de Aperfeiçoamento de Pessoal de Nível Superior* – Brazil (CAPES) – Finance Code 001. We also thank *Conselho Nacional de Desenvolvimento Científico e Tecnológico* (CNPq) for the research scholarships to R.M.S. Isaias (304335/2019-2) and D.C. Oliveira (304981/2019-2). E.C. Costa (888877.199702/2018-00) was financially supported by the *Coordenação de Aperfeiçoamento de Pessoal de Nível Superior* (CAPES) – Brazil– Finance Code 001.

Author Contributions

Elaine Cotrim Costa: substantial contribution in the concept and design of the study, data collection, data analysis and interpretation, manuscript preparation, critical revision, adding intellectual content.

Denis Coelho de Oliveira: data analysis and interpretation, manuscript preparation, critical revision, adding intellectual content.

Rosy Mary dos Santos Isaias: substantial contribution in the concept and design of the study, data collection, data analysis and interpretation, manuscript preparation, critical revision, adding intellectual content.

Conflicts of Interest

The authors declare that they have no conflict of interest related to the publication of this manuscript.

References

AMARIZ, I.A., PEREIRA, E.C.V., FILHO, J.M.T.A., SILVA, J.P., SOUZA, N.A.C., OLIVEIRA, A.P., ROLIM, L.A. & PEREIRA, R.N. Chemical study of *Mimosa tenuiflora* barks. 2020. Nat. Prod. Res. 1-5.

AMORIM, D.O., FERREIRA, B.G. & FLEURY, G. 2017. Plant potentialities determine anatomical and histochemical diversity in *Mikania glomera*ta Spreng. Galls. Braz. J. Bot 40:517-527.

ARRIOLA, I.A. & ISAIAS, R.M.S. 2021. Extending the knowledge on the histological patterns of leaf galls induced by *Ditylenchus gallaeformans* (Nematoda) on *Miconia* (Melastomataceae) hosts. Flora 274:1-11.

ASCENDINO, S. & MAIA, V.C. 2018. Insects galls of Pantanal areas in the State of Mato Grosso do Sul, Brazil: characterization and occurrence. An. Acad. Bras. Ciênc. 90(02):1543-1564.

BARNEBY, R.C. 1991. Sensitivae censitae: A description of the genus *Mimosa* Linnaeus (Mimosaceae) in the New World. Mem. N. Y. Bot. Gard. 65: 1-835.

BARROS, F.S. 2010. Anatomia ecológica foliar de espécies da Caatinga. Dissertação de Mestrado, Universidade Federal do Ceará, Ceará.

BATISTA, L.M. & DE ALMEIDA, R.N.1997. Central effects of the constituents of *Mimosa ophthalmocentra* Mart. ex Benth. Acta farm. bonaer. 16: 83-86.

BATISTA L.M., ALMEIDA, R.N., DA-CUNHA, E.V.L, DA-SILVA, M.S. & BARBOSA-FILHO, J.M. 1999. Isolation and Identification of Putative Hallucinogenic Constituents from the Roots of *Mimosa ophthalmocentra*. Pharm. Biol. 37(1)50-53.

BAUTISTA, E. CALZADA, F. ORTEGA, A. & YÉPEZ-MULIA, L. (2011). Antiprotozoal Activity of Flavonoids Isolated from *Mimosa tenuiflora* (Fabaceae-Mimosoideae). J. Mex. Chem. Soc. 55(4):251-253.

BEDETTI, C.S., BRAGANÇA, G.P., MODOLO, L.V. & ISAIAS, R.M.S. 2017. Influence of auxin and phenolic accumulation on the patterns of cell differentiation in distinct gall morphotypes on *Piptadenia gonoacantha* (Fabaceae).Aust. J. Bot. 65(5): 411-420.

BEDETTI, C.S., JORGE, N.C., TRIGUEIRO, F., BRAGANÇA, G.P., MODOLO, L.V. & ISAIAS, R.M.S. 2018. Detection of cytokinins and auxin in plant tissues using histochemistry and immunocytochemistry. Biotech. Histochem. 93(2):1-6.

BEZERRA, J.J., PINHEIRO, A.A.V. & LUCENA, R.B. 2021. Phytochemistry and teratogenic potential of *Mimosa tenuiflora* (willd.) poir. (Fabaceae) in ruminants: A systematic review. (195):78-85.

BOMFIM, P.M.S., CARDOSO, J.C.F., REZENDE, U.C., MARTINI, V.C. & OLIVEIRA, D.C. 2019. Red galls: the different stories of two gall types on the same host. Plant Biol. 21(2):284-291.

BRITO, G.P., COSTA, E.C., CARVALHO-FERNANDES, S.P. & SANTOS-SILVA, J. 2018. Riqueza de galhas de insetos em áreas de Caatinga com diferentes graus de antropização do estado da Bahia, Brasil. Iheringia Ser. Zool. 108: e2018003.

BROOKS, S.E. & SHORTHOUSE, J.D. 1998. Developmental morphology of stem galls of *Diplolepis nodulosa* (Hymenoptera: Cynipidae) and those modified by the inquiline *Periclistus pirata* (Hymenoptera: Cynipidae) on *Rosa blanda* (Rosaceae). Can. J. Bot. 76(3):365-381.

BUCHANAN-WOLLASTON, V., EARL, S., HARRISON, E., MATHAS, E., NAVABPOUR, S., PAGE, T. & PINK., D. 2003. The molecular analysis of leaf senescence – a genomics approach. Plant Biotechnol. J. 1(1):3-22.

CARNEIRO, R.G.S., CASTRO, A.C. & ISAIAS, R.M.S. 2014. Unique histochemical gradients in a photosynthesis-deficient plant gall. S. Afr. J. Bot. 92: 97-104.

CARPANEZZI, A.A., LAURENT, J.M.E., CARVALHO, PER., PEGORARO, A., BAGGIO, A.J., ZANON, A., OLIVEIRA, E.B., LEDE, E.T., ROTTA, E., STURION, J.A.; PEREIRA, J.C.D., GRAÇA, L.R.; RAUEN, M.J., CARPANEZZI, O.T.T. & OLIVEIRA, Y.M.M. 1988. Manual Técnico da bracatinga: *Mimosa scabrella* Benth. EMBRAPA-CNPF (Documentos, 20).

CARVALHO, P.E.R. 2004. Maricá – *Mimosa bimucronata*. EMBRAPA Colombo – PR. Circular Técnica 94:1-10.

CARVALHO-FERNANDES, S.P., ALMEIDA-CORTEZ, J.S. & FERREIRA, A.L.N. 2012. Riqueza de galhas entomógenas em áreas antropizadas e preservadas de Caatinga. Rev. Árvore 36(2): 269-277.

COELHO, M.S., CARNEIRO, M.A.A. BRANCO, C. & FERNANDES, G.W. 2013. Gall-inducing insects from Serra do Cabral, Minas Gerais, Brazil. Biota Neotropica. 13(3):102-109. https://doi.org/10.1590/S1676-06032013000300013 (last access on 20/July/2021).

COLOMBO, A.F. & JOLY, C.A. 2010. Brazilian Atlantic Forest lato sensu: the most ancient Brazilian forest, and a biodiversity hotspot, is highly threatened by climate change. Braz. J. Biol. 70(3):697-708.

COSTA E.C. 2016. Galhas no Parque Estadual da Serra dos Montes Altos e Refúgio de Vida Silvestre: diversidade e desenvolvimento. Dissertação de Mestrado, Universidade do Estado da Bahia, Bahia.

COSTA, E.C., CARVALHO-FERNANDES, S.P. & SANTOS-SILVA J. 2014. Galhas de insetos em uma área de transição caatinga-cerrado no Nordeste do Brasil. Sitientibus, Sér. Ciênc. Biol. 14:1-9.

COSTA, E.C., CARNEIRO, G.S.C., SILVA-SANTOS, J. & ISAIAS, R.M.S. 2018. Biology and development of galls induced by *Lopesia* sp. (Diptera: Cecidomyiidae) on leaves of *Mimosa gemmulata* (Leguminosae: Caesalpinioideae). Aust. J. Bot. 66, 161-172.

COSTA, E.C., MARTINI, V.C., SOUZA-SILVA, A., LEMOS-FILHO, J.P., OLIVEIRA, D.C., ISAIAS, R.M.S. (2021a) How galling herbivores share a single super-host plant during their phenological cycle: the case of *Mimosa gemmulata* Barneby (Fabaceae). Trop. Ecol.

COSTA, E.C., OLIVEIRA, D.C., FERREIRA, D.K.L. & ISAIAS, R.M.S. (2021b). Structural and nutritional peculiarities related to lifespan differences on four *Lopesia* induced bivalve-shaped galls on the single super-host *Mimosa gemmulata*. Front. Plant Sci. 12:1-13.

CRUZ, M.P., ANDRADE, C.M.F., SILVA, K.O., DE SOUZA, E.P., YATSUDA, R., MARQUES, L.M., DAVID, J.P., DAVID, J.M., NAPIMOGA, M.H. & CLEMENTE-NAPIMOGA, J.T. 2016. Antinoceptive and Anti-inflammatory activities of the ethanolic extract, fractions and flavones isolated from *Mimosa tenuiflora* (Willd.) Poir (Leguminosae). PLoS One 11(3):e0150839.

DE MORAES, E.H.F., ALVARENGA, M.A. & FERREIRA, Z.M.G.S. 1990. As bases nitrogenadas de *Mimosa scabrella* Bentham. Quim. Nova, 13(4):308-309.

DIAS, G.G., MOREIRA, G.R.P., FERREIRA, B.G. & ISAIAS, R.M.S. 2013. Why do the galls induced by *Calophya duvauae* Scott on *Schinus polygamus* (Cav.) Cabrera (Anacardiaceae) change colors? Biochem. Syst. Ecol. 48:111-122.

DUTRA, V.F. & GARCIA, F.C.P. 2014. *Mimosa* L. (Leguminosae-Mimosoideae) dos campos rupestres de Minas Gerais. Brasil. Iheringia, Sér. Bot. 69(1):49-88.

DUTRA, V.F., MORALES, M., JORDÃO, L.S.B., BORGES, L.M., SILVEIRA, F.S., SIMON, M.F., SANTOS-SILVA, J., NASCIMENTO, J.G.A. & RIBAS, O.D.S. 2020. *Mimosa* in Flora do Brasil 2020. Jardim Botânico do Rio de Janeiro. Available in: <http://reflora.jbrj.gov.br/reflora/floradobrasil/FB18823>. (last access on 03/May/2021).

FABROWSKI, F.J., NAKASHIMA, T., MUÑIZ, G.I.B., MAZZA, M.C.M. & KLOCK, U. 2002. Caracterização químico-qualitativa das variedades populares da bracatinga (*Mimosa scabrella* Bentham). Boletim de Pesquisa Florestal 44:01-139.

FERREIRA, B.G., ÁLVAREZ, R., BRAGANÇA, G.P., ALVARENGA, D.R., HIDALGO, N.P. & ISAIAS, R.M.S. 2019. Feeding and other gall facets: patterns and determinants in gall structure. Bot. Rev. 85:78-106.

FERREIRA, D.M.C., AMORIM, B.S., MACIEL, J.R. & MARCCUS, A. 2016. Floristic checklist from an Atlantic Forest vegetation mosaic in Reserva Particular do Patrimônio Natural Fazenda Tabatinga, Pernambuco, Brazil. Check List 12(6):1-18.

GAGNÉ, R.J. & JASCHHOF, M. 2017. A catalog of the Cecidomyiidae (Diptera) of the world. 4rd Edition. Digital.

GARDNER, D., RIET-CORREA, F., LEMOS, D., WELCH, K., PFISTER, J., PANTER, K. 2014. Teratogenic effects of *Mimosa tenuiflora* in a rat model and possible role of *N*-methyl- and *N*,*N*- dimethyltryptamine J. Agric. Food Chem. 62(30):7398-7401.

GUPTA, M.P., ARIAS, T.D., ETHEART, J. & HATFIELD, G.M. 1979. The occurrence of tryptamine and N-methyltryptamine in *Mimosa somnians*. J. Nat. Prod. 42(2):234-236.

GUYER, L., HOFSTETTER, S.S., CHRIST, B., LIRA, B.S., ROSSI, M. & HÖRTENSTEINER, S. 2014. Different mechanisms are responsible for chlorophyll dephytylation during fruit ripening and leaf senescence in tomato. Plant Physiol. 116:44-56.

HOLANDA, A.E.R., SOUZA, B.C., CARVALHO, E.C.D., OLIVEIRA, R.S., MARTINS, F.R., MUNIZ, C.R., COSTA, R.C. & SOARES, A.A. 2019. How do leaf wetting events afect gas exchange and leaf lifespan of plants from seasonally dry tropical vegetation? Plant Biol 21(6):1097-1109.

HUANG, L-Y, MIAO S-Y, CHEN J-H, LI B-Y, LI L. 2011. Leaf anatomic structure of *Mimosa bimucronata*, Guangxi. Sciences 17.

INBAR, M., IZHAKI, I., KOPLOVICH, A., LUPO, I., SILANIKOVE, N., GLASSER, T., GERCHMAN, Y., PEREVOLOTSKY, A. & LEV- YADUN, S. 2010. Why do many galls have conspicuous colors? A new hypothesis. Arthropod Plant Interact. 4:1-6.

ISAIAS, R.M.S, CARNEIRO, R.G.S., OLIVEIRA, D.C. & SANTOS, J.C. 2013. Illustrated and annotated checklist of Brazilian gall morphotypes. Neotrop. Entomol. 42(3):230-239.

ISAIAS, R.M.S., OLIVEIRA, D.C., MOREIRA, A.S.F.P., SOARES, G.L.G. & CARNEIRO, R.G.S., 2015. The imbalance of redox homeostasis in arthropod-induced plant galls: Mechanisms of stress generation and dissipation. Biochim. Biophys. Acta 1850(8):1509-1517.

IUCN - International Union for Conservation of Nature's Red List of Threatened Species. 2021. Available on https://www.iucnredlist.org/. Accessed on 14.March.2021.

JORDÃO, L.S.B., MORIN, M.P., BAUMGRATZ, J.F.A. 2020. Trichomes in *Mimosa* (Leguminosae): towards a characterization and a terminology standardization. Flora 272:151702.

JULIÃO, G.R., AMARAL, M.E.C. & FERNANDES, G.W. 2002. Galhas de insetos e suas plantas hospedeiras no Pantanal Sul Mato-grossense. Naturalia 27(1):47-74.

KUSTER, V.C., REZENDE, U.C., CARDOSO, J.C.F., ISAIAS, R.M.S. & OLIVEIRA, D.C. 2019. How galling organisms manipulate the secondary metabolites in the host plant tissues? A histochemical overview in Neotropical gall systems. In Co-evolution of secondary metabolites. Reference series in phytochemistry. (J. Mérillon & K.G. Ramawat eds). Springer, International Publishing, p. 1-20.

LIMA, A.L.A. & RODAL, M.J.N. 2010. Phenology and wood density of plants growing in the semi-arid region of northeastern Brazil. J. Arid Environ. 74(11):1363-1373.

LUZ, F.A. & MENDONÇA JÚNIOR, M.D.S. 2019. Guilds in insect galls: who is who. Fla. Entomol. 102(1):207-210.

MAIA, V. C. 2019. Insect galls on Myrtaceae: richness and distribution in brazilian restingas. Biota Neotropica. 19(1):e20180526. https://doi.org/10.1590/1676-0611-BN-2018-0526 (last access on 20/July/2021).

MAIA, V.C. 2021. Cecidomyiidae (Diptera, Insecta): richness of species and distribution in Brazil. Biota Neotropica. 21(2):e20201038. https://doi.org/10.1590/1676-0611-BN-2020-1038 (last access on 20/July/2021).

MAIA, V.C. & MASCARENHAS, B. 2017. Insect galls of the Parque Nacional do Itatiaia (Southeast Region, Brazil). An. Acad. Bras. Ciênc. 89:505-575.

MAIA, V.C., FERNANDES, G.W., MAGALHÃES, H. & SANTOS, J.C. 2010. Two new species of *Lopesia* Rübsaamen (Diptera, Cecidomyiidae) associated with *Mimosa hostilis* (Mimosaceae) in Brazil. Rev. Bras. Entomol. 54: 578-583.

MANI, M.S. 1964. Ecology of Plant Galls. Dr. W. Junk Publishers, The Hague.

MARTINI, V., MOREIRA, A., KUSTER, V.C. & OLIVEIRA, D.C. 2020. Photochemical performance and source-sink relationships in galls induced by *Pseudophacopteron longicaudatum* (Hemiptera) on leaves of *Aspidosperma tomentosum* (Apocynaceae). Photosynthetica 58(3):827-835.

MATTOS-FILHO, A. 1971. Estudo comparativo entre duas espécies de Leguminosae latescentes do cerrado e da caatinga. Rodriguesia 26(38):9-33.

MENDES, T.P., SIMON, M.F., ALONSO, A.A. & SILVA, M.J. (2021). *Mimosa brevicalyx* (Leguminosae-Caesalpinioideae): a new species based on molecular, anatomical, and morphological data. Plant Syst. Evol. 307(32):1-19.

MENDONÇA-JÚNIOR, M.S., TOMA, T.S.P. & SILVA, J.S. 2014. Galls and Galling Arthropods of Southern Brazil. In: Neotropical Insect Galls. (G.W. Fernandes & J.C. Santos, eds). Springer, Dordrecht, p. 221-256.

MONÇÃO, N.B.N., ARAÚJO, B.Q. & CITÓ, A.M.G.L. 2019. Explorando a Química de Produtos Naturais e Propriedades Biológicas do Gênero *Mimosa* Linnaeus (Fabaceae-Mimosoideae). Rev. Virtual Quim. 11(3):970-1010.

MONÇÃO, N.B.N., ARAÚJO, B.Q., SILVA, J.N., LIMA, D.J.B., FERREIRA, P.M.P., AIROLDI, F.P.S., PESSOA, C. & CITÓ, A.M.G.L. 2015. Assessing Chemical Constituents of *Mimosa caesalpiniifolia* Stem Bark: Possible Bioactive Components Accountable for the Cytotoxic Effect of *M. caesalpiniifolia* on Human Tumour Cell Lines. Molecules 20(3):4204-4224.

MONÇÃO, N.B.N., COSTA, L.M., ARCANJO, D.D.R., ARAÚJO, B.Q., LUSTOSA, M.C.G., RODRIGUES, K.A.F., CARVALHO, F.A.A., COSTA, A.P.R. & CITÓ, A.M.G. 2014. Chemical constituents and toxicological studies of leaves from *Mimosa caesalpiniifolia* Benth., a Brazilian honey plant. Pharmacogn. Mag.10(39):456-462.

NOGUEIRA, R.M., COSTA, E.C., CARVALHO-FERNANDES, S.P. & SANTOS-SILVA, J. 2016. Insect galls from Serra Geral, Caetité, BA, Brazil. Biota Neotropica. 16(1):e20150035. https://doi.org/10.1590/1676-0611-BN-2015-0035 (last access on 20/July/2021).

NOGUEIRA, R.M., COSTA, E.C., SANTOS-SILVA, J. & ISAIAS, R.M.S. 2018. Structural and histochemical profile of *Lopesia* sp. Rübsaamen. 1908 pinnula galls on *Mimosa tenuiflora* (Willd.) Poir. in a Caatinga environment. Hoehnea 45(2):231-239.

OLIVEIRA, J.C. & MAIA, V.C. 2005. Ocorrência e caracterização de galhas de insetos na restinga de Grumari (Rio de Janeiro, RJ, Brasil). Arq. Mus. Nac. 63(4):669-675.

OLIVEIRA, D.C., ISAIAS, R.M.S., FERNANDES, G.W., FERREIRA, B.G., CARNEIRO, R.G.S. & FUZARO, L. 2016. Manipulation of host plant cells and tissues by gall-inducing insects and adaptive strategies used by different feeding guilds. J. Insect Physiol. 84:103-113.

PILATTI, D.M., FORTES, A.M.T., JORGE, T.C.M. & BOIAGO N.P. 2019. Comparison of the phytochemical profiles of five native plant species in two different forest formations. Braz. J. Biol. 79(2):233-242.

QGIS.ORG. 2020. QGIS Geographic Information System. Open Source Geospatial Foundation Project. http://qgis.org.

RAMAN, A. 2007. Insect-induced plant galls of India: unresolved questions. Current Science 92(6):748-757.

REFLORA - Herbário Virtual [continuamente atualizado]. 2020. Available on http://reflora.jbrj.gov.br/reflora/herbarioVirtual/. Accessed on 20.March.2021.

REZENDE, U.C., CARDOSO, J.C.F., KUSTER, V.C., GONÇALVES, L.A., & OLIVEIRA, D.C. 2019. How the activity of natural enemies changes the structure and metabolism of the nutritive tissue in galls? Evidence from the *Palaeomystella oligophaga* (Lepidoptera)-*Macairea radula* (Metastomataceae) system. Protoplasma 256(3):669-677.

REZENDE, U.C., FERNANDES CARDOSO, J.C., HANSON, P. & OLIVEIRA, D.C. 2021. Gall traits and galling insect survival in a multi-enemy context. Rev. Biol. Trop. 69(1):291-301.

REZENDE, U.C., MOREIRA, A.S.F.P., KUSTER, V.C. & OLIVEIRA D.C. 2018. Structural, histochemical and photosynthetic profiles of galls induced by *Eugeniamyia dispar* (Diptera, Cecidomyiidae) on the leaves of *Eugenia uniflora* (Myrtaceae). Rev. Biol. Trop. 66(4):1469-1480.

RIBEIRO, M.C., MARTENSEN, A.C., METZGER, J.P., TABARELLI, M., SCARANO, F.R., FORTIN, M-J. 2011. The Brazilian Atlantic forest: a shrinking biodiversity hotspot. In Biodiversity hotspots: distribution and protection of conservation priority areas (F.E. Zachos & J.C. Habel, eds) Springer-Verlag, Berlin, p. 405-434.

ROMANOSKI, V.S. & FONSECA SANTOS, R.A.F. 2017. Cytotoxic and Antioxidant Activity of *Mimosa verrucosa* Benth. Electron. J. Chem. 9(2):100-104.

SANO, E.E., RODRIGUES, A.A., MARTINS, E.S., BETTIOL, G.M., BUSTAMANTE, M.M.C., BEZERRA, A.S., COUTO JR. A.F., VASCONCELOS, V., SCHÜLER, J. & BOLFE, E.L. Cerrado ecoregions: A spatial framework to assess and prioritize Brazilian savanna environmental diversity for conservation. J. Environ. Manag. 235(15)818-828.

SANTOS, J.C., ALMEIDA-CORTEZ, J.S. & FERNANDES, G.W. 2011. Richness of gall-inducing insects in the tropical dry forest (Caatinga) of Pernambuco. Rev Bras Entomol 55(1):45-54.

SANTOS, M.E.P., MOURA, L.H.P., MENDES, M.B., ARCANJO, D.D.R., MONÇÃO, N.B.N., ARAÚJO, B.Q., LOPES, J.A.D., SILVA-FILHO, J.C., FERNANDES, R.M., OLIVEIRA, R.C.M., CITÓ, A.M.G.L. & OLIVEIRA, A.P. 2015. Hypotensive and vasorelaxant effects induced by the ethanolic extract of the *Mimosa caesalpiniifolia* Benth. (Mimosaceae) inflorescences in normotensive rats. J Ethnopharmacol. 164:120-128.

SANTOS-SILVA, J. & ARAÚJO, T.J. 2020. Are Fabaceae the principal super-hosts of galls in Brazil? An. Acad. Bras. Ciênc. 92(2):e20181115.

SANTOS-SILVA, J., SIMON, M.F., TOZZI & A.M.G.A. 2015. Revisão taxonômica das espécies de *Mimosa* ser. Leiocarpae sensu lato (Leguminosae - Mimosoideae). Rodriguésia 66(1):95-154

SANTOS-SILVA, J.S. 2013. Filogenia, estudos micromorfológicos e revisão taxonômica de *Mimosa* ser. Leiocarpae Benth.(Leguminosae-Mimosoideae). Tese de doutorado. Universidade Estadual de Campinas, Campinas.

SANTOS-SILVA, J., TOZZI, A.M.G.A., SIMON, M.F., URQUIZA, N.G. & MORALES, M. 2013. Evolution of trichome morphology in *Mimosa* (Leguminosae-Mimosoideae). Phytotaxa 119(1):1-20.

SCHLICKMANN, F., BOEING, T., MARIANO, L.N.B., SILVA, R.C.M.V.A.F., SILVA, L.M., ANDRADE, S.F., SOUZA, P. & CECHICEL-FILHO, V. 2018. Gallic acid, a phenolic compound isolated from *Mimosa bimucronata* (DC.) Kuntze leaves, induces diuresis and saluresis in rats. Naunyn-Schmied. Arch. Pharmacol. 391(6):649-655.

SCHLICKMANN, F., DE SOUZA, P., BOEING, T., MARIANO, L.N.B., STEIMBACH, V.M.B., KRUEGER, C.M.A., DA SILVA, L.M., DE ANDRADE, S.F. & CECHINEL-FILHO, V. 2017. Chemical composition and diuretic, natriuretic and kaliuretic effects of extracts of *Mimosa bimucronata* (DC.) Kuntze leaves and its majority constituent methyl gallate in rats. J Pharm Pharmacol 69(11):1615-1624.

SERAGLIO, S.K.T., VALESE, A.C., DAGUER, H., BERGAMO, G., AZEVEDO, M.S., NEHRING, P., GONZAGA, L.V., FETT, R. & COSTA, A.C.O. 2017. Effect of in vitro gastrointestinal digestion on the bioaccessibility of phenolic compounds, minerals, and antioxidant capacity of *Mimosa scabrella* Bentham honeydew honeys. Food Res. Int. 99(1):670-67.

SILVA, A.R., NOGUEIRA, R.M., COSTA, E.C., CARVALHO-FERNANDES, S.P. & SANTOS-SILVA, S.P. 2018. Occurrence and characterization of entomogenic galls in an area of Cerrado sensu stricto and Gallery forest of the state of Bahia, Brazil. An. Acad. Bras. Ciênc. 90(3):2903-2919.

SILVA, B., BILUCA, F.C., MOHR, E.T.B., CAON, T., GONZAGA, L.V.G., FETT, R., DALMARCO, E.M. & COSTA, A.C.O. 2020a. Effect of *Mimosa scabrella* Bentham honeydew honey on inflammatory mediators. J. Funct. Foods 72:1-7.

SILVA, J.M.C., LEAL, I.R. & TABARELLI, M. 2017a. Caatinga: the largest tropical dry forest region in South America. 1ed. Springer Nature.

SILVA, M.J.D., CARVALHO, A.J.S., ROCHA, C.Q., VILEGAS, W., SILVA, M.A. & GOUVÊA, C.M.C.P. 2014. Ethanolic extract of *Mimosa caesalpiniifolia* leaves: Chemical characterization and cytotoxic effect on human breast cancer MCF-7 cell line. S. Afr. J. Bot. 93:64-69.

SILVA, P.F., LIMA, J.R.D.S., ANTONINO, A.C.D., SOUZA, R., DE SOUZA, E.S., SILVA, J.R.I. & ALVES, E.M. 2017b. Seasonal patterns of carbon dioxide, water and energy fluxes over the Caatinga and grassland in the semi-arid region of Brazil. J. Arid Environ. 147:71-82.

SILVA, S.A.N.M., BARROS, A.B., SOUZA, J.M.T., MOURA, A.F., ARAÚJO, A.R., MENDES, M.G.A., DABOIT, T.C., SILVA, D.A., ARAÚJO, A.J., FILHO, J.D.B.M. 2020b. Phytochemical and biological prospection of *Mimosa* genus plants extracts from Brazilian northeast. Phytochem Lett.39:173-181.

SILVA, T.M.S., CAMARA, C.A., LINS, A.C.S., BARBOSA-FILHO, J.M., SILVA, E.M.S., FREITAS, B.M. & SANTOS, F.D.A.R. 2006. Chemical composition and free radical scavenging activity of pollen loads from stingless bee *Melipona subnitida* Ducke. J. Food Compos. Anal. 19(6-7):507-511.

SILVEIRA, F.S. 2015. Estudos taxonômicos em *Mimosa* L. seção *Mimosa* (Fabaceae, Mimosoideae) no Rio Grande do Sul. Dissertação de Mestrado, Universidade Federal do Rio Grande do Sul, Rio Grande do Sul.

SILVEIRA, F.S., BORDIGNON, S.A.L. & MIOTTO, S.T.S. 2019. *Mimosa cerifera*, a New Threatened Species from the Pampa Biome, Southern Brazil. Syst. Bot. 44(1):133-138.

SIMON, M.F. & PROENÇA, C. 2000. Phytogeographic patterns of *Mimosa* (Mimosoideae, Leguminosae) in the Cerrado biome of Brazil: an indicator genus of high-altitude centers of endemism? Biol. Conserv. 96(3):279-296.

SIMON, M.F., GRETHER, R., QUEIROZ, L.P., SÄRKINEN, T.E., DUTRA, V.F. & HUGHES, C.E. 2011. The evolutionary history of *Mimosa* (Leguminosae): toward a phylogeny of the sensitive plants. Am J Bot. 98(7):1201-1221.

SIMON, M.F., GRETHER, R., QUEIROZ, L.P., SKEMA, C., PENNINGTON, R.T. & HUGHES, C.E. 2009. Recent assembly of the cerrado, a neotropical plant diversity hotspot, by in situ evolution of adaptations to fire. Proc. Natl. Acad. Sci. 106(48):20359-20364.

SPECIESLINK (SPLink). 2021. Centro de Referência em Informação Ambiental (CRIA) – Fundação de Amparo à Pesquisa do Estado de São Paulo. Available on http://www.splink.org.br. Accessed on 20.May.2021.

STONE, G.N. & SCHÖNROGGE, K. 2003. The adaptive significance of insect gall morphology. Trends Ecol. Evol. 18(10):512-522.

TOMA, T.S.P. & MENDONÇA-JÚNIOR, M.S. 2013. Gall-inducing insects of an Araucaria Forest in southern Brazil. Rev Bras Entomol, 57(2):225-233.

WEIS, A.E., WALTON, R & CREGO, C.L. 1988. Reactive plant tissue sites and the population biology of gall makers. Annu Rev Entomol 33:467-486.

YUKAWA, J. 2000. Synchronization of gallers with host plant phenology. Popul Ecol 42(2):105-113.

YUKAWA, J. & AKIMOTO, K. 2006. Influence of synchronization between adult emergence and host plant phenology on the population density of *Pseudasphondylia neolitseae* (Diptera: Cecidomyiidae) inducing leaf galls on *Neolitsea sericea* (Lauraceae). Popul Ecol 48:13-21.

Figure captions

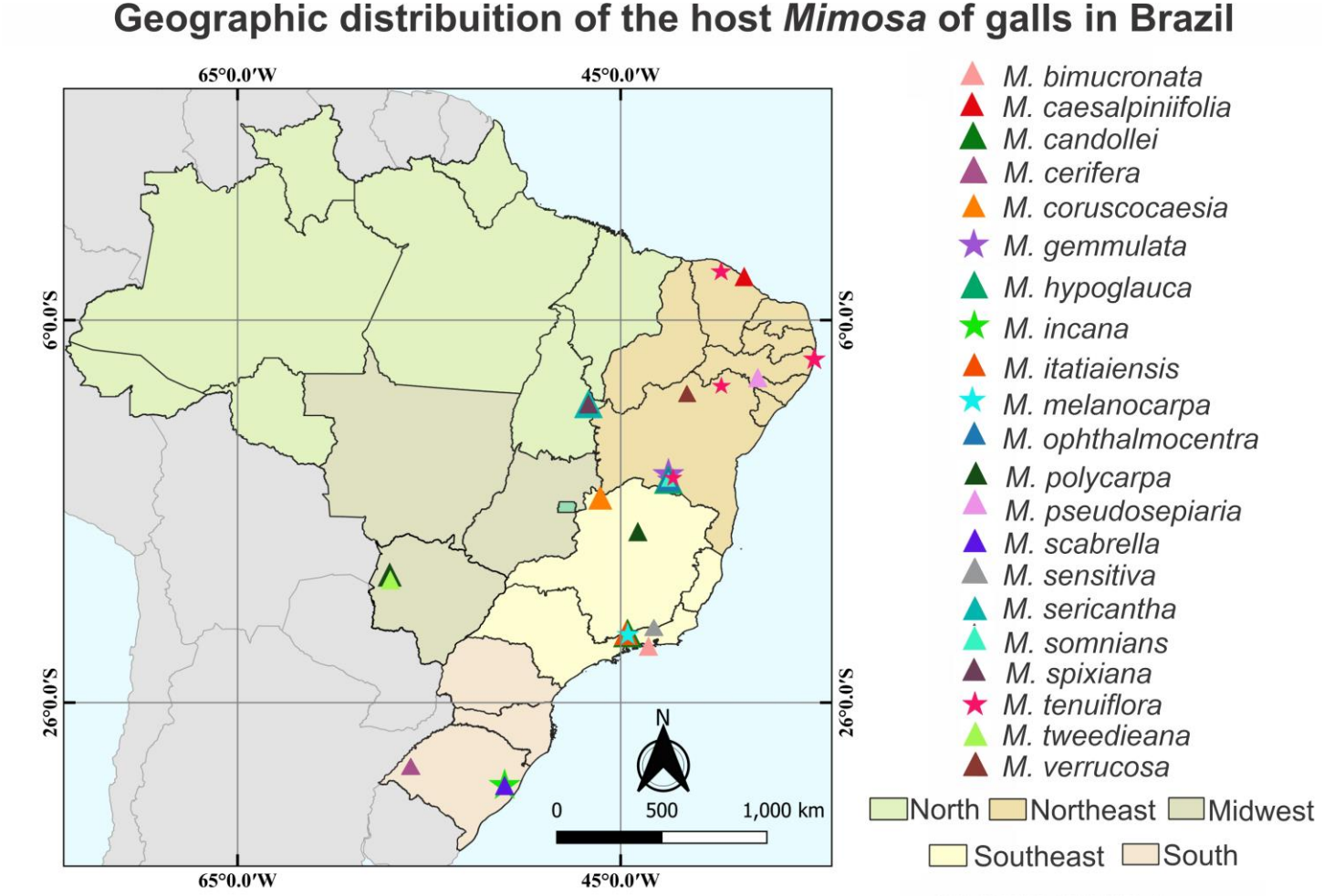

Figure 1. Geographic distribution of *Mimosa* spp. (Fabaceae) and their galls reported in Brazil. The triangles represent uni-host species, and the stars represent super-host species.

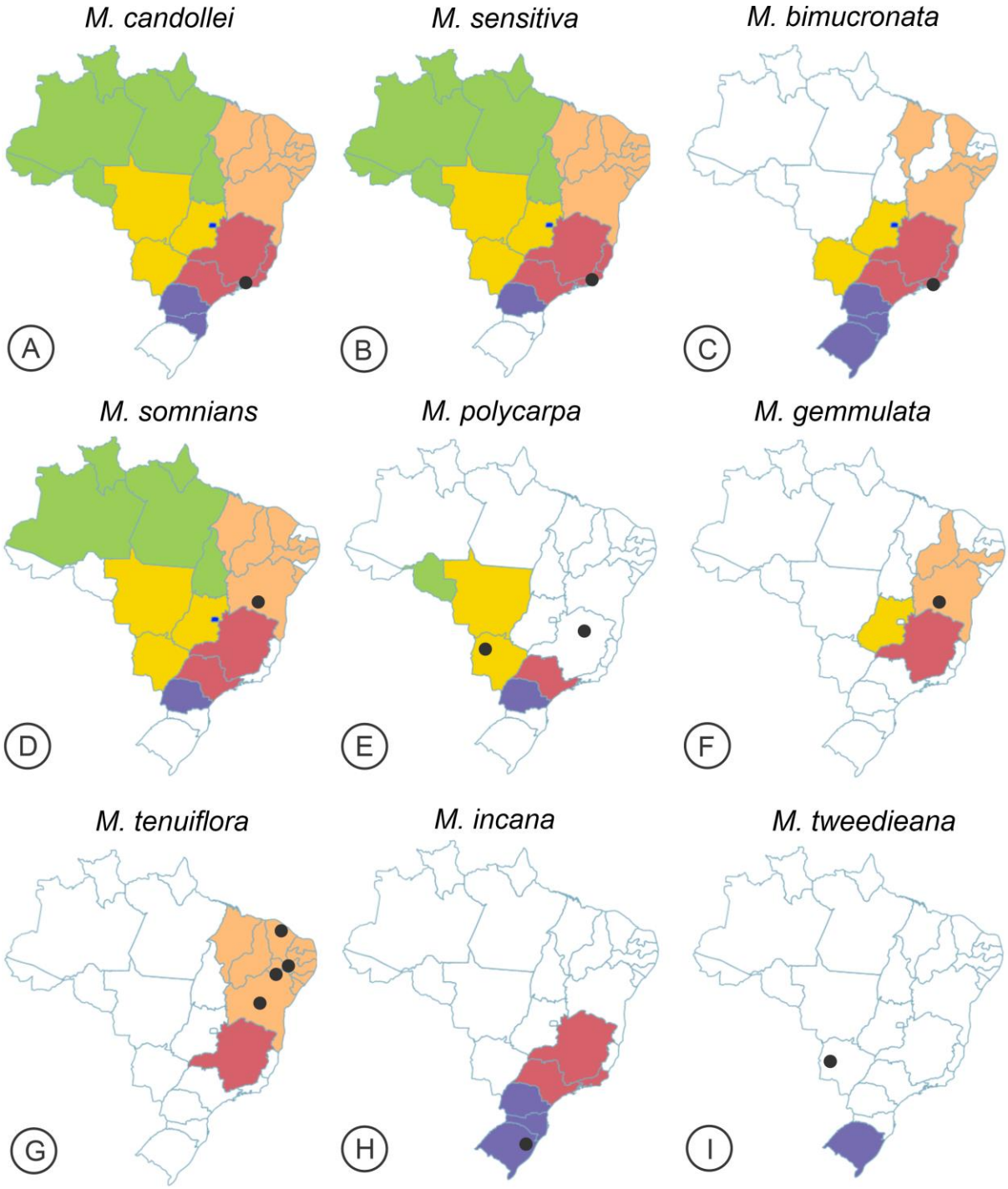

Figure 2. Current geographic distribution of some *Mimosa* spp. (Fabaceae) and their associated galls in Brazil. The colorful areas represent the geographic distribution of the host plants in Brazilian regions: green = North Region, orange = Northeast Region, red = Southeast Region, blue = South Region. The black circles represent the distribution of the galls. Maps adapted from the REFLORA, 2020.

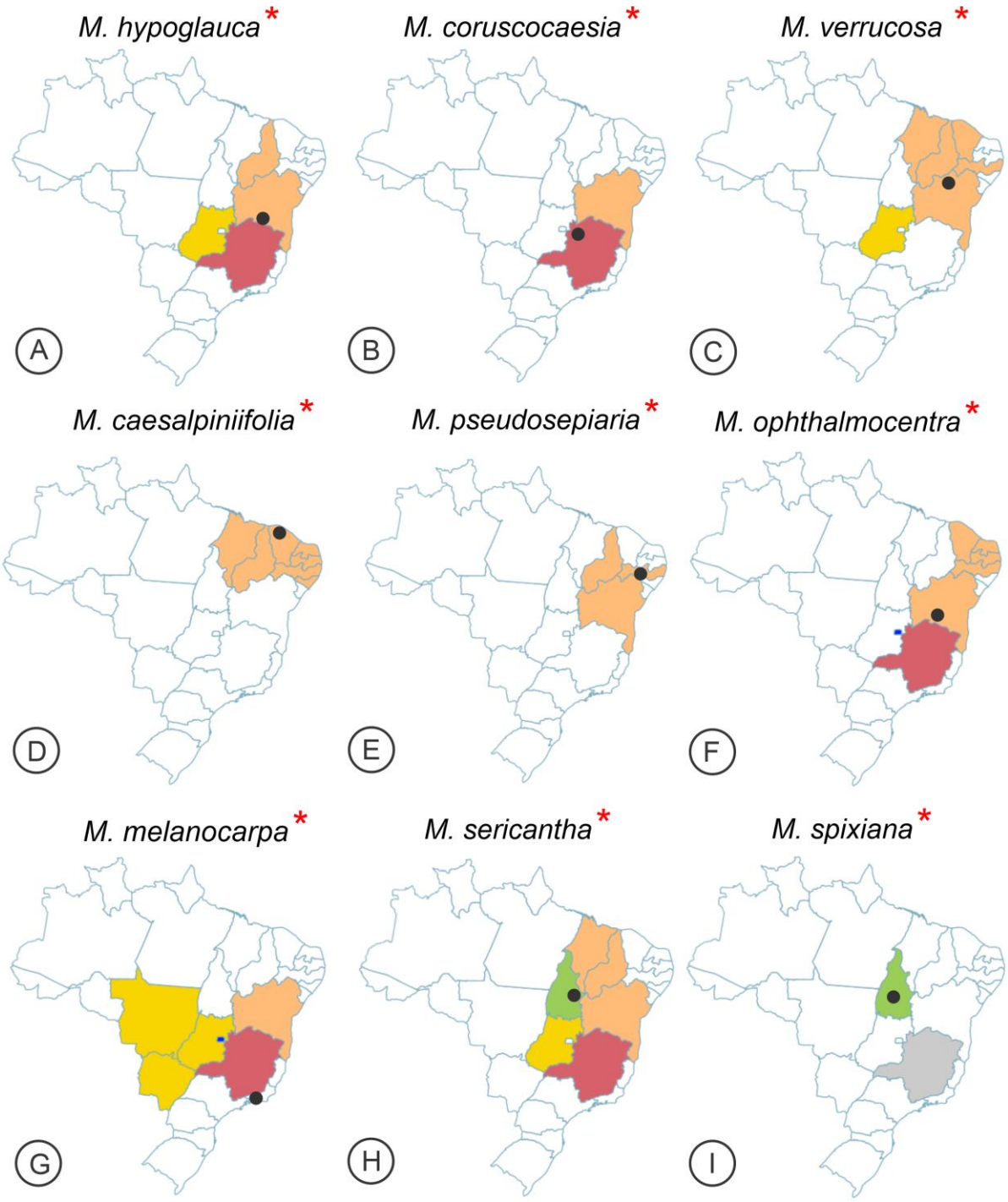

Figure 3. Current geographic distribution of some *Mimosa* spp. (Fabaceae) and their associated galls in Brazil. The colorful areas represent the geographic distribution of the host plants in Brazilian regions: green = North Region, orange = Northeast Region, red = Southeast Region, blue = South Region. The black circles represent the distribution of the galls. The red asterisks indicate endemic species. Maps adapted from the REFLORA, 2020.

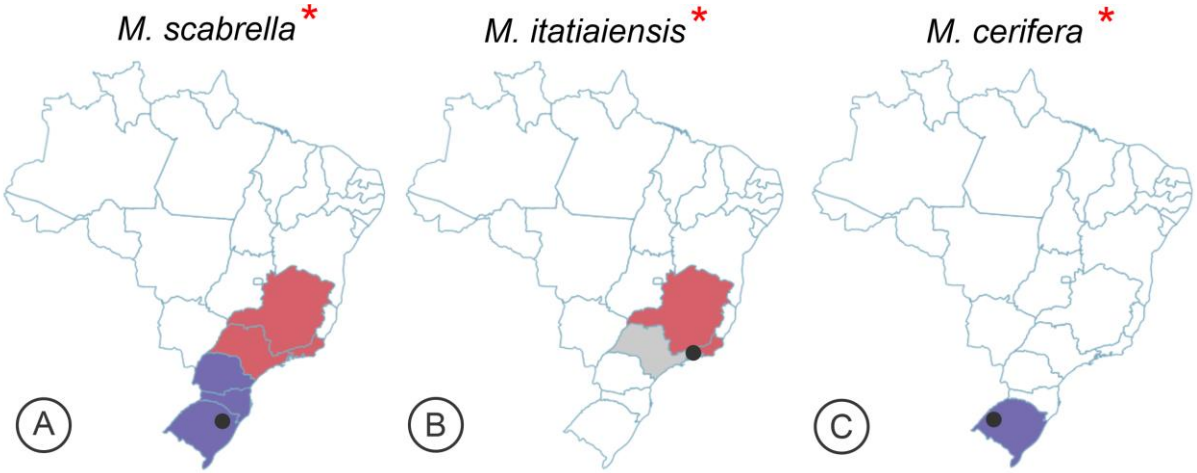

Figure 4. Current geographic distribution of some *Mimosa* spp. (Fabaceae) and their associated galls in Brazil. The colorful areas represent the geographic distribution of the host plants in Brazilian regions: green = North Region, orange = Northeast Region, red = Southeast Region, blue = South Region. The black circles represent the distribution of the galls. The red asterisks indicate endemic species. Maps adapted from the REFLORA, 2020.

Figure 5. Galls associated with *Mimosa* spp. (Fabaceae) observed in exsiccates of virtual herbaria. A. Galls on *M. gemmulata* of material from Bahia state (CEN00100529). B-C. Galls on *M. sericantha* of material from Tocantins state (CEN00052903/ CEN00041640).

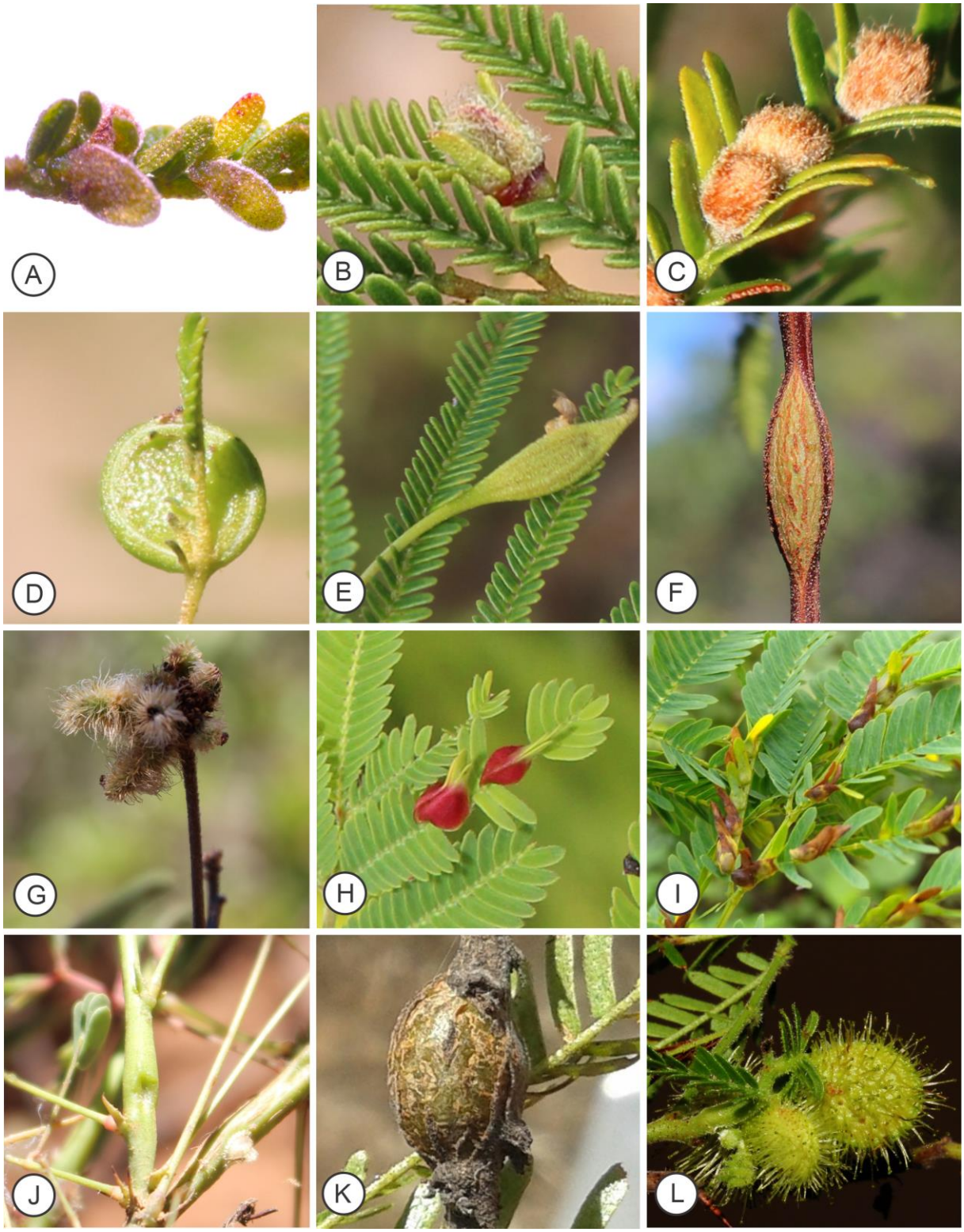

Figure 6. Gall morphotypes on *Mimosa* spp. (Fabaceae) in Brazil. A-F. Galls on *M. gemmulata.* A. Lenticular bivalve-shape gall. B. Green lanceolate bivalve-shaped gall. C. Brown lanceolate bivalve-shaped gall. D. Globoid bivalve-shaped gall. E. Clavate gall. F. Fusiform gall. G. Fusiform gall on *M. hypoglauca.* H-I. Bivalve-shaped galls on the *M. ophthalmocentra.* J. Fusiform galls on *M. somnians*. K-L. Galls on *M. tenuiflora.* K. Fusiform gall. L. Bivalve-shaped-gall.

Table 1: Literature data on *Mimosa* spp. and their galls in Brazil.

Host species	Uni/ super-host	Gall morphotype	Organ	Color	Trichomes (Yes/No)	Order and Family of inducers	Species of Gall-inducer	Literature
M. bimucronata (DC.) Kuntze	Uni-host	Fusiform	Bud	Brown	No data	Diptera-Cecidomyiidae	*Contarinia* sp.	Oliveira & Maia (2005)
M. caesalpiniifolia Benth.	Uni-host	No data	No data	No data	No data	Diptera-Cecidomyiidae	*Schizomyia mimosae* Tavares 1925	Gagné & Jaschhof (2017)
M. *candollei* R.Grether	Uni-host	Globoid	Bud	Brown	No	Undetermined	Undetermined	Maia & Mascarenhas (2017)
M. *coruscocaesia* Barneby	Uni-host	Bivalve-shaped	Leaf	Brown	Yes	Undetermined	Undetermined	Santos-Silva (2013)
M. gemmulata Barneby	Super-host	Lenticular bivalve-shaped	Pinna-rachis	Green/ brown	Yes	Diptera-Cecidomyiidae	*Lopesia* sp.	Costa et al. (2021a, b)
M. gemmulata Barneby	Super-host	Green lanceolate bivalve-shaped	Pinna-rachis	Green	Yes	Diptera-Cecidomyiidae	*Lopesia* sp.	Costa et al. (2014), Costa (2016), Costa et al. (2021a, b)
M. gemmulata Barneby	Super-host	Brown lanceolate bivalve-shaped	Pinna-rachis	Brown	Yes	Diptera-Cecidomyiidae	*Lopesia* sp.	Costa et al. (2014), Costa (2016), Costa et al. (2021a, b)
M. gemmulata Barneby	Super-host	Globoid bivalve-shaped	Pinna-rachis	Green/ black	Yes	Diptera-Cecidomyiidae	*Lopesia* sp.	Costa et al. (2014), Costa (2016), Costa et al. (2021a, b)
M. gemmulata Barneby	Super-host	Clavate	Pinna-rachis	Green/ brown	Yes	Diptera-Cecidomyiidae	*Lopesia* sp.	Costa (2016),
M. gemmulata Barneby	Super-host	Fusiform	Stem	Green/ brown	No	Lepidoptera	Undetermined	Costa et al. (2014), Costa (2016)
M. hypoglauca Mart.	Uni-host	Fusiform	Bud/ Leaf	Brown	Yes	Diptera-Cecidomyiidae	Undetermined	Costa (2016)
M. incana Benth.	Super-host	Fusiform	Stem	Brown	No	Undetermined	Undetermined	Mendonça-Júnior et al. (2014)
M. incana Benth.	Super-host	Globoid	Leaf	Green	Yes	Undetermined	Undetermined	Mendonça-Júnior et al. (2014)
M. itatiaiensis Dusén	Uni-host	Globoid	Bud	Brown	Yes	Undetermined	Undetermined	Maia & Mascarenhas (2017)
M. melanocarpa Benth.	Super-host	Fusiform	Stem	Brown	No	Undetermined	Undetermined	Maia & Mascarenhas (2017)
M. melanocarpa Benth.	Super-host	Fusiform	Stem	Green/ brown	Yes	Diptera-Cecidomyiidae	Undetermined	Maia & Mascarenhas (2017)
M. melanocarpa Benth.	Super-host	Globoid	Bud/ Leaf	Yellow	Yes	Diptera-Cecidomyiidae	Undetermined	Maia & Mascarenhas (2017)
M. melanocarpa Benth.	Super-host	Globoid	Leaf	Brown	No	Undetermined	Undetermined	Maia & Mascarenhas (2017)
M. ophthalmocentra Mart ex. Benth.	Uni-host	Bivalve-shaped	Leaflet	Red	Yes	Diptera-Cecidomyiidae	Undetermined	Costa (2016)

M. polycarpa Kunth	Uni-host	Globoid	Leaf	Green	Yes	Diptera-Cecidomyiidae	Undetermined	Coelho et al. (2013)
M. polycarpa Kunth	Uni-host	Globoid	Stem	Brown	Yes	Coleoptera	Undetermined	Julião et al. (2002)
M. pseudosepiaria Harms	Uni-host	Amorphous	Stem	Brown	No	Diptera-Cecidomyiidae	Undetermined	Carvalho-Fernandes et al. (2012)
M. scabrella Benth.	Uni-host	Amorphous	Leaf	Orange	Yes	Diptera-Cecidomyiidae	Undetermined	Toma & Mendonça-Júnior (2013)
M. scabrella Benth.	Uni-host	Fusiform	Stem	Brown	No	Diptera-Cecidomyiidae	Undetermined	Mendonça-Júnior et al. (2014)
M. sericantha Benth.	Uni-host	Bivalve-shaped	Bud/ Leaf/Inflorescence	Green/ Brown	Yes	Undetermined	Undetermined	Santos-Silva (2013)
M. somnians Humb. & Bonpl. ex Willd.	Uni-host	Fusiform	Stem	Brown	Yes	Diptera-Cecidomyiidae	Undetermined	Costa (2016)
M. spixiana Barneby	Uni-host	Bivalve-shaped	Bud/ Leaf/Inflorescence	Brown	Yes	Undetermined	Undetermined	Santos-Silva (2013)
M. tenuiflora (Willd.) Poir.	Super-host	Bivalve-shaped	Pinna-rachis	Green/ Brown	Yes	Diptera-Cecidomyiidae	*Lopesia pernambucensis* Maia, 2010	Maia et al. (2010), Santos et al. (2011), Carvalho-Fernandes et al. (2012), Brito et al. (2018)
M. tenuiflora (Willd.) Poir.	Super-host	Bivalve-shaped	Pinna-rachis	Green/ Black	Yes	Diptera-Cecidomyiidae	*Lopesia mimosae* Maia, 2010	Maia et al. (2010), Santos et al. (2011), Nogueira et al. (2018)
M. tenuiflora (Willd.) Poir.	Super-host	Fusiform	Stem	Brown	No	Coleoptera-Curculionidae	Undetermined	Brito et al. (2018)
M. tenuiflora (Willd.) Poir.	Super-host	Globoid	Stem	Brown	No	Lepidoptera	Undetermined	Carvalho-Fernandes et al. (2012)
M. tweedieana Barneby ex Glazier and Mackinder	Uni-host	Globoid	Stem	Red	Yes	Undetermined	Undetermined	Ascendino & Maia (2018)

Table 2: Herbarium data of *Mimosa* spp. and their galls in Brazil.

Host species	Uni/ super-host	Gall morphotype	Organ	Trichomes (Yes/No)	Herbarium/ voucher specimens	Plant collector/ year
M. cerifera Schmidt Silveira & Miotto*	Uni-host	-	Leaflet	Yes	CEN00113496	Fernanda Schmidt-Silveira, 2017
M. gemmulata Barneby	Super-host	Brown lanceolate bivalve-shaped	Pinna-rachis	Yes	CEN00100529	Laiana Moraes Brauner, 2017
M. sensitiva L.*	Uni-host	-	-	-	RFA29127	R.C. Lopes; M.S. Wangler, F.C. Alzer and G.F. Mazzoni, 2019
M. sericantha Benth.	Uni-host	Bivalve-shaped	-	Yes	CEN00052903	Taciana Barbosa Cavalcanti, 2003
M. sericantha Benth.	Uni-host	Bivalve-shaped	Leaflet and fruits	Yes	UEC051300	Cavalcanti, T.B. et al., 2013
M. sericantha Benth.	Uni-host	Bivalve-shaped	-	Yes	CEN00041640	Juliana S. Silva, 2013
M. tenuiflora Barneby	Super-host	-	-	-	MBM428260	Lozano, E.D.; Crivellari, L.B.; Seger, C.D.; Passos, E.; Becker, J.E.G.; Crivellari, L.B.; Seger, C.D.; Passos, E.; Becker, J.E.G., 2017
M. verrucosa Benth.*	Uni-host	-	Inflorescence	Yes	HVASF023838	M.M. Lira, 2021

Table 3. Anatomical traits of *Mimosa* spp..

***Mimosa* spp.**	**Pinnula or leaflets blade and stoma**	**Epidermis**	**cuticle**	**Mesophyll**	**Vascular system**	**Crystals or Sclereids**	**Laticifers**	**Reference**
M. caesalpiniifolia	Amphistomatic leaflets with paracitic stomata	Uniseriate with mucilage	Thin	Dorsiventral mesophyll 1-3-layered palisade parenchyma, and a 1-2-layered spongy parenchyma	Collateral	Pericyclic fibres with crystalliferous inclusions	Present in the phloem region	Mattos-Filho (1971), Barros (2010)
M. bimucronata	-	Uniseriate	Thick	Dorsiventral mesophyll	Collateral	Pericyclic fibres with crystalliferous inclusions	-	Huang et al. (2011)
M. gemmulata	Amphistomatic pinnula with anisocytic stomata	Uniseriate	Thin	Dorsiventral mesophyll 1-2-layered palisade parenchyma, and a 3-4-layered spongy parenchyma	Collateral	Parenchyma and pericyclic fibres with crystalliferous inclusions	-	Costa et al. (2018)
M. hypoglauca	Amphistomatic leaflets	Uniseriate	Thick	Dorsiventral mesophyll 1-2-layered palisade parenchyma, and a 3-6-layered spongy parenchyma	Collateral	Parenchyma with brachysclereids diffusely distributed		Mendes et al. (2021)
M. tenuiflora	Amphistomatic pinnula with paracitic stomata	Uniseriate with mucilage	Thin	Dorsiventral mesophyll 3-4-layered palisade parenchyma and a 3-4-layered spongy parenchyma	Collateral	Parenchyma and pericyclic fibres with crystalliferous inclusions	-	Nogueira et al. (2018)

Table 4. Types of glandular and non-glandular trichomes in *Mimosa* spp..

***Mimosa* spp.**	**Glandular trichomes**	**Non-glandular trichomes**	**Reference**
M. caesalpiniifolia	Granular	Filiform	Jordão et al. (2020)
M. candollei	Uniseriate-subsessile	Filiform	Jordão et al. (2020)
M. coruscocaesia	Sessile	Medusiform, stellate, unbranched trichomes	Santos-Silva et al. (2013)
M. cerifera	-	-	-
M. bimucronata	Uniseriate-subsessile	Filiform	Jordão et al. (2020)
M. gemmulata	Peltate	Filiform	Santos-Silva et al. (2013), Costa et al. (2018)
M. hypoglauca	Capitate and Clavate	Setiform	Mendes et al. (2021)
M. incana	-	Stellate and Plumose	Santos-Silva et al. (2013)
M. itatiaiensis	Granular	Filiform and Setiform	Jordão et al. (2020)
M. melanocarpa	Capitate	Filiform	Dutra et al. (2020)
M. ophthalmocentra	-	Unbranched trichomes	Santos-Silva et al. (2013)
M. polycarpa	-	Setose and Puberulous	Silveira (2015)
M. pseudosepiaria	Simple glandular trichomes	-	Ferreira et al. (2016)
M. scabrella	Capitate-filiform, Granular and Verrucose	Stellate, Tellate-lepidote, and Dendritic	Jordão et al. (2020)
M. sensitiva	-	-	-
M. sericantha	Sessile	Unbranched trichomes	Santos-Silva et al. (2013)
M. somnians	-	Filiform and Setiform	Jordão et al. (2020)
M. spixiana	Sessile	Unbranched trichomes	Santos-Silva et al. (2013)
M. tenuiflora	Sessile	Filiform	Santos-Silva et al. (2013)
M. tweedieana	-	-	-
M. verrucosa	Sessile	Verrucous trichomes	Santos-Silva et al. (2013)

Table 5. Chemical profiles of *Mimosa* spp..

Host species	Alkaloids	References
M. bimucronata	Alkaloids	Pilatti et al. (2019)
M. ophthalmocentra	*N*, *N*-dimethyl-tryptamine; *N*-Methyl-tryptamine and hordenine	Batista et al. (1997, 1999)
M. scabrella	*N*, *N*-dimethyl-tryptamine; *N*-Methyl-tryptamine; Tryptamine; and 2-Methyl-1,2,3,4-tetrahydro- β-carboline	De Moraes et al. (1990)
M. somnians	Tryptamine and *N*-Methyl-tryptamine	Gupta et al. (1979)
M. tenuiflora	*N*, *N*-Dimethyltryptamine; 2-methyl-tetrahydro-*β*-carboline and *N*-methyltryptamine	Gardner et al. (2014), Nogueira et al. (2018), Amariz et al. (2020), Bezerra et al. (2021)
Host species	**Phenolics**	**References**
M. bimucronata	Methyl gallate and gallic acid, and water-soluble tannins	Schlickmann et al. (2017, 2018)
M. caesalpiniifolia	Total phenolics; α-tocopherol; Pyrogallol; Gallic acid; Methyl gallate; 5-Hydroxy-40,7-dimethoxy-flavone; Quercetin; Quercetin-O-hexoside; Vicenin-2 and Rutin	Silva et al. (2014), Monção et al. (2014, 2015), Santos et al. (2015)
M. gemmulata	Total phenolics	Silva et al. (2006)
M. scabrella	3,4-dihydroxybenzoic acid; benzoic acid; salicylic acid; gallic acid; syringic acid; Coniferaldehyde; Syringaldehyde; *p*-Coumaric acid; Caffeic acid; Chlorogenic acid and Ferulic acid	Seraglio et al. (2017), Silva et al. (2020a)
M. tenuiflora	Total phenolics	Nogueira et al. (2018), Bezerra et al. (2021)
M. verrucosa	Flobabenic tannins; Pyrogalic tannins	Romanoski and Santos (2017), Silva et. (2020b)
Host species	**Flavonoids**	**References**
M. bimucronata	Flavonols	Pilatti et al. (2019)
M. caesalpiniifolia	Catechin, 2,3 dihydroquercetagetin, and procyanidin B2 [(epi)catechin–(epi)catechin)]	Silva et al. (2014), Monção et al. (2015)
M. gemmulata	6-naringenin and Flavonols	Silva et al. (2006)
M. scabrella	Kaempferol; Hesperidin; Isorhamnetin; Luteolin; Naringenin; Pinobanksin; Pinocembrin; Rutin and Quercetin	Seraglio et al. (2017), Silva et al. (2020a)
M. tenuiflora	Catechin; 5,4'-dihydroxy-7-methoxyflavanone (sakuranetin); 5,4'-dihydroxy-7-methoxyflavone (genkwanin); 5,6,4'-trihydroxy-7-methoxyflavone (sorbifolin); 5,4'-dihydroxy-7,8-dimethoxyflavone; 4',5,7-Trihydroxy-3,6-dimethoxyflavone; 5,7,4'-trihydroxy-3-methoxyflavone and the minor flavonols; 5,7,4'-trihydroxy-6-methoxyflavonol; 5,6-dihydroxy-7,4'-dimethoxyflavonol; 5-hydroxy-7,8,4'-trimethoxyflavonol; Tenuiflorin A; Tenuiflorin B; Tenuiflorin C; 4′,5-dihydroxy-7,8-dimethoxyflavone; 6-Methoxynaringenin; 6-methoxy-4′-*O*-methylnaringenin; Santin; 4′,5,7-trihydroxy-3,6-dimethoxyflavone; 6-methoxykaempferol; Kaempferol;	Bautista et al. (2011), Cruz et al. (2016), Bezerra et al. (2021)
M. verrucosa	Flavones; Flavonois,	Romanoski and Santos (2017), Silva et. (2020b)
Host species	**Saponins**	**References**
M. bimucronata	Saponins	Pilatti et al. (2019)
M. tenuiflora	Mimonosides A; Mimonosides B; Mimonosides C; Campesterol-3-*O*-*β*-D-glucopyranosyl; Stigmasterol-3-*O*-*β*-D-glucopyranosyl; *β*-Sitosterol-3-*O*-*β*-D-glucopyranosyl	Bezerra et al. (2021)
Host species	**Terpenoids**	**References**
M. bimucronata	Steroids and triterpenoids	Pilatti et al. (2019)

M. caesalpiniifolia	Triterpenic acid derivatives: betulinic acid (3β-hydroxy-lup-20(29)-en-28-oic acid)	Monção et al. (2015)
M. gemmulata	Terpenoids (essential oils)	Costa et al. (unpublished data)
M. scabrella	Steroids and triterpenoids	Fabrowski et al. (2002)
M. tenuiflora	Mimosasides A; Mimosasides B; Mimosasides C; 8,15-labdanediol and *ent*-8(17)-labden-15-ol	Nogueira et al. (2018), Bezerra et al. (2021)

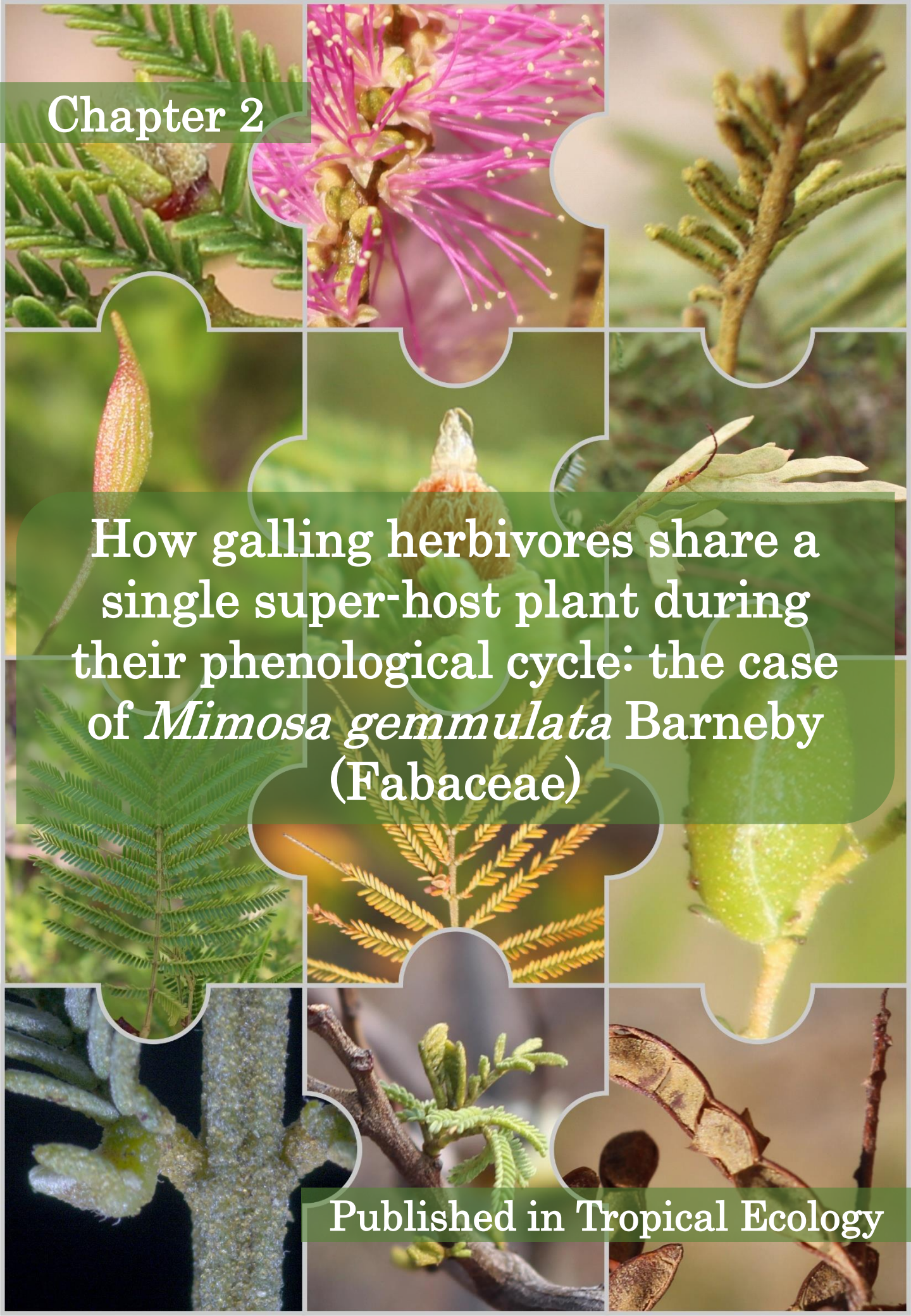

Chapter 2

How galling herbivores share a single super-host plant during their phenological cycle: the case of *Mimosa gemmulata* Barneby (Fabaceae)

Published in Tropical Ecology

Tropical Ecology
https://doi.org/10.1007/s42965-021-00182-1

International Society for Tropical Ecology

RESEARCH ARTICLE

How galling herbivores share a single super-host plant during their phenological cycle: the case of *Mimosa gemmulata* Barneby (Fabaceae)

Elaine C. Costa[1] · Vitor C. Martini[2] · Aline Souza-Silva[3] · José P. Lemos-Filho[1] · Denis C. Oliveira[2] · Rosy M. S. Isaias[1]

Received: 2 March 2020 / Revised: 1 March 2021 / Accepted: 1 July 2021

Abstract
The success of the galling insects sharing the same microhabitat depends both on the synchrony of their life cycles with the leaf flushing of the super-host plant and to the asynchrony among their life cycles. The asynchrony of the multivoltine life cycles of *Lopesia* spp. (Diptera—Cecidomyiidae) is favored by the constant leaf flushing in *M. gemmulata,* and favors the non-overlapping of gall induction periods. Peculiarly, the univoltine life cycle of the galling Lepidoptera on its stem galls is synchronized to the availability of mature host leaves during the rainy season, which is important for the water potential in host stem branches. The abundance of the *Lopesia* gall morphotypes follow the phenology of *M. gemmulata,* which obeys the seasonal pattern of water availability in the neotropical savanna climate.

Keywords Gall abundance · Gall-induction overlapping · Multivoltinism · Plant-interaction · Phenological synchronism · Seasonality

Introduction

Galls are sophisticated relationships between specialist herbivores, which include mites, nematodes, fungi, and more extensively insects, and their host plants (Stone and Schönrogge 2003; Shorthouse et al. 2005). The guild of galling insects include six orders, Coleoptera, Diptera, Hemiptera, Hymenoptera, Lepidoptera, and Thysanoptera (Fernandes and Santos 2014; Miller and Raman 2018; Ferreira et al. 2019) with a global estimation of 211,000 species in the last century (Espírito-Santo and Fernandes 2007). In face of the high specificity of this host plant-galling arthropod interaction, both richness and abundance of the galling insects can be estimated in nature by the distinct structural features of gall morphotypes (Carneiro et al. 2009; Isaias et al. 2013). Structural features, such as pubescence, shape, and size, as well as gall coloration are tools for the interpretation of gall developmental stages (Dias et al. 2013; Carneiro et al. 2013; Oliveira et al. 2013; Costa et al. 2018), and can be used to estimate the life cycles of the galling insects.

The life cycles of the galling insects can be defined by the type of voltinism, which indicates the number of generations of an organism within a one-year time (Yukawa 2000). Galling insects can have univoltine, bivoltine or multivoltine cycles (Yukawa 2000; Oliveira et al. 2016). Univoltine galling insects have only one generation throughout one-year time (Magalhães et al. 2014; Pfeffer et al. 2018; Guedes et al. 2018a, b), while the bivoltine and the multivoltine galling insects have two (Carneiro et al. 2013) or more generations over a year (Mendonça and Romanowski 2012; Dias et al. 2013; Costa et al. 2018), respectively. The periodicity of their cycles demands different and efficient strategies of the galling insects to exploit the resources during the host plant phenology (Oliveira et al. 2016).

The plant phenological pattern depends on environmental factors such as seasonality, precipitation, and temperature, as well as on the water potential of the plants (Lemos-Filho and Mendonça-Filho 2000; Franco et al. 2005; Garcia et al. 2017; García-Núñez et al. 2019). These abiotic and

✉ Rosy M. S. Isaias
rosy@icb.ufmg.br

[1] Departamento de Botânica, Instituto de Ciências Biológicas, Universidade Federal de Minas Gerais, Avenida Antônio Carlos, 6627, Pampulha, Belo Horizonte, Minas Gerais 31270-901, Brazil

[2] Instituto de Biologia, Universidade Federal de Uberlândia, Campus Umuarama, Rua Ceará s/n, Uberlândia, Minas Gerais 38402-018, Brazil

[3] Laboratório de Botânica, Universidade do Estado da Bahia, Campus VI, Avenida Contorno s/n, Caetité, São José, Bahia 46400-000, Brazil

Published online: 22 July 2021

physiological variables can impose constraints to the host plant species and, consequently, to the life cycles of the galling insects, and to gall abundance (Oliveira et al. 2013). Several studies demonstrated strategies of phenological synchronism between galling insects and the phenology of their host plants in temperate (Yukawa 2000; Tokuda 2012), tropical (Oliveira et al. 2016), and mediterranean (Guedes et al. 2018a, b) climatic conditions. Based on that, the seasonal leaf flushing of Neotropical plant species, that occur at the end of the dry season or early rainy season (Garcia et al. 2017; García-Núñez et al. 2019), can provide a large amount of resources for galling insect exploitation (Oliveira et al. 2016). One of the most efficient strategies of the galling insects is ovipositing in young tissues (sensu Weis et al. 1988). Nevertheless, the oviposition is not exclusive on the young tissues. Galling insects can induce their galls in mature leaves, whose cells keep the capacity for reedifferentiation (Oliveira and Isaias 2009; Oliveira et al. 2013). The ability to exploit both young and mature tissues is important for the success of the galling insects, which widens the opportunities of galling insects to synchronize their life cycles with the phenology of their host plants (Oliveira et al. 2013). The synchronization between galling insects and their host plants is a critical event for the first, because a time lag synchronization determines the quality and quantity of available food resources, and the abundance of population dynamics of galling herbivores (Yukawa 2000; Mendonça 2001; Oliveira et al. 2013, 2016). Interactive systems involving a super-host plant and several galling insects can reveal peculiar temporal strategies involving niche overlapping during gall induction by generations of galling insects (Weis et al. 1988; Toma and Mendonça 2014), which share the same induction site. The niche overlapping refers to the use of the same resources or conditions by two or more species, and the greater the number of resources shared by the species, the greater the overlapping (Pianka 1974). *Mimosa gemmulata* Barneby is a super-host Fabaceae, the mean host family of galling herbivores in the Neotropical region (Fernandes and Santos 2014). This species occurs in Venezuela and Brazil (Bahia, Minas Gerais, Goiás, Pernambuco, and Piauí), and grows naturally in areas of Caatinga, Savanna, and Campos Rupestres vegetation (Santos-Silva et al. 2015). *Mimosa gemmulata* hosts five leaf gall morphotypes induced by five species of *Lopesia* Rübsaamen, 1908 (Diptera—Cecidomyiidae, Maia and Carvalho-Fernandes, personal communication), and one fusiform stem gall induced by a Lepidoptera (Costa 2016; Silva et al. 2018). The five leaf galls on *M. gemmulata* share the same induction microsite, i.e., the pinna-rachis (Costa 2016), a peculiarity of the galls associated with this super-host plant.

The first approach toward the six gall morphotypes associated with *M. gemmulata* deals with the host plant phenology and the life cycles of the six associated galling insects. Currently, the life cycles of the six galling insects are evidenced by the developmental stages of their specific gall morphotypes (Carneiro et al. 2009; Isaias et al. 2013), herein referred as the life cycles of the galls. We hypothesize that the galling insects alternate their phenological synchrony with that of the host plant, and asynchrony among their life cycles as strategies to share the same microsite of induction. All processes involving this super-host plant-galling herbivore systems are directly influenced and dependent on climatic factors, which directed the following questions: (1) how are the gall life cycles distributed along a one-year period? (2) Do the periods of gall induction and leaf flushing on *M. gemmulata* overlap for the five galling herbivores? And (3) what are the abiotic and physiological factors that best relates to gall abundance?

Materials and methods

Study area

This study was carried out in Serra Geral of Caetité (14°04′ 36. 8″ S, 42°29′59″ W), state of Bahia, northeast Brazil. The area has 974 m of altitude with the vegetation comprising a savanna, where the individuals of *M. gemmulata* may be isolated or grouped in low density populations. According to the Köppen system, the climate of the region is classified as *Aw* (tropical with dry winters, and rainy summers; Alvares et al. 2013), with marked seasonality. The rainy season ranges from November to April, when monthly rainfall is >60 mm, and dry season ranges from May to October, when monthly rainfall is <60 mm (Fig. 1). The mean annual rainfall is 608 mm and the mean temperature is above 23 °C (Fig. 1). The data of precipitation and of mean temperature were obtained from the meteorological station of Caetité, and from the meteorological station of Lençóis, Bahia state, respectively. The second station is the nearest (~350 km) and with climate (*Aw*) similar to that of the study

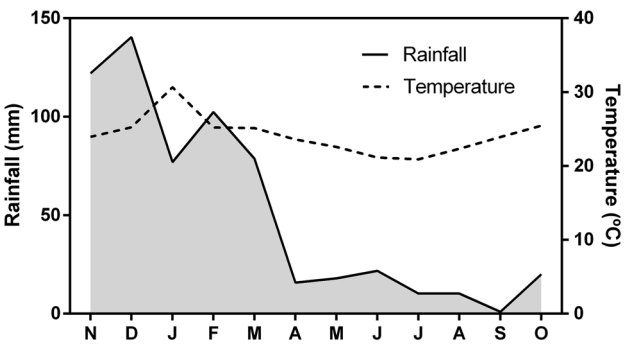

Fig. 1 Climatic diagram with mean annual rainfall (mm) and temperature (°C) during the year of study: from November 2017 to October 2018

site (Alvares et al. 2013; meteorological data for the years 1961–1990; INMET 2019).

Super-host plant phenology

The phenology of *M. gemmulata* (voucher specimens: herbarium of the Universidade do Estado da Bahia, HUNEB-25044) was monitored every 15-day intervals from November 2017 to October 2018 on individuals ($n = 12$) selected by order of appearance along trails previously traced (*cf.* Eça-Neves and Morellato 2004). The vegetative phenophases (leaf flushing, mature leaves, and leaf falling) and the reproductive phenophases (inflorescence buds, inflorescence anthesis, immature, and mature fruits) were monitored according to the methods proposed by Fournier (1974) in each *M. gemmulata* individual. This method is semi-quantitative, ranking five categories of phenophases (0 = absence of the phenophase; 1 = 1–25%; 2 = 26–50%; 3 = 51–75%; and 4 = 76–100% intensity of the phenophases). The presence and absence of the vegetative and reproductive phenophases were evaluated for each plant, and phenological synchrony was estimated (Bencke and Morellato 2002). Leaf flushing was considered valid from the beginning of the first leaves until their complete expansion (Pedroni et al. 2002) with light green leaflets (Fig. 2A, B). Mature leaves were considered as those with dark green leaflets (Fig. 2C), and leaf falling was considered when the leaflets are yellowish and fell off the branches easily (Fig. 2D). The phenophase of inflorescence buds reffered to the presence of inflorescences with flower buds (Fig. 2E), and the phenophase of inflorescence anthesis reffered to the presence of inflorescences with flower in anthesis (Fig. 2F). The phenophase of immature fruits reffered to the presence of fruits with green collor (Fig. 2G), while the phenophase of mature fruits reffered to the presence of fruits with brown collor (Fig. 2H). The observation of the phenology was based on the percentage categories for the canopy covering.

Life cycles of the galls

The definition of the life cycles was based on the most abundant of the developmental stages for the six galls in each field observation period throughout the year (Arduin et al. 1994; adapted). Terminal branches ($n = 4$) were randomly marked on each individual of *M. gemmulata* ($n = 12$), in a total of 48 branches. At each branch, the presence and abundance of each morphotype were counted every 15-day intervals from November 2017 to October 2018. The life cycles of the six galling insects were differentiated in the field based on structural features such as, the gall shape, and size, and color (Isaias et al. 2013). Galls stages were later registered as gall induction, growth and development, maturation and senescence (Fig. 2 I-B′, Table 1). For the five leaf galls, the induction stage was characterized as a small intumescence on the pinna-rachis. The induction stage of the stem gall could not be observed in field conditions. The growth and development stage was determined by the higher dimensions of the intumescence (1–3 mm of height, and 0.1–0.4 mm of width) or color. The mature stage was determined by the gall shape and color, and the senescent stage was determined by the presence of the open galls, pupal exuviae, or scape channel of the galling insects. Samples of mature leaf galls ($n = 24$ for each gall morphoespecies) were collected and opened on the stereomicroscope to obtain the fauna associated with the galls. The stem gall induced by a Lepidoptera was not collected due to its low abundance.

Water potential measurements

The water potential (Ψ) of terminal branches sectioned about 10 cm from the apex of the individuals ($n = 6$) of *M. gemmulata* (Scholander et al. 1965) was determined using a pressure chamber (Model 600 PMS, EUA). The water potential was measured at the predawn (Ψ_{PD} 05:00 a.m.), and midday (Ψ_{MD} 12:00 p.m.). The measurements were taken in the rainy season (November and December 2017, and January and April 2018), and in the dry season (July, September and October 2018).

Data analysis

The phenological data of the six-gall morphotypes was organized in histograms evidencing the annual gall life cycles. The stem gall induced by a Lepidoptera was not subjected to the analyses of distribution, overlapping, and correlation due to its low abundance. We tested the distribution and overlapping of the phenophases of *M. gemmulata* and the life cycles of five leaf gall morphotypes using the circular analysis (Agostinelli and Lund 2017), and the Pianka index (Pianka 1974). To circular analyses of the abundance of the gall life cycles, and the phenophases of the host plant, the Watson-Wheeler test was made using von Mises distribution. The mean angles of the induction of the five leaf gall life cycles and leaf flushing was compared. The data were standardized for adjusting the unities and create evenness on the variance. The overlapping of gall inductions and leaf flushing, and within gall morphotypes per month were quantified (Pianka 1974). To compare the overlapping of gall induction and leaf flushing, gall values were transformed in percentages. The overlapping was compared to a stochastic distribution of the data using the null model with Pianka metric and Ra3 algorithm running 5000 randomizations. The Pianka index ranged from 0 (no overlap) to 1 (complete overlap), which overlap was classified as high (> 0.6), intermediate (between 0.4 and 0.6) or low (< 0.4). To verify

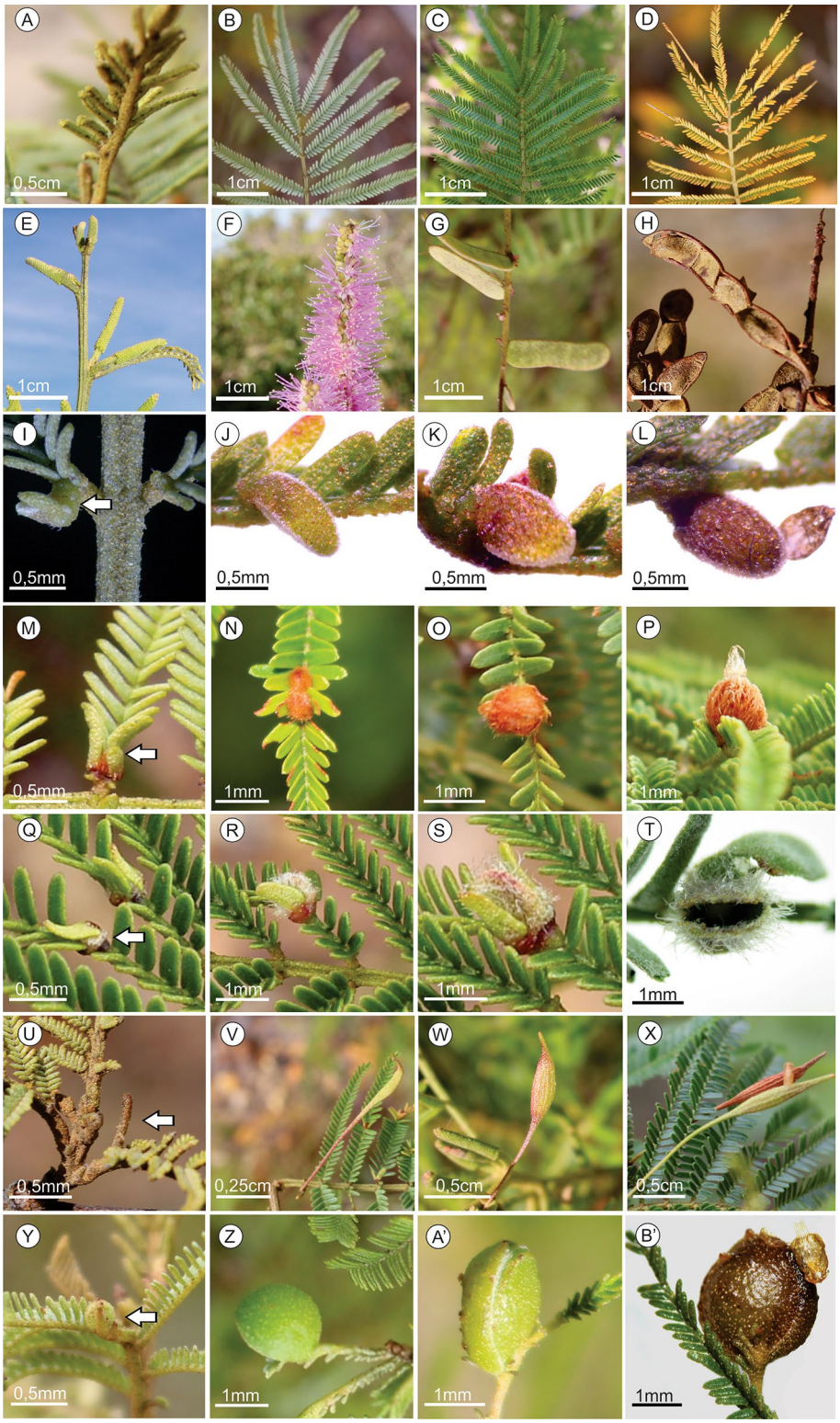

Fig. 2 Phenology of *Mimosa gemmulata* Barneby (Fabaceae) and the *Lopesia* gall life cycles (Diptera–Cecidomyiidae). **A**, **B** Leaf flushing. **C** Mature leaves. **D** Leaf falling. **E** Inflorescence buds. **F** Inflorescence anthesis. **G** Immature fruit. **H** Mature fruit. **I–L** Lenticular bivalve-shaped gall. **I** Induction (arrow). **J** Growth and development. **K** Maturation. **L** Senescence. **M–P** Brown lanceolate bivalve-shaped gall. **M** Induction (arrow). **N** Growth and development. **O** Maturation. **P** Senescence. **Q–T** Green lanceolate bivalve-shaped gall. **Q** Induction (arrow). **R** Growth and development. **S** Maturation. **T** Senescence. **U–X**) Clavate gall. **U** Induction (arrow). **V** Growth and development. **W** Maturation. **X** Senescence. **Y-B′** Globoid bivalve-shaped gall. **Y** Induction (arrow). **Z** Growth and development. **A′** Maturation. **B′** Senescence

the relationships between water potential (predawn and midday) and abundance of leaf gall morphotypes, we performed a generalized linear mixed model (GLMM), using the plant water potential as fixed variable and the gall morphotypes as random effect. The correlation between the abundance of the five leaf gall morphotypes with climatic factors (temperature, and rainfall), water potential, and plant phenophases were evaluated using a canonical analysis of principal coordinates (Legendre and Anderson 1999), based on Euclidian distance and standardized

Table 1 General features of the six gall morphotypes induced by insects on *Mimosa gemmulata* Barneby (Fabaceae) at Serra Geral, Caetité, Bahia state, Brazil

Morphotypes at MG	Inducing-insect	Host organ	Attachment at MG	Color at GD and MG	Size ($n=5$ galls) of GD (height and width; mm)
Lenticular bivalve-shaped gall	*Lopesia* sp. (Cecidomyiidae)	Pinna-rachis	Extralaminar	Green	1.24 ± 0.20; 0.54 ± 0.32
Brown lanceolate bivalve-shaped gall	*Lopesia* sp. (Cecidomyiidae)	Pinna-rachis	Extralaminar	Brown	1.96 ± 0.23; 0.93 ± 0.69
Green lanceolate bivalve-shaped gall	*Lopesia* sp. (Cecidomyiidae)	Pinna-rachis	Extralaminar	Green	1.72 ± 0.12; 0.86 ± 0.04
Clavate gall	*Lopesia* sp. (Cecidomyiidae)	Pinna-rachis	Pedunculated	Green	1.67 ± 0.25; 0.80 ± 0.02
Globoid-shaped bivalve gall	*Lopesia* sp. (Cecidomyiidae)	Pinna-rachis	Extralaminar	Green	3.30 ± 0.40; 1.41 ± 0.53
Fusiform gall	Lepidoptera	Stem	Intralaminar	Green (GD) and Brown (MG)	–

Values are mean—mm ± standard deviation. The number of samples was insufficient to average the size of the fusiform gall

GD growth and development, *MG* mature gall

data. All analyses were made using the R software (R Core Team 2020), with EcoSimR and Vegan packages (Oksanen et al. 2007).

Results

General features of the galls

Mimosa gemmulata hosts five gall morphotypes induced by five species of *Lopesia* (Cecidomyiidae) on the pinna-rachis, four of these galls are bivalve-shaped and one is clavate (CG), a sixth gall morphotype is fusiform (FG) and is induced on stems by a Lepidoptera. The bivalve-shaped galls are: (1) the lenticular bivalve-shaped (LG); (2) the brown lanceolate bivalve-shaped (BLG); (3) the green lanceolate bivalve-shaped (GLG); and (4) the globoid bivalve-shaped (GG) (Fig. 2I-B', Table 1). The *Lopesia* larvae of the LG, GLG, and BLG can be parasitized by *Eupelmus* sp. (Hymenoptera – Eupelmidae), while the *Lopesia* larvae of the CL and GG can be parasitized by *Torymus* sp. (Hymenoptera–Torymidae).

Life cycles of the galls

The lenticular bivalve-shaped gall had six generations over the year, each one of about 2 months (Fig. 3A). The induction stage was observed on the second fortnights of December, February, April, June, August, and October. The growth and development stage lasted about 15 days, and the maturation stage lasted about 30–45 days. The BLG, the GLG, and the CG had at least four generations over a year of about 3 months each (Fig. 3B–D). The induction of the BLG was observed on the second fortnights of December and February, on the first fortnight of May, and on the second fortnight of August (Fig. 3B). The induction of the GLG was observed on the second fortnight of December, on the first fortnight of March, on the second fortnight of May, and on the first fortnight of August (Fig. 3C). The induction of the CG was observed on the second fortnight of December, on the first fortnight of April, and on the second fortnights of June and September (Fig. 3D). The growth and development stage of these three gall morphotypes lasted approximately 30 days, and the maturation stage lasted 45–60 days. The life cycle of the GG lasted approximately 4 months, with three generations over a year (Fig. 3E). The induction was observed on the second fortnights of December and April, and on the first fortnight of August; the growth and development stage lasted 45–60 days, and the maturation stage lasted 60–75 days. The FG had one generation a year, which lasted about 5 months, beginning on the first fortnight of January and getting final development in May, when the gall reached senescence (Fig. 3F).

Phenology of the super-host plant

Mimosa gemmulata is a semi-deciduous host plant with all its vegetative, and reproductive phenophases synchronized (100%). The vegetative phenophases were distributed during the year, and the reproductive phenophases occurred at specific periods (Fig. 4A). The leaf flushing had the maximum intensity on the first fortnight of November (48%), and on the second fortnight of December (62%) with the mean vector directed to November. The intensity of leaf flushing decreased from March (15%) to October. At the second fortnight of February, the mature leaves intensity

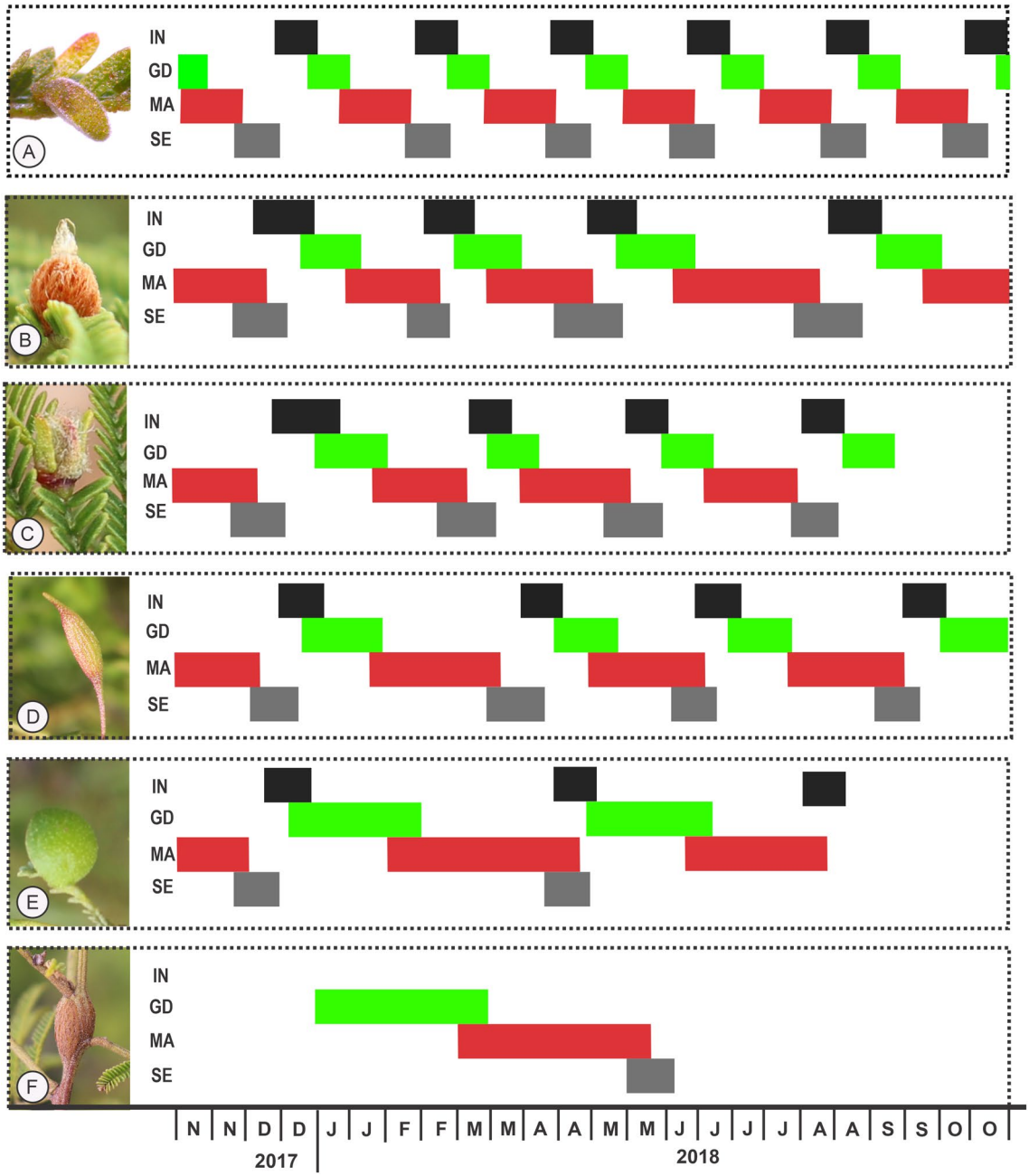

Fig. 3 Diagram of the life cycles of the gall morphotypes induced by insects (*Lopesia* spp.–Diptera–Cecidomyiidae and Lepidoptera) on *Mimosa gemmulata* Barneby (Fabaceae). **A**–**E**. Leaf galls induced by five *Lopesia* spp.. **A** Lenticular bivalve-shaped gall. **B** Brown lanceolate bivalve-shaped gall. **C** Green lanceolate bivalve-shaped gall. **D** Clavate gall. **E** Globoid bivalve-shaped gall. **F** Stem fusiform gall induced by Lepidoptera. The bars indicate to the specific temporal window of the stages of gall development: Induction (IN) ( ); Growth and development (GD) ( ); Maturation (MA) ( ) and Senescence (SE) ( )

increased and was constant throughout March (76%). The mean vector directed to concentration between February and March. The leaf falling occurrence increased from June (46%) to October (66%), and was more intense in September (73%) with the mean vector directed to August. The inflorescence buds occurred from December to February and had the maximum intensity in January (100%) with the mean vector pointed to January. At the second fortnight of February to the first fortnight of March, the vector pointed to the mean concentration of the inflorescence anthesis. The immature fruits occurred from March to August with the maximum intensity in July (90%), and the direction of the mean vector pointed between May and June. The mature fruits occurred from July to September

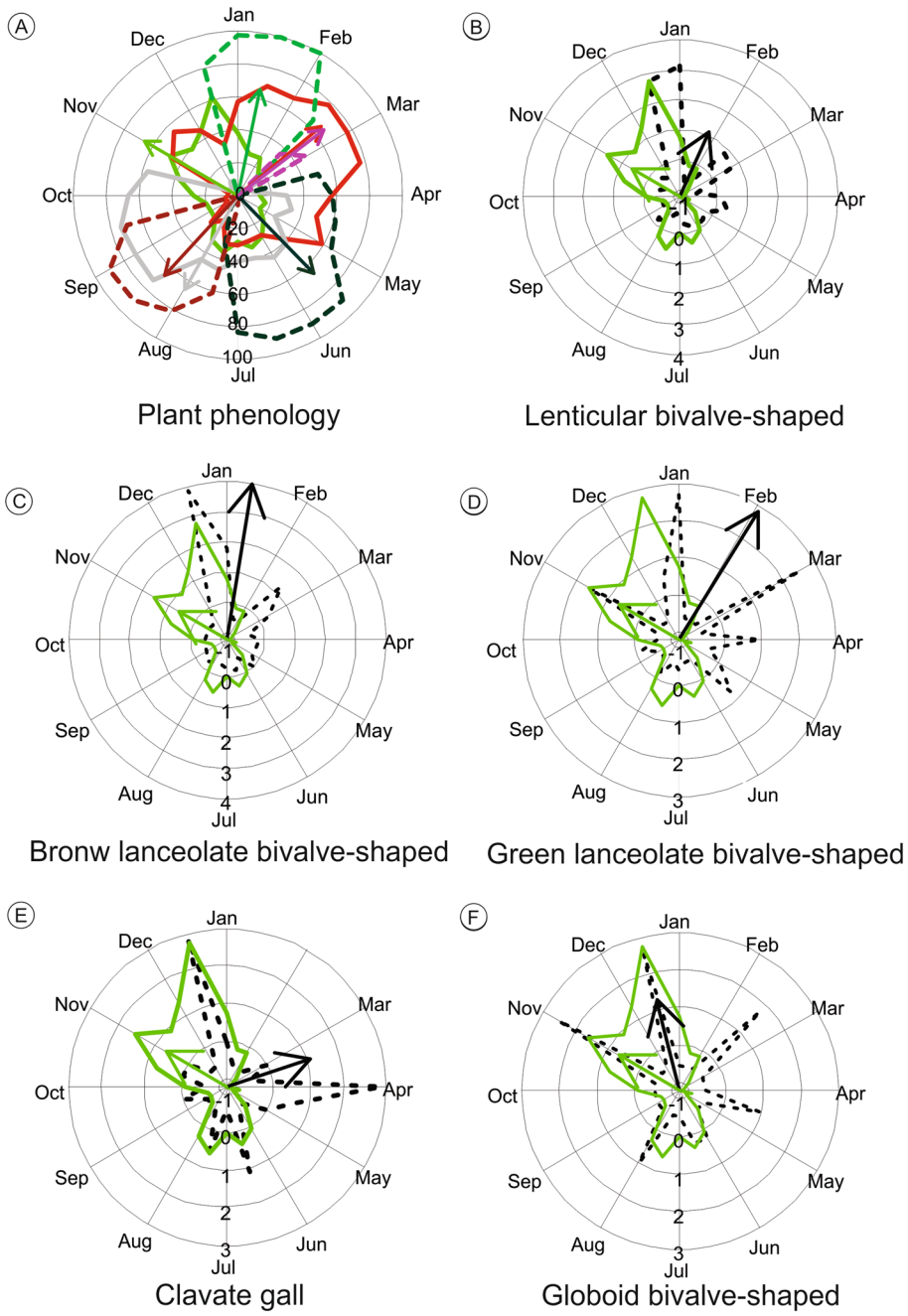

Fig. 4 Circular analysis of index of intensity of the vegetative and reproductive phenology of *Mimosa gemmulata* Barneby (Fabaceae) and induction of the five leaf galls induced by five *Lopesia* spp. from November 2017 to October 2018. **A** Phenology [Immature fruit (dark green); Inflorescence anthesis (pink); Inflorescence buds (light green); Leaf falling (gray); Leaf flushing (fluorescent green); Mature leaves (red); Mature fruit (brown)]. **B** Lenticular bivalve-shaped gall. **C** Brown bivalve-shaped gall. **D** Green bivalve-shaped gall. **E** Clavate gall. **F** Globoid bivalve-shaped gall

with the intensity peak in August (90%), observed by the direction of the mean vector.

Relationship between the induction of the leaf gall morphotypes and leaf flushing

The galling insects induce their galls throughout the year by the time of the leaf flushing. However, more events of gall induction than peaks of leaf flushing were observed (Fig. 4A). The Watson-Wheeler test showed different mean angles of inductions of the five leaf gall morphotypes comparing to leaf flushing (P values < 0.001). The LG had the highest peaks of induction along the second fortnight of December and first fortnight of January with the mean vector direction pointing to February (Fig. 4B). The highest peak of induction events of the BLG was observed on the second fortnight of December, with the mean vector pointing to January (Fig. 4C). The peaks of induction of the GLG were observed on the first fortnights of January and March, with the mean vector direction pointing to February (Fig. 4D).

The CG had the highest peaks of induction on the second fortnight of December, and on the first fortnight of April, with mean vector direction pointing to March (Fig. 4E). The highest peak of inductions of the GG was observed on the second fortnight of December, which coincided with the direction of the vector (Fig. 4F). The inductions of the five leaf gall morphotypes decreased from May to October. The highest overlapping occurred between the leaf flushing and the induction of the BLG (Pianka index = 0.74), and there was an intermediate overlapping between leaf flushing and the induction of GG (Pianka index = 0.40). However, there was no significant overlapping between the inductions of the three leaf galls (LG, GLG, CG) with leaf flushing. The overlapping between the events of induction was significant only for the BLG and the LG (Pianka index = 0.94). There was no significant difference in the values of overlapping of the induction events among the GLG, CG, and the GG, when compared to the null-model.

Gall morphotypes abundance versus abiotic and physiological factors

The six gall morphotypes co-occurred on *M. gemmulata* from January to May, during the rainy season. The numbers of gall morphotypes decreased in September and October, during the dry season, when the GLG, the GG, and the FG were not observed. The total abundance of the galls was higher from November to April, during the rainy season, with the highest abundance (2197) in January (Fig. 5A, B). In this month, the BLG was the most abundant (1135), followed by the LG (992), the GLG (39), the CG (21), the GG (9), and the FG (1). The seasonal pattern of the gall morphotypes was concomitant with the intensity of the leaf flushing (November to January) and mature leaves (February and March), and with the highest values of water potential (−0.3 MPa at predawn and −0.5 MPa at midday) during the rainy season (Fig. 5). Gall abundance decreased from May to October, and the lowest gall abundance was observed in September (185) and October (144). There was a positive correlation between the total gall abundance and the increasing of the water potential (Fig. 6) at predawn ($R^2 = 0.24$, P values < 0.001), and midday ($R^2 = 0.25$, P values < 0.001).

The Canonical analysis of the principal coordinates showed the five leaf gall morphotypes clustered in an environment with water potential, rainfall, temperature, mature leaves, inflorescence buds, inflorescence anthesis and no leaf falling, immature, and mature fruits. The eigenvalues were 3.305 for the axis 1 and 0.306 for axis 2, with a total of 82 and 7% of the total explained variance of abundance of the five galling Cecidomyiidae in the rainy season, respectively (Fig. 7, Supplementary table S1). The abundance of the LG was more correlated to the occurrence of mature leaves. The abundance of the BLG and GLG were correlated with the temperature. The CG and GG were more correlated with the rainfall, and the water potential. The flowering phases were positively correlated with the five leaf galls. The leaf falling, and immature and mature fruits were negatively correlated with the distribution of the five gall morphotypes.

Discussion

The distribution of the five gall morphotypes induced by five *Lopesia* spp. (Diptera—Cecidomyiidae) along the one-year cycle confirmed different strategies of synchronizing to *M. gemmulata* leaf flushing. The five species of galling *Lopesia* had a peculiar asynchronism among them, which favored the sharing of the same microsite of induction on host plant. This asynchronism was peculiar for the five multivoltine species of *Lopesia*, while the univoltine Lepidoptera exploited another site of induction on the same host species, the stem. The strategies of synchronism were influenced by seasonal water availability during the dry and the rainy seasons in neotropical savanna of Brazil, which defined the abundance and presence of the different gall morphotypes.

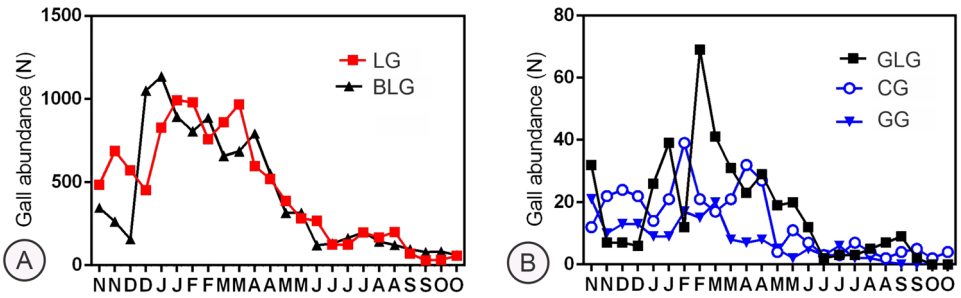

Fig. 5 Abundance of *Lopesia* galls (Diptera-Cecidomyiidae) on *Mimosa gemmulata* Barneby (Fabaceae) from November 2017 to October 2018. **A** Lenticular bivalve-shaped gall (LG) and Brown lanceolate bivalve-shaped gall (BLG). **B** Green lanceolate bivalve-shaped gall (GLG), Clavate gall (CG) and Globoid bivalve-shaped gall (GG)

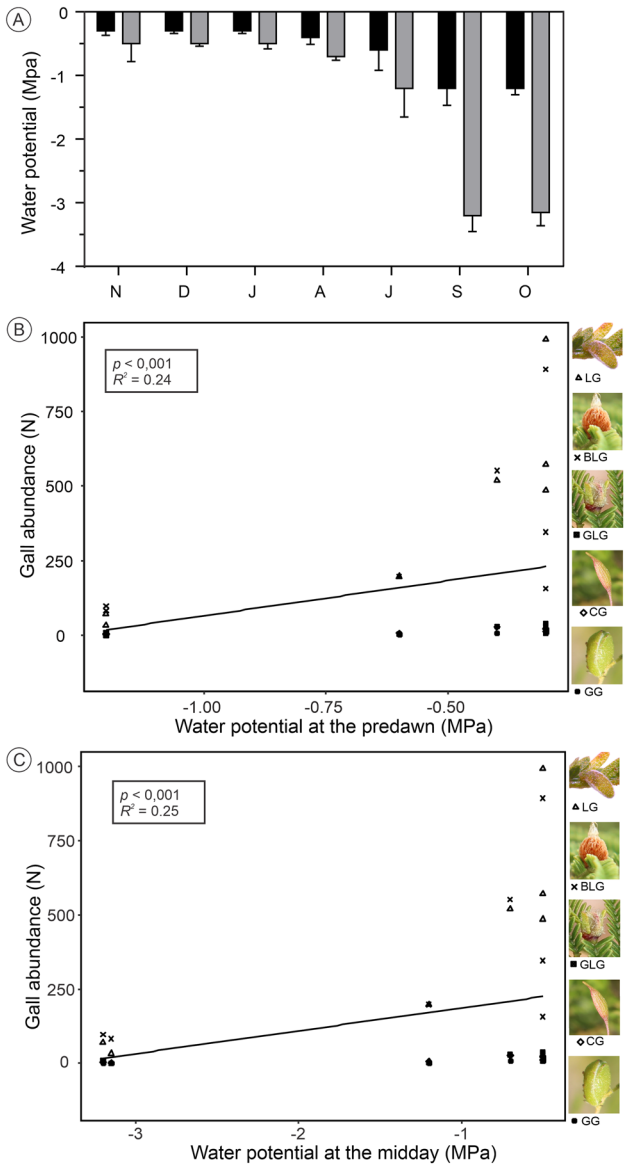

Fig. 6 Relationships between water potential (predawn and midday) and abundance of the five leaf *Lopesia* galls (Diptera–Cecidomyiidae) on *Mimosa gemmulata* Barneby (Fabaceae). **A** Leaf water potential (MPa) at predawn (■) and midday (■) in the *M. gemmulata* population on rainy (November and December 2017, and January and April 2018), and dry (July, September, and October 2018) seasons. **B** Relation of the predawn with gall abundance. **C** Relation of the midday with gall abundance. Clavate gall (CG). Brown lanceolate bivalve-shaped gall (BLG). Globoid bivalve-shaped gall (GG). Green lanceolate bivalve-shaped gall (GLG). Lanceolate bivalve-shaped gall (LG)

Univoltinism versus multivoltinism

The Lepidoptera stem gall on *M. gemmulata* had a univoltine life cycle. In the Neotropical region other galls induced by Lepidoptera have been reported, as the *Tibouchina trichopoda* (DC.) Baill. (Melastomataceae)-*Palaeomystella beckeri* Moreira and Basilio 2015 (Momphidae) and *Schinus weinmannifolius* Mart. ex Engl (Anacardiaceae)-*Cecidonius pampeanus* Moreira and Gonçalves 2017 (Cecidosidae) systems (Basilio et al. 2015; Moreira et al. 2017). The stem galls synchronized the growth and development and maturation phases with the high intensity of mature leaves during the rainy season. Such synchronization favored a high nutritional support to gall development due to the allocation of photoassimilates (Castro et al. 2012, 2013; Oliveira et al. 2017; Zorić et al. 2019), and water supply favoring the development of the Lepidoptera larvae.

The generations of the five leaf gall morphotypes on *M. gemmulata* revealed multivoltine life cycles for the *Lopesia* spp. (Cecidomyiidae). Generally, the Cecidomyiidae have univoltine or bivoltine life cycles, and rarely multivoltine life cycles in the Temperate region, despite the synchronism with deciduous plants (Tokuda 2012; Yukawa et al. 2015, 2019). In the Neotropical region, the Cecidomyiidae have univoltine life cycles as observed in the *Copaifera langsdorffii* Desf. (Fabaceae)-Cecidomyiidae systems (Oliveira et al. 2013; Carneiro et al. 2017), bivoltine life cycles as observed in the *Aspidosperma spruceanum* Benth. ex Müll.Arg. (Sapindaceae)-Cecidomyiidae system (Campos et al. 2010) or multivoltine life cycles, as described for *Eugenia uniflora* L. (Myrtaceae)-*Eugeniamyia dispar* Maia, Mendonça and Romanowski, 1996 system (Mendonça and Romanowski 2012; Rezende et al. 2018).

The multivoltine life cycles are the most common for the galling Cecidomyiidae in the Neotropical region (Hawkins and Gagné 1989), because of the evergreen or semi-deciduous habits that frequently provide sites of inductions in the neotropical savanna (Dalmolin et al. 2015; Garcia et al. 2017; Camargo et al. 2018; García-Núñez et al. 2019). Although the strategies of synchronism with their host plants are not completely clear for the galling insects with multivoltine life cycles (Mendonça and Romanowski 2012; Toma and Mendonça 2014; Oliveira et al. 2016), the multivoltine *Lopesia* spp. associated with *M. gemmulata* had peculiar strategies of synchronism. The continuous leaf flushing during the year support the multivoltine life cycles. *Mimosa gemmulata* is a semi-deciduous shrub, with periods of leaf flushing and leaf falling related to the contrasting periods of drought and raining in the neotropical savanna climate. The periods of leaf flushing were continuous throughout the year, but with main peaks in the rainy season, which coincided with the main peaks of Cecidomyiidae gall induction. Such synchronization indicated an advantage over the best windows of opportunity (Mendonça 2001; Yukawa 2000; Tokuda 2012; Oliveira et al. 2016). The induction phase of the five leaf gall morphotypes synchronized with the semi-deciduous habit of *M. gemmulata*, which was discussed herein based on the overlapping of resources.

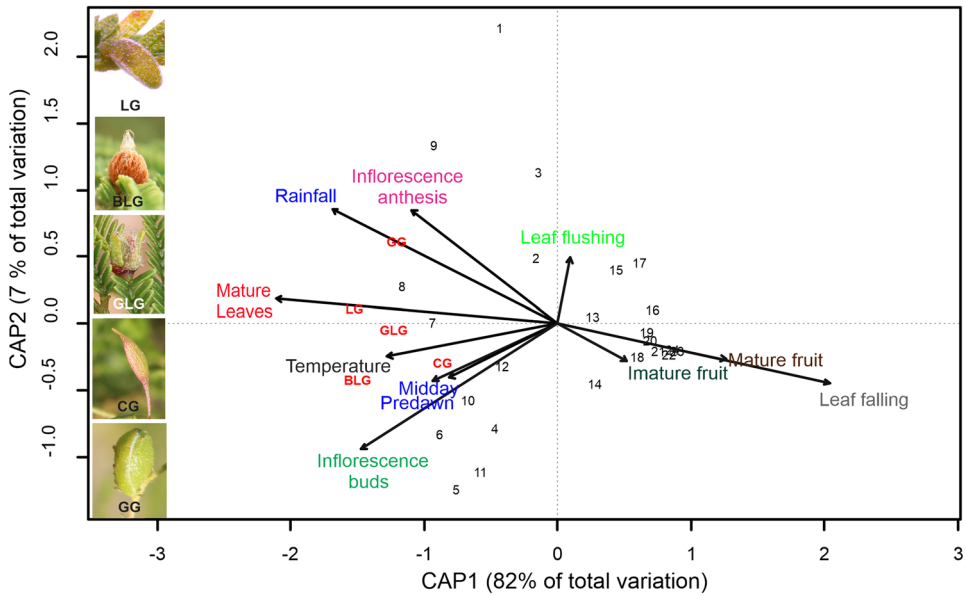

Fig. 7 Canonical analysis of principal coordinates (CAP) of the five leaf *Lopesia* galls (Diptera-Cecidomyiidae) on *Mimosa gemmulata* Barneby (Fabaceae). Vectors represent explanatory variables derived from host physiology: water potential at predawn (blue) and midday (blue); from host phenology: immature fruit (dark green), inflorescence anthesis (pink), inflorescence buds (light green), leaf falling (gray), leaf flushing (fluorescent green), mature leaves (red), mature fruit (brown), and from climatic factors: temperature (black) and rainfall (blue). Numbers represent each data collected from November 2017 (1) to October 2018 (24). Clavate gall (CG). Brown lanceolate bivalve-shaped gall (BLG). Globoid bivalve-shaped gall (GG). Green lanceolate bivalve-shaped gall (GLG). Lanceolate bivalve-shaped gall (LG)

Temporal strategies of multivoltine galling insects

The success of galling insects depends on the selection of the host plant, the most vigorous organ (quality of resources), and the number of oviposition sites (abundance of resources) available for their development (Höglund 2014; Oliveira et al. 2016). In addition, the parasitoids are the main causes of the death of gall-inducing insects, and can affect the life cycle and abundance of galls on their host plants (Rezende et al. 2019), as is true for *Eupelmus* sp. and *Torymus* sp., parasitoids of *Lopesia* larvae in galls on *M. gemmulata*. The abundance of gall inductions in the rainy season revealed the performance of the five galling *Lopesia* spp. in synchronizing with the best quality of resources and water availability in *M. gemmulata.* Our results suggested that, despite the non-synchronism among the multivoltine gall life cycles and the host plant over the year, the abundance of gall inductions followed the dry and rainy seasonal of the neotropical savanna climate imposed to the phenology of *M. gemmulata*. Herbivores that share host plants sometimes use leaves at different ages (Oliveira and Isaias 2009; Condon et al. 2014; Nakadai et al. 2018) or different microsites on the same leaves (Oliveira et al. 2013). The nine leaf galls on *Copaifera langsdorffii*, for example, are induced by Cecidomyiidae species on distinct microsites of young or mature leaves, such as leaf bud, petiole, lamina, and midrib (Oliveira and Isaias 2009; Oliveira et al. 2013; Carneiro et al. 2017). This is a spatial–temporal strategy for the co-occurrence of the galling insects, and the avoidance of the overlapping in the use of resources. Differently, the five *Lopesia* spp. associated with *M. gemmulata* had temporal strategies to the induction of the five leaf-gall morphotypes, and shared the same microsite of induction, i.e., the pinna-rachis. The multivotine galling *Lopesia* spp. emerged and induced their galls in distinct temporal scales in the pinna-rachis, as evidenced by the overlapping dynamics of the induction phases.

The high overlapping of the induction between the most abundant gall morphotypes, the LG, and the BLG, were explained by the temporal adjustments with the leaf flushing. The species of *Lopesia* associated with the LG had the strategy that better adjusted to the availability of leaf flushing, evidenced by the short life cycles and six gall generations throughout the year. The induction of the BLG had the highest overlapping with the leaf flushing peaks, and consequently the highest chance of finding available microsites of induction. For the inducers of the GLG, the CG, and the GG, the overlapping is not completely clear. We believed that the gall induction in different temporal scales was an adaptive strategy to avoid the overlapping of inductions in the pinna-rachis of *M. gemmulata*. These strategies of synchronism with seasonal availability of resources during the

leaf flushing of *M. gemmulata* promoted the temporal partitioning of resources and the success of the multivoltine life cycles of the galling *Lopesia* spp.

Seasonal abundance of insect galls and climatic factors, water potential, and plant phenology

The presence and abundance of each *Lopesia* gall morphotype were related to the phenological behavior of the host *M. gemmulata,* which was regulated by the seasonal climate of the neotropical Savanna. We could distinguish seasonal patterns of gall abundance in a year-time, which resembled a wave pattern with the abundance rarely decreasing to zero in the dry season, as proposed for free-living insects (Wolda 1988; Kishimoto-Yamada and Itioka 2015). We assumed that this pattern was true for the galling insects associated with *M. gemmulata*. In the neotropical savanna climate, the rainfall is one of the environmental factors that most influences the seasonal dynamics in the populations of the tropical free-living insects (Kishimoto-Yamada and Itioka 2015), and influence the abundance of the galling Cecidomyiidae on *M. gemmulata*, as well. The high rainfall values increased the amount of water available in the soil, which led to better water conditions for *M. gemmulata*, as evidenced by the values of water potential in many other plants (Franco et al. 2005; Garcia et al. 2017). As a response to the excellent water status, the highest intensity of leaf flushing and mature leaves in *M. gemmulata* favored the total abundance of galls. The pattern of abundance of galls on *M. gemmulata* differed from the pattern on the super-host *Copaifera langsdorffii* (Oliveira et al. 2013). For *C. langsdorffii*, the hygrothermal stress defined the pattern of gall richness (Fernandes and Price 1988) during the dry season, while the abundance of the nine gall morphotypes of Cecidomyiidae were distributed by seasonal syndromes during the rainy and the dry season. Similarly to *M. gemmulata*, *C. langsdorffii* is a semideciduous host plant, but with the peak of leaf flushing at the end of the dry season. The galls on *C. langsdorffii* could be induced on young or mature leaves, while on *M. gemmulata* the leaf flushing was continuous, but the induction occured only on young leaves. These phenological patterns evidenced that the water availability, which the host plants were exposed to, directly influenced gall abundance and richness in each system.

The specific abundance of the five *Lopesia* leaf gall morphotypes in the rainy season on *M. gemmulata* could be explained by the rainfall, water potential, temperature and mature leaves, as evidenced by the canonical analysis of principal coordinates. The GG, and the CG were more associated with the rainfall, and water potential. These were the two largest leaf galls on *M. gemmulata,* so they probably required large quantities of water for their cellular developmental and physiological processes (Tyree and Jarvis 1982; Gall et al. 2015). The water stress in the dry season seemed to be a limiting factor for the development of the GG, and could result in the interruption of the gall life cycle. The temperature was more associated with the abundance of the BLG and the GLG. In the BLG, the redifferentiation and hypertrophy of the non-glandular trichomes confered protection against natural enemies, as well as against unfavorable environmental factors, such as temperature (Stone and Schönrogge 2003; Costa et al. 2018; Ferreira et al. 2019). Additionally, the trichomes could be related to the maintenance of an internal stable microclimate for the development of the Cecidomyiidae larvae (Dias et al. 2013; Carneiro et al. 2017; Costa et al. 2018), which could also occur due to the non-glandular trichomes of the GLG. The abundance of the LG was more influenced by the occurrence of mature leaves. As the LG had more generations throughout the year, its associated Cecidomyiidae adjusted better to the higher available photoassimilates of mature leaves, as proposed by Castro et al. (2013), Carneiro et al. (2014), Oliveira et al. (2017), and Zorić et al. (2019) for other gall systems. The increase on the production of photoassimilates due to the maximum intensity of mature leaves, and the abiotic variables in the rainy season were responsible for modulating the flowering in *M. gemmulata*. This result evidenced that the flowering phase did not affect the life cycles of the five leaf *Lopesia* gall morphotypes, and that the development of the galls and the flowering phase shared temporal photoassimilated resources.

For the *M. gemmulata-Lopesia* systems, leaf falling, and low water potential were direct strategies for reducing future losses to the nutrient sinks, and the investment in fruit development. These phenological responses were indirect strategies to the potential increasing in the mortality risk imposed to the populations of the galling Cecidomyiidae, and the low gall abundance (Williams and Whitham 1986). We believe that the abundance of the populations of the five galling *Lopesia* spp. were adjusted to the phenology of *M. gemmulata*, and to the seasonal water availability of the Neotropical climate.

Conclusions

As expected, water availability both in the environment and inside plant body was determinant for plant phenology and consequently for the gall life cycles, and for the patterns of gall abundance. The continuous leaf flushing of *M. gemmulata* favored the asynchrony among the *Lopesia* gall life cycles. This asynchronism indicated a temporal strategy for the multivoltine galling *Lopesia* spp. sharing the pinna-rachis as the microsite for their gall establishment.

The univoltine Lepidoptera gall cycle seemed to benefit from the peaks of mature leaves in *M. gemmulata* and the high production of photoassimilates drained to the stem gall. Altogether, current results evidenced peculiar phenological dynamics within a super-host plant toward guaranteeing favorable microsites for the success of their associated galling herbivores.

Supplementary Information The online version contains supplementary material available at https://doi.org/10.1007/s42965-021-00182-1.

Acknowledgements We thank Dra. Valéria Cid Maia and Dra. Sheila P. Carvalho-Fernandes of the Museu Nacional at Universidade Federal do Rio de Janeiro for confirming the five *Lopesia* associated with *M. gemmulata* are distinct but undescribed species. We thank to Dr. Paul Hanson of the Universidad de Costa Rica for help in the identification of the parasitoids. We thank Flávio Cotrim Costa, and Jorge Ferreira Silva for help in the sampling. E.C. Costa was financially supported by the Coordenação de Aperfeiçoamento de Pessoal de Nível Superior (CAPES) -Brazil fellowship (888877.199702/2018-00). We also thank Conselho Nacional de Desenvolvimento Científico e Tecnológico (CNPq) for the research scholarships to R.M.S. Isaias (304535/2019-2) and D.C. Oliveira (304981/2019-2).

Declarations

Conflict of interest The authors declare no conflict of interest.

References

Agostinelli C, Lund U (2017) R package circular: circular statistics (version 0.4-3). https://rforge.r-project.org/projects/circular

Alvares CA, Stape JL, Sentelhas PC, Moraes G, Leonardo J, Sparovek G (2013) Köppen's climate classification map for Brazil. Meteorol Z 22:711–728. https://doi.org/10.1127/0941-2948/2013/0507

Arduin M, Kraus JE, Montenegro G (1994) Morfologia e fenologia de galhas foliares de *Piptadenia gonoacantha* (Fabales, Mimosaceae). Revta Bras Ent 38:79–89

Basilio DS, Casagrande MM, Bordignon SAL, Moreira GRP (2015) Description and life history of a new cecidogenous species of *Palaeomystella Fletcher* (Lepidoptera. Momphidae) from Brazil. Rev Bras Entomol 59:188–196. https://doi.org/10.1016/j.rbe.2015.06.005

Bencke CSA, Morellato LPC (2002) Comparação de dois métodos de avaliação da fenologia de plantas, sua interpretação e representação. Rev Bras Bot 25:269–275

Camargo MGG, Carvalho GH, Alberton BC, Morellato LPC (2018) Leafing patterns and leaf exchange strategies of a cerrado woody community. Biotropica 50:442–454. https://doi.org/10.1111/btp.12552

Campos PT, Costa MCD, Isaias RMS, Moreira ASFP, Oliveira DC, Lemos-Filho JP (2010) Phenological relationships between two insect galls and their host plants: *Aspidosperma australe* and *A. spruceanum* (Apocynaceae). Acta Bot Bras 24:727–733. https://doi.org/10.1590/S0102-33062010000300016

Carneiro MA, Branco CSA, Braga CED, Almada ED, Costa MBM, Maia VC, Fernandes GW (2009) Are gall midge species (Diptera, Cecidomyiidae) host-plant specialists? Rev Bras Entomol 53:365–378. https://doi.org/10.1590/S0085-56262009000300010

Carneiro RGS, Burckhardt D, Isaias RMS (2013) Biology and systematics of gall-inducing triozids (Hemiptera: Psylloidea) associated with *Psidium* spp. (Myrtaceae). Zootaxa 3620:129–146

Carneiro RGS, Castro AC, Isaias RMS (2014) Unique histochemical gradients in a photosynthesis-deficient plant gall. S Afr J Bot 92:97–104. https://doi.org/10.1016/j.sajb.2014.02.011

Carneiro RGS, Isaias RMS, Moreira ASFP, Oliveira DC (2017) Reacquisition of new meristematic sites determines the development of a new organ, the Cecidomyiidae gall on *Copaifera langsdorffii* Desf. (Fabaceae). Front Plant Sci 8:1–10. https://doi.org/10.3389/fpls.2017.01622

Castro AC, Oliveira DC, Moreira ASFP, Lemos-Filho JP, Isaias RMS (2012) Source–sink relationship and photosynthesis in the horn-shaped gall and its host plant *Copaifera langsdorffii* Desf. (Fabaceae). S Afr J Bot 83:121–126. https://doi.org/10.1016/j.sajb.2012.08.007

Castro AC, Moreira ASFP, Oliveira DC, Isaias RMS (2013) Synchronism between *Aspidosperma macrocarpon* Mart. (Apocynaceae) resources allocation and the establishment of gall inducer *Pseudophacopteron* sp. (Hemiptera: Psylloidea). Rev Biol Trop 61:1891–1900

Condon MA, Scheffer SJ, Lewis ML, Wharton R, Adams DC, Forbes AA (2014) Lethal interactions between parasites and prey increase niche diversity in a tropical community. Science 343:1240–1244. https://doi.org/10.1126/science.1245007

Costa EC (2016) Galhas no Parque Estadual da Serra dos Montes Altos e Refúgio de Vida Silvestre: diversidade e desenvolvimento. Masters dissertation, Universidade do Estado da Bahia, Paulo Afonso

Costa EC, Carneiro GSC, Silva-Santos J, Isaias RMS (2018) Biology and development of galls induced by Lopesia sp (Diptera: Cecidomyiidae) on leaves of Mimosa gemmulata (Leguminosae: Caesalpinioideae). Aust J Bot 66:161–172. https://doi.org/10.1071/BT17099

Dalmolin AC, Lobo FA, Vourlitis G, Silva PR, Dalmagro HJ, Antunes MZ, Ortíz CER (2015) Is the dry season an important driver of phenology and growth for two Brazilian savanna tree species with contrasting leaf habits? Plant Ecol 2161:407–417. https://doi.org/10.1007/s11258-014-0445-5

Dias GG, Ferreira BG, Moreira GRP, Isaias RMS (2013) Developmental pathway from leaves to galls induced by a sap-feeding insect on Schinus polygamus (Cav) Cabrera (Anacardiaceae). An Acad Bras Ciênc 85:187–200. https://doi.org/10.1590/S0001-37652013000100010

Eça-Neves FF, Morellato LPC (2004) Métodos de amostragem e avaliação utilizados em estudos fenológicos de florestas tropicais. Acta Bot Bras 18:99–108. https://doi.org/10.1590/S0102-33062004000100009

Espirito-Santo MM, Fernandes GW (2007) How many species of gall-inducing insects are there on earth, and where are they? Ann Entomol Soc Am 100:95–99. https://doi.org/10.1603/0013-8746(2007)100[95:HMSOGI]2.0.CO;2

Fernandes GW, Price PW (1988) Biogeographical gradients in galling species richness: tests of hypotheses. Oecologia 76:161–167. https://doi.org/10.1007/BF00379948

Fernandes GW, Santos JC (eds) (2014) Neotropical insect galls. Springer, Dordrecht. https://doi.org/10.1007/978-94-017-8783-3_1

Ferreira BG, Álvarez R, Bragança GP, Alvarenga DR, Pérez-Hidalgo N, Isaias RMS (2019) Feeding and other gall facets: patterns and determinants in gall structure. Bot Rer 85:1–29. https://doi.org/10.1007/s12229-019-09207-w

Fournier LA (1974) Un método cuantitativo para la medición de características fenológicas en árboles. Turrialba 24:422–423

Franco AC, Bustamante MM, Caldas LS, Goldstein G, Meinzer FC, Kozovits AR, Rundel P, Coradin VTR (2005) Leaf functional

traits of Neotropical savanna trees in relation to seasonal water deficit. Trees 19:326–335. https://doi.org/10.1007/s00468-004-0394-z

Gall HL, Philippe F, Domom JM, Gilllet F, Pelloux J, Rayon C (2015) Cell wall metabolism in response to abiotic stress. Plants Basel 4:112–166. https://doi.org/10.3390/plants4010112

Garcia LC, Barros FV, Lemos-Filho JP (2017) Environmental drivers of leaf phenology of ironstone outcrops species under seasonal climate. An Acad Bras Ciênc 89:131–143

García-Núñez C, Pirela M, Fariñas M, Azócar A (2019) Seasonal patterns of gas exchange and water relations in juveniles of two Neotropical savanna tree species differing in leaf phenology. Acta Oecol 95:57–67. https://doi.org/10.1016/j.actao.2019.01.005

Guedes LM, Aguilera N, Ferreira BG, Becerra J, Hernández V, Isaias RMS (2018a) Anatomical and phenological implications between *Schinus polygama* (Cav.) (Cabrera) (Anacardiaceae) and the galling insect *Calophya rubra* (Blanchard) (Hemiptera: Psylloidea). Plant Biol 20:507–515. https://doi.org/10.1111/plb.12696

Guedes LM, Aguilera N, Ferreira BG, Becerra J, Pérez C, Hernández V, Isaias RMS (2018b) Factors influencing the morphogenesis of galls induced by *Calophya mammifex* (Calophyidae) on *Schinus polygama* (Anacardiaceae) leaves. Botany 96:589–599. https://doi.org/10.1139/cjb-2018-0078

Hawkins BA, Gagné RJ (1989) Determinants of assemblage size for the parasitoids of Cecidomyiidae (Diptera). Oecologia 81:75–88. https://doi.org/10.1007/BF00377013

Höglund S (2014) Timing of growth determines fitness and performance of a galling insect on willow. Ecol Entomol 39:159–167. https://doi.org/10.1111/een.12078

INMET-Instituto Nacional de Meteorologia (2019) Normais Climatológicas do Brasil 1981–2010. http://www.inmet.gov.br/portal/index.php?r=clima/normaisClimatologicas

Isaias RMS, Carneiro RGS, Oliveira DC, Santos JC (2013) Illustrated and annotated checklist of Brazilian gall morphotypes. Neotrop Entomol 42:230–239. https://doi.org/10.1007/s13744-013-0115-7

Kishimoto-Yamada K, Itioka T (2015) How much have we learned about seasonality in tropical insect abundance since Wolda (1988)? Entomol Sci 18:407–419. https://doi.org/10.1111/ens.12134

Legendre P, Anderson MJ (1999) Distance-based redundancy analysis: testing multispecies responses in multifactorial ecological experiments. Ecol Monogr 69:1–24. https://doi.org/10.1890/0012-9615(1999)069[0001:DBRATM]2.0.CO;2

Lemos-Filho JP, Mendonça-Filho CV (2000) Seasonal changes in the water status of three wood legumes from the Atlantic forest, Caratinga, Brazil. J Trop Ecol 16:21–32

Magalhães TA, Oliveira DC, Isaias RMS (2014) Population dynamics of the gall inducer *Eriogallococcus isaias* (Hemiptera: Coccoidea: Eriococcidae) on *Pseudobombax grandiflorum* (Malvaceae). J Nat Hist 49:7891–7913. https://doi.org/10.1080/00222933.2014.951083

Mendonça MS (2001) Galling insect diversity patterns: the resource synchronization hypothesis. Oikos 95:171–176. https://doi.org/10.1034/j.1600-0706.2001.950120.x

Mendonça MS, Romanowski HP (2012) Population ecology of the multivoltine Neotropical gall midge *Eugeniamyia dispar* (Diptera, Cecidomyiidae). Iheringia Sér Zool 102:170–176. https://doi.org/10.1590/S0073-47212012000200009

Miller DG, Raman A (2018) Host–plant relations of gall-inducing insects. Ann Entomol Soc Am 10:1–19. https://doi.org/10.1093/aesa/say034

Moreira GRP, Eltz RP, Pase RB, Silva GT, Bordignon SAL, Mey W, Gonçalves GL (2017) *Cecidonius pampeanus*, gen. et sp. n.: an overlooked and rare, new gall-inducing micromoth associated with *Schinus* in southern Brazil (Lepidoptera, Cecidosidae). ZooKeys 695:37–74. https://doi.org/10.3897/zookeys.695.13320

Nakadai R, Hashimoto K, Iwasaki T, Sato Y (2018) Geographical co-occurrence of butterfly species: the importance of niche filtering by host plant species. Oecologia 186:995–1005. https://doi.org/10.1007/s00442-018-4062-1

Oksanen J, Kindt R, Legendre P, O'Hara B, Stevens MHH, Oksanen MJ, Suggests MASS (2007) The vegan package. Commun Ecol Package 10:631–637

Oliveira DC, Isaias RMS (2009) Influence of leaflet age in anatomy and possible adaptive values of the midrib gall of *Copaifera langsdorffii* (Fabaceae: Caesalpinioideae). Rev Biol Trop 57:293–302. https://doi.org/10.15517/rbt.v57i1-2.11322

Oliveira DC, Mendonça MS, Moreira ASFP, Lemos-Filho JP, Isaias RMS (2013) Water stress and phenological synchronism between *Copaifera langsdorffii* (Fabaceae) and multiple galling insects: formation of seasonal patterns. J Plant Interact 8:225–233. https://doi.org/10.1080/17429145.2012.705339

Oliveira DC, Isaias RMS, Fernandes GW, Ferreira BG, Carneiro RGS, Fuzaro L (2016) Manipulation of host plant cells and tissues by gall-inducing insects and adaptive strategies used by different feeding guilds. J Insect Physiol 84:103–113. https://doi.org/10.1016/j.jinsphys.2015.11.012

Oliveira DC, Moreira ASFP, Isaias RMS, Martini VC, Rezende UC (2017) Sink Status and Photosynthetic Rate of the Leaflet Galls Induced by *Bystracoccus mataybae* (Eriococcidae) on *Matayba guianensis* (Sapindaceae). Front Plant Sci 8:1–12. https://doi.org/10.3389/fpls.2017.01249

Pedroni F, Sanchez M, Santos FAM (2002) Fenologia da copaíba (*Copaifera langsdorffii* Desf. Leguminosae, Caesalpinioideae) em uma floresta semidecídua no sudeste do Brasil [Phenology of copaiba (*Copaifera langsdorffii* Desf. Leguminosae, Caesalpinioideae) in a semideciduous forest in southeast Brazil. Rev Bras Bot 25:183–194. https://doi.org/10.1590/S0100-84042002000200007

Pfeffer L, Rezende UC, Barônio GJ, Oliveira DC (2018) Building two houses on a single host plant: galling insect synchronizes its life cycle with plant phenology. Oecol Aust 22:438–448. https://doi.org/10.4257/oeco.2018.2204.07

Pianka ER (1974) Niche overlap and diffuse competition. Proc Natl Acad Sci 71:2141–2145. https://doi.org/10.1073/pnas.71.5.2141

R Core Team (2020) R: a language and environment for statistical computing. R Foundation for Statistical Computing, Vienna, Austria. https://www.R-project.org/

Rezende UC, Moreira ASFP, Kuster VC, Oliveira DC (2018) Structural, histochemical and photosynthetic profiles of galls induced by *Eugeniamyia dispar* (Diptera: Cecidomyiidae) on the leaves of *Eugenia uniflora* (Myrtaceae). Rev Biol Trop 66:1469–1480. https://doi.org/10.15517/rbt.v66i4.32531

Rezende UC, Custódio JF, Kuster VC, Gonçalves LA, Oliveira DC (2019) How the activity of natural enemies changes the structure and metabolism of the nutritive tissue in galls? Evidence from the *Palaeomystella oligophaga* (Lepidoptera)—*Macairea radula* (Metastomataceae) system. Protoplasma 256:669–667. https://doi.org/10.1007/s00709-018-1321-2

Santos-Silva J, Simon MF, Tozzi AMGA (2015) Revisão taxonômica das espécies de Mimosa ser. Leiocarpae *sensu lato* (Leguminosae Mimosoideae). Rodriguésia 66:95–154. https://doi.org/10.1590/2175-7860201566107

Scholander PF, Bradstreet ED, Hemmingsen EA, Hammel HT, Bradstreet DE, Hemmingsen EA (1965) Sap pressure in vascular plants: negative hydrostatic pressure can be measured in plants. Science 148:339–346. https://doi.org/10.1126/science.148.3668.339

Shorthouse JD, Wool D, Raman A (2005) Gall-inducing insects—nature's most sophisticated herbivores. Basic Appl Ecol 6:407–411. https://doi.org/10.1016/j.baae.2005.07.001

Silva AR, Nogueira RM, Costa EC, Carvalho-Fernandes SP, Silva-Santos J (2018) Occurrence and characterization of entomogenic galls in an area of Cerrado sensu stricto and the state of Bahia, Brazil. An Acad Bras Ciênc 90:2903–2919. https://doi.org/10.1590/0001-3765201820170522

Stone GN, Schönrogge K (2003) The adaptive significance of insect gall morphology. Trends Ecol Evol 18:512–522. https://doi.org/10.1016/S0169-5347(03)00247-7

Tokuda M (2012) Biology of Asphondyliini (Diptera: Cecidmyiidae). Entomol Sci 15:361–383. https://doi.org/10.1111/j.1479-8298.2012.00539.x

Toma TSP, Mendonça MS (2014) Population ecology of galling arthropods in the Neotropics. In: Fernandes GW, Santos JC (eds) Neotropical insect galls. Springer, New York, pp 69–98. https://doi.org/10.1007/978-94-017-8783-3_5

Tyree M, Jarvis PG (1982) Water in tissues and cells. In: Lange OL, Nobel PS, Osmond CB, Ziegler H (eds) Physiological plant ecology II. Springer, Berlin, pp. 36–77. https://doi.org/10.1007/978-3-642-68150-9_3

Weis AE, Walton R, Crego CL (1988) Reactive plant tissue sites and the population biology of gall makers. Annu Rev Entomol 33:467–486. https://doi.org/10.1146/annurev.en.33.010188.002343

Williams AG, Whitham TG (1986) Premature leaf abscission: an induced plant defense against gall aphids. Ecology 67:1619–1627

Wolda H (1988) Insect seasonality: why? Annu Rev Ecol Evol Syst 19:1–18. https://doi.org/10.1146/annurev.es.19.110188.000245

Yukawa J (2000) Synchronization of gallers with host plant phenology. Popul Ecol 42:105–113. https://doi.org/10.1007/2FPL00011989

Yukawa J, Ichinose M, Kim W, Uechi N, Gyotoku N, Fujii T (2015) Lower development threshold temperatures and thermal constants for four species of *Asphondylia* (Diptera: Cecidomyiidae) in Japan and their larval developmental delay caused by heat stress. Appl Entomol Zool 51:71–80. https://doi.org/10.1007/s13355-015-0372-5

Yukawa J, Moriya T, Kanmiya K (2019) Comparison in the flight ability between the soybean pod gall midge, *Asphondylia yushimai* and the aucuba fruit gall midge, *A. aucubae* (Diptera: Cecidomyiidae). Appl Entomol Zool 54:167–174. https://doi.org/10.1007/s13355-019-00609-1

Zorić AS, Morina F, Toševski I, Tosti T, Jović J, Krstić O, Veljović-Jovanović S (2019) Resource allocation in response to herbivory and gall formation in *Linaria vulgaris*. Plant Physiol Biochem 135:224–232. https://doi.org/10.1016/j.plaphy.2018.11.032

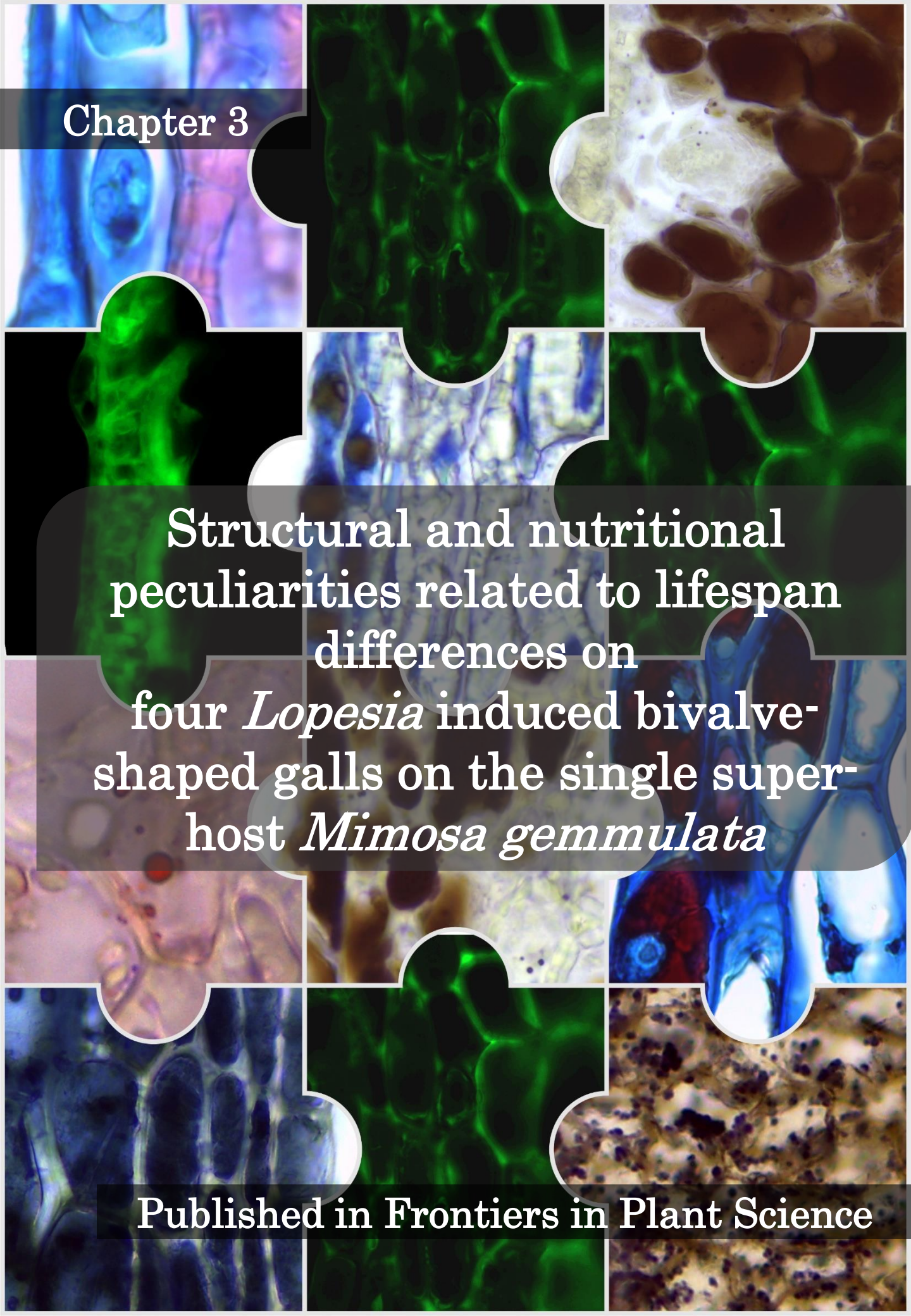

Chapter 3

Structural and nutritional peculiarities related to lifespan differences on four *Lopesia* induced bivalve-shaped galls on the single super-host *Mimosa gemmulata*

Published in Frontiers in Plant Science

frontiers in Plant Science

ORIGINAL RESEARCH
published: 17 May 2021
doi: 10.3389/fpls.2021.660557

Structural and Nutritional Peculiarities Related to Lifespan Differences on Four *Lopesia* Induced Bivalve-Shaped Galls on the Single Super-Host *Mimosa gemmulata*

*Elaine C. Costa[1], Denis C. Oliveira[2], Dayse K. L. Ferreira[1] and Rosy M. S. Isaias[1]**

[1] Departamento de Botânica, Instituto de Ciências Biológicas, Universidade Federal de Minas Gerais, Belo Horizonte, Brazil,
[2] Instituto de Biologia, Universidade Federal de Uberlândia, Uberlândia, Brazil

Super-host plants are elegant models to evaluate the peculiarities of gall structural and nutritional profiles due to the stimuli of distinct gall inducers in temporal and spatial perspectives. Galls induced by congeneric insects, *Lopesia* spp. (Diptera, Cecidomyiidae) on the same host plant, *Mimosa gemmulata* Barneby (Fabaceae) were analyzed to estimate if variations of 1 or 2 months in gall lifespans may result in differences over the accumulation of nutritional resources, and their compartmentalization both in cell walls and protoplasm. *Mimosa gemmulata* hosts four *Lopesia*-induced galls: the lenticular bivalve-shaped gall (LG) with a 2-month life cycle, the brown lanceolate bivalve-shaped gall (BLG) and the green lanceolate bivalve-shaped gall (GLG) with 3 month-life cycles, and the globoid bivalve-shaped gall (GG) with a 4 month-life cycle. The comparisons among the four *Lopesia* galls, using anatomical, histometric, histochemical, and immunocytochemical tools, have demonstrated that the longest lifespan of the GG related to its highest increment in structural and nutritional traits compared with the LG, GLG, and BLG. The differences among the tissue stratification and cell wall thickness of the galls with the 2-month and the 3-month lifespans were subtle. However, the GG had thicker cell walls and higher stratification of the common storage tissue, schlerenchymatic layers and typical nutritive tissue than the other three gall morphospecies. The higher tissue thickness of the GG was followed by the formation of a bidirectional gradient of carbohydrates in the protoplasm, and the detection of xyloglucans in cell walls. Current data supported the presumption that the longest the lifespan, the highest the impact over the structural and nutritional metabolism of the *Lopesia* galls associated to *M. gemmulata*.

Keywords: cell walls, gall anatomy, hemicelluloses, histochemistry, immunocytochemistry, *Lopesia* galls

OPEN ACCESS

Edited by:
Brigitte Mauch-Mani, Université de Neuchâtel, Switzerland

Reviewed by:
Valéria Maia, Federal University of Rio de Janeiro, Brazil
Man-Miao Yang, National Chung Hsing University, Taiwan

***Correspondence:**
Rosy M. S. Isaias
rosy@icb.ufmg.br

Specialty section:
This article was submitted to Plant Pathogen Interactions, a section of the journal Frontiers in Plant Science

Received: *29 January 2021*
Accepted: *19 April 2021*
Published: *17 May 2021*

Citation:
Costa EC, Oliveira DC, Ferreira DKL and Isaias RMS (2021) Structural and Nutritional Peculiarities Related to Lifespan Differences on Four Lopesia Induced Bivalve-Shaped Galls on the Single Super-Host Mimosa gemmulata. Front. Plant Sci. 12:660557. doi: 10.3389/fpls.2021.660557

INTRODUCTION

The gall lifespans depend on structural, cytological, and chemical traits on the host plant cells stimulated by the associated galling organisms (Mani, 1964; Oliveira et al., 2010, 2016; Jorge et al., 2018; Ferreira et al., 2019; Chen et al., 2020). Any changes in the galling organism behavior may lead to the disruption of the gall life cycle (Rezende et al., 2019) and compromise gall

developmental stages. In mature galls, the specialized tissues are established and organized in specific compartments (Bragança et al., 2017), which store energy-rich molecules that support the galling organism nutritional requirements (Mani, 1964; Ferreira et al., 2017). Cecidomyiidae galls, for instance, can have two types of storage tissues: the common storage tissue and the typical nutritive tissue, which are commonly spatially separated by schlerenchymatic layers (Meyer and Maresquelle, 1983; Bronner, 1992; Rohfritsch, 1992). The common storage tissue is located in the gall outer tissue compartment, while the typical nutritive tissue is located in the gall inner tissue compartment, which is in contact with the larval chamber (Bragança et al., 2017).

The cells of the common storage tissue have inconspicuous nuclei, large vacuoles, thin cytoplasm, and accumulate energetic metabolites related to gall growth and metabolism. The storage tissue also supports the nutritive tissue by cell-to-cell translocation of solutes (Moura et al., 2008; Oliveira et al., 2010; Ferreira and Isaias, 2014). The cells of the typical nutritive tissue have conspicuous nuclei, fragmented vacuoles, and dense protoplasm, which accumulate energetic metabolites related to the nutrition of the gall inducer (Bronner, 1992; Oliveira et al., 2010, 2011a; Ferreira et al., 2015). The additional accumulation of carbohydrates in cell walls have been recently evaluated in nematode-induced galls (Ferreira et al., 2020) and in insect-galls (Bragança et al., 2020a), with peculiarities regarding the type and distribution of hemicellulose epitopes. The hemicelluloses, xyloglucans and heteromannans, integrate the primary or secondary cell walls, may regulate cell expansion (Cosgrove, 2016, 2018), and have also been related to the galling organism maintenance (Bragança et al., 2020a; Ferreira et al., 2020). In an overall analysis, the storage and nutritive tissues accumulate different metabolites in Cecidomyiidae galls (Bronner, 1992; Moura et al., 2008; Oliveira et al., 2010) but can perform specific functions in the diverse host plant-galling insect systems (Amorim et al., 2017; Bragança et al., 2017). Accordingly, the longer the galling insect stay inside the gall, the higher the gall demand is (Carneiro et al., 2017), therefore, the long-life cycle of the galling insect may determine more complex gall structural profiles (Gonçalves et al., 2005). Such presumption may be analyzed in the nutritional perspective, and the accumulation of energetic resources in gall storage tissues can be higher, the longer the gall lifespan is, which may be elegantly evaluated in super-host plants with several associated galling-insects (Formiga et al., 2014; Amorim et al., 2017; Bragança et al., 2020a; Costa et al., submitted).

Currently, we use anatomical, histometric, histochemical, and immunocytochemical tools to evaluate the structural and nutritional profiles of four bivalve-shaped galls induced by four undescribed new species of *Lopesia* (Rübsaamen, 1908) (Diptera-Cecidomyiidae; Maia and Carvalho-Fernandes personal communication) in temporal and spatial perspectives on the super-host *Mimosa gemmulata* Barneby (Fabaceae). These galls have distinct lifespans and their gall-inducing *Lopesia* species have multivoltine life cycles whose durations vary in 2-, 3-, or 4-months (Costa et al., submitted). We expect that variations of 1 or 2 months in gall lifespans may result in differences over the accumulation of nutritional resources, and their compartmentalization both in cell walls and protoplasm. The following questions are addressed: (1) are there distinct peculiarities in the structural profiles among the four *Lopesia* galls regarding tissue compartments? And (2) may the nutritional profiles of the four *Lopesia* galls vary in response to the 1–2-month-temporal distinction?

MATERIALS AND METHODS

The Lifespans of *Lopesia* Galls on *M. gemmulata*

The four *Lopesia* galls induced on *M. gemmulata* pinna-rachis are the lenticular bivalve-shaped gall (LG), the green lanceolate bivalve-shaped gall (GLG), the brown lanceolate bivalve-shaped gall (BLG), and the globoid bivalve-shaped gall (GG). The four *Lopesia* spp. have multivoltine life cycles and each bivalve-shaped gall have distinct developmental times, with the maturation as the longest stage of development. The LG has six life cycles a year, the BLG and GLG have four life cycles a year, and the GG has three cycles a year (Costa et al., submitted). The LG has a 2-month life cycle, with the maturation stage lasting ≅ 30–45 days. The BLG and GLG have 3 month-life cycles, with the maturation stage lasting ≅ 45–60 days. The GG has a 4 month-life cycle, with the maturation stage lasting ≅ 60–75 days.

Structural Analysis

Samples of the non-galled pinna-rachis (control) and of the LG, GLG, BLG, and GG (mature galls with live larvae) were collected (n = 5 for each gall system) from individuals of *M. gemmulata* (n = 5) in a Cerrado area located at Serra Geral, municipality of Caetité, state of Bahia, Brazil (14°04′36.8″S, 42°29′59″W) on March 2019. For anatomical and immunocytochemical analyses, a set of fragments of the pinna-rachis, LG, GLG, BLG, and GG (n = 8 for each gall morphospecies) were fixed in 2.5% glutaraldehyde and 4.5% formaldehyde in 0.1 mol.L^{-1} (Karnovsky, 1965, modified to pH 7.2 phosphate buffer), for 48 h at room temperature. The fixed fragments were dehydrated in an ethanol series and embedded in Paraplast® (Kraus and Arduin, 1997). The sections (12 μm) were obtained in a rotary microtome (Leica® BIOCUT 2035), deparaffinized in butyl acetate, and hydrated in an ethanol series (Kraus and Arduin, 1997). The sections (n = 5 for each category) were stained in Astra blue and safranin (9:1, v/v) (Bukatsch, 1972, modified to 0.5%) dehydrated in an ethanol-butyl acetate series (Kraus and Arduin, 1997), and mounted using colorless varnish Acrilex® (Paiva et al., 2006). A second set of fragments of the pinna-rachis and of the four mature *Lopesia* galls (n = 17 for each gall morphospecies) was used for histochemical analysis. The histological slides were analyzed and photographed under a light microscope (Leica® DM500) with a coupled digital camera (Leica® ICC50 HD).

Histometric Analysis

The thickness of the common storage tissue, schlerenchymatic layers, and typical nutritive tissue, as well as the respective cell walls, were measured in the LG, BLG, GLG, and GG (n = 5 galls,

one section per gall, 5 measurement fields per section, totalizing 25 measurements by tissue for each gall morphospecies). The data were compared using one-way ANOVA followed by Tukey's test, using $\alpha = 0.05$. The tests were performed with SigmaStat® (Systat Software, Inc., Chicago, Illinois) and the graphics were done with GraphPad prism 5.0®.

Histochemical Analysis

Free-handmade sections from fresh samples of the pinna-rachis, LG, GLG, BLG, and GG ($n = 7$ for each gall morphospecies) and Paraplast® embedded sections obtained in a rotary microtome were submitted to histochemical analyses. Starch grains were detected with Lugol's reagent (1% potassium iodine-iodide solution) for 5 min (Johansen, 1940). Reducing sugars were detected by Fehling's reagent (Solution A: 7.9% copper sulfate, and solution B: 34.6% sodium potassium tartrate and 1% sodium hydroxide) heated to pre-boiling temperature (Sass, 1951). Proteins were detected by 0.1% bromophenol blue in a saturated solution of 10% magnesium chloride in ethanol during 15 min, washed in 0.5% acetic acid in water during 20 min, and water for 3 min (Mazia et al., 1953). Lipids were detected with a saturated solution of Sudan Red B in 70 GL ethanol during 5 min (Brundett et al., 1991). Black sections were used as controls. The sections were analyzed and photographed under a light microscope (Leica® DM500) coupled to a digital camera (Leica® ICC50 HD).

Immunocytochemical Analysis

The detection of hemicelluloses was performed in the sections of the pinna-rachis, LG, GLG, BLG, and GG ($n = 3$ for each category) obtained in a rotary microtome. The sections were pre-incubated in pectate lyase at 10 μg/mL, diluted in 50 mM N-cyclohexyl-3-aminopropane sulfonic acid (CAPS) and 2 mM $CaCl_2$ buffer, pH 10, for 2 h at room temperature (Marcus et al., 2008). Afterward, the sections were incubated in the primary monoclonal antibodies (MAbs), LM15 and LM21, diluted in block solution [5% powder milk in phosphate-buffered saline-PBS) 0.1 mol L^1, pH 7.2 (1:5, *w*/*v*)] for the labeling of the epitopes of xyloglucans (Marcus et al., 2008) and heteromannans (Marcus et al., 2010), respectively, for 90 min in the darkness. The sections were washed in PBS and incubated in the secondary antibody anti-rat IgG linked to FITC, diluted in 5% powder milk/PBS (1:100, *w*/*v*), for 90 min in darkness. The slides were mounted in 50% glycerin, analyzed and photographed under a fluorescence microscope (Leica® DM 2500 LED), with blue excitation light (450–490 nm) and green emission light (515 nm), coupled to a digital camera (Leica® DFC 7000T). The immunocytochemical images were submitted to intensity measurement using ImageJ version 1.51k[1]. The fluorescence intensities of the epitopes of hemicelluloses were evaluated by grayscale methodology (Gy = Gray value) with triplicate analysis for each tissue. After the measurements, we proposed the following categories: (−) negative (= 0 Gy values); (+) weak (10–20 Gy values); (++) moderate (21–39.99 Gy values); and (+++) intense (≥40 Gy values).

[1]http://rsb.info.nih.gov/ij

RESULTS

Non-galled Pinna-Rachis Profile (Control)

The pinna-rachis of *M. gemmulata* (**Figure 1A**) has uniseriated epidermis with glandular and non-glandular trichomes (**Figure 1B**). The adaxial cortical parenchyma is homogeneous with 3–4 cell layers. The vascular tissues have bicollateral arrangement and are surrounded by two layers of pericyclic fibers (**Figure 1B**). Starch (**Figure 1C**), reducing sugars (**Figure 1D**), proteins (**Figure 1E**), and lipidic droplets (**Figure 1F**) accumulate in the protoplasm of parenchyma cells. In the pinna-rachis, the epitopes of xyloglucans recognized by LM15 (24 Gy; **Figure 1G**) and the epitopes of heretomannans recognized by LM21 (30.4 Gy; **Figure 1H**) are moderately labeled in the parenchyma cell walls.

Profiles of *Lopesia* Galls

Structural Profiles

The *Lopesia* galls are green (LG, GLG, and GG) or brown (BLG), isolated, pubescent (**Figures 2A–D**), and developed by pinna-rachis cell redifferentiation and tissue reorganization. In the four *Lopesia* galls, the epidermis, common storage tissue, vascular tissues, and schlerenchymatic layers form the gall outer compartment and the typical nutritive tissue forms the gall inner compartment (**Figures 2E–H**). In the LG, the common storage tissue has 4–5 cell layers (**Figure 2I**), the schlerenchyma has 1–2 layers, and the typical nutritive tissue has 1–2 cell layers (**Figure 2J**). In the GLG, the common storage tissue has 10–11 cell layers (**Figure 2K**), the schlerenchyma has 1–2 layers, and the typical nutritive tissue has 1–2 cell layers (**Figure 2L**). In the BLG, the common storage tissue has 8–9 cell layers (**Figure 2M**), the schlerenchyma has 4–5 layers, and the typical nutritive tissue has 1–2 cell layers (**Figure 2N**). In the GG, the common storage tissue has 10–11 cell layers (**Figure 2O**), the schlerenchyma has 7–8 layers, and the typical nutritive tissue has 5–6 cell layers (**Figure 2P**).

Histometric Profiles

In accordance with structural description, GG tissues are thicker than the tissues of the other three *Lopesia* galls (**Figure 3**). The GG common storage tissue is 177% thicker than that of the LG ($p < 0.001$), and 249% thicker than that of the BLG ($p < 0.001$), but there is no significant difference between the GG and the GLG regarding the thickness of the common storage tissue (**Figure 3A**). The GLG common storage tissue is 249% thicker than that of the BLG ($p < 0.001$). The GG schlerenchyma is 2,009% thicker than that of the LG ($p < 0.001$), and 2,495% thicker than that of the GLG ($p < 0.001$), but there is no significant difference between the GG and the BLG regarding the thickness of the schlerenchyma (**Figure 3B**). The BLG schlerenchyma is 348% thicker than that of the GLG ($p < 0.001$). There is no significant difference among the schlerenchyma thickness of the GL, the GLG and the BLG (**Figure 3B**). The GG typical nutritive tissue is 772% thicker than that of the LG ($p < 0.001$), and 813% thicker than that of the GLG ($p < 0.001$), but there is no significant difference between the GG and the BLG

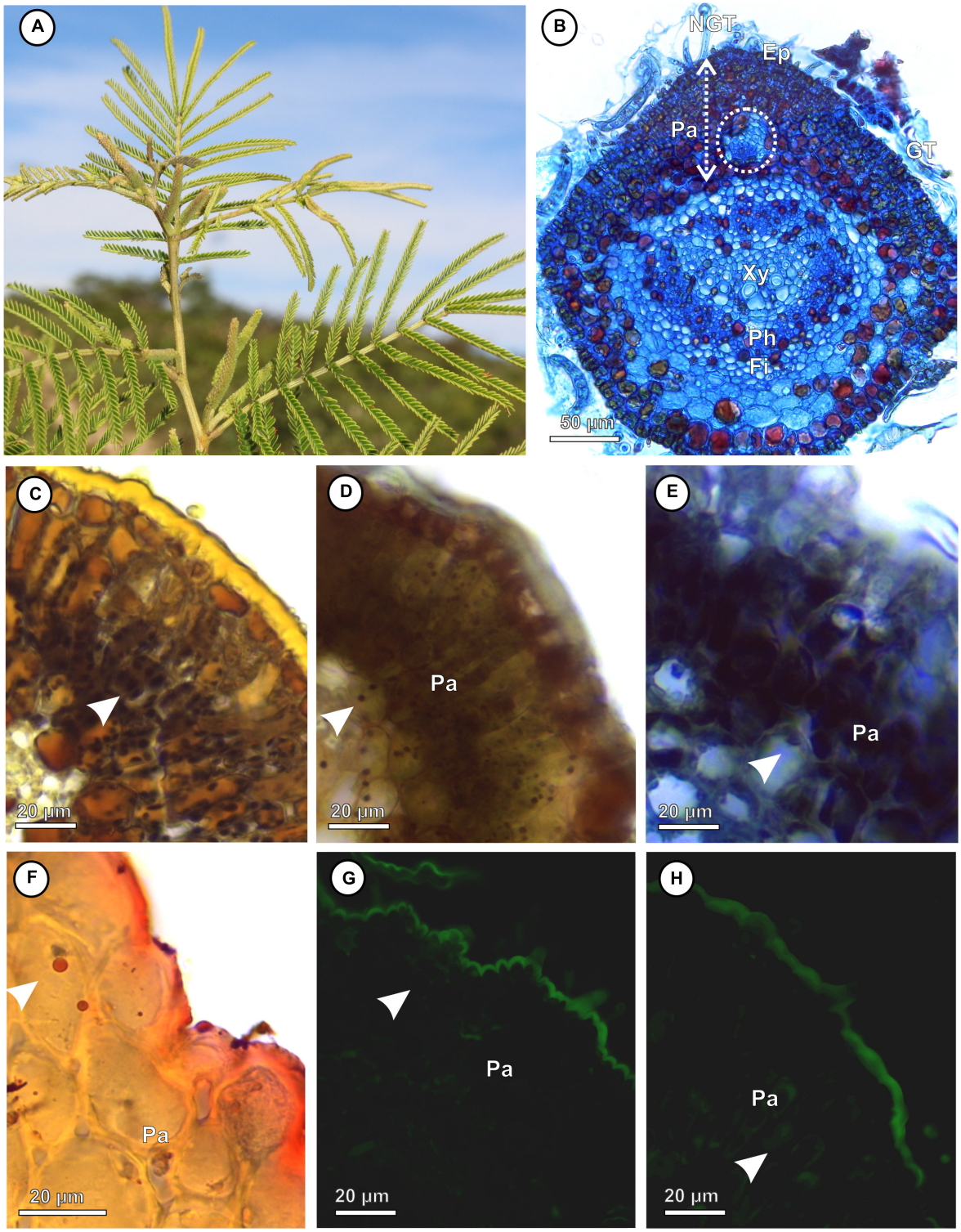

FIGURE 1 | Non-galled pinna-rachis of *Mimosa gemmulata* Barneby (Fabaceae). **(A)** General aspect of non-galled leaves. **(B–H)** Transverse sections. **(B)** Anatomical profile. **(C,D)** Immunocytochemical profile. **(C–F)** Histochemical profile. **(C)** Starch grains stained in black (white arrowhead). **(D)** Reducing sugars stained in brown (white arrowhead). **(E)** Proteins stained in blue (white arrowhead). **(F)** Lipidic droplets stained in red (white arrowhead). **(G,H)** Xyloglucans detected by LM15 in cell walls of parenchyma (white arrowhead). **(H)** Heteromannans detected by LM21 in cell walls of parenchyma (white arrowheads). Ep, Epidermis; Fi, fibers; GT, glandular trichomes; NGT, non-glandular trichomes; Pa, parenchyma; Ph, Phloem; Xy, Xylem.

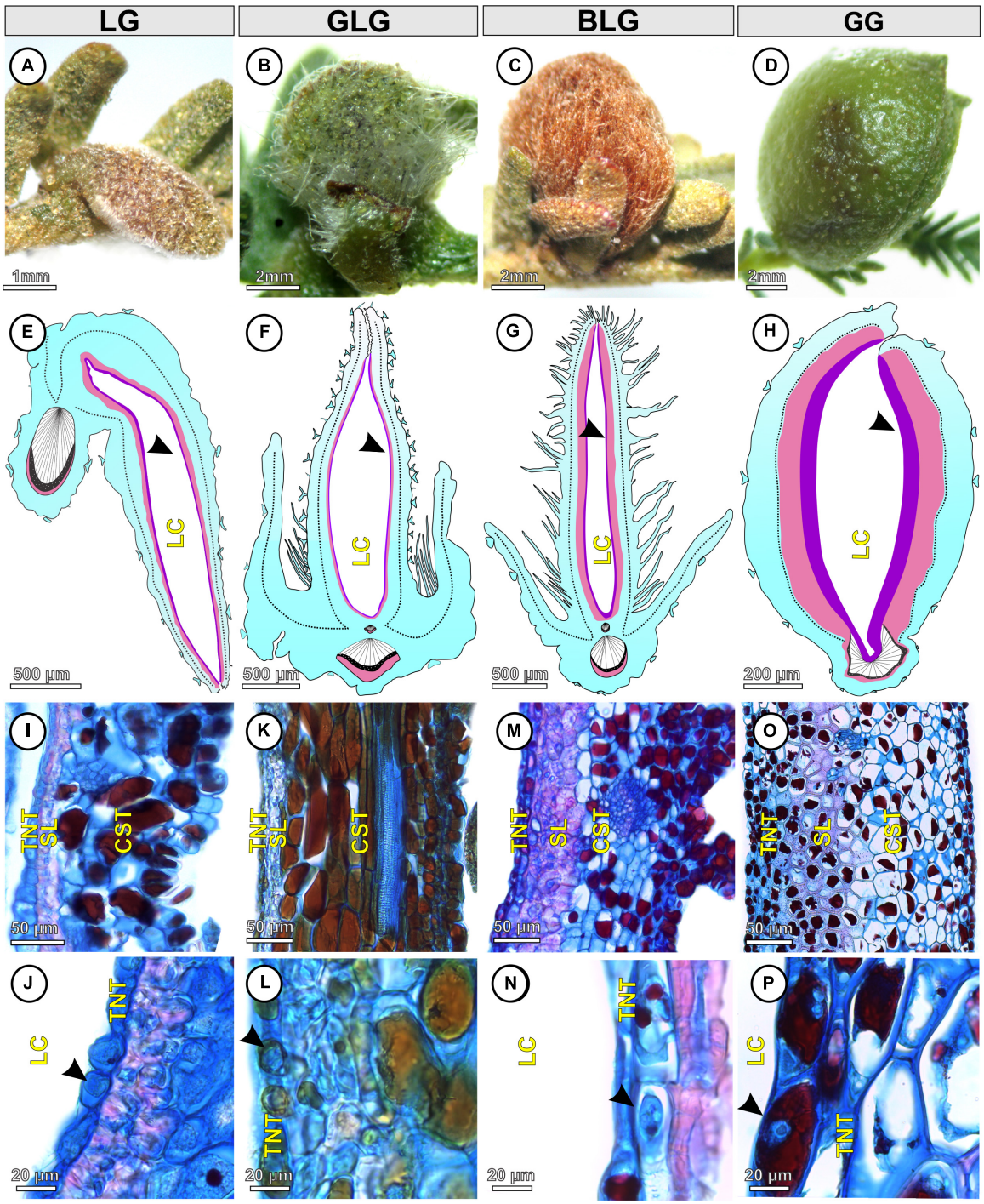

FIGURE 2 | Structural profiles of the four *Lopesia* galls on *Mimosa gemmulata* Barneby (Fabaceae) pinna-rachis in transverse sections. **(A–D)** Macroscopic aspect of the galls. **(A,E)** Lenticular bivalve-shaped gall. **(B,F)** Green lanceolate bivalve-shaped gall. **(C,G)** Brown lanceolate bivalve-shaped gall. **(D,H)** Globoid bivalve-shaped gall. **(E–H)** Diagram of the *Lopesia* galls, evidencing common storage tissues (blue), schlerenchymatic layers (pink) in the outer tissue compartments, and typical nutritive tissues (purple–black arrowheads) in the inner tissue compartments. **(I,J)** Lenticular bivalve-shaped gall, evidencing common storage tissue, schlerenchymatic layer and typical nutritive cells with evident nuclei (black arrowhead). **(K,L)** Green lanceolate bivalve-shaped gall, evidencing common storage tissue, schlerenchymatic layer and typical nutritive cells with evident nuclei (black arrowhead). **(M,N)** Brown lanceolate bivalve-shaped gall, evidencing common storage tissue, schlerenchymatic layer and typical nutritive cells with evident nuclei (black arrowhead). **(O,P)** Globoid bivalve-shaped gall, evidencing common storage tissue, schlerenchymatic layer and typical nutritive cells with evident nuclei (black arrowhead). BLG, brown lanceolate bivalve-shaped gall; CST, common storage tissue; GG, globoid bivalve-shaped gall; GLG, green lanceolate bivalve-shaped gall; LC, larval chamber; LG, lenticular bivalve-shaped gall; SL, schlerenchymatic layer; TNT typical nutritive tissue.

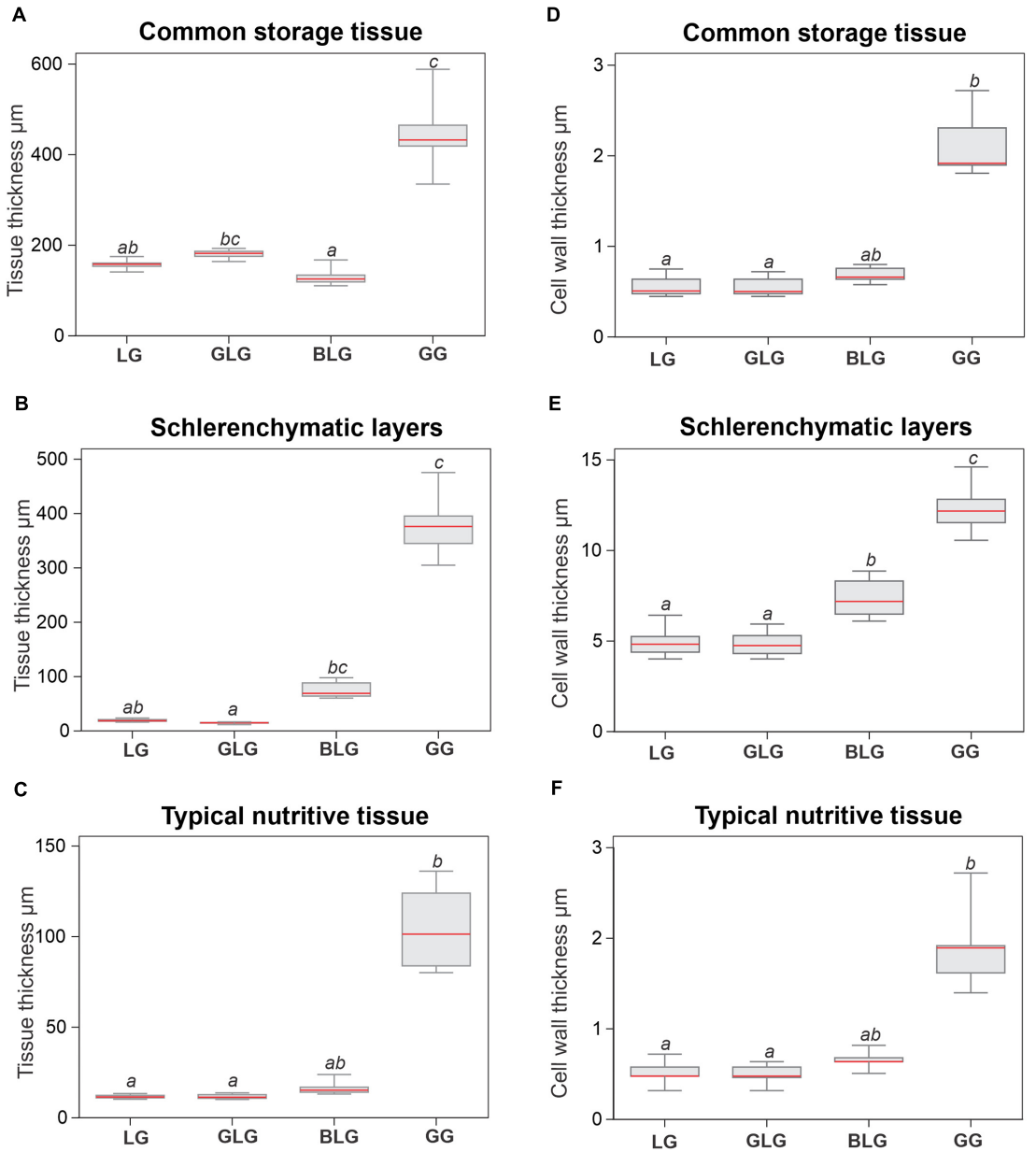

FIGURE 3 | Histometry of the tissues and cell walls of the four *Lopesia* galls on *Mimosa gemmulata* Barneby (Fabaceae) pinna-rachis **(A–C)** Tissue thickness. **(D–F)** Cell wall thickness. BLG, brown lanceolate bivalve-shaped gall, GG, globoid bivalve-shaped gall, GLG, green lanceolate bivalve-shaped gall, LG, lenticular bivalve-shaped gall. $n = 5$ per gall systems (5 regions per section from 1 sections); $p < 0.05$. Same letters on bars indicate statistically equal values for the same variable, and different letters indicate different values.

regarding the thickness of the typical nutritive tissue (**Figure 3C**). There is no significant difference of the typical nutritive tissue thickness among the LG, GLG, and BLG.

The cell walls of the schlerenchyma are thicker than the cell walls of the common storage and typical nutritive tissues on the four *Lopesia* galls (**Figures 3D–F**). The cell walls of the GG schlerenchyma are 141% thicker than the cell walls of the LG, 160% thicker than the cell walls of the GLG, and 76% thicker than the cell walls of the BLG ($p < 0.001$). The cell walls of the BLG schlerenchyma are 48% thicker than the cell walls of the GLG, and 37% thicker than the cell walls of the LG ($p < 0.001$). There is no significant statistical difference between the cell wall thickness of the schlerenchyma of the LG and GLG ($p = 0.958$). The cell walls of the GG storage and typical nutritive tissues are thicker than the cell walls of the GL and GLG ($p < 0.001$). There is no significant difference among in the cell wall thickness of the common storage tissues (**Figure 3D**) and typical nutritive tissues (**Figure 3F**) among the GL, GLG, and GBG.

TABLE 1 | Histochemical profiles of the four *Lopesia* galls on *Mimosa gemmulata* (Fabaceae).

	Outer compartment								Inner compartment			
	Common storage tissue				Schlerenchymatic layer				Typical nutritive tissue			
	LG	GLG	BLG	GG	LG	GLG	BLG	GG	LG	GLG	BLG	GG
Histochemistry												
Starch	+	+	+	+	−	−	−	+		−	−	+
Reducing sugars	+	+	+	+	−	−	−	+	+	+	+	+
Proteins	+	+	+	+	−	−	+	+	+	+	+	+
Lipids	+	+	+	+	+	+	−	+	+	+	+	+

BLG, brown lanceolate bivalve-shaped gall; LG, lenticular bivalve-shaped gall; GG, globoid bivalve-shaped gall; GLG, green lanceolate bivalve-shaped gall. The symbols indicate (−) absence and (+) presence.

Histochemical Profiles

Starch, reducing sugars, proteins, and lipids are detected both in the non-galled pinna-rachis and in the *Lopesia* galls (**Table 1**). Starch grains are detected only in the protoplasm of the common storage tissue of the LG (**Figure 4A**), GLG (**Figure 4B**), and BLG (**Figure 4C**). Starch grains (**Figure 4D**) are detected in the protoplasm of the GG common storage tissue, schlerenchyma and typical nutritive tissue. Reducing sugars are detected in the protoplasm of the common storage tissue and typical nutritive tissue of the LG (**Figure 4E**), GLG (**Figure 4F**), BLG (**Figure 4G**), and GG (**Figure 4H**). There is a centripetal gradient of reducing sugars in the LG, GLG, and BLG. In the GG, the reducing sugars accumulate in a bidirectional gradient. Proteins are detected in the protoplasm of the common storage tissue, schlerenchyma and typical nutritive tissue of the LG (**Figure 4I**), GLG (**Figure 4J**), BLG (**Figure 4K**), and GG (**Figure 4L**), forming a centripetal gradient toward the nutritive cells. Lipidic droplets are detected in the protoplasm of the common storage tissue and typical nutritive tissue of the LG (**Figure 4M**), GLG (**Figure 4N**), BLG (**Figure 4O**), and GG (**Figure 4P**).

Immunocytochemical Profiles

The epitopes of xyloglucans recognized by LM15 are moderately labeled in the cell walls of the BLG (34 Gy) and GG (36.7 Gy) common storage tissue; intensely labeled in the cell walls of the LG schlerenchyma (63 Gy), and typical nutritive tissue (47.6 Gy) (**Figure 5A**); and moderately labeled in the cell walls of the GLG schlerenchyma (39.8 Gy), and weakly labeled in the cell walls of the typical nutritive tissue (17.26 Gy) (**Figure 5B**). The xyloglucans are moderately detected in the cell walls of the BLG typical nutritive tissue (38.6 Gy; **Figure 5C**), and intensely detected in the GG typical nutritive tissues (47.1 Gy; **Figure 5D**). The epitopes of heteromannans recognized by LM21 are weakly labeled in the cell walls of the typical nutritive tissue of the LG (20.6 Gy; **Figure 5E**), GLG (19.7 Gy; **Figure 5F**), BLG (12 Gy; **Figure 5G**), and moderately labeled in the cell walls of the GG typical nutritive tissue (31.6 Gy; **Figure 5H** and **Table 2**).

DISCUSSION

The four *Lopesia* galls on *Mimosa gemmulata* have peculiarities regarding the investment in cell walls, tissue stratification, and accumulation of metabolites. The *Lopesia* species associated to the GG has the longest lifespan and distinct structural and nutritional profiles compared with the other three *Lopesia* galls (**Figure 6**). The GG has peculiar bidirectional gradients of starch and reducing sugars, which indicate additional substrates to the synthesis of xyloglucans and heteromannans in cell walls. In the typical nutritive tissues, the cell wall xyloglucans and heteromannans together with the protoplasm accumulated reducing sugars, proteins and lipids constitute the pool of energetic resources for the four galling *Lopesia*. Peculiarly, the GG with its 4 month-life cycle has the highest structural and nutritional investment in the storage and the nutritive tissues, and schlerenchymatic layers, which relates to the highest demand for gall development and galling insect establishment.

Structural Peculiarities in the *Lopesia* Galls

Gall development and tissue compartmentalization depend on the galling insect behavior and how long the galling insect stimulus lasts (Bronner, 1992; Bragança et al., 2017; Oliveira et al., 2016). The duration of the gall cycle can determine the rate of cell divisions, elongation, and tissue complexity (Carneiro et al., 2017; Costa et al., 2018), and determine the structural profile of the storage tissues (Rohfritsch, 1992), which are distinct among the *Lopesia* galls. The GG with the 4-month life cycle has the highest stratification of the common storage tissue, when compared with the other gall morphospecies with the 2-month life cycle (LG) and 3-month life cycles (GLG and BLG) due both to higher hyperplasia and cell hypertrophy. In addition, the thicker cell walls of the GG common storage tissue indicate a distinct metabolic investment for the synthesis of cell wall components as cellulose, hemicellulose and pectins than observed in the other three *Lopesia* galls. This investment in cell wall thickness is important to control the turgor pressure during cell hypertrophy (Chanliaud et al., 2002), and confers an additional support for the GG. The structural and physiological traits of the common storage tissue have been related to the sink and storage of water and energetic resources (Castro et al., 2012; Oliveira et al., 2017; Bragança et al., 2020b). Water and energetic molecules accumulation increase gall succulence (tissue thickness) (Oliveira et al., 2017), and can also be consequence of the longest lifespan,

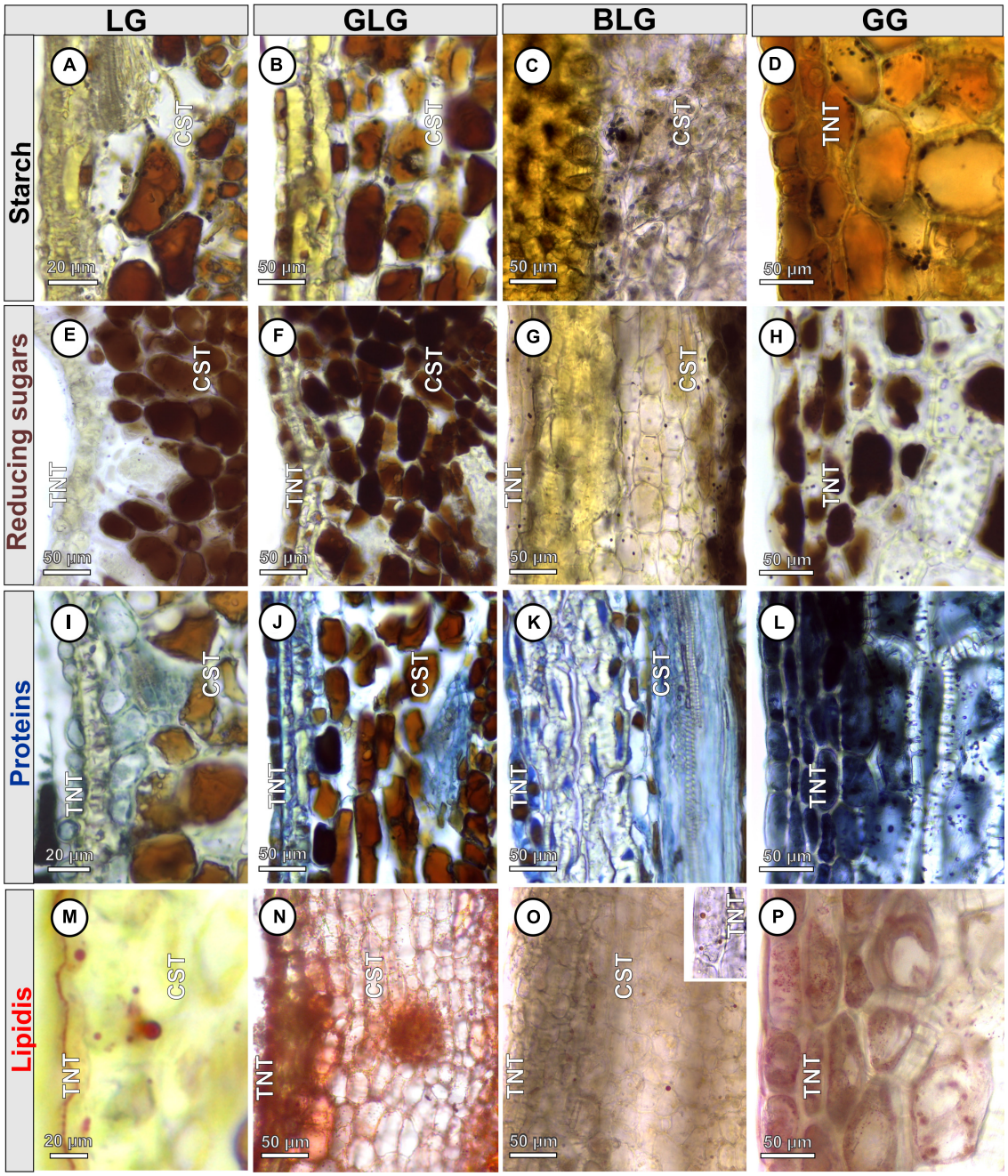

FIGURE 4 | Histochemical profiles of the four *Lopesia* galls on *Mimosa gemmulata* Barneby (Fabaceae) pinna-rachis in transverse sections. **(A–D)** Starch grains stained in black. **(E–H)** Reducing sugars stained in brown. **(I–L)** Proteins stained in blue **(M–P)** Lipidic droplets stained in red. BLG, brown lanceolate bivalve-shaped gall; CST, common storage tissue; GG, globoid bivalve-shaped gall; GLG, green lanceolate bivalve-shaped gall; LG, lenticular bivalve-shaped gall; TNT, typical nutritive tissue.

as evidenced in the GG on *M. gemmulata* with the thickest cell walls as well as higher stratification of the common storage tissue.

The differentiation of the schlerenchymatic cell layers is associated with life cycle of the *Lopesia* galls on *M. gemmulata*. Secondary walls are mainly composed of cellulose, hemicelluloses (xylans and glucomannans), and lignins, whose biosynthesis is involved in the scavenging of free radicals (Liu et al., 2018; Zhong et al., 2019). The lignification process confers mechanical support and may also protect gall tissues against the high oxidative stress originated from the galling organism respiration and cell metabolism (Oliveira et al., 2010, 2011b, 2017; Isaias et al., 2015). The higher thickness of the GG cell walls indicates that the biosynthesis and deposition of the secondary wall components can be more expressive in galls with longer lifespans. The longest

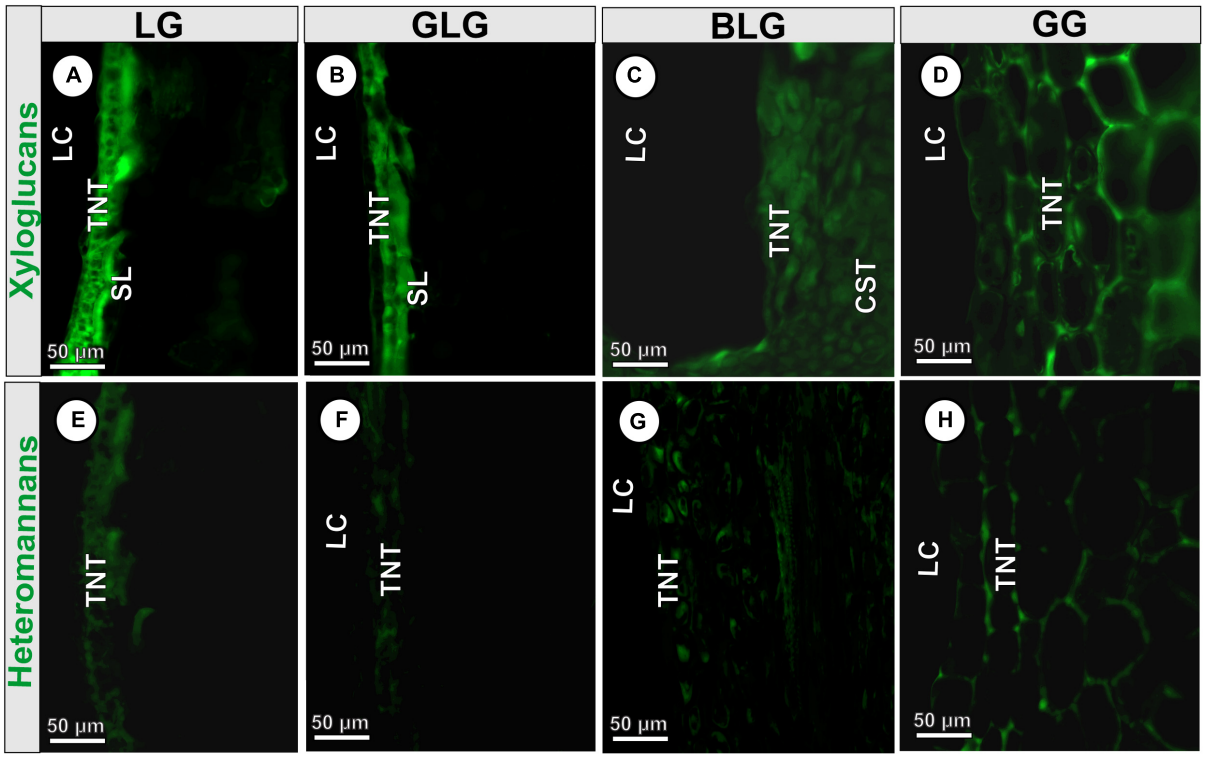

FIGURE 5 | Immunocytochemical profiles of the four *Lopesia* galls on *Mimosa gemmulata* Barneby (Fabaceae) pinna-rachis in transverse sections. **(A–D)** Xyloglucans labeled by LM15. **(E–H)** Heteromannans labeled by LM20. BLG, brown lanceolate bivalve-shaped gall; CST, common storage tissue; GG, globoid bivalve-shaped gall; GLG, green lanceolate bivalve-shaped gall; LC, larval chamber; LG, lenticular bivalve-shaped gall; TNT, typical nutritive tissue; SL, schlerenchymatic layer.

TABLE 2 | Average of gray value and intensity of reaction of the epitopes for hemicelluloses in the tissues of the four *Lopesia* galls on *Mimosa gemmulata* (Fabaceae).

	Outer compartment								Inner compartment			
	Common storage tissue				Schlerenchymatic layer				Typical nutritive tissue			
	LG	GLG	BLG	GG	LG	GLG	BLG	GG	LG	GLG	BLG	GG
Immunocytochemistry												
Xyloglucans	0	0	34.0	36.7	63	39.8	0	0	47.6	17.2	38.6	47.1
Intensity	–	–	++	++	+++	++	–	–	+++	+	++	+++
Heteromannans	0	0	19.7	0	0	0	0	0	20.6	19.7	12	31.6
Intensity	–	–	+	–	–	–	–	–	+	+	+	++

BLG, brown lanceolate bivalve-shaped gall; LG, lenticular bivalve-shaped gall; GG, globoid bivalve-shaped gall; GLG, green lanceolate bivalve-shaped gall. Intensity of reaction: (–) negative (=0 Gy value); (+) weak (10–20 Gy value); (++) moderate (21–39.99 Gy value); (+++) intense (≥40 Gy value).

time the galling *Lopesia* associated to the GG remains inside the gall, and the higher impact of its breathing and feeding seem to result in the thick schlerenchymatic layers, which may favor the dissipation of oxidative stress and gall maintenance. Controversly, the LG and the GLG also have conspicuous schlerenchymatic layers, but with the thinnest cell walls amongst the *Lopesia* galls, while the BLG has an intermediate condition in cell wall and schlerenchymatic layer thickness among the four *Lopesia* galls on *M. gemmulata*. The differences in the duration of the life cycles even in 1–2 months relate to the thickness of the cell walls and the stratification of the schlerenchymatic layers on the *Lopesia* galls associated to *M. gemmulata*, which support the premise that the lignification process is triggered and supported by the galling insect activity and is more intense the longer the galling insect lifespan is.

The cells of the typical nutritive tissue develop due to the galling insect stimuli over the host plant tissues, as they are directly impacted by the nutrition of the inducers (Bronner, 1992). The cell walls and stratification of the typical nutritive tissues of the galls with 2- and the 3-month-life cycles (LG,

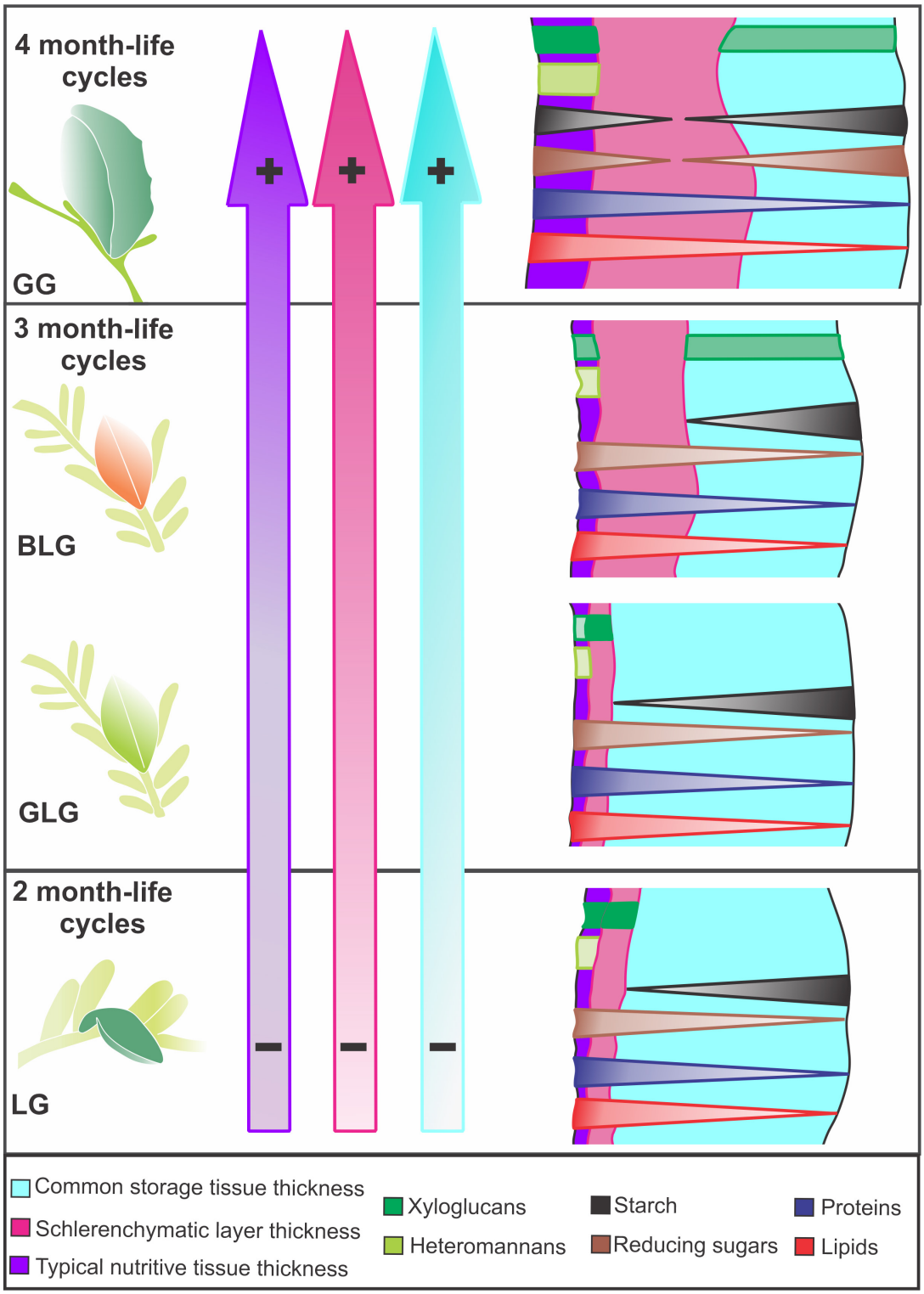

FIGURE 6 | Diagrams of the structural and nutritional profiles of the four *Lopesia* galls on *Mimosa gemmulata* with their respective lifespans. The color gradients in the purple, pink and blue arrows, and the symbols (– and +) indicate tissue thickness investment. The diagrams of the transverse sections illustrate the gradients of the nutritive molecules in gall tissues. BLG, brown lanceolate bivalve-shaped gall; GG, globoid bivalve-shaped gall; GLG, green lanceolate bivalve-shaped gall; LG, lenticular bivalve-shaped gall.

BLG, and GLG) have similar thickness, which can indicate the low and constant nutritional demand of the three gall-inducing *Lopesia*. Differently, the primary cell walls and stratification of the typical nutritive tissue of the GG are thicker, which seems to be consequence of the greater feeding stimulus and high nutritional demand of the *Lopesia* larvae with the longest lifespan (4 month-life cycle).

Nutritional Profiles in the Protoplasm of the *Lopesia* Galls

The life cycles did not alter the evaluated compounds linked to the nutritional profiles of the four *Lopesia* galls on *M. gemmulata*. However, the histochemical gradients of carbohydrates are bidirectional in the GG. The common storage tissues of four *Lopesia* galls are starch-rich, and, unexpectedly, starch grains also accumulate in the GG nutritive tissue. Starch is an insoluble polysaccharide that must be broken down in monosaccharides or disaccharides by invertases, such as D-glucose, activity (Morris and Arthur, 1984) in gall storage tissues (Oliveira et al., 2010, 2011a; Bragança et al., 2017). The inverse gradients of accumulation of starch and reducing sugars in the four *Lopesia* galls implies in the activity of enzymes and may result in adequate substrate for the biosynthesis of new cell wall components (Taylor, 2008; Polko and Joseph, 2019), such as xyloglucans (Pauly and Keegstra, 2016) and heteromannans (Voiniciuc et al., 2019) in *Lopesia* galls. These hemicelluloses are synthesized by Golgi-localized glycosyltransferases (GTs), and the resulting polysaccharides are secreted to the plant cell wall via exocytosis (Driouich et al., 2012; Voiniciuc et al., 2019). Accordingly, the bidirectional gradients of starch and reducing sugars in the common storage and typical nutritive tissues of the GG may be associated with additional substrates to biosynthesis of xyloglucans and heteromannans, and the composition of the primary cell walls (Pauly and Keegstra, 2016).

The proteins and lipids are energetic molecules that support the four gall-inducing *Lopesia* nutrition and gall structural maintenance. The proteins can act in the scavenging of free radicals and the maintenance of redox-potential homeostasis in tissues of plants (Meyer et al., 2019; Foyer et al., 2020) and of galls induced by different galling organisms (Schönrogge et al., 2000; Oliveira et al., 2010; Isaias et al., 2015; Silva et al., 2019). The protein accumulation in the nutritive cells of the *Lopesia* galls can have antioxidant function due to highest cellular metabolism in this tissue compartment. The accumulation of lipids in the storage, and/or typical nutritive tissue of Cecidomyiidae galls on different host plants are linked to the intrinsic metabolism of the host plants (Moura et al., 2008; Oliveira et al., 2010; Ferreira and Isaias, 2014; Amorim et al., 2017; Nogueira et al., 2018), as is true for *M. gemmulata*. The lipid droplets accumulated in the common storage tissue are related to the maintenance of the cellular machinery, while in the nutritive cells, they are food resources for the *Lopesia* galls. In the typical nutritive tissue, the lipids may become available by the activity of a lipase-like protein expressed in the salivary glands of Cecidomyiidae larvae during feeding, which can be involved in extra-oral digestion (Hatchett et al., 1990; Shukle et al., 2009; Al-Jbory et al., 2018).

Nutritional Profiles in Cell Walls of *Lopesia* Galls

Xyloglucans and heteromannans are hemicelluloses involved in cell expansion and rigidity (Park and Cosgrove, 2015; Cosgrove, 2016, 2018; Voiniciuc et al., 2019), which also work out as reserve of carbohydrates accumulated in plant cell walls of some cotyledons, mainly in seeds of Fabaceae species (Buckeridge et al., 2000; Santos et al., 2004). Recently, the xyloglucans were reported as reserve carbohydrates in cell walls of nematode-induced galls on *Miconia* spp. (Melastomaceae) (Ferreira et al., 2020), and cell walls of the common storage and of the typical nutritive tissues of Cecidomyiidae-induced galls on *Inga ingoides* (Fabaceae) (Bragança et al., 2020a). Herein, the epitopes of xyloglucans labeled by LM15 in the common storage tissue of the BLG and the GG, and in the schlerenchymatic layers of the LG and GLG can influence the dynamics of cell wall expansion and rigidity. Both the xyloglucans and the heteromannans are detected in the primary cell walls of the typical nutritive tissue of the four *Lopesia* galls on *M. gemmulata*. While the overall labeling of heteromannans in the four *Lopesia* galls relates to structural function, the labeling of the xyloglucans in the typical nutritive tissues relates not only to the structural, but also to the nutritional function.

We demonstrated that the primary walls of the GG are thicker, and therefore a greater investment in the synthesis of xyloglucans as reserve carbohydrates occurs, which indicate the support for the galling *Lopesia* with the longest life cycle high nutritional demands. The xyloglucan monosaccharides can become available for the galling *Lopesia* nutrition by the activity of β-D-galactosidase and β-D-glucosidase, which may be found in salivary glands and/or midgut of Cecidomyiidae larvae (Grover et al., 1988). Even though the heteromannans and the xyloglucans are labeled in primary cell walls of the four *Lopesia* galls independently of their lifespans, the GG thickest cell walls and typical nutritive tissue indicate a higher support for the 4-month life cycle.

CONCLUSION

The 1–2-month variation of *Lopesia* gall lifespans did not impact the type of energetic molecules, but the investment in cell walls and tissue stratification, especially regarding the common storage tissue. Moreover, cell walls have configured as sites of additional carbohydrate accumulation not only for structural, but for nutritional purposes. The bivalve-shaped globoid galls with the 4-month lifespan associated to *M. gemmulata* demanded the highest structural and nutritional support, as expected.

DATA AVAILABILITY STATEMENT

The raw data supporting the conclusions of this article will be made available by the authors, without undue reservation.

AUTHOR CONTRIBUTIONS

EC, DO, and RI designed the experiments, analyzed the data, and drafted the manuscript. EC and DF performed the experiments. All authors contributed to the article and approved the submitted version.

FUNDING

This work was supported by the Coordenação de Aperfeiçoamento de Pessoal de Nível Superior—Brazil (CAPES)—Finance Code 001. We thank CAPES-Brazil for doctoral grant to EC (888877.199702/2018-00). We thank Conselho Nacional de Desenvolvimento Científico e Tecnológico (CNPq) for the research scholarships to RI (304535/2019-2) and DO (304981/2019-2).

ACKNOWLEDGMENTS

We thank to Dra. Valéria Cid Maia and Dra. Sheila P. Carvalho-Fernandes for confirming the four *Lopesia* associated to *M. gemmulata* are distinct but undescribed species.

REFERENCES

Al-Jbory, Z., Anderson, K. M., Harris, M. O., Mittapalli, O., Whitworth, R. J., and Chen, M. S. (2018). Transcriptomic analyses of secreted proteins from the salivary glands of wheat midge larvae. *J. Insect Sci.* 18:17. doi: 10.1093/jisesa/iey009

Amorim, D. O., Ferreira, B. G., and Fleury, G. (2017). Plant potentialities determine anatomical and histochemical diversity in *Mikania glomerata* Spreng. galls. *Braz. J. Bot.* 40, 517–527. doi: 10.1007/s40415-016-0357-9

Bragança, G. P., Oliveira, D. C., and Isaias, R. M. S. (2017). Compartmentalization of metabolites and enzymatic mediation in nutritive cell of Cecidomyiidae galls on *Piper arboretum* Aubl. (Piperaceae). *J. Plant Stud.* 6, 11–22. doi: 10.5539/jps.v6n1p11

Bragança, G. P. P., Alencar, C. F., Freitas, M. S. C., and Isaias, R. M. S. (2020a). Hemicelluloses and associated compounds determine gall functional traits. *Plant Biol.* 22, 981–991. doi: 10.1111/plb.13151

Bragança, G. P. P., Freitas, M. S. C., and Isaias, R. M. S. I. (2020b). The influence of gall position over xylem features in leaflets of *Inga ingoides* (Rich.) willd. (Fabaceae: Caesalpinioideae). *Trees* 35, 199–209. doi: 10.1007/s00468-020-02027-1

Bronner, R. (1992). "The role of nutritive cells in the nutrition of cynipids and cecidomyiids," in *Biology of Insect-Induced Galls*, eds J. D. Shorthouse, and O. Rohfritsch (New York, NY: Oxford University Press), 118–140.

Brundett, M. C., Kendrick, B., and Peterson, C. A. (1991). Efficient lipid staining in plant material with sudan red 7B or fluoral yellow 088 in polyethylene glycol–glycerol. *Biotech. Histochem.* 66, 111–116. doi: 10.3109/10520299109110562

Buckeridge, M. S., Santos, H. P., and Tiné, M. A. S. (2000). Mobilisation of storage cell wall polysaccharides in seeds. *Plant Physiol.* 38, 141–156. doi: 10.1016/S0981-9428(00)00162-5

Bukatsch, F. (1972). Bermerkungen zur doppelfärbung astrablau-safranin. *Mikrokosmos* 61:255.

Carneiro, R. G. S., Isaias, R. M. S., Moreira, A. S. F. P., and Oliveira, D. C. (2017). Reacquisition of new meristematic sites determines the development of a new organ, the Cecidomyiidae gall on *Copaifera langsdorffii* Desf. (Fabaceae). *Front. Plant Sci.* 8:1622. doi: 10.3389/fpls.2017.01622

Castro, A. C., Oliveira, D. C., Moreira, A. S. F. P., Lemos-Filho, J. P., and Isaias, R. M. S. (2012). Source-sink relationship and photosynthesis in the horn-shaped gall and its host plant *Copaifera langsdorffii* Desf. (Fabaceae). *S. Afr. J. Bot.* 83, 121–126. doi: 10.1016/j.sajb.2012.08.007

Chanliaud, E., Burrows, K. M., Jeronimidis, G., and Gidley, M. J. (2002). Mechanical properties of primary plant cell wall analogues. *Planta* 215, 989–996. doi: 10.1007/s00425-002-0783-8

Chen, X., Yang, Z., Chen, H., Qian, Q., Liu, J., Wang, C., et al. (2020). A complex nutrient exchange between a gall-forming aphid and its plant host. *Front. Plant Sci.* 11:811. doi: 10.3389/fpls.2020.00811

Cosgrove, D. J. (2016). Plant cell wall extensibility: connecting plant cell growth with cell wall structure, mechanics, and the action of wall modifying enzymes. *J. Exp. Bot.* 67, 463–476. doi: 10.1093/jxb/erv511

Cosgrove, D. J. (2018). Diffuse growth of plant cell walls. *Plant Physiol.* 176, 16–27. doi: 10.1104/pp.17.01541

Costa, E. C., Carneiro, G. S. C., Silva-Santos, J., and Isaias, R. M. S. (2018). Biology and development of galls induced by *Lopesia* sp. (Diptera: Cecidomyiidae) on leaves of *Mimosa gemmulata* (Leguminosae: Caesalpinioideae). *Aust. J. Bot.* 66, 161–172. doi: 10.1071/BT17099

Driouich, A., Follet-Gueye, M. L., Bernard, S., Kousar, S., Chevalier, L., Vicré-Gibouin, M., et al. (2012). Golgi-mediated synthesis and secretion of matrix polysaccharides of the primary cell wall of higher plants. *Front. Plant Sci.* 3:79. doi: 10.3389/fpls.2012.00079

Ferreira, B. G., Álvarez, R., Avritzer, S. C., and Isaias, R. M. S. (2017). Revisiting the histological patterns of storage tissues: beyond the limits of gall-inducing taxa. *Botany* 95, 173–184. doi: 10.1139/cjb-2016-0189

Ferreira, B. G., Álvarez, R., Bragança, G. P., Alvarenga, D. R., Pérez-Hidalgo, N., and Isaias, R. M. S. (2019). Feeding and other gall facets: patterns and determinants in gall structure. *Bot. Rev.* 85, 78–106. doi: 10.1007/s12229-019-09207w

Ferreira, B. G., Bragança, G. P., and Isaias, R. M. S. (2020). Cytological attributes of storage tissues in nematode and eriophyid galls: pectin and hemicellulose functional insights. *Protoplasma* 257, 229–244. doi: 10.1007/s00709-019-01431-w

Ferreira, B. G., Carneiro, R. G. S., and Isaias, R. M. S. (2015). Multivesicular bodies differentiate exclusively in nutritive fast-dividing cells in *Marcetia taxifolia* galls. *Protoplasma* 252, 1275–1283.

Ferreira, B. G., and Isaias, R. M. S. (2014). Floral-like destiny induced by a galling Cecidomyiidae on the axillary buds of *Marcetia taxifolia* (Melastomataceae). *Flora* 209, 391–400.

Formiga, A. T., Silveira, F. A. O., Fernandes, G. W., and Isaias, R. M. S. (2014). Phenotypic plasticity and similarity among gall morphotypes on a superhost, *Baccharis reticularia* (Asteraceae). *Plant Biol.* 17, 512–521.

Foyer, C. H., Baker, A., Wright, M., Sparkes, I. A., Mhamdi, A., Schippers, J. H. M., et al. (2020). On the move: redox-dependent protein relocation in plants. *J. Exp. Bot.* 71, 620–631. doi: 10.1093/jxb/erz330

Gonçalves, S. J. M. R., Isaias, R. M. S., Vale, F. H. A., and Fernandes, G. W. (2005). Sexual dimorphism of *Pseudotectococcus rolliniae* Hodgson & Gonçalves 2004 (Hemiptera Coccoidea Eriococcidae) influences gall morphology on *Rollinia laurifolia* Schltdl. (Annonaceae). *Trop. Zool.* 18, 161–169. doi: 10.1080/03946975.2005.10531219

Grover, P. B., JR., Ross, D. R., and Shukle, R. H. (1988). Identification and partial characterization of digestive carbohydrases in larvae of the Hessian fly, *Mayetiola destructor* (Say) (Diptera: Cecidomyiidae). *Arch. Insect Biochem. Physiol.* 5, 59–72. doi: 10.1002/arch.940080106

Hatchett, J. H., Kreitner, G. L., and Elzinga, R. J. (1990). Larval mouthparts and feeding mechanism of the Hessian fly (Diptera: Cecidomyiidae). *Ann. Entomol. Soc. Am.* 83, 1137–1147.

Isaias, R. M. S., Oliveira, D. C., Moreira, A. S. F. P., Soares, G. L. G., and Carneiro, R. G. S. (2015). The imbalance of redox homeostasis in arthropod-induced plant galls: mechanisms of stress generation and dissipation. *Biochim. Biophys. Acta* 1850, 1509–1517. doi: 10.1016/j.bbagen.2015.03.007

Johansen, D. A. (1940). *Plant Microtechnique*. New York, NY: McGraw-Hill Book.

Jorge, N. C., Souza-Silva, E. A., Alvarenga, D. R., Saboia, G., Soares, G. L. G., Zini, C. A., et al. (2018). Structural and chemical profiles of *Myrcia splendens* (Myrtaceae) leaves under the influence of the galling *Nexothrips* sp. (Thysanoptera). *Front. Plant Sci.* 9:1521. doi: 10.3389/fpls.2018.01521

Karnovsky, M. J. (1965). A formaldehyde-glutaraldehyde fixative of high osmolarity for use in electron microscopy. *J. Cell Biol.* 27, 137–138.

Kraus, J. E., and Arduin, M. (1997). *Manual Básico de Métodos em Morfologia Vegetal*. Rio de Janeiro: Editora da Universidade Rural.

Liu, Q., Luo, L., and Zheng, L. (2018). Lignins: biosynthesis and biological functions in plants. *Int. J. Mol. Sci.* 19:335. doi: 10.3390/ijms19020335

Mani, M. S. (1964). *Ecology of Plant Galls*. The Hague: Dr. W. Junk Publishers. doi: 10.1007/978-94-017-6230-4

Marcus, S. E., Blake, A. W., Benians, T. A. S., Lee, K. J. D., Poyser, C., Donaldson, L., et al. (2010). Restricted access of proteins to mannan polysaccharides in intact plant cell walls. *Plant J.* 61, 191–203. doi: 10.1111/j.1365-313X.2010.04319.x

Marcus, S. E., Verhertbruggen, Y., Herve, C., Ordaz-Ortiz, J. J., Farkas, V., Pedersen, H. L., et al. (2008). Pectic homogalacturonan masks abundant sets of xyloglucan epitopes in plant cell walls. *BMC Plant Biol.* 8:60. doi: 10.1186/1471-2229-8-60

Mazia, D., Brewer, P. A., and Alfert, M. (1953). The cytochemistry staining and measurement of protein with mercuric bromophenol blue. *Biol. Bull.* 104, 57–67.

Meyer, A. J., Riemer, J., and Rouhier, N. (2019). Oxidative protein folding: state-of-the-art and current avenues of research in plants. *New Phytol.* 221, 1230–1246. doi: 10.1111/nph.15436

Meyer, J., and Maresquelle, H. J. (1983). *Anatomie des Galles*. Berlin: Gerbrüder Borntrager.

Morris, D. A., and Arthur, E. D. (1984). Invertase and auxin-induced elongation in internodal segments of *Phaseolus vulgaris*. *Phytochemistry* 23, 2163–2167.

Moura, M. Z. D., Soares, G. L. G., and Isaias, R. M. S. (2008). Species-specific changes in tissue morphogenesis induced by two arthropod leaf gallers in *Lantana camara* L. (Verbenaceae). *Aust. J. Bot.* 56, 153–160. doi: 10.1071/BT07131

Nogueira, R. M., Costa, E. C. C., Santos-Silva, J., and Isaias, R. M. S. (2018). Structural and histochemical profile of *Lopesia* sp. Rübsaamen. 1908 pinnula galls on *Mimosa tenuiflora* (Willd.) Poir. in a Caatinga environment. *Hoehnea* 45, 231–239. doi: 10.1590/2236-8906-80/2017

Oliveira, D. C., Carneiro, R. G. S., Magalhães, T. A., and Isaias, R. M. S. (2011a). Cytological and histochemical gradients on two *Copaifera langsdorffii* Desf. (Fabaceae) – Cecidomyiidae gall systems. *Protoplasma* 248, 829–837. doi: 10.1007/s00709-010-0258-x

Oliveira, D. C., Isaias, R. M. S., Fernandes, G. W., Ferreira, B. G., Carneiro, R. G. S., and Fuzaro, L. (2016). Manipulation of host plant cells and tissues by gall-inducing insects and adaptive strategies used by different feeding guilds. *J. Insect Physiol.* 84, 103–113. doi: 10.1016/j.jinsphys.2015.11.012

Oliveira, D. C., Isaias, R. M. S., Moreira, A. S. F. P., Magalhães, T. A., and Lemos-Filho, J. P. (2011b). Is the oxidative stress caused by *Aspidosperma* spp. galls capable of altering leaf photosynthesis? *Plant Sci.* 180, 489–495. doi: 10.1016/j.plantsci.2010.11.005

Oliveira, D. C., Magalhães, T. A., Carneiro, R. G. S., Alvim, M. N., and Isaias, R. M. S. (2010). Do Cecidomyiidae galls of *Aspidosperma spruceanum* (Apocynaceae) fit the pre-established cytological and histochemical patterns? *Protoplasma* 242, 81–93. doi: 10.1007/s00709-010-0128-6

Oliveira, D. C., Moreira, A. S. F. P., Isaias, R. M. S., Martini, V., and Rezende, U. C. (2017). Sink status and photosynthetic rate of the leaflet galls induced by *Bystracoccus matayba* (Eriococcidae) on *Matayba guianensis* (Sapindaceae). *Front. Plant Sci.* 8:1249. doi: 10.3389/fpls.2017.01249

Paiva, J. G. A., Fank-de-Carvalho, S. M., Magalhães, M. P., and Graciano-Ribeiro, D. (2006). Verniz vitral incolor 500® : uma alternativa de meio de montagem economicamente viável. *Acta Bot. Bras.* 20, 257–264. doi: 10.1590/S0102-33062006000200002

Park, Y. B., and Cosgrove, D. J. (2015). Xyloglucan and its interactions with other components of the growing cell wall. *Plant Cell Physiol.* 56, 180–194. doi: 10.1093/pcp/pcu204

Pauly, M., and Keegstra, K. (2016). Biosynthesis of the plant cell wall matrix polysaccharide xyloglucan. *Annu. Rev. Plant Biol.* 67, 235–259. doi: 10.1146/annurev-arplant-043015-112222

Polko, J. K., and Joseph, J. K. (2019). The regulation of cellulose biosynthesis in plants. *Plant Cell* 31, 282–296. doi: 10.1105/tpc.18.00760

Rezende, U. C., Custódio, J. F., Kuster, V. C., Gonçalves, L. A., and Oliveira, D. C. (2019). How the activity of natural enemies changes the structure and metabolism of the nutritive tissue in galls? Evidence from the *Palaeomystella oligophaga* (Lepidoptera) –*Macairea radula* (Metastomataceae) system. *Protoplasma* 256, 669–677.

Rohfritsch, O. (1992). "Patterns in gall development," in *Biology of Insect-Induced Galls*, eds J. D. Shorthouse, and O. Rohfritsch (New York, NY: Oxford University Press), 60–86.

Rübsaamen, E. H. (1908). Beitrage zur Kenntnis aussereuropaischer Zoocecidien. III. Beitrag: Gallen aus Brasilien und Peru. *Marcellia* 7, 15–79.

Santos, H. P., Purgatto, E., Mercier, H., and Buckeridge, M. S. (2004). The control of storage xyloglucan mobilization in cotyledons of *Hymenaea courbaril*. *Plant Physiol.* 135, 287–299. doi: 10.1104/pp.104.040220

Sass, J. E. (1951). *Botanical Microtechnique*. Ames, IA: Iowa State College Press.

Schönrogge, K., Harper, L. J., and Lichtenstein, C. P. (2000). The protein content of tissues in cynipid galls (Hymenoptera: Cynipidae): similarities between cynipid galls and seeds. *Plant Cell Environ.* 23, 215–222. doi: 10.1046/j.1365-3040.2000.00543.x

Shukle, R. H., Mittapalli, O., Morton, P. K., and Chen, M. S. (2009). Characterization and expression analysis of a gene encoding a secreted lipase-like protein expressed in the salivary glands of the larval Hessian fly, *Mayetiola destructor* (Say). *J. Insect Physiol.* 55, 105–112. doi: 10.1016/j.jinsphys.2008.10.008

Silva, A. F. D. M., Kuster, V. C., Rezende, U. C., and Oliveira, D. C. (2019). The early developmental stages of gall-inducing insects define final gall structural and histochemical profiles: the case of *Bystracoccus mataybae* galls on *Matayba guianensis*. *Botany* 97, 427–438. doi: 10.1139/cjb-2019-0017

Taylor, N. G. (2008). Cellulose biosynthesis and deposition in higher plants. *New Phytol.* 178, 239–252.

Voiniciuc, C., Dama, M., Gawenda, N., Stritt, F., and Pauly, M. (2019). Mechanistic insights from plant heteromannan synthesis in yeast. *Proc. Natl. Acad. Sci. U.S.A.* 116, 522–527. doi: 10.1073/pnas.1814003116

Zhong, R., Cui, D., and Ye, Z.-H. (2019). Secondary cell wall biosynthesis. *New Phytol.* 221, 1703–1723. doi: 10.1111/nph.15537

Conflict of Interest: The authors declare that the research was conducted in the absence of any commercial or financial relationships that could be construed as a potential conflict of interest.

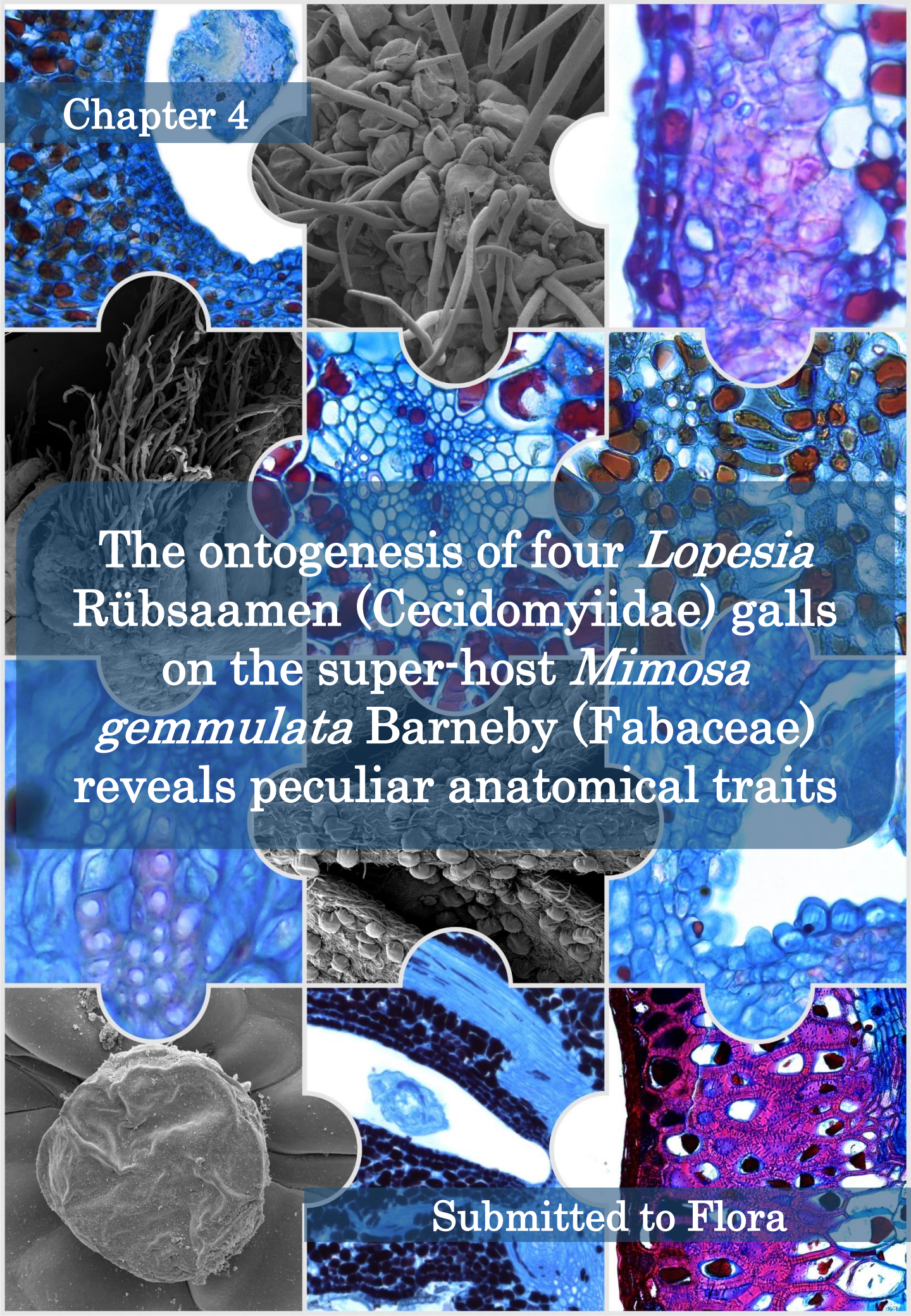

Chapter 4

The ontogenesis of four *Lopesia* Rübsaamen (Cecidomyiidae) galls on the super-host *Mimosa gemmulata* Barneby (Fabaceae) reveals peculiar anatomical traits

Submitted to Flora

The ontogenesis of four *Lopesia* Rübsaamen (Cecidomyiidae) galls on the super-host *Mimosa gemmulata* Barneby (Fabaceae) reveals peculiar anatomical traits

Elaine C. Costa[1], Mariana S. C. Freitas[1], Renê G. S. Carneiro[2], Denis C. Oliveira[3], Rosy M. S. Isaias[1, *]

[1]Departamento de Botânica, Instituto de Ciências Biológicas, Universidade Federal de Minas Gerais, Avenida Antônio Carlos, 6627, Pampulha, Belo Horizonte, Minas Gerais Zip code: 31270-901, Brazil.

[2]Departamento de Botânica, Instituto de Ciências Biológicas, Universidade Federal de Goiás, Campus Samambaia, Avenida Esperança, s/n, Goiânia, Goiás, Zip code: 74690-900, Brazil.

[3]Instituto de Biologia, Universidade Federal de Uberlândia, Campus Umuarama, Rua Ceará s/n, Uberlândia, Minas Gerais, Zip code: 38402-018, Brazil.

[*]Corresponding author: rosy@icb.ufmg.br

Highlights

- The ordinary developmental anatomy deviates differently toward the four *Lopesia* galls.
- Trichome types vary in size, number of cells, and distribution among the galls.
- The nutritive tissue has mixed tissue origin only in the globoid gall.
- The gall common traits relate to the induction site and to the original cell lineages.

Abstract: The super-host *Mimosa gemmulata* has four bivalve-shaped galls induced on the pinna-rachis by congeneric *Lopesia* spp., which are distinguishable as the lenticular (LG), the green lanceolate (GLG), the brown lanceolate (BLG), and the globoid (GG) galls. The ontogenesis of each gall is related to the capacity of each inducer to differentially access the host plant tissues, resulting in specific phenotypes. The ontogenesis of these galls reveals that the differentiation of two types of trichomes is a conservative anatomical trait of *M. gemmulata.* Nevertheless, under the influence of the four *Lopesia* spp., these trichome types are altered in size, number of cells, and distribution in the dermal system of each gall. Another conservative trait in regard to the vascular system is the collateral arrangement in non-galled and galled conditions, but with an increment in vascular elements in the GG. The nutritive cells of three out of the four galls originate exclusively from the epidermis, while parenchyma cell lineages participate in the formation of the nutritive tissue of the GG. The intrinsic anatomical features of the four *Lopesia* galls relate to the site of induction and to the original cell lineages recruited toward the ontogenesis of similar bivalve-shaped morphotypes. However, specific ontogenetic deviations determine each *Lopesia* gall morphospecies. In contrast, the peculiar structural-functional traits of the GG develop due to its longest lifespan, which consequently leads to highest stimuli-induced responses in all host plant cell lineages.

Keywords: cell redifferentiation; gall anatomy; gall development; plant cell lineages.

1. Introduction

The super-host plants of galling herbivores have been explored as study models to investigate the potential of one host plant genome to generate specific phenotypes under the stimuli of different galling insect species. Such study models have provided numerous insights on plant tissue reorganization leading to the variety of gall structures found in nature (Isaias et al. 2013; Formiga et al., 2014; Kurzfeld-Zexer et al., 2015; Martinez et al., 2018; Álvarez et al., 2020). Gall ontogenesis is influenced by the galling insect taxa, but also by the induction site, the origin of gall tissues, and by the morphogenetic potentialities of the host plants (Moura et al., 2008; Formiga et al., 2014; Amorim et al., 2017; Bragança et al., 2021). In addition, the lifespan of the inducer, i.e., the amount of time the inducer stays inside plant tissues stimulating gall development, can influence the dynamics of cell hypertrophy, tissue hyperplasia, and differentiation along gall development (Carneiro et al., 2017; Costa et al., 2021b). The anatomical peculiarities of each gall morphotype configure the cellular and subcellular phenotypes of the inducers (Stone and Schönrogge, 2003; Carneiro et al., 2015; Kurzfeld-Zexer et al., 2015), as irrefutable traits of the specificity of each plant gall.

The super-host *Mimosa gemmulata* Barneby (Fabaceae) hosts four bivalve-shaped galls induced by four distinct undescribed species of *Lopesia* Rübsaamen, 1908 (Diptera-Cecidomyiidae; Maia and Carvalho-Fernandes personal communication). The four *Lopesia* species select the same microsite for the induction of their galls on *M. gemmulata*, the immature pinna-rachis. The four species of *Lopesia* are multivoltine with distinct lifespans, varying from 2- to 3- or 4-months (Costa et al. 2021a). The four *Lopesia* galls on *M. gemmulata* are the lenticular bivalve-shaped galls (LG) with a 2-month life cycle, the green lanceolate bivalve-shaped galls (GLG) and the brown lanceolate bivalve-shaped galls (BLG) with 3-month life cycles, and the globoid bivalve-shaped galls (GG)

with a 4-month life cycle (Costa et al. 2021a). The variation of one or two months in gall lifespans results in differences in the structural and nutritional traits in cell walls and protoplasm of gall tissues (Costa et al., 2021b).

Currently, we focus on the comparative ontogenetic approach of the four bivalve-shaped galls induced on the pinna-rachis of *M. gemmulata* by four congeneric species of *Lopesia* to verify anatomical peculiarities. We assume that each *Lopesia* gall develops diagnostic anatomical traits along its ontogenesis, and address the following questions to guide our discussion: (1) how diverse is the assembly of cell lineages recruited for the ontogenetical steps of the four *Lopesia* galls? And (2) do the bivalve-shaped gall morphotypes have anatomical intrinsic features related to common structural-functional traits in the four *Lopesia* galls?

2. Materials and methods

2.1. Sampling and collection

Samples of immature and mature non-galled pinna-rachis (NGP), non-galled pinnulae, and of the four *Lopesia* galls (LG, GLG, BLG, and GG) at the induction, growth and development, maturation, and senescent stages (n = 10 per category) were collected from individuals (n = 12) of *M. gemmulata* in a Cerrado area at the Serra Geral, municipality of Caetité, state of Bahia, Brazil (14º04’36.8’’S, 42°29’59’’W). The developmental stages of the four *Lopesia* galls were distinguished by their size, color, and shape along their phenological life cycles (Costa et al. 2021a).

2.2.Light microscopy analysis

98 The samples of NGP, non-galled pinnulae, LG, GLG, BLG and GG were fixed in
99 2.5% glutaraldehyde and 4.5% formaldehyde 0.1mol L^{-1} (Karnovsky, 1965; modified to
100 phosphate buffer, pH 7.2) for 48 hours. The samples were dehydrated in ethanol series
101 and embedded in Paraplast® (Leica Biosystems, St. Louis, MO, USA; Kraus and Arduin,
102 1997). Serial transverse sections (12 μm) were obtained using a rotatory microtome
103 (Leica® BIOCUT 2035), deparaffinized in butyl acetate, and hydrated in an ethanol series
104 (Kraus and Arduin, 1997). The sections were stained with Astra blue–safranin (9: 1, v/v)
105 (Bukatsch, 1972; modified to 0.5%), dehydrated, and mounted with colorless varnish
106 Acrilex® (Paiva et al., 2006). The sections were analyzed under a light microscope
107 (Leica® DM500) and photographed with a coupled digital camera (Leica® ICC50 HD).

108 *2.3.Scanning electron microscopy analysis*

109 Samples of the immature and mature NGP, non-galled pinnulae, and of the LG,
110 GLG, BLG, and GG at the four developmental stages (n = 3 per category) were fixed in
111 4% Karnovsky in 0.1 mM phosphate buffer for 48 hours (O'Brien and McCully, 1981;
112 modified to pH = 7.2). The samples were post-fixed in 1% osmium tetroxide in 0.1 mM
113 phosphate buffer (pH 7.2), and dehydrated in an ethanol series (Johansen, 1940), followed
114 by critical point drying with carbon dioxide (Bal-Tec® CPD 030). The samples were
115 sputter-coated with 30 nm of gold (Bal-Tec SCD® 050) and the images were obtained in
116 a scanning electron microscope (LEO EVO® 40) at the *Centro de Microscopia* of the
117 *Universidade Federal de Minas Gerais* (CM-UFMG).

118

119 **3. Results**

120 *3.1. Non-galled Pinna-rachis (NGP) and Pinnula*

121 The NGP is arranged between opposite pinnula pairs on the pinnately composite
122 leaves (Fig. 1A). The dermal tissue system of the immature pinna-rachis is formed by a
123 single-layered ordinary epidermal cells and distinct types of trichomes covered by thick
124 cuticle. The non-glandular trichomes are unicellular and filiform, while the glandular
125 trichomes are multicellular and peltate (Fig. 1B). The ground tissue system consists of
126 homogeneous parenchyma with isodiametric cells and large vacuoles. The central
127 vascular system has bicollateral organization, and the vascular bundles immersed in the
128 adaxial cortical parenchyma have collateral organization; vessel elements and pericyclic
129 fibers are in the early differentiation process (Fig. 1C). The mature pinna-rachis is
130 characterized by the complete differentiation of the vessel elements and pericyclic fibers,
131 which have lignified cell walls (Fig. 1D). The dermal tissue system of the pinnula has
132 single-layered ordinary epidermal cells, unicellular filiform trichomes covering the
133 adaxial surface (Fig. 1E), and multicellular peltate trichomes covering the abaxial surface
134 (Fig. 1F), where anisocytic stomata occur. The dorsiventral mesophyll has a 3-4 layered
135 palisade parenchyma and 4-5 layered spongy parenchyma; the vascular bundles are
136 collateral (Fig. 1G).

137 *3.2.General aspects of the four* Lopesia *galls*

138 The four *Lopesia* galls are formed by valve-like appendages. The LG are green,
139 extralaminar, and formed by an upper and a lower valve, which grow toward the abaxial
140 surface of the pinnulae (Fig. 2A). The GLG are green (Fig. 2B) and the GBG are brown
141 (Fig. 2C); both lanceolate galls are extralaminar and formed by valves of the same length.
142 The GG are green, extralaminar, and formed by a larger valve projected over a minor
143 valve (Fig. 2D).

144 *3.3. Lenticular bivalve-shaped galls (LG)*

The LG originates from the epidermal and parenchyma cells of the NGP, which lead to the development of the two valve-like appendages (Fig. 3A). In the induction stage, the epidermal cells of the NGP divide anticlinally, and originate ordinary epidermal cells and trichoblasts, which are differentiated either into unicellular filiform or into multicellular peltate trichomes covering the galls. The stomata are absent. The divisions of cortical parenchyma cells of the NGP originate the LG ground tissue system, formed by homogeneous parenchyma. New procambial strands differentiate from the parenchyma cells of the NGP. The epidermal cells of the NGP also originate the typical nutritive tissue around the larval chamber (Fig. 3A). In the growth and development stage, the LG has an increase in cell divisions and expansion in all regions of the valves, which lead to the reorganization of the ground tissue into three distinct regions, as well as to the gall closure (Fig. 3B). The filiform and the peltate trichomes together with the papillose epidermal cells in the two valves assist in the LG closure (Figs. 3C-D). The ground tissue has 3-4 layered outer parenchyma, 3-4 layered median parenchyma (Fig. 3B), and 1-2 layered inner sclerenchyma cells differentiated in the median and basal zones of the valves (Fig. 3E). The typical nutritive tissue has 1-2 cell layers with dense cytoplasm, and evident nuclei (Fig. 3E). The cells of the collateral vascular bundles complete the differentiation (Fig. 3F), and are connected to the central vascular system of the NGP. In the maturation stage, the trichomes sparsely cover the LG. The outer and median parenchyma cells are differentiated into the common storage tissue, and the sclerenchyma development toward the distal zone is complete (Figs. 3G-H), which lead to the compartmentalization of the LG tissues. The epidermis, common storage tissue, vascular bundles, and sclerenchyma layers comprise the outer tissue compartment, while the typical nutritive tissue comprises the inner tissue compartment (Fig. 3H). During senescence, the common storage and nutritive cells are collapsed in the median (Fig. 3I)

and distal zones. The walls of the papillose epidermal cells lignify, and the trichomes in the distal zone at the junction of the two valves fall off.

3.4.Green lanceolate bivalve-shaped galls (GLG)

The GLG originates from epidermal and parenchyma cells of the NGP, which lead to the development of the two valve-like appendages (Fig. 4A). During the induction stage, epidermal cells of the NGP divide anticlinally, and originate ordinary epidermal cells and trichoblasts. The trichoblasts are differentiated into hypertrophied unicellular filiform, and into multicellular peltate trichomes covering the GLG (Figs. 4A-B). Stomata are absent. The divisions of the NGP cortical parenchyma cells in different directions originate the GLG ground tissue system formed by homogeneous parenchyma (Fig. 4C). New procambial strands of the GLG differentiate from the newly formed homogeneous parenchyma (Fig. 4D), and the epidermal cells of the NGP originate the typical nutritive tissue around the larval chamber (Fig. 4C). In the growth and development stage, the GLG have an increase in cell divisions, which leads to the reorganization of the ground tissue, and to the gall closure. The hypertrophied, unicellular filiform and the multicellular peltate trichomes (Fig. 4E-F), as well as the papillose epidermal cells (Fig. 4G) assist the GLG closure. The ground system has 4-5 layered outer parenchyma, 4-5 layered median parenchyma, and 1-2 layered inner parenchyma with small cells with cuboid crystals. The cells of the collateral vascular bundles complete the differentiation, and are connected to the vascular system of the NGP. The typical nutritive tissue has 1-2 layers (Fig. 4H). During the maturation stage, a dense covering of trichomes remain at the surface of the GLG. The outer and median parenchyma cells differentiate into the common storage tissue, and the inner parenchyma cells differentiate into homogeneous sclerenchyma layers, which lead to the compartmentalization of the GLG tissues. The epidermis,

common storage tissue, vascular bundles, and sclerenchyma layers comprise the outer tissue compartment, while the typical nutritive tissue comprises the inner tissue compartment (Fig. 4I). During senescence, some common storage cells are collapsed at the median and distal zones. At the junction of the two valves in the distal zone, the papillose epidermal cells have lignified walls (Fig. 4J), and the trichomes fall off.

3.5. Brown lanceolate bivalve-shaped galls (BLG)

The BLG originates from epidermal cells of the pinnula, and epidermal and parenchyma cells of the NGP, which lead to the development of the two valve-like appendages (Fig. 5A). During the induction stage, the epidermal cells of the pinnula divide anticlinally, and originate ordinary epidermal cells and trichoblasts, which differentiate into hypertrophied and multicellular filiform trichomes (Fig. 5B). Stomata are absent. The divisions of cortical parenchyma cells of the NGP in different directions originate the BLG ground tissue system formed by homogeneous parenchyma. New procambial strands of the BLG differentiate from the homogeneous parenchyma. The epidermal cells of the NGP originate the typical nutritive tissue around the larval chamber. During the growth and development stage, the BLG has an increase in cell divisions, as well as in expansion, which lead to the reorganization of the ground tissue system and to the BLG closure (Fig. 5B-C). The hypertrophied, multicellular filiform trichomes, as well as papillose epidermal cells assist the BLG closure. The ground tissue system has 3-4 layered outer parenchyma, 4-5 layered median parenchyma, and 4-5 layered inner parenchyma. The cells of the vascular system complete their differentiation, and are connected to the central vascular system of the pinna-rachis. The nutritive tissue has 2 layers (Fig. 5D). During the maturation stage, the hypertrophied, multicellular filiform trichomes densely cover the BLG. The outer and median parenchyma cells

220 differentiate into the common storage tissue, and the inner parenchyma cells differentiate
221 into the homogeneous sclerenchyma layers, which lead to the compartmentalization of
222 the BLG tissues (Fig. 5E). The epidermis, common storage tissue, collateral vascular
223 bundles (Fig. 5F), and sclerenchyma layers comprise the outer tissue compartment, while
224 the typical nutritive tissue comprises the inner tissue compartment. During the senescent
225 stage, some common storage cells collapse. At the junction of the two valves in the distal
226 zone, the papillose epidermal cells have lignified walls (Figs. 5G-H), and the trichomes
227 fall off.
228
229 *3.6. Globoid bivalve-shaped galls (GG)*

230 The GG originates from epidermal and parenchyma cells of the NGP, which lead
231 to the development of the two valve-like appendages (Fig. 6A). During the induction
232 stage, the epidermal cells of the NGP divide anticlinally, and originate the GG dermal
233 tissue system with ordinary epidermal cells, and trichoblasts; abnormal anisocytic
234 stomata occur. The trichoblasts differentiate into multicellular peltate trichomes covering
235 the GG, and into unicellular filiform trichomes only in the region of the GG closure. The
236 divisions of the cortical parenchyma cells of the NGP in different directions originate the
237 homogenous GG ground tissue system (Fig. 6B). New procambial strands redifferentiate
238 from the newly formed homogenous parenchyma. The epidermal and parenchyma cells
239 of the NGP originate the typical nutritive tissue. During the growth and development
240 stage, the GG has an increase in cell divisions and expansion, which lead to the
241 reorganization of the ground tissue, and to the GG closure (Figs. 6C-D). The union of the
242 two valves occurs by the growth of the larger valve over the minor valve (Fig. 6C), as
243 well as by intertwining of the unicellular filiform trichomes (Fig. 6D). The multicellular
244 peltate trichomes densely cover the outer surface of the GG (Fig. 6E), whose ground

245 system has 6-7 layered outer parenchyma, 7-8 layered median parenchyma, and 3-4
246 layered inner parenchyma (Fig. 6F). The nutritive tissue has 6 layers; 2-3 layers around
247 the larval chamber are derived from the epidermis, while the outer 3-4 layers are derived
248 from the adjacent inner parenchyma (Fig. 6F).

249 The cells of the collateral vascular system complete the redifferentiation (Fig. 6F),
250 and are connected to the vascular system of the NGP. During the maturation stage, the
251 multicellular peltate trichomes are sparsely distributed on the GG. The outer parenchyma
252 cells differentiate into the common storage tissue, and the median parenchyma cells
253 differentiate into the homogeneous sclerenchyma layers, forming a continuuum with the
254 pericyclic fibers of the NGP (Fig. 6G). These anatomical changes lead to the
255 compartmentalization of the GG tissues. The epidermis, common storage tissue, vascular
256 system, and sclerenchyma layers comprise the outer tissue compartment, while the typical
257 nutritive tissue comprises the inner tissue compartment. In the vascular system, an
258 increment of vascular elements is observed (Fig. 6H). During senescence, the common
259 storage and nutritive cells collapse in the median and the distal zones (Figs. 6I-J). In the
260 distal zone, the nutritive cells have lignified walls, and the filiform trichomes fall off.

261

262 **4. Discussion**

263 The ontogenesis of the four *Lopesia* galls involves the recruitment and
264 differentiation of cell lineages of the dermal, ground, and vascular systems. The epidermal
265 cell lineages recruited from the *M. gemmulata* pinna-rachis originate ordinary epidermal
266 cells and trichoblasts, which differentiate in the two conservative types of trichomes. The
267 alterations in the dermal system relates to the size, number of cells, and distribution of
268 the trichomes in the all the four *Lopesia* galls. The recruitment of parenchyma cell
269 lineages from the NGP originates the parenchyma, the sclerenchyma, and the vascular
270 cell lineages of the four *Lopesia* galls, but the GG has a special feature, the increment in

271 the vascular elements, which may be linked to its longer lifespan (Costa et al., 2021).
272 Peculiarly, the nutritive cells of the GG are originated from the epidermal and
273 parenchyma cell lineages of the pinna-rachis, while the nutritive cells of the other three
274 *Lopesia* galls are only of epidermal origin (Fig. 7). There are anatomical intrinsic features
275 related to common structural-functional traits in the four *Lopesia* galls. The trichomes
276 together with papillose epidermal cells are involved in the closure of the galls. The
277 homogeneous parenchyma and the collateral vascular system are related to the storage
278 and trasport of water and metabolites, which support gall metabolism. The specialized
279 nutritive cells are redifferentiated from epidermal cells. By senescence, parenchyma cell
280 dehydration is important for the opening of the galls. The common structural-functional
281 traits in the four *Lopesia* galls are related to the same induction site, the pinna-rachis, and
282 to their original cell lineages toward the bivalve-shaped morphospecies, with evident
283 increment in cell redifferentiation in the GG.
284
285 *4.1. Diversity of cell lineages in the development of the* Lopesia *galls*
286 The dermal system is the first plant tissue system to differentiate in the four
287 *Lopesia* galls, similar to the ordinary ontogenesis of the non-galled pinnulae of *M.*
288 *gemmulata* (Costa et al., 2018), and of other plants that host galling herbivores (Moura et
289 al., 2008; Oliveira et al., 2006; 2010; Isaias et al., 2011; Martinez et al., 2018). The over-
290 differentiation of non-glandular and glandular trichomes in the induction stage of the four
291 *Lopesia* galls indicates the recruitment of ordinary cells toward trichoblasts, and the
292 longer maintenance of a juvenile developmental feature of the host plant leaves. The
293 differentiation of trichoblasts into trichomes occurs while ordinary epidermal cells are
294 still in the division process, and before the differentiation of the other tissue systems
295 (Glover, 2000; Hülskamp, 2004; Tominaga-Wada et al. 2011), which explains their

296 higher density in the four *Lopesia* galls on *M. gemmulata*. The dermal tissue system
297 covering the two valves have peculiar trichome distribution in each *Lopesia* gall, and is
298 involved in their closure in the growth and development stage. The closure of the LG
299 involves the differentiation of the unicellular filiform and the multicellular peltate
300 trichomes, as well as of the papillose cells. Additionally to these epidermal traits, the
301 hypertrophying process of the unicellular filiform trichomes works out in the GLG
302 closure, while the BLG closure also involves the hypertrophying process, but of the
303 multicellular filiform trichomes. The peltate trichomes do not differentiate in the BLG,
304 as an ontogenetic constraint of the trichoblasts of the pinnulae adaxial epidermis, where
305 only unicellular filiform trichomes differentiate (Costa et al., 2018). Peculiarly, in the
306 GG, the peltate trichomes cover the valves, and only the unicellular filiform trichomes
307 differentiate in the closure zone. The sparse distribution of the peltate trichomes in the
308 maturation stage of the LG and of the GG is related to the expansion of the ordinary
309 epidermal cells, and represents a common epidermal trait to the non-galled abaxial surface
310 of *M. gemmulata* mature pinnulae. The GLG and BLG valves remain densely covered by
311 trichomes, probably due to the recruitment of more ordinary cells toward trichoblasts.
312 During the senescent stage, the falling of the trichomes in the ostiolar region helps the
313 Cecidomyiidae gall opening (Meyer and Maresquelle, 1983; Meyer, 1987), as occurs on
314 the distal zone of the four *Lopesia* galls associated with *M. gemmulata.*

315 The plant ground tissue system has the most plastic cell lineages, with the
316 totipotency of parenchyma cells activated toward the redifferentiation of new cell types
317 (Lev-Yadun, 2003), as also demonstrated for several galls (Dreger-Jauffret and
318 Shorthouse, 1992; Oliveira and Isaias, 2010; Isaias et al., 2014). The recruitment of
319 parenchyma cell lineages from the *M. gemmulata* pinna-rachis toward the ground tissue
320 systems of the four *Lopesia* galls occurs during the induction stage. The increment in cell

divisions ends up in the reorganization of the ground tissue system into the outer and median parenchyma during the growth and development stage. Along maturation, the outer and median parenchyma cells redifferentiate into the common storage tissue of the LG, GLG and BLG. Peculiarly, in the GG, only the outer parenchyma cells redifferentiate toward the common storage tissue. Together with the cell divisions, parenchyma cell hypertrophy in the growth and development stage ends up in the expansion of the larger valve over the minor valve as a particular feature of the GG *Lopesia* gall, which also assists in its closure. In the senescent stage, the dehydration of the cells of the common storage tissue is important for gall opening, due to a tension force created along the median and distal regions of the gall walls. Such force exerted by cell collapse in the valves work as a mechanism for gall opening and for the emergence of the adults of the four *Lopesia*.

Some of the *M. gemmulata* pinna-rachis parenchyma cells are also recruited to originate the mechanical zone of the GLG, the BLG, and the GG, which starts with the deposition of secondary cell walls and lignification in the maturation stage, a common trait of Cecidomyiidae galls (Meyer and Maresquelle, 1983; Rohfritsch, 1992; Oliveira and Isaias, 2010; Bragança et al., 2017; Molas et al., 2017). Curiously, the lignification process in the LG is peculiar, for the sclerenchyma cells differentiate in the gall basal and median zones during the growth and development stage, and proceeds toward the gall distal zone along maturation. In the LG, GLG, and BLG, the sclerenchyma layers redifferentiate from the inner parenchyma cells, while in the GG, the sclerenchyma layers develop through redifferentiation of the median parenchyma cells, forming a connection with the pericyclic fibers of the pinna-rachis.

The vascular tissue system in Cecidomyiidae galls may originate from the procambium, vascular cambium or parenchyma cells (Bragança et al., 2021). In the four

346 *Lopesia* galls, the parenchyma cells of *M. gemmulata* pinna-rachis are recruited and
347 redifferentiated toward the vascular cells in the induction stage, and proceeds toward the
348 growth and development stage. Peculiarly, in the GG an increment of vascular elements
349 occurs, which may be associated with water and nutrient support for its longer lifespan
350 among the galls on *M. gemmulata* (Costa et al., 2021).

351 The typical nutritive tissue of Cecidomyiidae galls can be originated from the
352 epidermal and the parenchyma cells of the host organs (Bronner, 1992; Rohfritsch, 1992),
353 as is true for the GG on *M. gemmulata*, and culminates in the highest tissue stratification
354 along the growth and development and the maturation stages. The mixed origin of the
355 typical nutritive tissue has been demonstrated previously in Cecidomyiidae galls (*cf.*
356 Oliveira and Isaias, 2010), but in the case of the LG, the GLG, and the BLG, the nutritive
357 cells are originated exclusively from the epidermal cells of the pinna-rachis in the
358 induction stage.

359

360 *4.2. Anatomical features related to the structural-functional traits of* Lopesia *galls*

361 The determination of the extralaminar bivalve-shaped galls seems to be related to
362 the site of induction, and to the feeding of the *Lopesia* larvae on epidermal cells next to
363 the vascular system. The dynamics of anticlinal divisions of the epidermis, and anticlinal
364 and periclinal divisions of the parenchyma cells of the pinna-rachis leads to the expansion
365 of the valve-like appendages that enclose the *Lopesia* larvae into the gall chambers.
366 Similarly, during the ontogenesis of compound leaves, the pinnula emerges from the
367 dermal and ground tissue systems of the pinna-rachis (Costa et al., 2018), with similar
368 ontogenetical steps herein described for the valves of the galls. In fact, the valve-like
369 appendages reflect the deviation of a previously determined ontogenetical pattern toward
370 the formation of valves instead of pinnulae, thus reflecting the structural and functional

371 change from photosynthesis-related tissues of leaves toward nutrition and protection-
372 related tissues of galls. The ontogenesis of other bivalve-shaped galls on Fabaceae species
373 corroborates the interpretation of the valves as leaflet-like appendages (Isaias et al., 2011;
374 Molas et al., 2017; Nogueira et al., 2018), but deviated from its ordinary structural and
375 functional patterns.

376 The ordinary epidermal cells covering the four bivalve-shaped galls remains
377 single-layered in all the developmental stages, evidencing that periclinal divisions of
378 epidermal cells are not triggered by any of the four *Lopesia* species on *M. gemmulata*.
379 The anticlinal divisions of epidermal cells represent a morphogenetical constraint of *M.*
380 *gemmulata* pinnulae, as of other host plants associated to other bivalve-shaped galls
381 (Isaias et al., 2011; Molas et al., 2017; Nogueira et al., 2018). The manipulation of
382 epidermal cell redifferentiation, however, has the impressive feature of the recruitment of
383 ordinary cells toward trichoblasts, which in the case of the *M. gemmulata-Lopesia*
384 systems followed diverse new patterns to fit the same solution, the gall closure. The
385 differentiation of trichomes and papillose cells has been observed in the galls on
386 *Lonchocarpus muehlbergianus* (Isaias et al., 2011) and on *Prosopis caldenia* (Molas et
387 al. 2017), respectively. These two epidermal traits, trichomes and papillose epidermal
388 cells, are involved in the closure of the galls on *M. gemmulata*, but with specificities
389 regarding each of the four *Lopesia* galls. Such specificity is also expressed in the stomata,
390 which may be abnormal (GG) or absent (LG, GLG and BLG), and demonstrate the
391 impairment of the *M. gemmulata* pinnula developmental pattern. The alteration in stomata
392 differentiation reduces the ability for gas exchange, configuring the new structural-
393 functional patterns of Cecidomyiidae galls (Huang et al., 2014, 2015; Amorim et al.,
394 2017).

The new ontogenetical fates of the cells and tissues of the four *Lopesia* galls culminate in parenchyma homogenization, with reduced intercellular spaces and cells with few chloroplasts. The most noticeable anatomical trait regarding the cells of the ground tissue system of the four *Lopesia* galls and of the *M. gemmulata* pinnulae is the redifferentiation of the mechanical zone in the outer tissue compartment. The homogeneous parenchyma and the sclerenchyma layers are common to other insect galls (Rohfritsch, 1992; Kurzfeld-Zexer et al., 2015; Bragança et al., 2021), and perform structural and storage functions for gall establishment and survivor (Ferreira et al., 2017). The common storage tissue of *Lopesia* galls on *M. gemmulata* accumulates carbohydrates, proteins, and lipids in the protoplast, as well as xyloglucans in the cell walls, which are mobilized for the nutritional and structural maintenance of the galls (Costa et al., 2021). The sclerenchyma layers confer mechanical support to the valves and form a thicker mechanical zone in the GG than in the other three *Lopesia* galls on *M. gemmulata*, which is possibly a time-related feature, since GG has the longest lifespan among the four *Lopesia* galls (Costa et al., 2021).

The redifferentiation of the sclerenchyma cells is involved in the opening of the bivalve-shaped galls on *L. muehlbergianus* (Isaias et al., 2011) and on *P. caldenia* (Molas et al. 2017), while in the four *Lopesia* galls, the dehydration of the common storage cells is important for the mechanical opening of the bivalve-shaped galls on *M. gemmulata*. These anatomical features in the outer tissue compartment create tension in the two valves, which leads to the rupturing of cell layers in the ostiolar area, and the adult inducers are able to escape. In the bivalve-shaped galls of Cecidomyiidae on Fabaceae species (Mani, 1964; Maia and Fernandes, 2006; Maia et al., 2010; Molas et al., 2017), as well as in the *M. gemmulata-Lopesia* systems (Costa et al., 2018; Costa et al.,

submitted), the pupae movements also assist the gall opening, and the pupal exuviae are left between the gall valves after the emergence of the adult galling *Lopesia*.

The hydric status of the galls is maintained by the cell-to-cell water transport favored by the reduced intercellular spaces and also by the vascularization network (Oliveira et al., 2017; Aloni et al., 2021; Bragança et al., 2021). The neovascularization of the four *Lopesia* galls is connected to the central vascular system of the host pinna-rachis, being a crucial anatomical trait established in extralaminar bivalve-shaped galls (Molas et al., 2017; Nogueira et al., 2018) for their organogenesis as adventitious new organs (Isaias et al., 2011, 2013). As in other leaf galls (Kurzfeld-Zexer et al., 2015; Álvarez et al., 2020), the xylem is directed toward the inner side, and the phloem is oriented toward the outer side, keeping the collateral arrangement. This is a conservative pattern of the vascular tissues of the pinnulae and pinna rachis of *M. gemmulata*, and is a strong support for the leaf nature of the valve-like appendages of the four *Lopesia* galls.

The epidermal cells are functional barriers against water loss and abiotic stresses in non-galled tissues (Javelle et al., 2010), but in galls are cytologically decharacterized and redifferentiated in the nutritive cells that serve as food source (Bronner, 1992; Oliveira et al., 2011). The nutritive cells, redifferentiated from the ordinary epidermal cells of the host plant, accumulate energetic molecules, such as the lipids and reducing sugars in the protoplasm, and xyloglucans and heteromannans in the cell walls (Costa et al., 2021). They are typical nutritive cells in the four *Lopesia* galls, but the *Lopesia*-GG system expressed the additional advantage of the mixed origin of its nutritive cells, culminating in higher stratification. Such stratification reflects the potential of parenchyma cells to divide not only anticlinally but also periclinally, which has not been observed for the nutritive cells of other *Lopesia* galls. .

5. Conclusion

The ontogenetic studies in the four bivalve-shaped galls revealed that the specificity of each *M. gemmulata-Lopesia* system is mainly expressed in the epidermal cell lineages, by the recruitment of new trichoblasts at different sites, and by breaking their developmental patterns. Trichome types are manipulated by the four species of *Lopesia* in peculiar ways, with differences in size, number of cells, and distribution in the dermal system of each gall. However, as variable as the trichomes may be, they are involved not only in the covering of the galls, but also in the mechanism of gall closure. The parenchyma of the valves, which are leaflet-like appendages, deviate from the standard photosynthetic function, and assumes the structural-functional traits of nutrient storage and mechanical protection in the four *Lopesia* galls; in the GG it also contributes to the formation of the nutritive tissue. In the other three galls, the typical nutritive tissues are exclusively originated from the epidermis. The vascular system, as conservative as it is in the four *Lopesia* galls, has a higher increment of cells in the GG, the most peculiar amongst the four bivalve-shaped galls on *M. gemmulata*. The intrinsic anatomical features of the four *Lopesia* galls relate both to their common site of induction and to the original cell lineages recruited toward the ontogenesis of similar bivalve-shaped morphotypes. However, specific ontogenetic deviations characterize each *Lopesia* gall morphospecies, within which the GG peculiar structural-functional traits develop due to its highest potential for stimuli-induced cell responses in all host plant cell lineages and to its longest lifespan.

Credit author statement

ECC, DCO and RMSI designed sampling methods. ECC and MSCF collected material and performed the experiments. ECC, MSCF, RGSC, DCO and RMSI analyzed the results, discussed data, wrote, and reviewed the manuscript.

Funding

Coordenação de Aperfeiçoamento de Pessoal de Nível Superior (*CAPES*) – Brazil– Finance Code 001 for doctoral grant (888877.199702/2018-00 – ECC). *Conselho Nacional de Desenvolvimento Científico e Tecnológico* (*CNPq*) for the research fellowships granted to R.M.S. Isaias (304335/2019-2 – RMSI and 304981/2019 – DCO).

Declaration of Competing Interest

None.

Acknowledgments

We thank Dra. Valéria Cid Maia and Dra. Sheila Patrícia Carvalho-Fernandes (*Museu Nacional*/UFRJ) for the identification of insects.

References

Aloni, R., 2021. How vascular differentiation in hosts is regulated by parasitic plants and gall inducing insects. In: Aloni, R. (Ed.), Vascular differentiation and plant hormones. Springer, Switzerland, pp. 293–305. https://doi.org/10.1007/978-3-030-53202-4_20

Álvarez, R., Moreno-Gonzalez, V., Martinez, J.J.I., Ferreira, B.G., Hidalgo N.P., 2020. Microscopic study of nine galls induced in *Populus nigra* by aphids of the Iberian Peninsula. Arth.-Plant Int. 14, 1–11. https://doi.org/10.1007/s11829-020-09778-1.

492 Amorim, D.O., Ferreira, B.G., Fleury, G., 2017. Plant potentialities determine anatomical
493 and histochemical diversity in *Mikania glomerata* Spreng. galls. Braz J Bot 40,
494 517–527. https://doi.org/doi:10.1007/s40415-016-0357-9.
495 Bragança, G.P., Oliveira, D.C., Isaias, R.M.S., 2017. Compartmentalization of
496 metabolites and enzymatic mediation in nutritive cells of Cecidomyiidae galls on
497 *Piper arboreum* Aubl. (Piperaceae). J. Plant Tiss 6, 11–22.
498 https://doi.org/10.5539/jps.v6n1p11.
499 Bragança, G.P., Alencar, C.F., Freitas, M.S.C., Isaias R.M.S., 2021. The influence of gall
500 position over xylem features in leaflets of *Inga ingoides* (Rich.) Willd. (Fabaceae:
501 Caesalpinioideae). Trees 35, 199–209. https://doi.org/10.1007/s00468-020-02027-
502 1.
503 Bronner, R., 1992. The role of nutritive cells in the nutrition of cynipids and cecidomyiids.
504 In: Shorthouse, J.D., Rohfritsch, O. (Eds), Biology of insect induced-galls. Oxford
505 University Press, Oxford, pp. 118–140.
506 Bukatsch, F., 1972. Bermerkungen zur Doppelfärbung Astrablau-Safranin. Mikrokosmo,
507 61, 255.
508 Carneiro, R.G.S., Pacheco, P., Isaias, R.M.S., 2015. Could the Extended Phenotype
509 Extend to the Cellular and Subcellular Levels in Insect-Induced Galls? Plos one 8,
510 1–20. https://doi.org/10.1371/journal.pone.0129331.
511 Carneiro, R.G.S, Isaias, R.M.S., Moreira, A.S.F.P., Oliveira, D.C., 2017. Reacquisition
512 of new meristematic sites determines the development of a new organ, the
513 Cecidomyiidae gall on *Copaifera langsdorffii* Desf. (Fabaceae). Front. Plant Sci. 8,
514 1–10. https://doi.org/10.3389/fpls.2017.01622.
515 Costa, E.C., Carneiro, R.G.S., Silva, J.S., Isaias, R.M.S., 2018. Biology and development
516 of galls induced by *Lopesia* sp. (Diptera: Cecidomyiidae) on leaves of *Mimosa*

517 *gemmulata* (Leguminosae: Caesalpinioideae). Aust. J. Bot. 66, 161–172.
518 https://doi.org/ 10.1071/BT17099.

519 Costa, E.C., Martini, V.C., Souza-Silva, A., Lemos-Filho, J.P., Oliveira, D.C., Isaias,
520 R.M.S. 2021a. How galling herbivores share a single super-host plant during their
521 phenological cycle: the case of *Mimosa gemmulata* Barneby (Fabaceae). Tropical
522 Ecology

523 Costa, E.C., Oliveira, D.C., Ferreira, D.K.L., Isaias, R.M.S., 2021b. Structural and
524 nutritional peculiarities related to lifespan differences on four *Lopesia* induced
525 bivalve-shaped galls on the single super-host *Mimosa gemmulata*. Front. Plant Sci.
526 12, 1-13. https://doi.org/10.3389/fpls.2021.660557.

527 Dreger-Jauffret, F., Shorthouse. J. D., 1992. Diversity of gall-inducing insects and their
528 galls. In: Shorthouse, J. D., Rohfritsch O. (Eds.), Biology of Insect-Induced Galls,
529 Oxford University Press, New York, pp. 8–33.

530 Ferreira, B.G., Álvarez, R., Avritzer, S.C., Isaias, R.M.S., 2017. Revisiting the
531 histological patterns of storage tissues: beyond the limits of gall-inducing taxa.
532 Botany 95, 173–184. https://doi.org/10.1139/cjb-2016-0189.

533 Formiga, A.T., Silveira, F.A.O., Fernandes, G.W., Isaias, R.M.S., 2014. Phenotypic
534 plasticity and similarity among gall morphotypes on a superhost, *Baccharis*
535 *reticularia* (Asteraceae). Plant Biol. 17, 512–521.
536 https://doi.org/10.1111/plb.12232.

537 Glover, B.J., 2000. Differentiation in plant epidermal cells. J. Exp. Bot. 51, 497–505.
538 https://doi.org/10.1093/jexbot/51.344.497.

539 Hulskamp, M., 2004. Plant trichomes: A model for cell differentiation. Nat. Rev. Mol.
540 Cell Biol. 5, 471–480. https://doi.org/10.1038/nrm1404

541 Huang, M.Y., Huang, W.D., Chou, H.M., Lin, K.H., Chen, C.C., Chen, P.J., Chang, Y.T.,
542 Yang, C.M., 2014. Leaf-derived cecidomyiid galls are sinks in *Machilus thunbergii*

(Lauraceae) leaves. Physiol. Plantarum 152, 475–485. https://doi.org/10.1111/ppl.12186.

Huang, M.Y., Huang, W.D., Chou, H.M., Chen, C.C., Chen, P.J., Chang, Y.T., Yang, C.M., 2015. Structural, biochemical, and physiological characterization of photosynthesis in leaf-derived cup-shaped galls on *Litsea acuminate*. BMC Plant Biol. 61, 2-12. https://doi.org/10.1186/s12870-015-0446-0.

Isaias, R.M.S., Oliveira, D.C., Carneiro, R.G.S., 2011. Role of *Euphalerus ostreoides* (Hemiptera: Psylloidea) in manipulating leaflet ontogenesis of *Lonchocarpus muehlbergianus* (Fabaceae). Botany 89, 581–592. https://doi.org/10.1139/b11-048.

Isaias, R.M.S., Carneiro, R.G.S., Oliveira, D.C., Santos, J.C., 2013. Illustrated and annotated checklist of Brazilian gall morphotypes. Neotrop. Entomol. 42, 230–239. https://doi.org/10.1007/s13744-013-0115-7.

Isaias, R.M.S., Oliveira, D.C., Carneiro, R.G.S., Kraus, J.E., 2014. Developmental anatomy of galls in the Neotropics: arthropods stimuli versus host plant constraints. In: Fernandes, G.W., Santos, J.C. (Eds.), Neotropical Insect Galls. Springer, Netherlands, Dordrecht, pp. 15–34.

Javelle, M., Vernoud., V., Depège-Fargeix, N., Arnould, C., Oursel, D., Domergue, F., Sarda, X., Rogowsky, P.M., 2010. Overexpression of the epidermis-specific homeodomain-leucine zipper IV transcription factor Outer Cell Layer1 in maize identifies target genes involved in lipid metabolism and cuticle biosynthesis. Plant Physiol 154, 273–286. https://doi.org/10.1111/j.1469-8137.2010.03514.x

Johansen, D.A., 1940. Plant Microtechnique. McGraw-Hill Book Co. Inc., New York.

Karnovsky, M., 1965. A formaldehyde-glutaraldehyde fixative of high osmolality for use in electron microscopy. J Cell Biol 27, 137–138.

567 Kraus, J.E., Arduin, M., 1997. Manual básico de métodos em morfologia vegetal. Editora
568 da Universidade Federal Rural do Rio de Janeiro, Seropédica.
569 Kurzfeld-Zexer, L., Lev-Yadun, S., Inbar, M., 2015. One aphid species induces three gall
570 types on a single plant: Comparative histology of one genotype and multiple
571 extended phenotypes. Flora 210, 19–30.
572 https://doi.org/10.1016/j.flora.2014.10.007.
573 Lev-Yadun, S., 2003. Stem cells in plants are differentiated too. Curr Opin Plant Biol 4,
574 93–102.
575 Maia, V.C., Fernandes, G.W., 2006. A new genus and species of gall midge (Diptera,
576 Cecidomyiidae) associated with *Parkia pendula* (Fabaceae, Mimosoideae). Rev.
577 bras. entomol. 50, 1–5. https://doi.org/10.1590/S0085-56262006000100001.
578 Maia, V.C., Fernandes, G.W., Magalhães, H., Santos, J.C., 2010. Two new species of
579 *Lopesia* Rübsaamen (Diptera, Cecidomyiidae) associated with *Mimosa hostilis*
580 (Mimosaceae) in Brazil. Rev. bras. entomol. 54, 578–583.
581 https://doi.org/10.1590/S0085-56262010000400007.
582 Mani, M.S., 1964. Ecology of Plant Galls. Dr. W. Junk Publishers, The Hague.
583 Martinez, J.J., Moreno-González, V., Jonas-Levi, A., Álvarez, R., 2020. Quantitative
584 differences detected in the histology of galls induced by the same aphid species in
585 different varieties of the same host. Plant Biol. 20, 516–524.
586 https://doi.org/10.1111/plb.12705.
587 Meyer, J., 1987. Plant galls and gall inducers. Gebrüder Borntraeger.
588 Meyer, J., Maresquelle, H.J., 1983. Anatomie des galles. Gebrüder Borntraeger.
589 Molas, B.M.C., Martínez, J.J., Nacaratti, S., Arrese, J.J., Testa, N., Álvarez, M.N., 2017.
590 Exomorfología y anatomía dela agalla bivalva foliar inducida por *Rhopalomyia* sp.

(Insecta, Diptera, Cecidomyiidae) en *Prosopis caldenia* (Fabaceae). Bol. Soc. Argent. Bot. 52, 535–547. https://doi.org/10.31055/1851.2372.v52.n3.18032.

Moura, M.Z.D., Soares, G.L.G., Isaias, R.M.S., 2008. Species-specific changes in tissue morphogenesis induced by two arthropod leaf gallers in *Lantana camara* L. (Verbenaceae). Aust. J. Bot. 56, 153–160. https://doi.org/10.1071/BT07131.

Nogueira, R.M., Costa, E.C.C., Santos-Silva, J., Isaias, R.M.S., 2018. Structural and histochemical profile of *Lopesia* sp. Rübsaamen. 1908 pinnula galls on *Mimosa tenuiflora* (Willd.) Poir. in a Caatinga environment. Hoehnea 45, 231-239. https://doi.org/10.1590/2236-8906-80/2017.

O'Brien, T.P., McCully, M.E., 1981. The Study of Plant Structure Principles and Selected Methods. Termarcarphi Pty. Ltd., Melbourne.

Oliveira, D.C., Christiano, J.C.S., Soares, G.L.G., Isaias, R.M.S., 2006. Reações de defesas químicas e estruturais de *Lonchocarpus muehlbergianus* Hassl. (Fabaceae) à ação do galhador *Euphalerus ostreoides* Crawf. (Hemiptera: Psyllidae). Rev. Bras. Bot. 29, 657–667. https://doi.org/10.1590/S0100-84042006000400015.

Oliveira, D.C., Isaias, R.M.S., 2010. Redifferentiation of leaflet tissues during midrib gall development in *Copaifera langsdorffii* (Fabaceae). S. Afr. J. Bot. 76, 239–248. https://doi.org/10.1016/j.sajb.2009.10.011.

Oliveira, D.C., Carneiro, R.G.S., Magalhães, T.A., Isaias, R.M.S., 2011. Cytological and histochemical gradients on two *Copaifera langsdorffii* Desf. (Fabaceae) Cecidomyiidae gall systems. Protoplasma 248, 829–837. https://doi.org/10.1007/s00709-010- 0258-x.

Oliveira, D.C., Moreira, A.S.F.P., Isaias, R.M.S., Martini, V., Rezende, U., 2017. Sink status and photosynthetic rate of the leaflet galls induced by *Bystracoccus mataybae*

(Eriococcidae) on *Matayba guianensis* (Sapindaceae). Front. Plant Sci 8, 1–12. https://doi.org/10.3389/fpls.2017.01249.

Paiva, J.G.A., Fank-De-Carvalho, S.M., Magalhães, M.P., Graciano-Ribeiro, D., 2006. Verniz vitral incolor 500®: uma alternativa de meio de montagem economicamente viável. Acta bot. bras. 20, 257–264. https://doi.org/10.1590/S0102-33062006000200002.

Rohfritsch, O., 1992. Patterns in gall development. In: Shorthouse, J.D., Rohfritsch, O. (Eds.), Biology of insect-induced galls. Oxford University Press, Oxford, pp. 60–86.

Stone, G.N., Schonrögge, K., 2003. The adaptive significance of insect gall morphology. Trends Ecol. Evol. 18, 512–522. https://doi.org/10.1016/S0169-5347(03)00247-7.

Tominaga-Wada, R., Ishida, T, Wada, T., 2011. New insights into the mechanism of development of arabidopsis root hairs and trichomes. Int Rev Cell Mol Biol. 286, 67-106. https://doi.org/10.1016/B978-0-12-385859-7.00002-1.

637 **Figures**

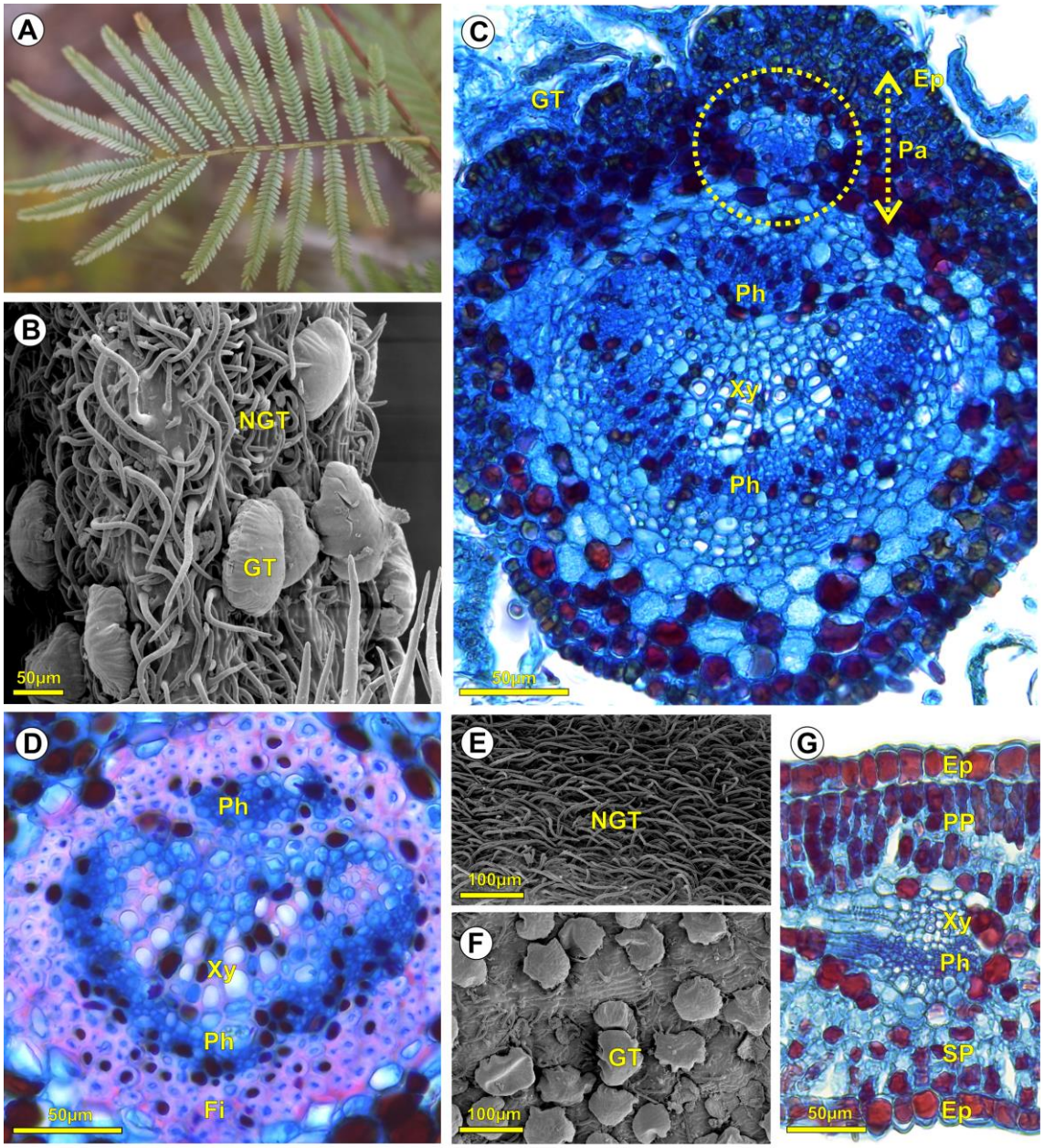

638

639

640

641

642 Fig. 1. Non-galled leaves of *Mimosa gemmulata* Barneby (Fabaceae). A) Macroscopic
643 aspect of a non-galled leaf. B-D) Pinna-rachis. B) Non-glandular unicellular filiform and
644 glandular multicellular peltate trichomes under scanning electron microscopy. C-D)
645 Transverse anatomical sections. C) imature stage, evidencing small vascular bundles
646 (yellow circle), central vascular system, and cortical parenchyma (yellow double arrow).
647 D) Vascular system in mature stage evidencing tissue arrangement and lignified fibers.
648 E-G) Mature pinnula. E) Non-glandular unicellular filiform trichomes in the adaxial
649 surface, and F) glandular multicellular peltate trichomes in the abaxial surface under
650 scanning electron microscopy. G) Transverse anatomical section evidencing tissue
651 arrangement. Ep: epidermis; Fi: fibers; GT: glandular trichomes; NGT: non-glandular
652 trichomes; Pa: parenchyma; Ph: phloem; PP: palisade parenchyma; SP: spongy
653 parenchyma; Xy: xylem.

654

655

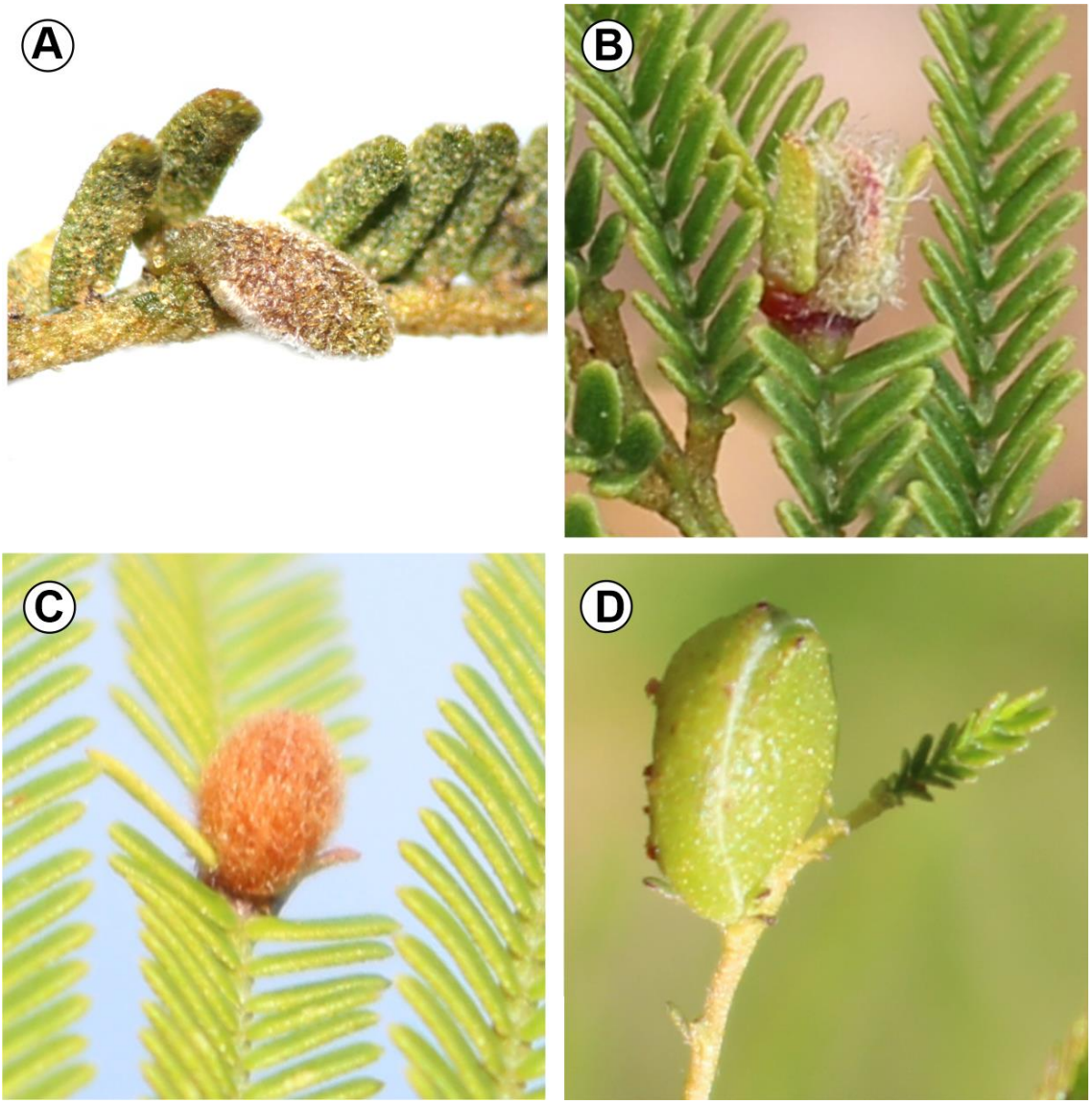

Fig. 2. Mature *Lopesia* galls on *Mimosa gemmulata* Barneby (Fabaceae). A) Lenticular bivalve-shaped gall. B) Green lanceolate bivalve-shaped gall. C) Brown lanceolate bivalve-shaped gall. D) Globoid bivalve-shaped gall.

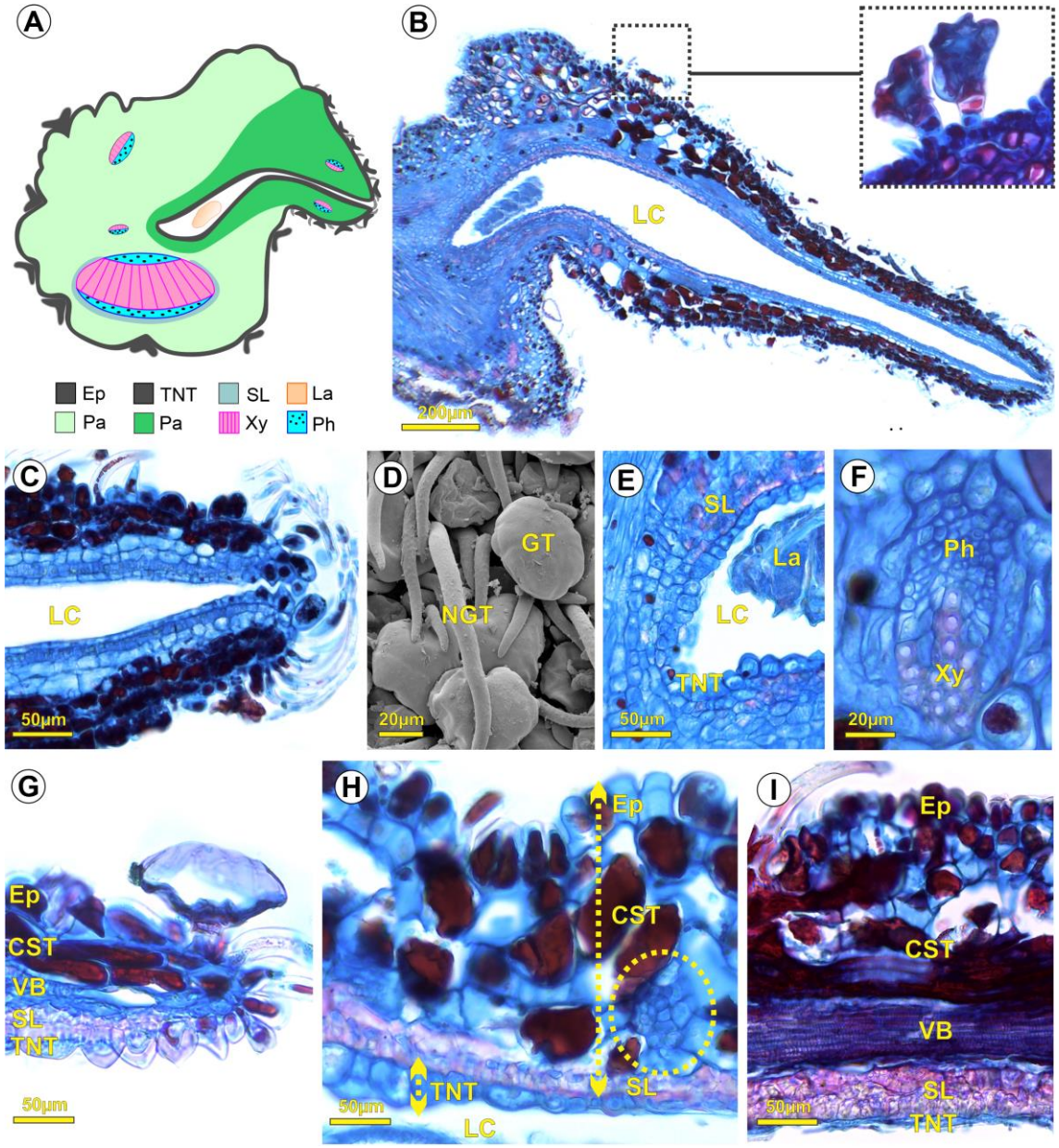

663

664

665

666

667

668

669 Fig. 3. Ontogenesis of the lenticular bivalve-shaped gall induced by *Lopesia* sp. (Diptera-
670 Cecidomyiidae) on *Mimosa gemmulata* Barneby (Fabaceae). A-C; E-I) Transverse
671 anatomical sections. A) Diagram illustrating tissue organization in the gall induction
672 stage. B-F) Growth and development stage. B) Anatomical aspect of the valves
673 evidencing tissue organization and glandular multicellular peltate trichomes (detail in
674 box) covering the gall. C) Gall closure with trichomes and papillose epidermal cells. D)
675 Non-glandular unicellular filiform and glandular multicellular peltate trichomes under
676 scanning electron microscopy. E) Sclerenchyma cells in the basal zone and typical
677 nutritive tissue around the larval chamber. F) Vascular bundle. G-H) Mature stage. G)
678 Sclerenchyma layer in distal zone. H) Outer and inner tissue compartments (yellow
679 double arrows), highlighting a vascular bundle (yellow circle). I) Senescent stage
680 evidencing tissue organization. CST: common storage tissue; Ep: epidermis; GT:
681 glandular trichomes; La: larva; LC: larval chamber; NGT: non-glandular trichomes; Pa:
682 parenchyma; Ph: phloem; SL: sclerenchyma layers; TNT: typical nutritive tissue; VB:
683 vascular bundles; Xy: xylem.

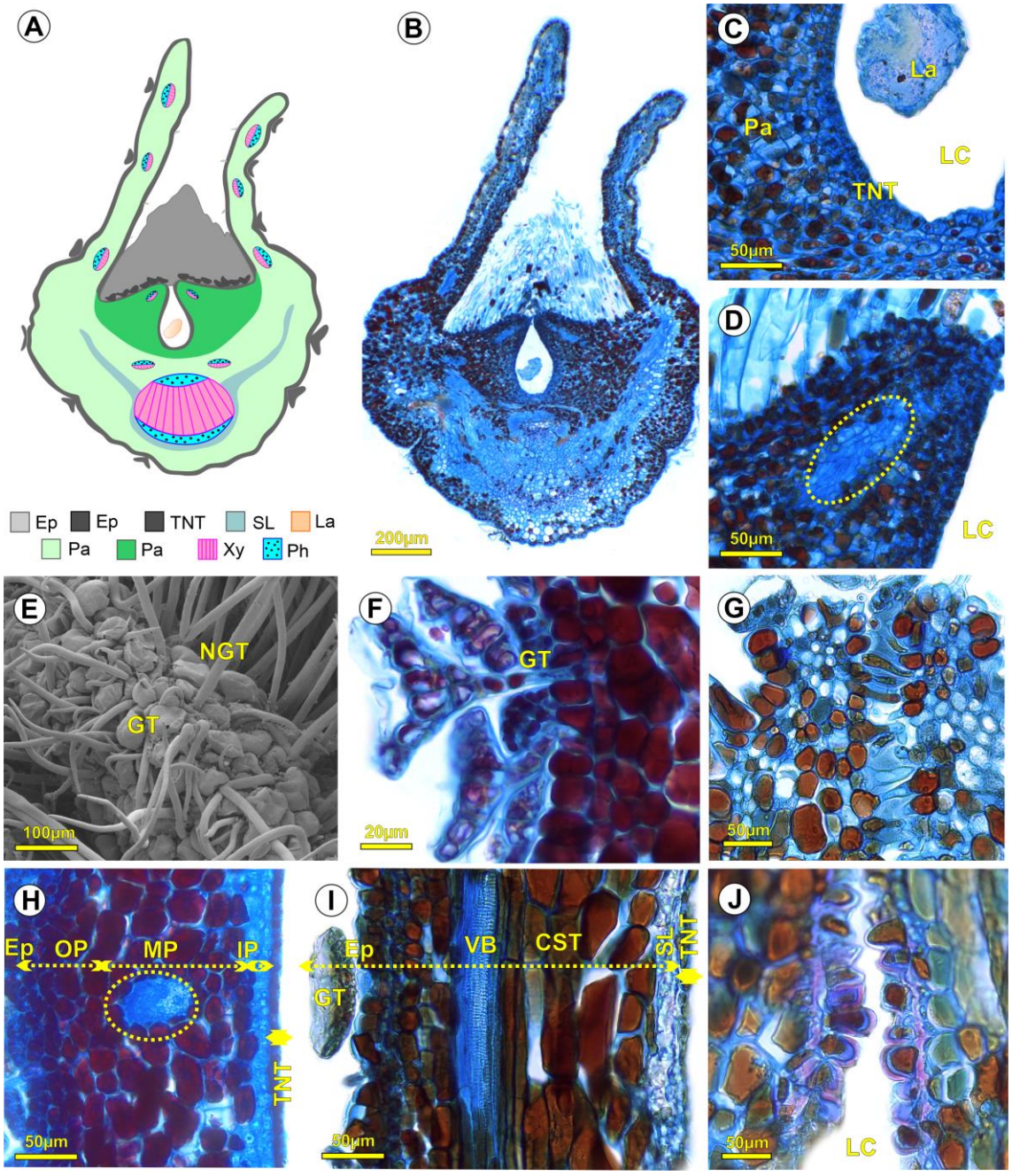

684

685

686

687

688

689 Fig. 4. Ontogenesis of the green lanceolate bivalve-shaped gall induced by *Lopesia* sp.
690 (Diptera-Cecidomyiidae) on *Mimosa gemmulata* Barneby (Fabaceae). A-D; F-J)
691 Transverse anatomical sections. A) Diagram illustrating the gall induction stage. B-D)
692 Induction stage. B) Anatomical aspect evidencing valve-like projections. C)
693 Homogeneous hyperplasic parenchyma and typical nutritive tissue around the larval
694 chamber. D) Undifferentiated vascular cells (yellow circle). E-H) Growth and
695 development stage. E) Gall closure with glandular multicellular peltate and hypertrophied
696 non-glandular unicellular filiform trichomes under scanning electron microscopy. F)
697 Glandular peltate trichomes. G) Papillose epidermal cells in the distal zone. H) General
698 anatomy evidencing tissue organization with epidermis, outer, median and inner
699 parenchymatic regions, and typical nutritive tissue (yellow double arrows); and vascular
700 system (yellow cycle). I) Outer and inner tissue compartments (yellow double arrows) in
701 mature stage. J) Gall opening in senescent stage. CST: common storage tissue; Ep:
702 epidermis; GT: glandular trichomes; IP: inner parenchyma; La: larva; LC: larval
703 chamber; MP: median parenchyma; NGT: non-glandular trichomes; OP: outer
704 parenchyma; Pa: parenchyma; Ph: phloem; SL: Sclerenchyma layers; TNT: typical
705 nutritive tissue; VB: Vascular bundles; Xy: xylem.

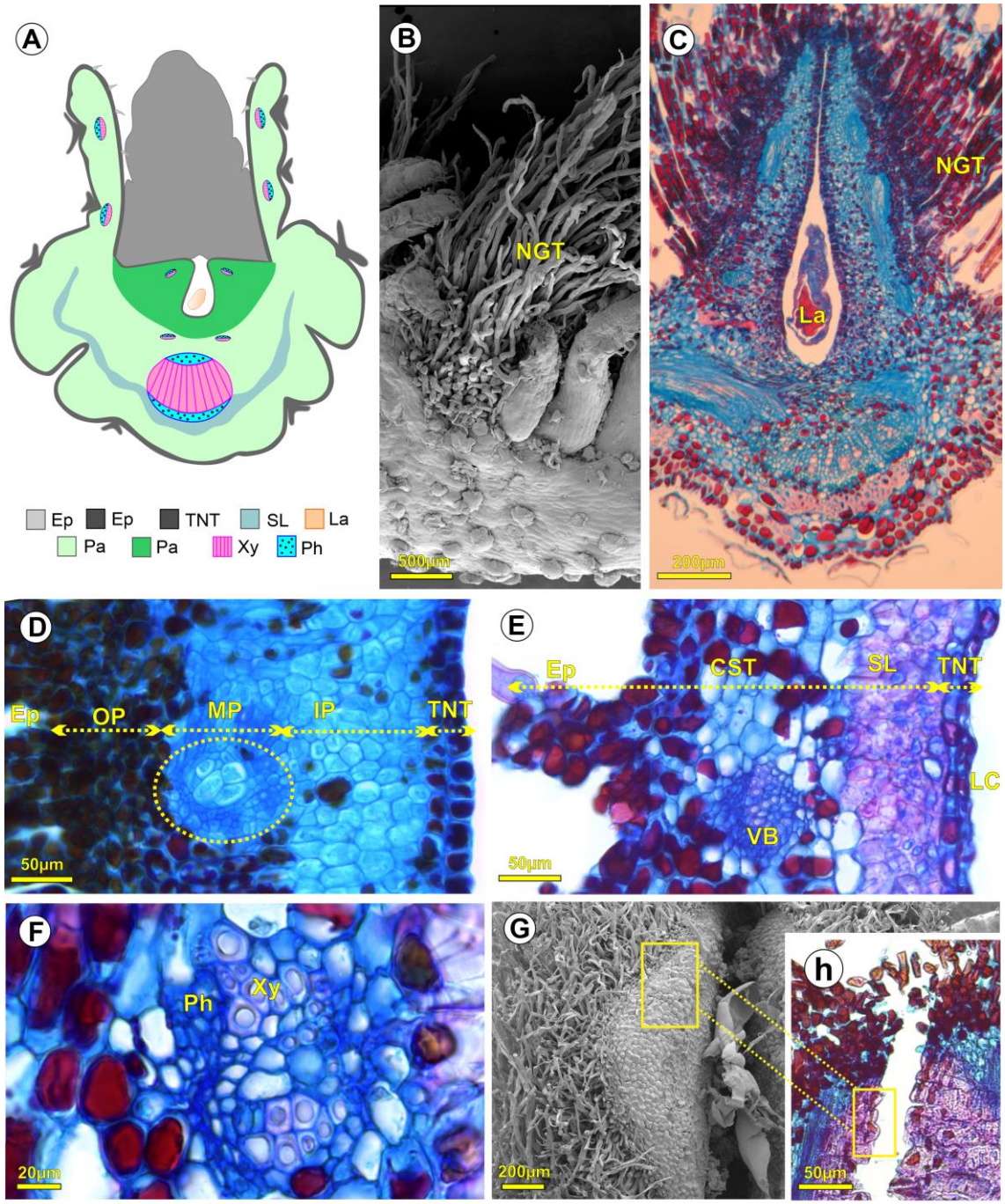

706

707

708

709

Fig. 5. Ontogenesis of the brown lanceolate bivalve-shaped gall induced by *Lopesia* sp. (Diptera-Cecidomyiidae) on *Mimosa gemmulata* Barneby (Fabaceae). A; C-F; H) Transverse anatomical section. A) Diagram illustrating the gall induction stage. B) Induction stage evidencing the hypertrophied glandular multicellular filiform trichomes covering the gall under scanning electron mycroscopy. C-D) General anatomy in growth and development stage. C) Gall closure. D) Tissue organization with epidermis, outer, median and inner parenchyma regions, and typical nutritive tissue (yellow double arrows); and vascular system (yellow cycle). E-F) Mature stage. E) Outer and inner tissue compartments (yellow double arrows). F) Vascular bundles. G-H) Senescent stage. Papillose epidermal cells in gall opening. G) Scanning electron microscopy (yellow box). H) Lignified cell walls (yellow box). CST: common storage tissue; Ep: epidermis; IP: inner parenchyma; La: larva; LC: larval chamber; MP: median parenchyma; NGT: non-glandular trichomes; OP: outer parenchyma; Pa: parenchyma; Ph: phloem; SL: sclerenchyma layer; TNT: typical nutritive tissue; VB: vascular bundles; Xy: xylem.

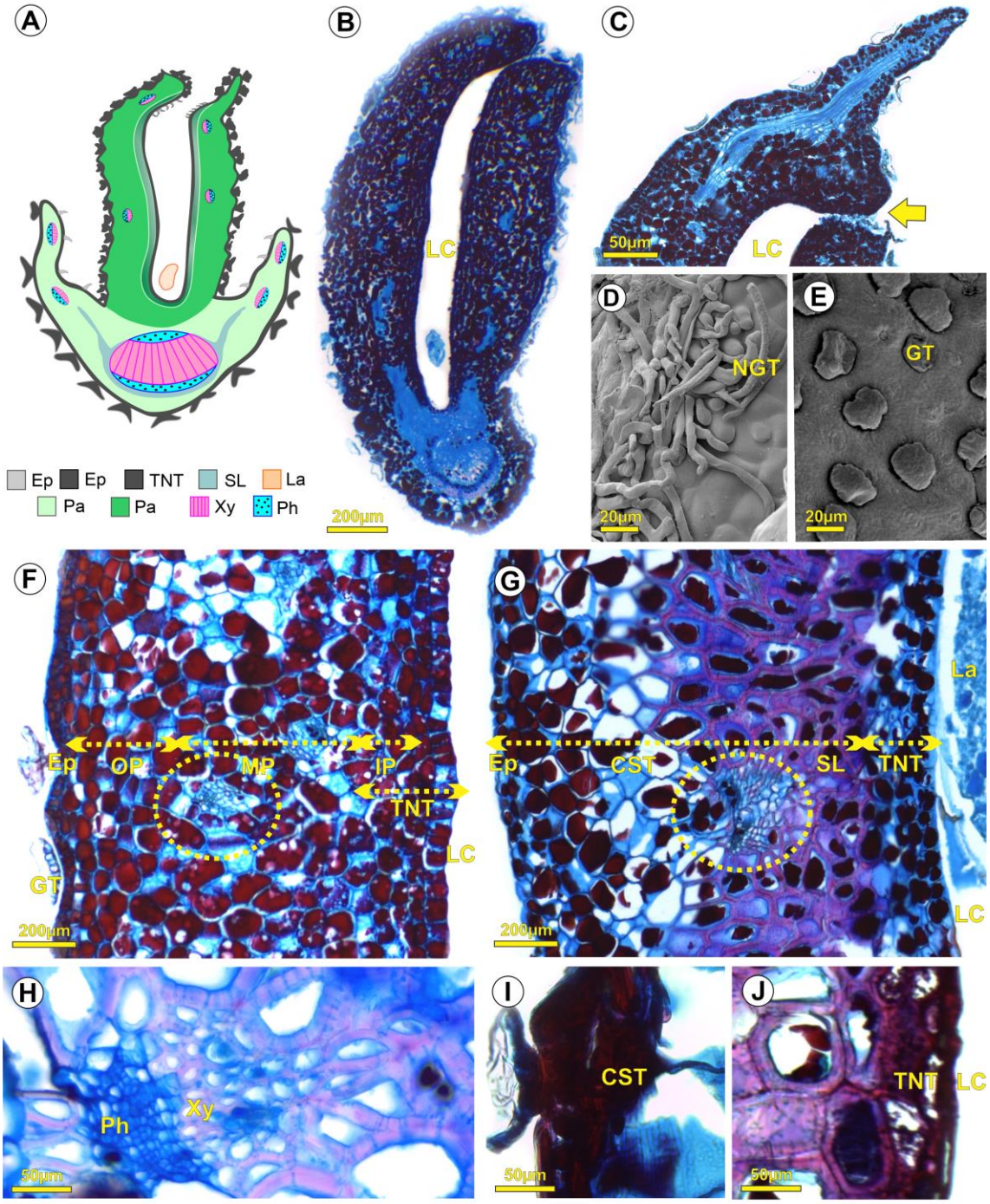
A
B
C
LC
50μm
LC
D
E
NGT
GT
20μm
20μm
Ep
Ep
TNT
SL
La
Pa
Pa
Xy
Ph
200μm
F
G
Ep
OP
MP
IP
TNT
LC
GT
200μm
La
Ep
CST
SL
TNT
LC
200μm
H
I
J
Ph
Xy
50μm
CST
50μm
TNT
LC
50μm

724

725

Fig. 6. Ontogenesis of the globoid bivalve-shaped gall induced by *Lopesia* sp. (Diptera-Cecidomyiidae) on *Mimosa gemmulata* Barneby (Fabaceae). A-C; F-J) Transverse anatomical section. A) Diagram illustrating the gall induction stage. B-F) Growth and development stage. B) General anatomical aspect evidencing tissue organization. C) Non-glandular trichomes in the closure of the two valves (yellow arrow). D-E) Scanning electron microscopy. D) Non-glandular unicellular filiform trichomes. E) Glandular multicellular peltate trichomes. F) General anatomical aspect evidencing the epidermis, outer, median and inner parenchymatic regions, and typical nutritive tissue (yellow double arrows); and vascular system (yellow circle). G-H) Mature stage. G) Outer and inner tissue compartments (yellow double arrows). H) Vascular bundle. I-J) Senescent stage. I) Common storage tissue. J) Typical nutritive tissue. CST; common storage tissue; Ep: epidermis; GT: glandular trichomes; IP: inner parenchyma; La: larva; LC: larval chamber; MP: median parenchyma; NGT: non-glandular trichomes; OP: outer parenchyma; Pa: parenchyma: Ph: phloem. SL: sclerenchyma layer; TNT: typical nutritive tissue; VB: vascular bundles. Xy: xylem.

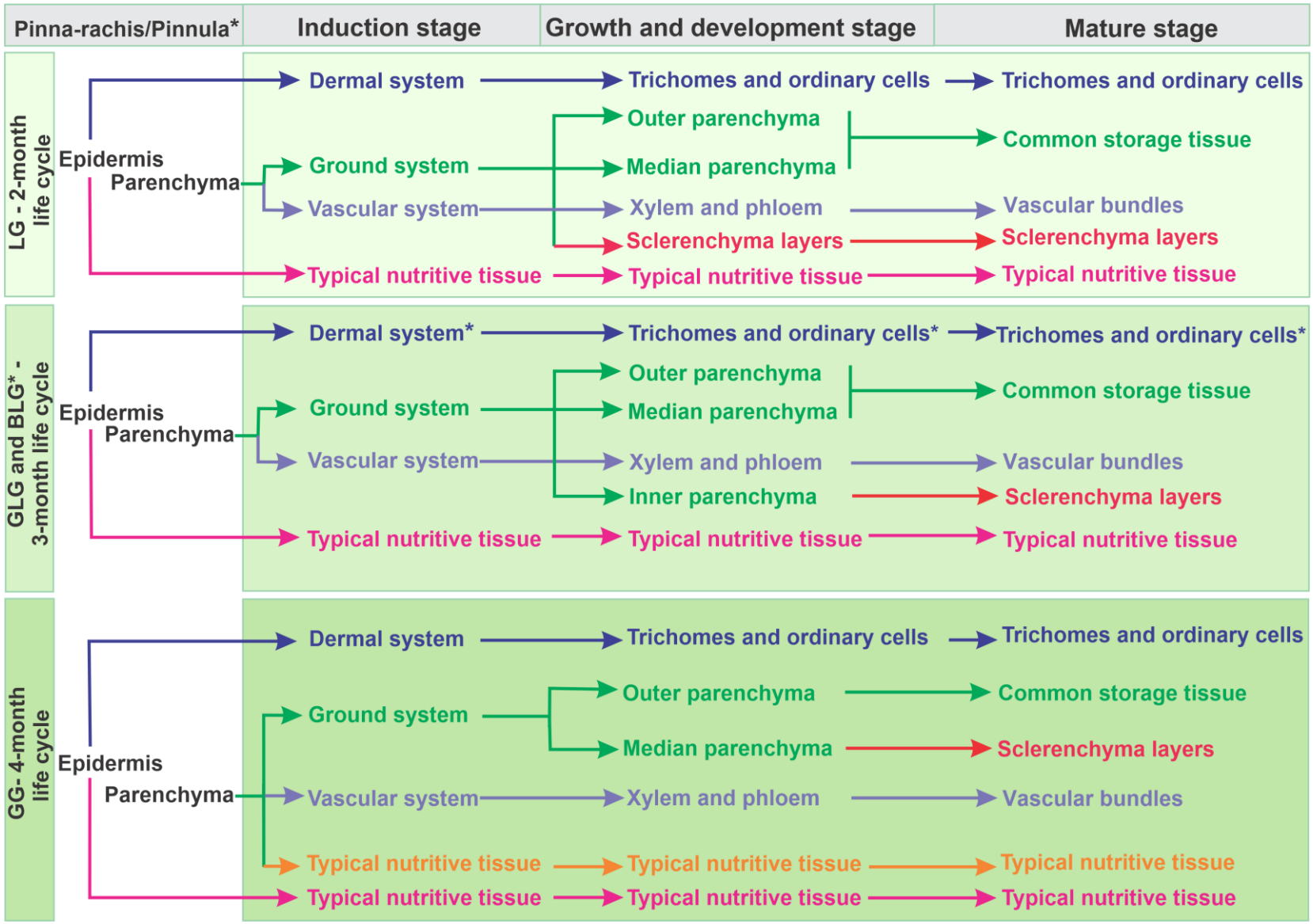
Pinna-rachis/Pinnula*
Induction stage
Growth and development stage
Mature stage
LG - 2-month life cycle
Epidermis
Parenchyma
Dermal system
Trichomes and ordinary cells
Trichomes and ordinary cells
Ground system
Outer parenchyma
Median parenchyma
Common storage tissue
Vascular system
Xylem and phloem
Vascular bundles
Sclerenchyma layers
Sclerenchyma layers
Typical nutritive tissue
Typical nutritive tissue
Typical nutritive tissue
GLG and BLG* - 3-month life cycle
Epidermis
Parenchyma
Dermal system*
Trichomes and ordinary cells*
Trichomes and ordinary cells*
Ground system
Outer parenchyma
Median parenchyma
Common storage tissue
Vascular system
Xylem and phloem
Vascular bundles
Inner parenchyma
Sclerenchyma layers
Typical nutritive tissue
Typical nutritive tissue
Typical nutritive tissue
GG- 4-month life cycle
Epidermis
Parenchyma
Dermal system
Trichomes and ordinary cells
Trichomes and ordinary cells
Ground system
Outer parenchyma
Common storage tissue
Median parenchyma
Sclerenchyma layers
Vascular system
Xylem and phloem
Vascular bundles
Typical nutritive tissue
Typical nutritive tissue
Typical nutritive tissue
Typical nutritive tissue
Typical nutritive tissue
Typical nutritive tissue

741

742 Fig. 7. Diagram of the origins and fates of the cell lineages from pinna-rachis or pinnulae
743 toward the ontogenesis of the four *Lopesia* galls on *Mimosa gemmulata* Barneby
744 (Fabaceae). BLG: brown lanceolate bivalve-shaped gall; GG: globoid bivalve-shaped
745 gall; GLG: green lanceolate bivalve-shaped gall; LBG: lenticular bivalve-shaped gall.

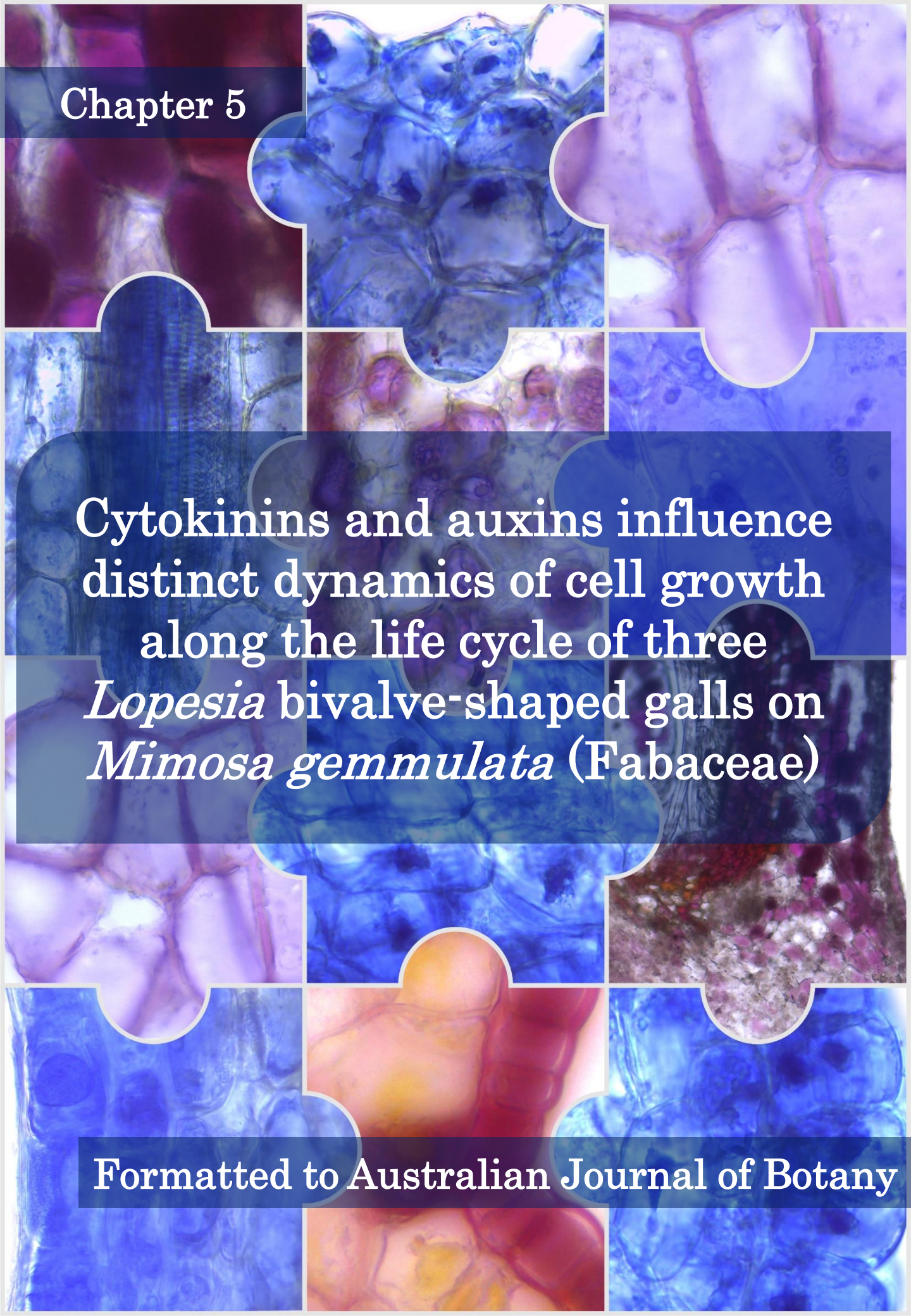

Chapter 5

Cytokinins and auxins influence distinct dynamics of cell growth along the life cycle of three *Lopesia* bivalve-shaped galls on *Mimosa gemmulata* (Fabaceae)

Formatted to Australian Journal of Botany

Cytokinins and auxins influence distinct dynamics of cell growth along the life cycle of three *Lopesia* bivalve-shaped galls on *Mimosa gemmulata* (Fabaceae)

Abridged title: Cytokinins and auxins in *Lopesia* galls

Elaine C. Costa[1], Renê G. S. Carneiro[2], Mario A. Cozzuol[3], Denis C. Oliveira[4], Rosy M. S. Isaias[1, *]

[1]Departamento de Botânica, Instituto de Ciências Biológicas, Universidade Federal de Minas Gerais, Avenida Antônio Carlos, 6627, Pampulha, Belo Horizonte, Minas Gerais Zip code: 31270-901, Brazil.

[2]Departamento de Botânica, Instituto de Ciências Biológicas, Universidade Federal de Goiás, Campus Samambaia, Avenida Esperança, s/n, Goiânia, Goiás, Zip code: 74690-900, Brazil.

[3]Departamento de Zoologia, Instituto de Ciências Biológicas, Universidade Federal de Minas Gerais, Avenida Antônio Carlos, 6627, Pampulha, Belo Horizonte, Minas Gerais Zip code: 31270-901, Brazil.

[4]Instituto de Biologia, Universidade Federal de Uberlândia, Campus Umuarama, Rua Ceará s/n, Uberlândia, Minas Gerais, Zip code: 38402-018, Brazil.

[*]Corresponding author: rosy@icb.ufmg.br

Summary text for the Table of Contents: The histolocalization of cytokinins and auxins relates to the cell and tissue dynamics along the developmental stages of the three bivalve-shaped *Lopesia* galls on *Mimosa gemmulata* pinna-rachis. The cytokinins associate with sites of hyperplasia and the projection of the valves, while the auxins associate with cell hypertrophy and its distinct anisotropic growth mainly in the common storage tissue of the three *Lopesia* galls. The specific cell and tissue dynamics are linked to the lifespan of each *Lopesia* sp. in its bivalve-shaped gall.

Abstract: The accumulation sites of cytokinins (CKs) and indole-3-acetic acid (IAA), and their influence on cell elongation patterns during the development of the lenticular (LG), the green lanceolate (GLG), and the globoid (GG) bivalve-shaped galls induced by congeneric species of *Lopesia* (Cecidomyiidae) on the pinna-rachis of *Mimosa gemmulata* (Fabaceae), are investigated. The similar accumulation sites of CKs in the three bivalve-shaped galls relate to the sites of hyperplasia and the projection of the valves in the induction stage, as well as in the maintenance of cell cycles in the typical nutritive tissue until the mature stage. The accumulation sites of IAA, mainly in the common storage tissue, coincided with the periclinal or anticlinal cell elongation in the growth and development stage of the LG, and in the mature stage of the BLG and the GG. The anticlinal elongation of the sclerenchyma cells and the detection of auxins in the typical nutritive cells are a specific trait of the GG. In *M. gemmulata,* the differences among the three bivalve-shaped galls are determined by the temporal dynamics of cell elongation patterns mediated by the balance of CKs and of IAA, which are manipulated by each *Lopesia* species along its lifespan.

Keywords: cell elongation patterns; cytometry; cell hypertrophy; hyperplasia; indole-3-acetic acid; phytohormones.

Introduction

Galls are modified and fascinating plant structures formed by hyperplasia (increased cell number) and/or hypertrophy (increased cell size) induced by parasitic or pathogenic organisms (Mani 1964). Gall development has been well studied in host plant-galling insect systems (Rohfritsch 1992; Arduin and Kraus 1995; Isaias *et al*. 2011; Ferreira and Isaias 2013; Bedetti *et al*. 2017), which led scientists to understand the ontogenesis of several shapes of galls frequently found in nature (Isaias *et al*. 2013). As new organs and along with structural changes, galls also have peculiar physiology, which confer them special functional traits (Mani 1964; Shorthouse *et al*. 2005; Carneiro *et al*. 2017).

Cytokinins and auxins are plant hormones that play important roles in gall development by controlling the dynamics of cell division and expansion (Yamaguchi *et al*. 2012; Tooker and Helms 2014; Bedetti *et al*. 2018; Schultz *et al*. 2019). Sites of cytokinin accumulation have been associated with hyperplasia (Bedetti *et al*. 2018). The sites that accumulate indole-3-acetic acid (IAA), the most common auxin in plants (Casanova-Sáez *et al*. 2021; Sheldrake 2021), have been related to cell hypertrophy and expansion during gall development (Bedetti *et al*. 2014, 2017; Suzuki *et al*. 2015; Bragança *et al*. 2020). Besides regulating cell growth, these two phytohormones also play key roles on the differentiation of vascular tissues in plant organs (Cheng *et al*. 2006; Hwang *et al*. 2012), including galls (Bragança *et al*. 2021).

As far as cell expansion is concerned, gall development may involve either isotropic and anisotropic cell growth (Isaias *et al*. 2011; Magalhães *et al*. 2014; Carneiro *et al*. 2015; Suzuki *et al*. 2015). When cells grow isotropically, the expansion occurs in all directions (and cells turn into spheroids), while the anisotropic expansion determines

either periclinal or anticlinal axis of cell elongation (Baskin 2005; Magalhães *et al*. 2014). Generally, galls tend to have isotropic cell growth during young stages, when tissues are not fully differentiated, and tend to anisotropic cell growth during mature stages, when their final shapes are achieved (Magalhães *et al*. 2014; Carneiro *et al*. 2015; Suzuki *et al*. 2015). The dynamics of cell expansion in each gall depends on the induction site selected by the galling organism, but also on its *taxon* and feeding habit (Meyer and Maresquelle 1983; Bronner 1992; Rohfritsch 1992; Raman 2010; Isaias *et al*. 2013; Ferreira *et al*. 2019a; Miller and Raman 2019).

Currently, we investigate the super-host *Mimosa gemmulata* Barneby (Fabaceae) and three associated bivalve-shaped galls induced on the same site, the young pinna-rachis, by three *Lopesia* species (Diptera: Cecidomyiidae) with different lifespans (Costa *et al*. 2021*a*, *b*). The bivalve galls are distinguished by their peculiar shapes and colours in mature stage, being lenticular (LG), green lanceolate (GLG), and globoid (GG). To understand the development of such a variety of shapes for the same morphotype, we map the sites of accumulation of cytokinins (CKs) and IAA, as well as the dynamic patterns of cell elongation along the stages of the three galls. We hypothesize that the sites of accumulation of CKs and of IAA, and the cell and tissue dynamics vary along the developmental stages, which explain the structural peculiarities of each bivalve-shaped gall. Two questions guide our discussion: (1) do the histolocalization of CKs and IAA equally relate to the dynamics of cell division and expansion in the three bivalve-shaped galls? And (2) what are the key factors that determine the peculiar shapes of the bivalve morphotypes?

Materials and methods

Sampling and collection

The young non-galled pinna-rachis (NGP) and the three *Lopesia* bivalve-shaped galls (LG, GLG, and GG) at the induction, growth and development, mature, and senescent stages (n = 10 per category) were collected from individuals (n = 12) of *M. gemmulata* in a Cerrado area at Serra Geral, municipality of Caetité, state of Bahia, Brazil (14º04'36.8''S, 42°29'59''W). The developmental stages of the galls were distinguished by their size, color, and shape along with their phenological life cycles (Costa *et al*. 2021*a*).

Histochemical analysis of phytohormones

Hand-made transverse sections of fresh samples of the young NGP and of the LG, the GLG, and the GG in the induction, growth and development, mature, and senescent stages (n = 3 per category) were used for the detection of CKs and IAA. For the detection of CKs, the anatomical sections were submitted to silver nitrate (0.5% silver nitrate in absolute ethanol) at room temperature for 5 min, followed by incubation in bromophenol blue (0.2% bromophenol blue and 0.15% silver nitrate in absolute ethanol: butyl acetate mixture; 1:1, v/v), also at room temperature for 5 min. The sections were washed three times in absolute ethanol and mounted on slides using absolute ethanol (Touchstone 1992; Bedetti *et al*. 2018). Blue staining indicated positive results for the accumulation sites of CKs (Bedetti *et al*. 2018). For the detection of IAA, the sections were submitted to Ehrlich's reagent (1% *p*- dimethylaminobenzaldehyde in 1 $mol \cdot l^{-1}$ HCl; w/v) at room temperature for 5 min (Leopold and Plummer 1961; Bedetti *et al*. 2018). Purple staining indicated positive results for the accumulation sites of IAA (Bedetti *et al*. 2014, 2017, 2018). Blank sections were used as the control for the two histochemical tests. The sections were analyzed under a light microscope (Leica® DM500) and photographed with a coupled digital camera (Leica® ICC50 HD).

116 *Cytometric analyses*

117 The samples of young NGP and LG, GLG, and GG at four developmental stages
118 (*n* = 10) were fixed in 2.5% glutaraldehyde and 4.5% formaldehyde 0.1mol L^{-1}
119 (Karnovsky, 1965; modified to phosphate buffer, pH 7.2) for 48 hours. The samples were
120 dehydrated in ethanol series and embedded in Paraplast® (Leica Biosystems, St. Louis,
121 MO, USA; Kraus and Arduin, 1997). Serial transverse sections (12 μm) were obtained
122 using a rotatory microtome (Leica® BIOCUT 2035), deparaffinized in butyl acetate, and
123 hydrated in an ethanol series (Kraus and Arduin, 1997). The sections were stained with
124 Astra blue–safranin (9: 1, v/v) (Bukatsch, 1972; modified to 0.5%), dehydrated, and
125 mounted with colorless varnish Acrilex® (Paiva et al., 2006). The transverse sections were
126 analyzed under a light microscope (Leica® DM500) and photographed with a coupled
127 digital camera (Leica® ICC50 HD).

128 The cytometric measurements were performed in transverse sections of young
129 NGP (*n* = 10), and LG, GLG, and GG at four developmental stages in the basal, median,
130 and distal zones of the gall valves (n = 10 galls per developmental stage; 10 images; two
131 cells of each tissue; *n* = 20 cells per tissue in each region) using the AxioVision 4.8
132 software (Carl Zeiss Microscopy GmbH, Jena, Germany). In the NGP, the area, height,
133 and width of the cells of the epidermis and of the cortical parenchyma were measured. In
134 the galls, the area, height and width of the cells of the epidermis, of the outer, of the
135 median (= the common storage tissue in the mature stage of the LG and the GLG, and the
136 common storage tissue and the sclerenchyma cells in the mature stage of the GG), and of
137 the inner parenchyma (= the sclerenchyma cells in the mature stage of the LG and the
138 GLG, and the typical nutritive cells of the GG), and of the typical nutritive tissue were
139 measured. The symmetrical valves of the GLG, the upper and lower valves of the LG,
140 and the minor and larger and minor valves of the GG were measured.

Statistical analyses

Cell areas, and cell height and width, of the young NGP and of the LG, the GLG and the GG in induction, growth and development, mature, and senescent stages were compared. The parametric data were compared by one-way ANOVA, followed by Tukey's test. The non-parametric data were compared by Kruskall-Wallis test and Dunn's test using the SigmaStat® (Systat software, Inc.) software. The level of significance used in all tests was $p < 0.05$. The type of cell expansion and the degree of anisotropy were measured by the ratio between the average anticlinal and periclinal axes (Baskin 2005). Ratio values ranging between 0.9 - 1.1 indicate a tendency to isotropic expansion. When the ratio value is lower than 0.9, the cell expansion is anisotropic with a tendency to periclinal direction, and when it is higher than 1.1, the cell expansion is considered anisotropic with a tendency to anticlinal direction of expansion (Carneiro *et al*. 2015).

The cytometric data of the height and the width of each cell lineage in all development stages of the three bivalve-shaped galls were compared by means of the Principal Component Analysis (PCA) to explore the distribution of the different galls in the morphometric space. The Statistical Software PAST 4.03 (Hammer *et al*. 2001) was used for the PCA analysis. The data were standardized using allometric Burnaby to remove size from distance and create evenness on the variance.

Results

Non-galled pinna-rachis - The young non-galled pinna-rachis (Fig. 1*a*) have anticlinally elongated epidermal cells and isodiametric parenchyma cells (Table S1). Cytokinins are detected in the protoplast of parenchyma and phloem cells (Fig. 1*b*), while IAA is sparsely detected in the cell walls of the epidermis and of the parenchyma (Fig. 1*c*).

Lopesia *galls* - The three mature bivalve-shaped galls found on *M. gemmulata* are extralaminar and formed by leaflet-like valves. The LG are green, and formed by an upper and a lower valve, which grow toward the abaxial surface of the pinnulae (Fig. 2*a*), and guarantee the peculiar lenticular shape. The GLG are green and formed by valves of the same length (Fig. 2*b*), which project upward getting the lanceolate aspect. The GG are green and formed by a larger valve projected over a minor valve (Fig. 2*c*), forming the globoid shape.

Histochemical analyses of the galls

LG - At the induction stage, the CKs are detected in the cytoplasm and in the nuclei of parenchyma (Fig. 3*a*) and nutritive cells (Fig. 3*b*), and overall in procambial strands (Fig. 3*c*). The IAA is sparsely detected in the cytoplasm of epidermal, parenchyma, and nutritive cells. At the growth and developmental stage, the CKs are detected overall in vascular bundles and in the cytoplasm of nutritive cells around the larval chamber, as well as in the *Lopesia* larva (Fig. 3*d*), while the IAA is detected overall in vascular bundles, and in the cytoplasm of the ordinary and papillose epidermal cells (Fig. 3*e*), and of the outer and the median parenchyma cells (Fig. 3*f*). At the mature stage, the patterns of accumulation of CKs and IAA are unchanged when compared to the previous stage, but in the senescence, the CKs are detected with low intensity in the vascular cells, and the IAA is detected in some parenchyma cells.

GLG - At the induction stage, the CKs are detected in the walls and in the nuclei of the parenchyma (Fig. 4*a*) and nutritive cells (Fig. 4*b*), as well as overall in procambial strands. The IAA is sparsely detected in the walls and in the cytoplasm of the epidermal and parenchyma cells. At the growth and development stage, the CKs are detected overall in vascular bundles and in the cytoplasm of parenchyma and nutritive cells (Fig. 4*c*),

189 while the IAA accumulates in the cytoplasm of the ordinary papillose epidermal cells,
190 trichomes, and parenchyma cells (Figs. 4*d-f*). At the mature stage, the CKs are detected
191 overall in vascular cells, and in the cytoplasm and in the nucleus of the nutritive cells
192 (Fig. 4*g*). The IAA is homogeneously detected in the cytoplasm of the ordinary epidermal
193 and common storage cells (Fig. 4*h*), and overall in vascular cells (Fig. 4*i*). In the
194 senescence, the CKs are detected at low intensity in the vascular cells (Fig. 4*j*), and the
195 IAA is not detected.

196 *GG* - At the induction stage, the CKs are detected in the nuclei, and in the cytoplasm of
197 ordinary epidermal (Fig. 5*a*), parenchyma (Fig. 5*b*), and nutritive cells (Fig. 5*c*), as well
198 as overall in procambial strands (Fig. 5*a*), while the IAA is sparsely detected in the
199 cytoplasm of epidermal and parenchyma cells. At the growth and development stage, the
200 sites of accumulation of CKs are similar to those of the induction stage, with more
201 intensity in nutritive and vascular cells. The IAA is detected in the walls and in the
202 cytoplasm of the ordinary epidermal cells, of the outer and median parenchyma and of
203 the nutritive cells (Figs. 5*d*, *e*), as well as overall in vascular cells (Fig. 5*f*). At the mature
204 stage, the CKs are detected in the cytoplasm of vascular parenchyma and phloem cells
205 (Fig. 5*g*, *h*), and in the cytoplasm and nucleus of the nutritive cells (Fig. 5*g*, *i*); the IAA
206 is detected in the cell walls of the epidermis, the common storage tissue (Figs. 5*j*, *k*), and
207 the typical nutritive tissue (Fig. 5*l*). In the senescence, the CKs are detected at low
208 intensity in the vascular bundles, and the IAA is not detected.

209 *Cytometric analyses*

210 *LG* – At the induction stage, the epidermal cells are anticlinally elongated, and the outer
211 and inner parenchyma cells are isodiametric, similar to the original pinna-rachis tissues.
212 The median parenchyma and the nutritive cells are periclinally elongated (Fig. 6*a*). The

epidermis and sclerenchyma layers differentiated from the inner parenchyma cells, as well as the typical nutritive tissue, maintain the patterns of cell expansion during all developmental stages, but at different expansion degrees (Fig. 6*a, b*). At the growth and development stage, a new pattern of cell elongation is established; the outer parenchyma cells of the two valves change the expansion pattern from isotropic to anisotropic on the periclinal axis, except for the cells at the basal zone of the upper valve, which remain isodiametric (Fig. 6*b*). At the mature stage, increased degrees of cell expansion are observed for the epidermis, the common storage tissue, and the typical nutritive tissue at the distal zone (Table S1). In the senescence, the cells of the common storage and nutritive tissues at the median and distal zones show decreased area.

GLG - At the induction stage, the epidermal and the nutritive cells have anisotropic expansion on the anticlinal axis, and the parenchyma cells are isodiametric, similar to the original pinna-rachis tissues (Fig. 6*c*). The elongation pattern of the epidermal cells is maintained during all developmental stages and zones of the GBG. At the growth and development stage, the axes of cell expansion are similar to those of the induction stage; an increased degree of cell expansion is observed in the median parenchyma of the median zone, and in all tissues of the distal zone (Table S1; Fig. 6*d*). At the mature stage, the patterns of cell elongation are characterized by the highest degree of cell expansion, especially in the common storage tissue of the median zone. When compared to the previous developmental stage, the direction of cell expansion is altered from isotropic to anisotropic with periclinal elongation in the median parenchyma cells of the common storage tissue, while the outer parenchyma cells remain isotropic. Similar periclinal elongation is observed for the sclerenchyma cells and the three zones, and the nutritive cells at the median and basal zones. In the distal zone, the nutritive cells maintain the

anticlinal pattern of cell elongation (Table S1; Fig. 6*e*). In the senescence, the cells of the common storage tissue of the distal zone decrease in size.

GG - At the induction stage, the patterns of cell elongation in all tissues are similar to the original tissues of the NGP, except for the typical nutritive tissue. The epidermal cells have anticlinal elongation, while the parenchyma and the typical nutritive tissue exhibit isotropic patterns of cell expansion (Fig. 6*f*). At the growth and development stage, the cell expansion axis alters from isotropic to anisotropic with anticlinal elongation in the median parenchyma, and with periclinal elongation in the typical nutritive tissue of the larger valve (Fig. 6*g*). At the mature stage, the epidermis, the common storage tissue, and the typical nutritive tissue have periclinally elongated cells. However, the common storage tissue cells tend to expand anisotropically with anticlinal elongation, only at the median zone. The sclerenchyma cell layers, differentiated from the median parenchyma cells, maintain the anticlinal elongation (Table S1; Fig. 6*h*). In the senescence, the common storage tissue and the nutritive tissue of the median and distal zones have cells with decreased area.

Principal-component analysis (PCA)

In the intersection of PC1 to PC2, and of PC1 to PC3, the PC1 explains the distribution of the bivalve-shaped galls during all the developmental stages (Table S2; Fig. 7, 8). However, at the intersection of PC2 to PC3, the three bivalve-shaped galls overlap (Table S2; Fig. S1-S4). During the induction stage, the LG separates from the GLG and the GG on the positive range of PC1, while the GLG and the GG partially overlap distributing from the center to the negative range of PC1 (Fig. 7*a*). The width of the median parenchyma cells in the median zone (WM-MP) and the width of the nutritive cells in the basal zone (WB-TNT) in the positive direction of the CP1 axis, and

261 the height of the nutritive cells in the distal (HD-TNT) and median (HM-TNT) zones in
262 the negative range of the CP1 contribute more strongly for separation of the LG. During
263 the growth and development stage, the LG maintains the separation from the other two
264 galls, but now on the negative range of PC1, while the overlap of GLG and the GG reduce,
265 now on the positive range of PC1 (Fig. 7*b*). During the mature stage, the three bivalve-
266 shaped galls are totally separated along the PC1 (Fig. 8*a*). The height of the nutritive cells
267 in the distal zone (HD-TNT) in the positive values of the CP1, and the height and width
268 of the outer parenchyma cells (HM-OP, WM-OP), and height of the median parenchyma
269 cells (HM-MP) in the median zone in the negative range of the CP1 axis are the variables
270 that contribute more strongly for the separation of the three bivalve-shaped galls. At the
271 senescent stage, the LG and the GG have a partial overlapping on the negative side of the
272 PC1 (Fig. 8*b*).

273

274 **Discussion**

275 *Influence of CKs and IAA in the bivalve-shaped galls*

276 The sites of accumulation of CKs in the parenchyma, vascular and nutritive cells
277 on the induction stages of the three *Lopesia* galls relate to the sites of hyperplasia and
278 projections of the valves. Such relation Cks-hyperplasia explains the overlapping of the
279 GLG and the GG in the PCA, and the separation of LG from the other two galls. The
280 intense cell division and the highest cell expansion in the median parenchyma and typical
281 nutritive tissue of the LG compared to the GLG and the GG are important for the
282 projection of their upper and the lower valves toward the abaxial surface of *M. gemmulata*
283 pinnulae. The source of CKs in galls may be both endogenous or exogenous, since the

larvae of gall-inducing insects are able to produce and ingest these phytohormones, which can be concentrated in their salivary glands and then be injected into plant tissues (Yamaguchi *et al*. 2012; Andreas *et al*. 2020). In *M. gemmulata*, the accumulation of CKs is also detected in the *Lopesia* larva of the LG in the growth and development stage, which indicates that the stimuli for cell divisions is most probably exogenous. Besides the CKs, the IAA is indispensable for the progression of cell dynamics in gall developmental stages (Tooker and Helms 2014; Yamaguchi *et al.* 2012; Ferreira et al. 2019*b*). The CKs and the IAA can trigger early procambial cell divisions toward the differentiation of vascular cells in leaves (Mähönen *et al*. 2000; Dettmer *et al*. 2009; Hwang *et al*. 2012; Furuta *et al*. 2014). Similarly, in galls, the redifferentiation of parenchyma cells toward vascular elements is well documented and has been related to the accumulation of CKs and IAA (Bragança *et al*. 2021). The overlapping of the histolocalization of CKs and IAA in the vascular cells of the three bivalve-shaped galls on *M. gemmulata* reinforces their key role on the establishment of vascularization in galls.

The accumulation of IAA in the parenchyma cells is associated with the isotropic cell expansion in the upper valve and the periclinal anisotropic elongation in the lower valve of the LG, which characterize the stage of growth and development and the separation of the LG from the other two *Lopesia* galls in the PCA. The LG is the bivalve morphotype with the shortest lifespan among the *Lopesia* galls on *M. gemmulata* (Costa *et al*. 2021*a*), and cellular mechanisms related to its shape determination are established sooner than in the other two galls. In fact, in the GLG and the GG morphotypes, the overlapping of the detection of CKs and of IAA in parenchyma cells relate to the sites of cell hypertrophy and hyperplasia, and explain these two galls overlapping in the PCA. In addition, the final shapes of the GLG and the GG are determined during the mature stage, when cells get to their maximum expansion size, mainly in the common storage tissue.

309 Despite the different patterns of the outer tissue compartments of the galls in mature stage,
310 the nutritive cells have similar cell dynamics, which may be a response to the congeneric
311 *Lopesia* stimuli.

312 The nutritive tissue plays a key role for the nutrition of the galling larva,
313 supporting its development, and determining the gall final shape (Rohfritsch 1992).
314 Accordingly, the nutritive cells have periclinal elongation during the maturation in the
315 three *Lopesia* bivalve-shaped-galls on *M. gemmulata*. The typical nutritive cells have
316 active metabolism (Costa *et al*. 2021*b*) and accumulate CKs during the stages of gall
317 growth and development, and maturation, which relate to the maintenance of continuous
318 cell dynamics. The accumulation of CKs in nutritive cells is also related to the strength
319 of physiological sinks, as they stimulate the activity of invertases, which metabolize
320 carbohydrates in galls (Ferreira *et al*. 2019*b*). For instance, the CKs in nutritive cells can
321 influence the breakdown of starch, and the production of reducing sugars for the
322 biosynthesis of xyloglucans. Even though xyloglucans are typical reserve carbohydrates
323 of the cell walls in general, in the bivalve-shaped galls they may be used as food resources
324 by the *Lopesia* spp. larvae (Costa *et al*. 2021*b*).

325 The patterns of cell growth and direction of elongation in the common storage
326 tissue are determinants for the separation of mature galls in the PCA. The accumulation
327 of IAA in the common storage cells of the GLG determines distinct cell expansion
328 patterns, i.e., isotropic growth in the outer cell layers and anisotropic expansion with
329 periclinal elongation in subjacent inner cell layers. Even though the GLG and the brown
330 lanceolate bivalve-shaped gall (BLG), a fourth gall morphotype on *M. gemmulata* studied
331 elsewhere (Costa *et al*. 2021*b*), have similar lifespans, their anatomical traits are distinct
332 (Costa *et al*. submitted). While the GLG presents both isotropic and anisotropic type of
333 cell growth in specific tissue layers, the BLG has periclinally elongated cells in all tissues

(Costa *et al*. 2018). The diversity of cell responses to IAA accumulation in the papillose epidermal cells, as well as in the common storage cells is important for the separation of the GLG from the LG and the GG in the stages of maturation and senescence in the PCA.

Among the three *Lopesia* galls on *M. gemmulata*, the GG has the highest complexity of cell elongation patterns, and also the longest lifespan (Costa *et al*. 2021 *a*, *b*). The spatial-temporal dynamics of cell divisions and expansion relate to IAA accumulation in the outermost cell layers of the common storage tissue during the stage of growth and development, when anisotropic cell growth with periclinal elongation is observed in the distal and median zones. Such IAA-periclinal cell elongation pattern persists in the distal and basal zones of the GG by the stage of maturation, but in the median zone, the direction of cell elongation changes to anticlinal. The cell dynamics for establishing the elongation patterns of the common storage tissue, of the sclerenchyma layers, and of the typical nutritive tissue is important for the separation of the GG from the other two galls in the stage of maturation in the PCA. In the nutritive cells of the GG, the IAA accumulates in the periclinally elongated cells of the larger valve, which grows over the minor valve. Along with IAA accumulation, the nutritive cells of the GG store phenolics (Costa et al. submitted). The overlapping detection of IAA and phenolics has been associated with the inhibiting action of the phenolics over the IAA oxidases (Hori 1992; Bedetti *et al*. 2014, 2017; Suzuki *et al*. 2015), thus potentializing cell periclinal elongation during the stage of GG maturation.

The CKs are positive regulators of leaf development and negative regulators of leaf senescence (Zwack and Rashotte 2013; Zhang *et al*. 2020), which also applies to galls. By the time of senescence, the detection of CKs weakens in the vascular cells, indicating reallocation of nutrients from the gall toward other plant structures (Zwack and

Rashotte 2013; Janečková *et al*. 2018). As nutrients and energy of galls are reallocated toward the leaflets of *M. gemmulata*, the investment in the development of gall tissues decreases accordingly.

Key factors that determine the bivalve-shaped galls

The induction site on the host plant, the gall-inducing *taxa*, and the feeding habit of the inducer are determinants for the final shape of the galls (Meyer and Maresquelle 1983; Bronner 1992; Rohfritsch 1992; Raman 2010; Isaias *et al*. 2013; Ferreira *et al*. 2019*a*; Miller and Raman 2019). In fact, the induction site on epidermal cells next to the vascular system is important for the establishment of the bivalve structure of galls, considered as leaflet-like appendages (Isaias *et al*. 2011; Nogueira *et al*. 2016; Costa et al. 2018). The CKs are related to the sites of hyperplasia in the induction stage that lead to the projection of the valves, and the maintenance of cell divisions in the typical nutritive tissue along the development of the three bivalve-shaped galls on *M. gemmulata*. The overlapping of accumulation of CKs and IAA overall in the vascular bundles indicates the functions of these two phytohormones in the vascularization of the three bivalve-shaped galls. The accumulation of IAA relates either to anticlinal or periclinal dynamics of anisotropic cell elongation, mainly in the common storage tissue during the growth and development stage of both the LG and the GG, and during maturation of both the GLG and the GG. In addition, the anticlinal elongation of sclerenchyma cells, and the detection of IAA in the nutritive cell walls are exclusive peculiarities of the GG, which may be explain their higher thickness of the nutritive cell walls and longer lifespans compare to other bivalve-shaped galls (Costa et al. 2021a). In the super-host *M. gemmulata,* the spatial-temporal dynamics of accumulation of CKs and IAA are key factors that drive the development of the three bivalve-shaped galls induced by the

congeneric *Lopesia* spp. at the same induction site, the pinna-rachis toward their peculiar final shapes, the lenticular, the lanceolate and the globoid.

Conflicts of Interest

The authors declare no conflicts of interest.

Declaration of Funding

This study was financed by the *Coordenação de Aperfeiçoamento de Pessoal de Nível Superior* (CAPES) – Brazil– Finance Code 001 for E.C. Costa (888877.199702/2018-00) scholarship, and by *Conselho Nacional de Desenvolvimento Científico e Tecnológico* (CNPq) for the research scholarships to R.M.S. Isaias (304335/2019-2) and D.C. Oliveira (304981/2019-2).

Acknowledgments

We thank Prof. Dr. Jane Kraus and the members of the Neotropical Gall Group for the critical reading and valuable suggestions on the manuscript.

References

Andreas P, Kisiala A, Emery RJ, Clerck-Floate D, Tooker JF, Price PW, Connor EF (2020) Cytokinins are abundant and widespread among insect species. *Plants* **9**, 208. doi:10.3390/plants9020208

Arduin M, Kraus JE (1995) Anatomia e ontogenia de galhas foliares de *Piptadenia gonoacantha* (Fabales, Mimosaceae). *Boletim de Botânica da Universidade de São Paulo* **14**, 109–130. doi: 10.11606/issn.2316-9052.v14i0p109-130

Baskin TI (2005) Anisotropic expansion of the plant cell wall. *Annual Review of Cell and Developmental Biology* **21**, 203–222. doi: 10.1146/annurev.cellbio.20.082503.103053

Bedetti CS, Modolo LV, Isaias RMS (2014) The role of phenolics in the control of auxin in galls of *Piptadenia gonoacantha* (Mart.) MacBr (Fabaceae: Mimosoideae). Biochemical *Systematics and Ecology* **55**, 53–59. doi: 10.1016/j.bse.2014.02.016

Bedetti CS, Bragança GP, Isaias RMS (2017) Influence of auxin and phenolic accumulation on the patterns of cell differentiation in distinct gall morphotypes on *Piptadenia gonoacantha* (Fabaceae). *Australian Journal of Botany* **65**, 411–420. doi: 10.1071/BT16257

Bedetti CS, Jorge NC, Trigueiro FCG, Bragança GP, Modolo LV, Isaias RMS (2018) Detection of cytokinins and auxin in plant tissues using histochemistry and immunocytochemistry. *Biotechnic & Histochemistry* **93**, 149–154. doi:10.1080/10520295.2017.1417640

Bragança GPP, Alencar CF, Freitas MSC, Isaias RMS (2020) Hemicelluloses and associated compounds determine gall functional traits. *Plant Biology* **22**, 981–991. doi: 10.1111/plb.13151

Bragança GPP, Freitas, MSC dos Santos Isaias, R. M. (2021) The influence of gall position over xylem features in leaflets of *Inga ingoides* (Rich.) Willd. (Fabaceae: Caesalpinioideae). Trees, 35(1):199-209. doi: 10.1007/s00468-020-02027-1

427 Bronner R (1992) The role of nutritive cells in the nutrition of cynipids and cecidomyiids.
428 In ‘Biology of insect-induced galls’. (Eds JD Shorthouse, O Rohfritsch) pp. 118–
429 140. (Oxford University Press: New York)
430 Carneiro RGS, Pacheco P, Isaias RMS (2015) Could the Extended Phenotype Extend to
431 the Cellular and Subcellular Levels in Insect-Induced Galls? *Plos one* **8**, 1–20. doi:
432 10.1371/journal.pone.0129331
433 Carneiro RGS, Isaias RMS, Moreira ASFP, Oliveira DC (2017) Reacquisition of new
434 meristematic sites determines the development of a new organ, the Cecidomyiidae
435 gall on *Copaifera langsdorffii* Desf. (Fabaceae). *Frontiers in Plant Science* **8**, 1622.
436 doi: 10.3389/fpls.2017.01622
437 Casanova-Sáez R, Mateo-Bonmatí E, Ljung K (2021) Auxin metabolism in plants. *Cold*
438 *Spring Harbor Perspectives in Biology* **13**, a039867.
439 Cheng Y, Dai X, Zhao Y (2006) Auxin biosynthesis by the YUCCA flavin
440 monooxygenases controls the formation of floral organs and vascular tissues in
441 *Arabidopsis*. *Genes & development* **20**, 1790–1799.
442 Costa EC, Carneiro GSC, Santos-Silva J, Isaias RMS (2018) Biology and development
443 of galls induced by *Lopesia* sp. (Diptera: Cecidomyiidae) on leaves of *Mimosa*
444 *gemmulata* (Leguminosae: Caesalpinioideae). *Australian Journal of Botany* **66**,
445 161–172. doi: 10.1071/BT17099
446 Costa EC, Oliveira DC, Ferreira DKL, Isaias RMS (2021a) Structural and nutritional
447 peculiarities related to lifespan differences on four *Lopesia* induced bivalve-shaped
448 galls on the single super-host *Mimosa gemmulata*. *Frontiers in Plant Science* **12**,
449 1–13. doi: 10.3389/fpls.2021.660557

Costa EC, Martini VC, Souza-Silva A, Lemos-Filho JP, Oliveira DC, Isaias RMS (2021b) How galling herbivores share a single super-host plant during their phenological cycle: the case of *Mimosa gemmulata* Barneby (Fabaceae). *Tropical Ecology*. doi: 10.1007/s42965-021-00182-1

Dettmer J, Elo A, Helariutta Y (2009) Hormone interactions during vascular development. *Plant molecular biology* **69**, 347–360.

Ferreira BG, Isaias RMS (2013) Developmental stem anatomy and tissue redifferentiation induced by a galling Lepidoptera on *Marcetia taxifolia* (Melastomataceae). *Botany* **91**, 752–760. doi: 10.1139/cjb-2013-0125

Ferreira BG, Álvarez R, Bragança GP, Alvarenga DR, Pérez-Hidalgo N, Isaias RMS (2019a) Feeding and other gall facets: patterns and determinants in gall structure. The *Botanical Review* **85**, 78–106. doi: 10.1007/s00709-021-01646-w

Ferreira BG, Freitas MSC, Bragança GP, Moreira ASFP, Carneiro RGS, Isaias RMS (2019b) Enzyme-mediated metabolism in nutritive tissues of galls induced by *Ditylenchus gallaeformans* (Nematoda: Anguinidae). *Plant Biology*, **21**, 1052–1062. doi: 10.1111/plb.13009

Furuta KM, Hellmann E, Helariutta Y (2014) Molecular control of cell specification and cell differentiation during procambial development. *Annual review of plant biology* **65**, 607–638. doi: 10.1146/annurev-arplant-050213-040306

Hammer Ø, Harper DAT, Ryan PD (2001) PAST: paleontological statistics software package for education and data analysis. *Paleontologia Electronica* **4**, 1–9.

Hori K. (1992) Insect secretions and their effect on plant growth, with special reference to hemipterans. In 'Biology of insect-induced galls'. (Eds JD Shorthouse, O Rohfritsch) (Eds JD Shorthouse, O Rohfritsch) pp 157–170 (Oxford University Press: New York)

475 Hwang I, Sheen J, Müller B (2012) Cytokinin signaling networks. *Annual review of plant*
476 *biology* **63**, 353–380.
477 Isaias RMS, Oliveira DC, Carneiro RGS (2011) Role of *Euphalerus ostreoides*
478 (Hemiptera: Psylloidea) in manipulating leaflet ontogenesis of *Lonchocarpus*
479 *muehlbergianus* (Fabaceae). *Botany* **89**, 581–592. doi: 10.1139/b11-048
480 Isaias RMS, Carneiro RGS, Oliveira DC, Santos JC (2013) Illustrated and annotated
481 checklist of Brazilian gall morphotypes. *Neotropical Entomology* **42**, 230–239. doi:
482 10.1007/s13744-013-0115-7
483 Janečková H, Husičková A, Ferretti U, Prčina M, Pilařová E, Plačková L, Špundová M
484 (2018) The interplay between cytokinins and light during senescence in detached
485 Arabidopsis leaves. *Plant, cell & environment* **41**, 1870–1885. doi:
486 10.1111/pce.13329
487 Leopold AC, Plummer TH (1961) Auxin–phenol complexes. *Plant Physiology* **36**, 589–
488 592. doi: 10.1104/pp.36.5.589
489 Magalhães TA, Oliveira DC, Suzuki AYM, Isaias RMS (2014) Patterns of cell elongation
490 in the determination of the final shape in galls of *Baccharopelma dracunculifoliae*
491 (Psyllidae) on *Baccharis dracunculifolia* DC (Asteraceae). *Protoplasma* **251**, 747–
492 753. doi: 10.1007/s00709-013-0574-z
493 Mähönen AP, Bishopp A, Higuchi M, Nieminen KM, Kinoshita K, Törmäkangas K,
494 Helariutta Y (2006) Cytokinin signaling and its inhibitor AHP6 regulate cell fate
495 during vascular development. *Science* **311**, 94–98. doi: 10.1126/science.1118875
496 Mani MS (1964) 'Ecology of plant galls.' (Dr. W. Junk: The Hague, Netherlands)
497 Meyer J, Maresquelle HJ (1983) 'Anatomie des galles.' (Gebrüder Borntraeger, Berlin,
498 Germany)

499 Miller III DG, RamanA (2019). Host–plant relations of gall-inducing insects. *Annals of*
500 *the Entomological Society of America* **112**, 1–19. doi: 10.1093/aesa/say034
501 Nogueira RM, Costa ECC, Santos-Silva J, Isaias RMS (2018) Structural and
502 histochemical profile of *Lopesia* sp. Rübsaamen. 1908 pinnula galls on *Mimosa*
503 *tenuiflora* (Willd.) Poir. in a Caatinga environment. *Hoehne*a **45**, 231–239. doi:
504 10.1590/2236-8906-80/2017
505 Raman, A (2010) Insect–plant interactions: the gall factor. In 'All Flesh Is Grass: Plant-
506 Animal Interrelationships' (Eds J Seckbach, Z Dubinsky) pp. 119–146 (Springer,
507 Dordrecht)
508 Rohfritsch O (1992) Patterns in gall development. In 'Biology of insect-induced galls'.
509 (Eds JD Shorthouse, O Rohfritsch) pp. 60–86. (Oxford University Press: New
510 York)
511 Schultz JC, Edger PP, Body MJ, Appel HM (2019) A galling insect activates plant
512 reproductive programs during gall development. *Scientific reports* **9**, 1–17. doi:
513 10.1038/s41598-018-38475-6
514 Sheldrake AR (2021) The production of auxin by dying cells. *Journal of Experimental*
515 *Botany* **72**, 2288–2300. doi: 10.1093/jxb/erab009
516 Shorthouse JD, Wool D, Raman A (2005) Gall-inducing insects–Nature's most
517 sophisticated herbivores. *Basic and Applied Ecology* **6**, 407–411. doi:
518 10.1016/j.baae.2005.07.001
519 Suzuki AYM, Bedetti CS, Isaias RMDS (2015) Detection and distribution of cell growth
520 regulators and cellulose microfibrils during the development of *Lopesia* sp. galls on
521 *Lonchocarpus cultratus* (Fabaceae). *Botany* **93**, 435–444. doi: 10.1139/cjb-2015-
522 0012

Tooker JF, Helms AM (2014) Phytohormone dynamics associated with gall insects, and their potential role in the evolution of the gall-inducing habit. J*ournal of Chemical Ecology* **40**, 742–753. doi: 10.1007/s10886-014-0457-6

Touchstone JC (1992) 'Practice of thin layer chromatography.' (John Wiley & Sons, New York)

Mani MS (1964) 'Ecology of plant galls.' (Dr. W. Junk: The Hague, Netherlands)

Yamaguchi H, Tanaka H, Hasegawa M, Tokuda M, Asami T, Suzuki Y (2012) Phytohormones and willow gall induction by a gall-inducing sawfly. *New Phytologist* **196**, 586–595. doi: 10.1111/j.1469-8137.2012.04264.x

Zwack PJ, Rashotte AM (2013) Cytokinin inhibition of leaf senescence. *Plant signaling & behavior* **8**, e24737. doi: 10.4161/psb.24737

Zhang Y, Wang HL, Li Z, Guo H. (2020) Genetic network between leaf senescence and plant immunity: crucial regulatory nodes and new insights. *Plants* **9**, 1–22. doi: 10.3390/plants9040495

Supplementary table 1. Dynamics of hyperplasia and cell hypertrophy during the gall developmental stages of the three bivalve-shaped galls induced by *Lopesia* spp. (Diptera: Cecidomyiidae) on *Mimosa gemmulata* Barneby (Fabaceae) pinna-rachis.

Pinna-rachis										
Young pinna-rachis	Ep	Pa								
	1.28	1.11	1.11	1.11	1.28					
LG	**Upper valve**					**Lower valve**				
Developmental stages	Ep	OP	MP	IP	TNT	Ep	OP	MP	IP	TNT
		CST		SL			CST		SL	
D - Induction	1.38	1.06	0.92	0.92	0.83	1.29	0.91	0.85	0.91	0.65
D - Growth and development	1.27	0.82	0.54	0.93	0.66	1.31	0.81	0.53	0.91	0.60
D - Maturation	1.33	0.89	0.48	0.91	0.52	1.39	0.82	0.48	0.90	0.50
D - Senescence	1.21	0.80	0.36	0.96	0.63	1.28	0.71	0.33	1.01	0.78
M - Induction	1.36	1.01	0.68	0.90	0.57	1.33	1.05	0.69	1.00	0.64
M - Growth and development	1.59	0.81	0.80	0.91	0.43	1.69	0.86	0.81	0.91	0.50
M - Maturation	1.60	0.86	0.65	0.93	0.54	1.59	0.87	0.65	0.91	0.56
M - Senescence	1.73	0.89	0.65	0.93	0.47	1.67	0.88	0.60	1.00	0.49
B - Induction	1.23	0.91	0.82	0.90	0.71	1.15	0.93	0.76	0.90	0.61
B - Growth and development	1.27	1.00	0.71	0.91	0.50	1.49	0.80	0.48	0.92	0.54
B - Maturation	1.25	0.95	0.81	0.99	0.59	1.37	0.85	0.41	0.91	0.66
B - Senescence	1.23	1.01	0.73	0.97	0.51	1.32	0.80	0.42	1.00	0.45
GLG	**Symmetrical valve**									
Developmental stages	Ep	OP	MP	IP	TNT	Ep	OP	MP	IP	TNT
		CST		SL			CST		SL	
D - Induction	1.52	0.90	1.04	1.00	1.25	1.28	0.94	0.93	0.90	1.12
D - Growth and development	1.66	0.96	1.00	0.94	3.19	1.69	1.00	1.03	0.97	1.34
D - Maturation	1.57	0.87	0.77	0.79	1.41	1.70	0.97	0.56	0.74	1.46
D - Senescence	1.40	0.90	0.55	0.78	1.03	1.48	0.90	0.63	0.82	1.04
M - Induction	1.46	0.93	0.96	0.96	1.32	1.35	0.94	0.93	0.94	1.42
M - Growth and development	1.80	0.95	1.04	0.95	1.07	1.77	1.00	1.03	0.96	1.79
M - Maturation	2.00	0.91	0.51	0.60	0.48	1.81	0.97	0.56	0.52	0.48
M - Senescence	1.72	0.90	0.52	0.59	0.49	1.68	0.90	0.63	0.58	0.45
B - Induction	1.22	0.90	0.98	1.05	1.16	1.35	0.96	1.00	0.90	1.19
B - Growth and development	1.51	0.97	0.98	0.98	0.91	1.56	1.00	0.94	1.09	1.23
B - Maturation	1.77	1.00	0.59	0.53	0.50	1.75	0.91	0.59	0.64	0.55
B - Senescence	1.49	0.96	0.58	0.66	0.58	1.63	0.96	0.59	0.65	0.57
GG	**Minor valve**					**Larger valve**				
Developmental stages	Ep	OP	MP	IP	TNT	Ep	OP	MP	IP	TNT
		CST	SL		TNT		CST	SL		TNT
D - Induction	1.32	1.02	1.17	0.92	1.13	1.24	1.17	1.05	0.90	1.13
D - Growth and development	1.19	0.92	1.22	0.78	1.02	1.14	0.84	1.42	0.75	0.89
D - Maturation	0.94	0.74	1.45	0.54	0.68	0.99	0.89	1.48	0.54	0.58
D - Senescence	0.93	1.06	1.31	0.42	0.38	1.01	0.98	1.46	0.44	0.40
M - Induction	1.14	1.01	1.16	1.00	1.15	1.42	0.99	0.90	0.97	0.98
M - Growth and development	1.21	0.75	1.27	0.76	0.95	1.38	0.85	1.42	0.74	0.82
M - Maturation	0.73	1.21	1.63	0.56	0.65	0.74	1.24	1.69	0.51	0.53
M - Senescence	0.80	1.31	2.12	0.41	0.34	0.92	1.28	2.07	0.40	0.33
B - Induction	1.26	1.04	0.95	0.91	0.99	1.36	1.10	1.16	0.94	1.07
B - Growth and development	1.26	0.91	1.14	0.73	0.94	1.30	0.91	1.22	0.74	0.81
B - Maturation	0.64	0.69	1.14	0.50	0.72	0.76	0.79	1.07	0.51	0.55
B - Senescence	0.83	0.75	1.21	0.39	0.31	0.83	0.74	1.42	0.41	0.36

Lines labelled "**R**" correspond to the **A/P ratio** from the same **cell lineage at different developmental stages**. Values lower than **0.9** indicate tendency to **anisotropic** growth with **periclinal elongation**; values between **0.9** and **1.1** indicate tendency to **isotropic** growth, and values higher than **1.1** indicate tendency to **anisotropic** growth with **anticlinal elongation**. D, Distal zone; B, Basal zone; E, Epidermis; CST, Common Storage tissue; GG, Globoid bivalve-shaped gall; GLG, Green lanceolate bivalve-shaped gall; IP, Inner Parenchyma; LG, Lenticular bivalve-shaped gall; M, Median zone; MP, Median Parenchyma; OP, Outer parenchyma; Pa, Parenchyma; SL, Schlerenchymatic layers; TNT, Typical nutritive tissue.

548

Supplementary table 2. Principal components 1 (PC1), 2 (PC2) and 3 (PC3) obtained from the correlation matrix of cytometric characters of the three bivalve-shaped galls induced by *Lopesia* spp. (Diptera: Cecidomyiidae) on *Mimosa gemmulata* Barneby (Fabaceae) pinna-rachis.

	Induction stage			Growth and development stage		
	PC1	PC2	PC3	PC1	PC2	PC3
HD-Ep	0.019268	0.31012	-0.07508	0.14186	0.35674	-0.06424
HD-OP	-0.15572	-0.14604	-0.00507	0.15821	0.052709	-0.06762
HD-MP	-0.04157	0.05339	-0.27939	0.26526	-0.15741	-0.12488
HD-IP	-0.11321	-0.1867	-0.06971	0.11494	-0.21269	-0.31328
HD-TNT	-0.39206	0.14184	0.053291	0.4982	0.51734	0.014267
HM-Ep	0.18913	0.2773	0.087937	-0.09698	0.35084	-0.19644
HM-OP	-0.00638	-0.02154	0.21054	-0.13136	-0.01761	0.31129
HM-MP	0.099651	0.069184	-0.08081	-0.28732	0.18441	0.11942
HM-IP	-0.21684	-0.00264	-0.19562	0.015067	-0.01349	0.032441
HM-TNT	-0.40504	0.34708	0.11632	0.16249	-0.14921	-0.16397
HB-Ep	0.085539	-0.07904	0.4621	-0.07531	0.28356	0.12546
HB-OP	0.015046	-0.04769	0.31546	0.034862	-0.09039	0.099443
HB-MP	0.026571	0.44224	0.062599	0.33678	-0.14332	0.57698
HB-IP	-0.05993	-0.14347	-0.0141	0.065215	-0.12366	0.15031
HB-TNT	-0.22282	0.22888	0.005639	0.12458	-0.15576	0.02274
WD-Ep	0.15339	0.011665	-0.01329	0.056166	-0.1646	-0.1276
WD-OP	-0.00515	-0.17347	-0.00305	0.055236	0.21671	-0.00983
WD-MP	0.20128	-0.06065	-0.32186	-0.1064	0.014002	0.026322
WD-IP	-0.09254	-0.2063	-0.30149	0.15791	0.041332	-0.11791
WD-TNT	0.14609	-0.09312	-0.05786	-0.23646	0.10315	-0.00589
WM-Ep	0.27427	-0.15627	-0.00957	-0.11425	-0.03629	-0.20021
WM-OP	0.041795	0.038616	0.086307	-0.09121	-0.0267	-0.00665
WM-MP	0.32342	0.30232	-0.20701	-0.3563	0.10295	0.079743
WM-IP	-0.10416	-0.15728	0.079324	0.045746	0.082938	-0.2687
WM-TNT	0.1849	0.070124	-0.04462	-0.21746	0.095376	-0.09237
WB-Ep	0.19283	-0.20538	0.29213	-0.11756	-0.28884	-0.15402
WB-OP	0.027352	0.033423	0.34556	-0.03348	-0.00204	0.070336
WB-MP	0.23798	0.23862	0.10029	-0.05534	0.026424	0.078962
WB-IP	0.02929	-0.04353	0.092099	0.085358	-0.05902	0.23052
WB-TNT	0.26983	0.10369	-0.03161	-0.16057	0.030842	0.26786

D, Distal zone; Ep, Epidermis; H, Height of the cells; IN, Inner parenchyma; M, Median zone; MP, Median parenchyma; OP, Outer parenchyma; TNT, Typical nutritive tissue; W, Width of the cells.

549

550

551

552

553

554

555

556

557

Supplementary table 3. Principal components 1 (PC1), 2 (PC2) and 3 (PC3) obtained from the correlation matrix of cytometric characters of the three bivalve-shaped galls induced by *Lopesia* spp. (Diptera: Cecidomyiidae) on *Mimosa gemmulata* Barneby (Fabaceae) pinna-rachis.

	Mature stage			Senescent stage		
	PC1	PC2	PC3	PC1	PC2	PC3
HD-Ep	0.16942	0.019389	-0.09872	0.13688	0.091353	0.19017
HD-OP	0.01202	0.06231	-0.03718	0.076572	-0.19945	-0.03211
HD-MP	0.18068	-0.0665	-0.30089	0.24049	-0.11005	-0.35901
HD-IP	0.04561	-0.08601	-0.13498	0.24831	0.24339	-0.15143
HD-TNT	0.71596	0.34383	0.2867	0.51228	0.45965	0.32434
HM-Ep	-0.00144	-0.21356	0.28299	-0.00778	0.043872	0.23661
HM-OP	-0.18066	-0.07925	0.16907	-0.26024	0.094449	0.063728
HM-MP	-0.25131	0.39901	-0.29647	-0.35303	0.3943	-0.07554
HM-IP	-0.16625	0.12077	-0.03627	-0.12051	0.21313	0.040865
HM-TNT	-0.08156	0.23838	-0.15344	0.081174	0.065022	0.065288
HB-Ep	0.053607	0.008321	0.21222	0.10391	0.006614	0.15785
HB-OP	-0.04188	0.2823	0.10243	-0.04192	-0.2304	0.14749
HB-MP	0.20502	0.15546	-0.18996	0.17223	-0.36857	0.17775
HB-IP	0.002515	-0.08942	0.099909	0.017464	0.058066	0.28527
HB-TNT	0.005114	0.14973	0.1021	0.17569	0.05241	0.10405
WD-Ep	0.097006	-0.01334	-0.02913	0.10151	0.000131	0.11341
WD-OP	-0.03561	-0.03888	0.048542	-0.06281	-0.0987	0.10877
WD-MP	-0.04146	-0.3532	-0.28202	-0.04503	-0.03965	-0.27527
WD-IP	0.14538	-0.1991	-0.07656	0.29589	-0.02064	-0.27174
WD-TNT	0.005506	-0.09977	-0.2321	0.19012	0.10815	-0.034
WM-Ep	-0.13473	-0.01952	0.16279	-0.07273	0.085379	0.18673
WM-OP	-0.207	0.019043	0.19124	-0.16191	0.13654	0.15891
WM-MP	-0.08203	0.046215	-0.00438	-0.22779	0.13381	-0.12826
WM-IP	0.097192	-0.42247	0.12639	0.13459	0.009964	-0.13584
WM-TNT	0.049262	-0.17994	-0.07516	0.016109	-0.09319	-0.23224
WB-Ep	-0.07692	0.053832	0.33413	-0.02812	-0.09208	0.14114
WB-OP	-0.19432	0.05905	0.21847	-0.17276	-0.25714	0.31218
WB-MP	0.04944	0.091421	-0.21665	0.078315	-0.25655	0.12303
WB-IP	0.26654	-0.20594	0.003286	0.16733	-0.17227	0.067692
WB-TNT	0.12926	0.043642	-0.17597	-0.00755	0.10967	-0.04596

D, Distal zone; Ep, Epidermis; H, Height of the cells; IN, Inner parenchyma; M, Median zone; MP, Median parenchyma; OP, Outer parenchyma; TNT, Typical nutritive tissue; W, Width of the cells.

Figure captions

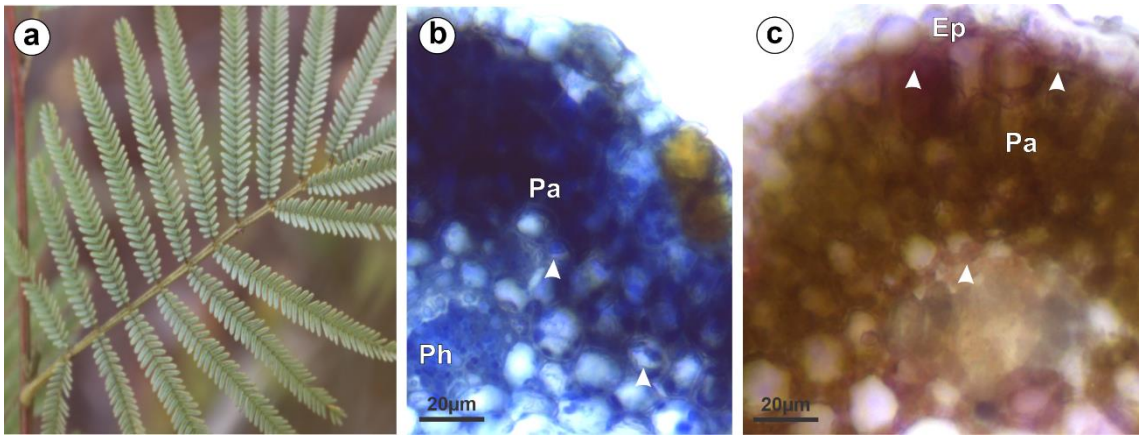

Fig. 1. The non-galled leaves of the *Mimosa gemmulata* Barneby (Fabaceae). (*a*) Macroscopic aspect of the leaf. (*b*, *c*) Histochemical tests of transverse sections of young pinna-rachis. (*b*) Cytokinins in the parenchyma and in the phloem cells (white arrowheads). (*c*) Indole acetic acid in the parenchyma cells (white arrowheads). Pa, Parenchyma; and Ph, Phloem.

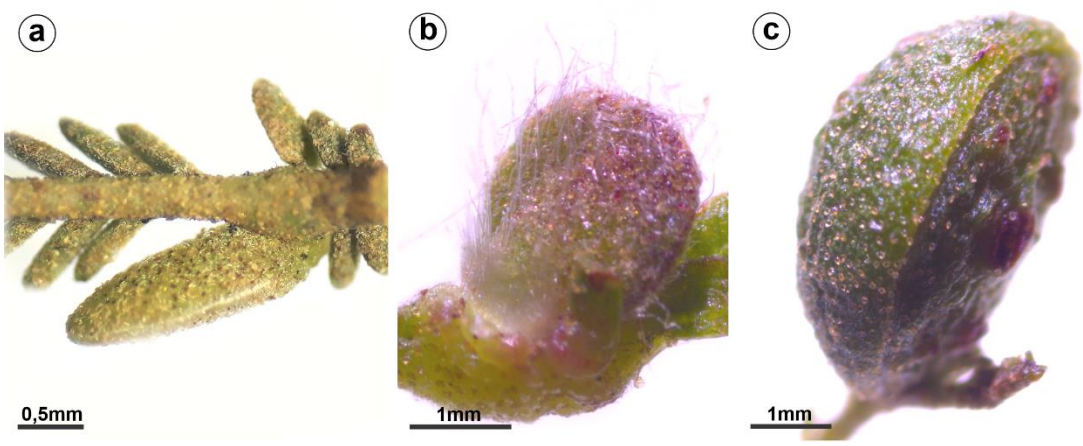

Fig. 2. Bivalve-shaped galls induced by *Lopesia* spp. (Diptera: Cecidomyiidae) on *Mimosa gemmulata* Barneby (Fabaceae) pinna-rachis. (*a*) Lenticular-bivalve-shaped gall. (*b*) Green lanceolate bivalve-shaped gall. (*c*) Globoid bivalve-shaped gall.

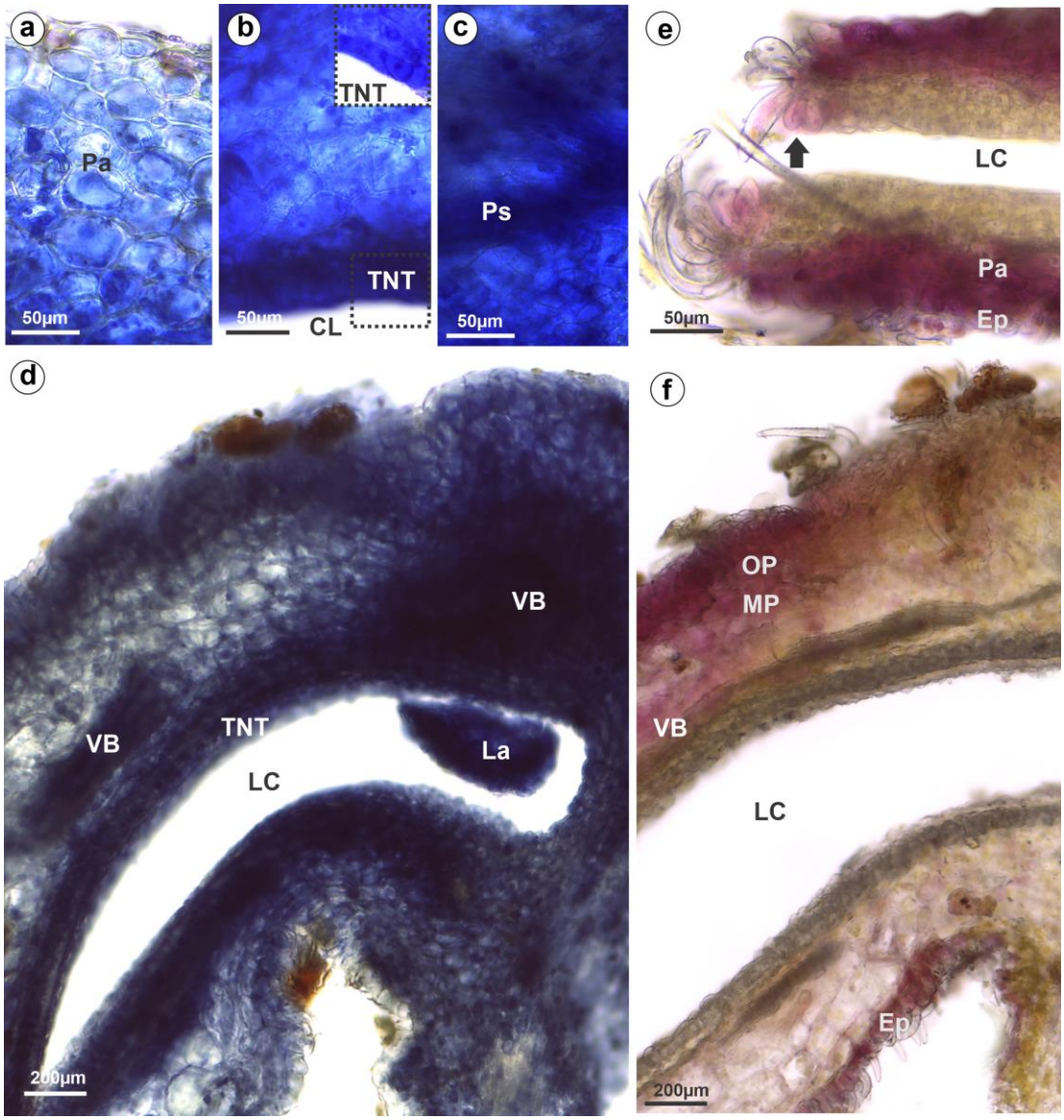

Fig. 3. Histochemical analyses of cytokinins (CKs) and indole acetic acid (IAA) in developmental stages of the lenticular bivalve-shaped galls induced by *Lopesia* sp. (Diptera: Cecidomyiidae) on *Mimosa gemmulata* Barneby (Fabaceae) pinna-rachis in transversal sections. (*a*-*d*) Detection of CKs. (*e*, *f*) Detection of IAA. (*a*-*c*) Induction stage. (*a*) Parenchyma cells. (*b*) Nutritive cells. (*c*) Procambial strands. (*d*) CKs detected in the vascular and in the nutritive cells, and in the body of the larva. (*e*, *f*) Growth and development stage. (*e*) Epidermal, vascular, and parenchyma cells. (*f*) Ordinary and papillose (black arrow) epidermal cells and parenchyma cells. Ep, Epidermis; La, Larva; LC, Larval chamber; MP, Median parenchyma; OP, Outer parenchyma; Pa, Parenchyma; Ps, Procambial strands; TNT, Typical nutritive tissue; VB, Vascular bundle.

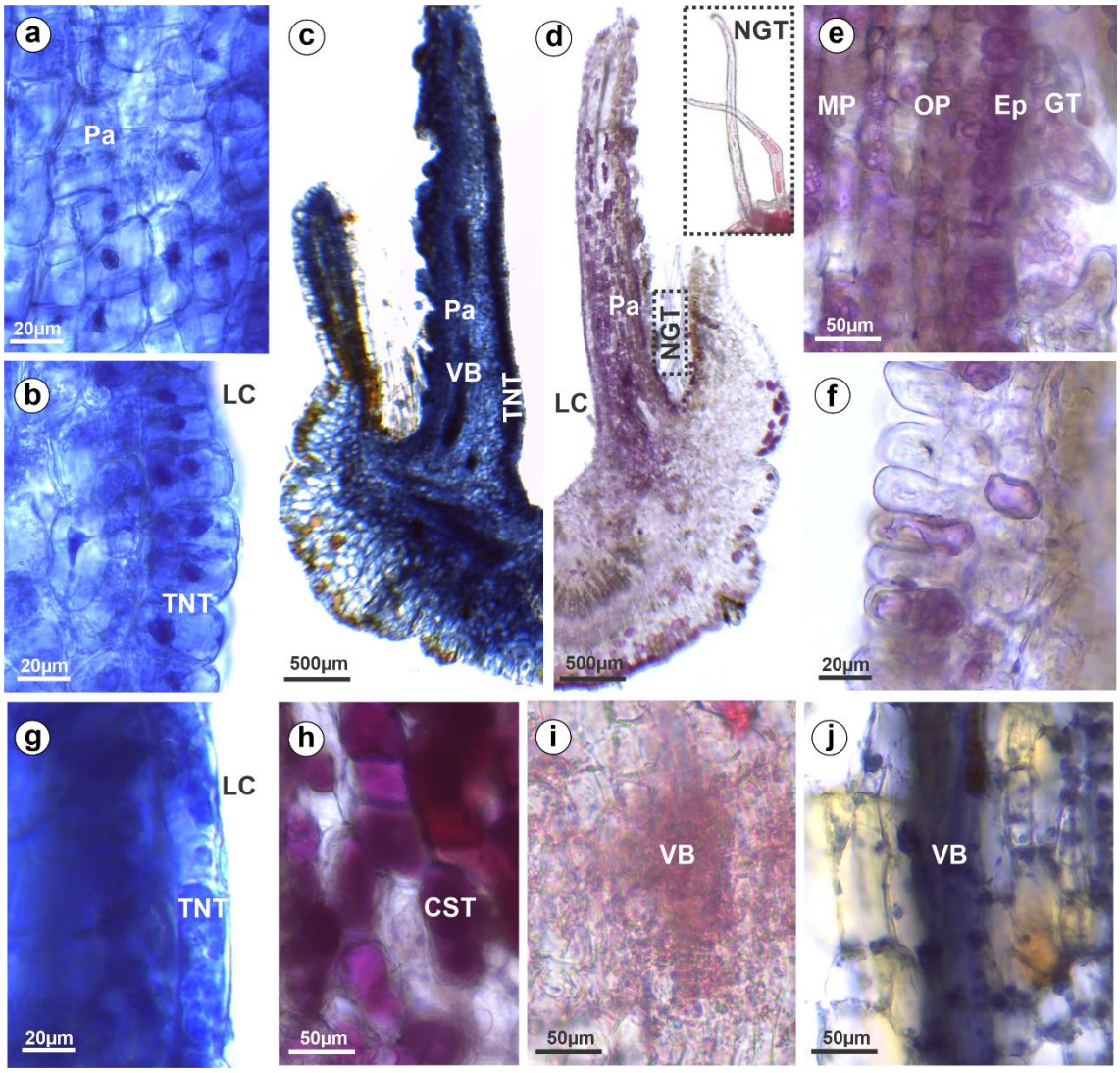

Fig. 4. Histochemical analyses of cytokinins (CKs) and indole acetic acid (IAA) in developmental stages of the green lanceolate bivalve-shaped galls induced by *Lopesia* sp. (Diptera: Cecidomyiidae) on *Mimosa gemmulata* Barneby (Fabaceae) pinna-rachis in transversal sections. (*a-c*, *g*, and *j*) Detection of CKs. (*d-f* and *h*, *i*) Detection of IAA. (*a*, *b*) Induction stage. (*a*) Parenchyma cells. (*b*) Nutritive cells. (*c-f*) Growth and development stage. (*c, d*) Geral aspect of the valve. (*e*) Trichomes, epidermal and parenchyma cells. (*f*) Papillose epidermal cells. (*g-i*) Mature stage. (*g*) Nutritive cells. (*h*) Parenchyma cells. (*i*) Vascular bundles. (*j*) Vascular bundle in the senescent stage. Ep, Epidermis; CST, Common storage tissue; GT, Glandular trichomes; LC, Larval chamber; MP, Median parenchyma; OP, Outer parenchyma; Pa, Parenchyma; Ps, Procambial strands; TNT, Typical nutritive tissue; VB, Vascular bundle.

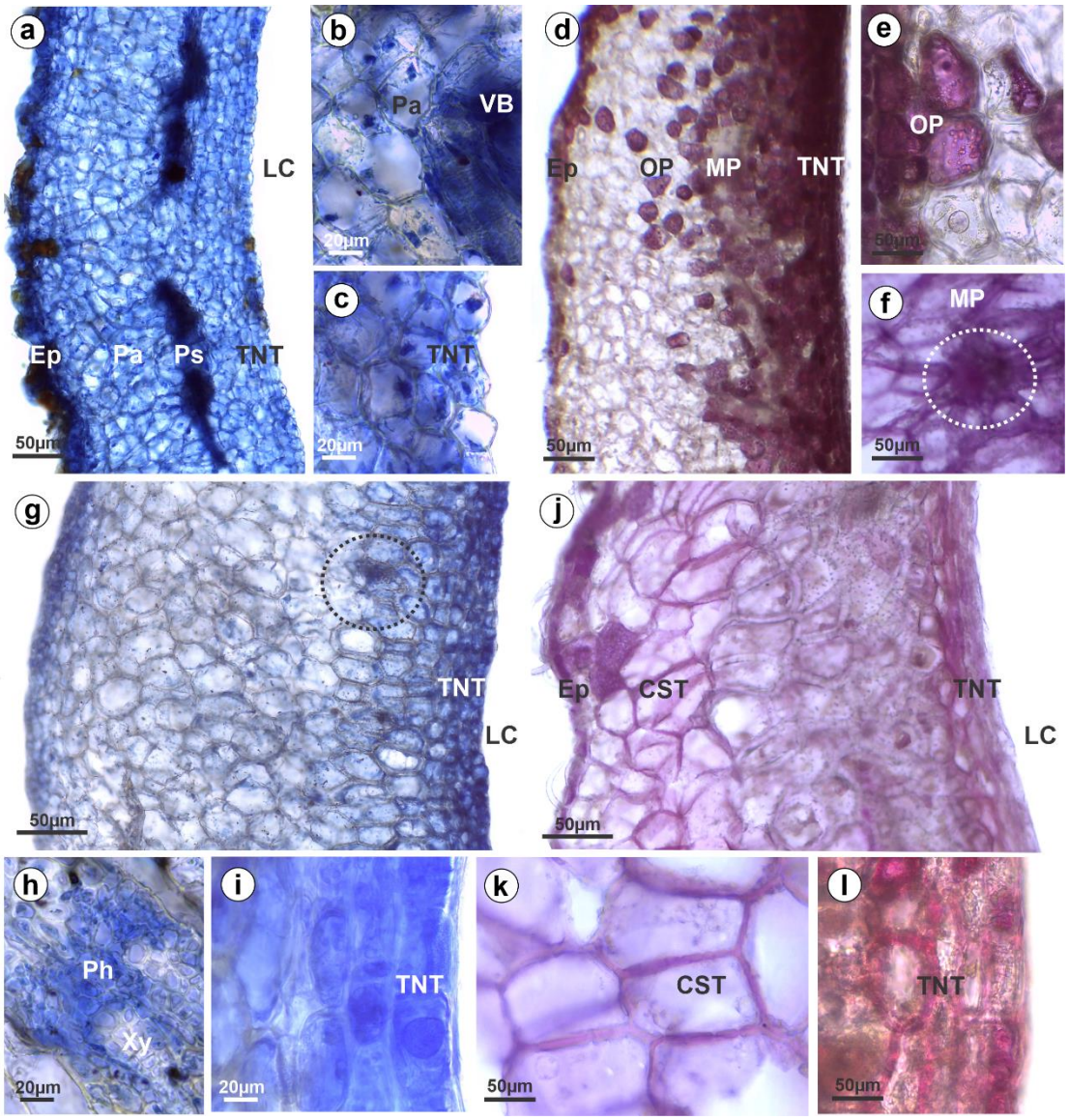

Fig. 5. Histochemical analyses of cytokinins (CKs) and indole acetic acid (IAA) in developmental stages of the globoid bivalve-shaped galls induced by *Lopesia* sp. (Diptera: Cecidomyiidae) on *Mimosa gemmulata* Barneby (Fabaceae) pinna-rachis in transversal sections. (*a-c*, *g*, and *h*, *i*) Detection of CKs. (*d-f* and *j-l*) Detection of IAA. (*a-c*) Induction stage. (*a*) Epidermal, parenchyma, vascular and nutritive cells. (*b*) Parenchyma and vascular cells. (*c*) Nutritive cells. (*d-f*) Growth and development stage. (*d*) Detection in the epidermal, parenchyma and nutritive cells. (*e*) Detection in the epidermal and outer parenchyma cells. (*f*) Vascular bundle. (*g-l*) Mature stage. (*g*) Vascular and nutritive cells. (*h*) Vascular bundle. (*i*) Nutritive cells. (*j*) Epidermal, common storage and nutritive cells. (*k*) Common storage cells. (*l*) Nutritive cells. Ep. Epidermis; CST. Common storage tissue; GT. Glandular trichomes; LC. Larval chamber; MP, Median parenchyma; OP, Outer parenchyma; Pa. Parenchyma; TNT. Typical nutritive tissue; VB. Vascular bundle.

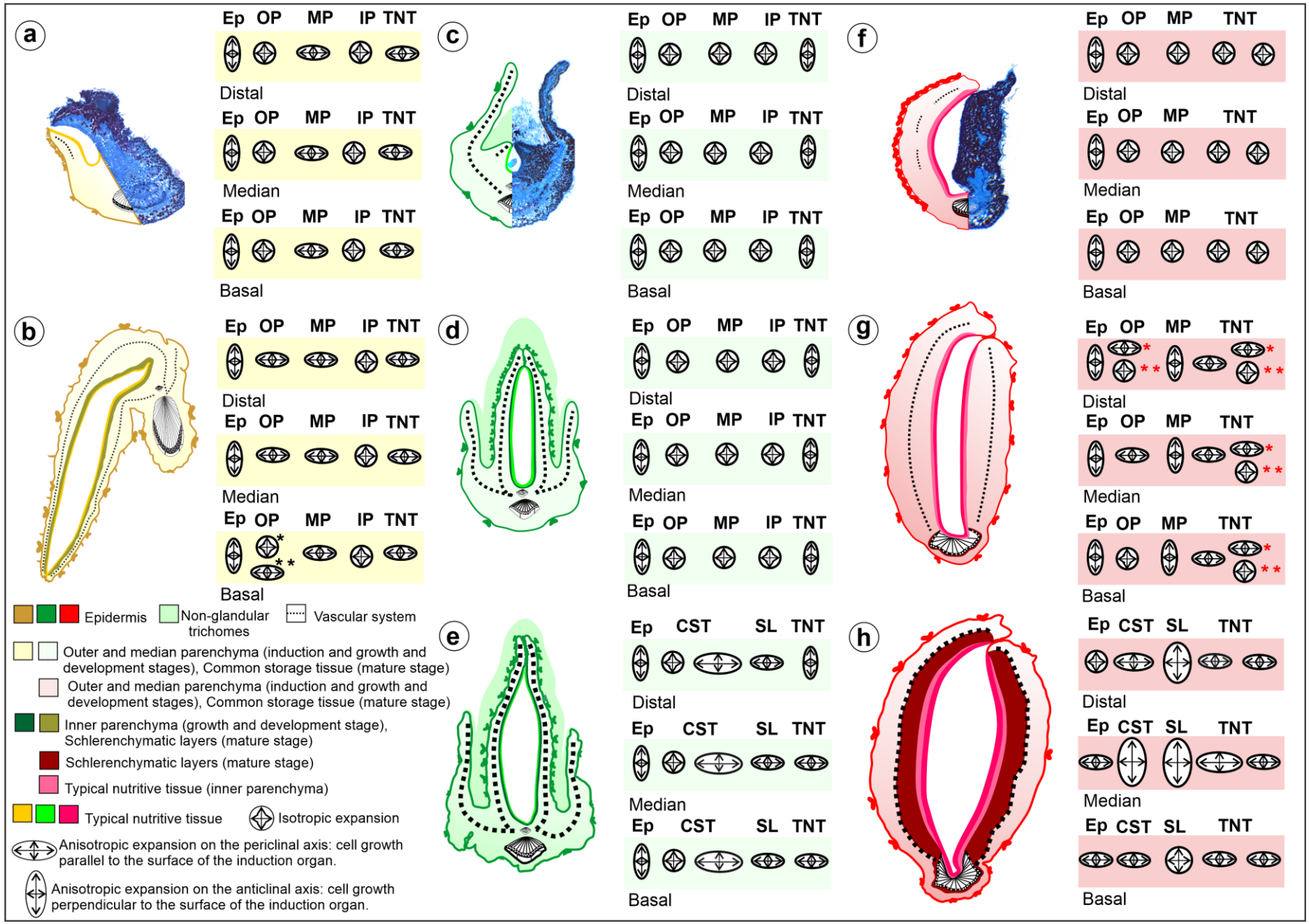
a
b
c
d
e
f
g
h
Ep OP MP IP TNT
Distal
Median
Basal
Ep CST SL TNT
Epidermis
Non-glandular trichomes
Vascular system
Outer and median parenchyma (induction and growth and development stages), Common storage tissue (mature stage)
Outer and median parenchyma (induction and growth and development stages), Common storage tissue (mature stage)
Inner parenchyma (growth and development stage), Schlerenchymatic layers (mature stage)
Schlerenchymatic layers (mature stage)
Typical nutritive tissue (inner parenchyma)
Typical nutritive tissue
Isotropic expansion
Anisotropic expansion on the periclinal axis: cell growth parallel to the surface of the induction organ.
Anisotropic expansion on the anticlinal axis: cell growth perpendicular to the surface of the induction organ.

Fig. 6. Diagrams of the cell elongation patterns in the developmental stages of the three bivalve-shaped galls induced by *Lopesia* spp. (Diptera: Cecidomyiidae) on *Mimosa gemmulata* Barneby (Fabaceae) pinna-rachis in transversal sections. The one black asterisk indicates the cell elongation pattern only of the upper valve, and the two black asterisks indicate the cell elongation pattern only of the lower valve. The one red asterisk indicates the cell elongation pattern only of the larger valve, and the two red asterisks indicate the cell elongation pattern only of the minor valve. (*a, b*) Lenticular bivalve-shaped gall. (*a, c, f*) Induction stage. (*b, d, e*) Growth and development stage. (*e, g*) Mature stage. *Anisotropic expansion on the periclinal axis*: cell growth parallel to the surface of the induction organ. *Anisotropic expansion on the anticlinal axis*: cell growth perpendicular to the surface of the induction organ. Ep, Epidermis; CST, Common storage tissue; MP, Median parenchyma; SL, Schlerenchymatic layers; IP, Inner parenchyma; OP, Outer parenchyma; Pa, Parenchyma; TNT, Typical nutritive tissue.

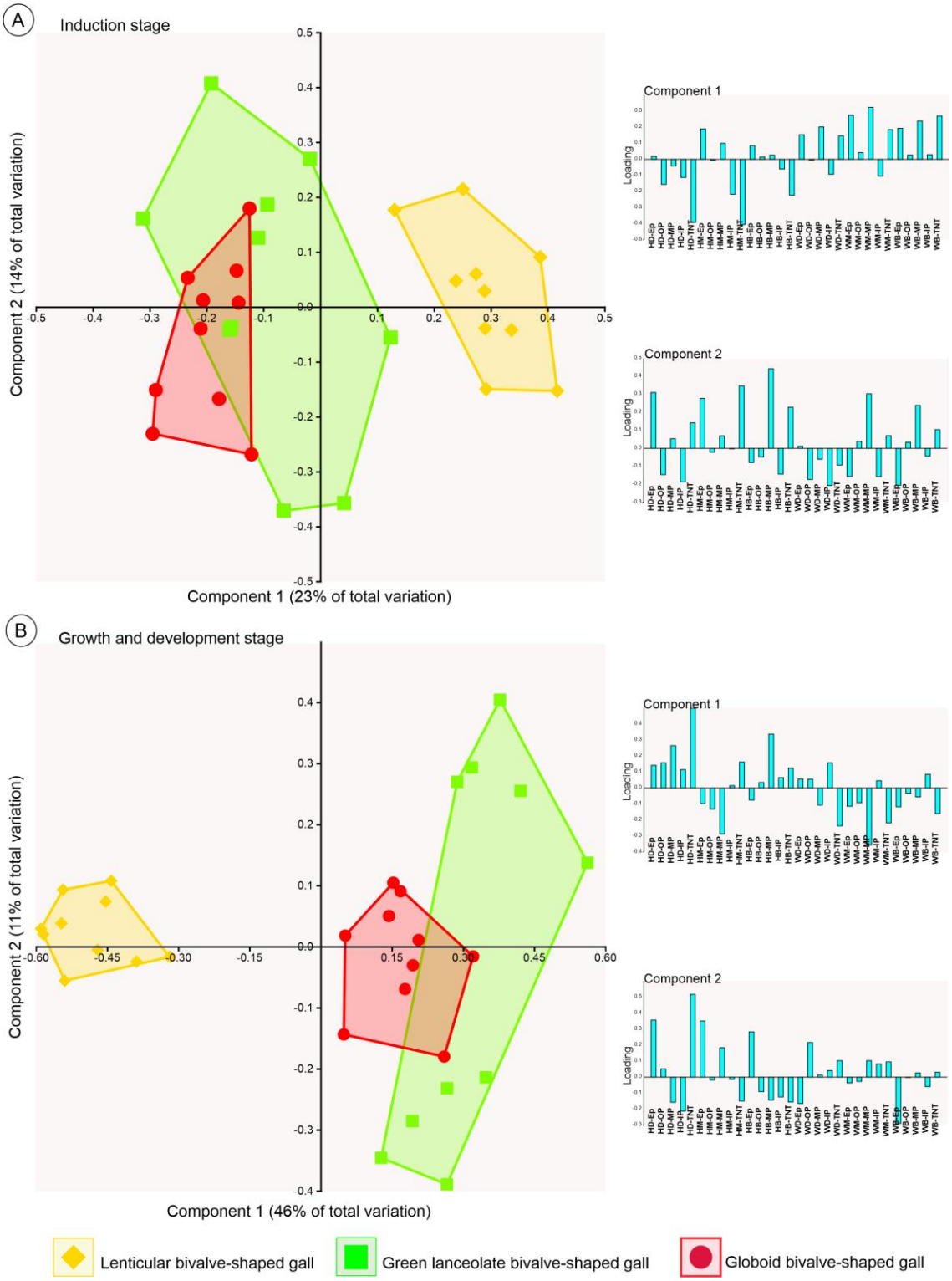

Fig. 7. Representation of the scores Principal component 1 (PC1) and 2 (PC2) in the developmental stages of the three *Lopesia* galls (Diptera: Cecidomyiidae) on *Mimosa gemmulata* Barneby (Fabaceae) pinna-rachis. (*a*) Induction stage. (*b*) Growth and development stage. Ep, Epidermis; B, Basal zone; D, Distal zone; H, Height of the cells; IP, Inner parenchyma; MP, Median parenchyma; OP, Outer parenchyma; TNT, Typical nutritive tissue; W, Width of the cells.

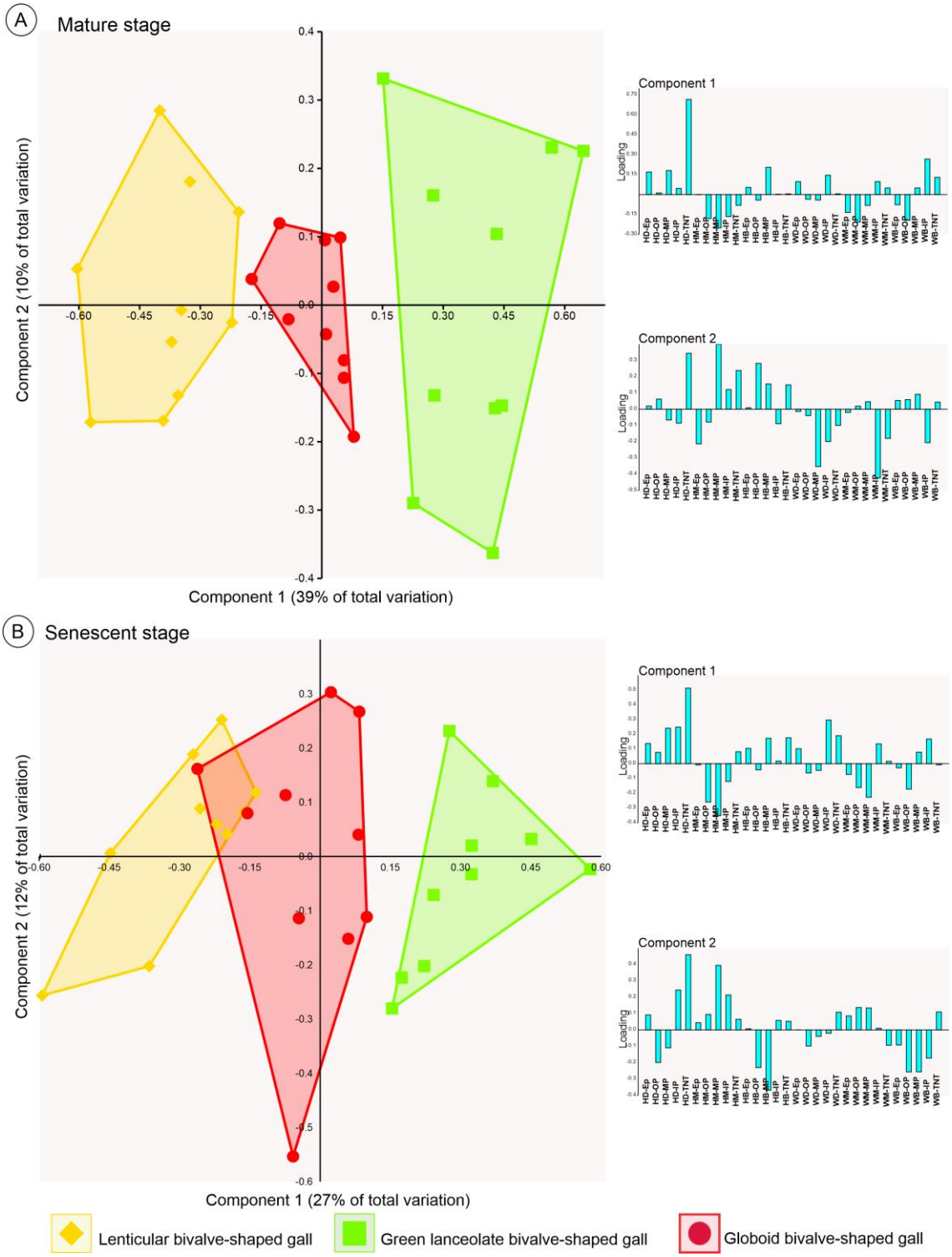

Fig. 8. Representation of the scores Principal component 1 (PC1) and 2 (PC2) in the developmental stages of the three *Lopesia* galls (Diptera: Cecidomyiidae) on *Mimosa gemmulata* Barneby (Fabaceae) pinna-rachis. (*a*) Mature stage. (*b*) Senescent stage. Ep, Epidermis; B, Basal zone; D, Distal zone; H, Height of the cells; IP, Inner parenchyma; MP, Median parenchyma; OP, Outer parenchyma; TNT, Typical nutritive tissue; W, Width of the cells.

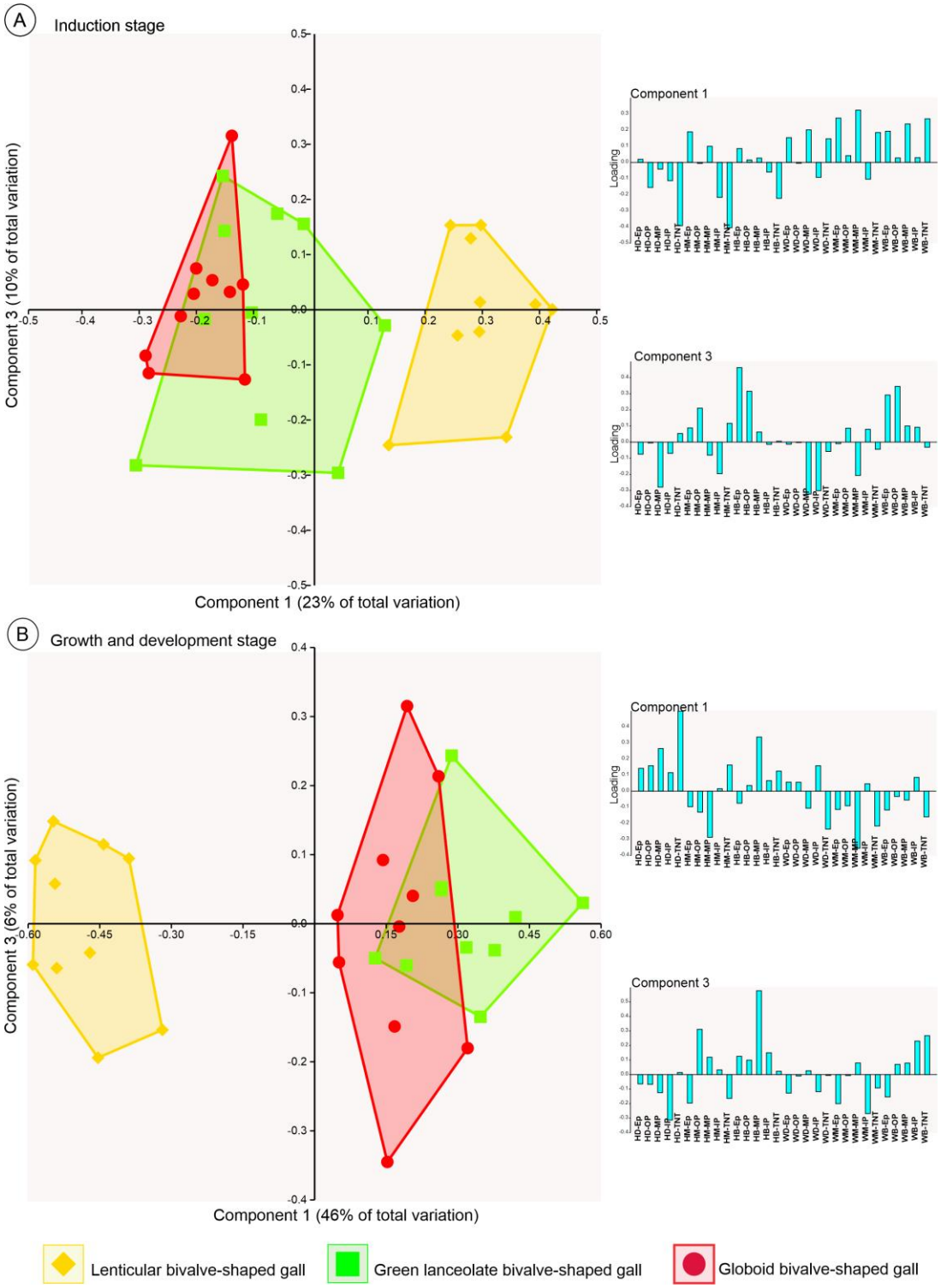

Supplementary fig. 1. Representation of the scores of the Principal component 1 (PC1) and 3 (PC3) in the developmental stages of the three *Lopesia* galls (Diptera: Cecidomyiidae) on *Mimosa gemmulata* Barneby (Fabaceae) pinna-rachis. (*a*) Induction stage. (*b*) Growth and development stage. Ep, Epidermis; B, Basal zone; D, Distal zone; H, Height of the cells; IP, Inner parenchyma; MP, Median parenchyma; OP, Outer parenchyma; TNT, Typical nutritive tissue; W, Width of the cells.

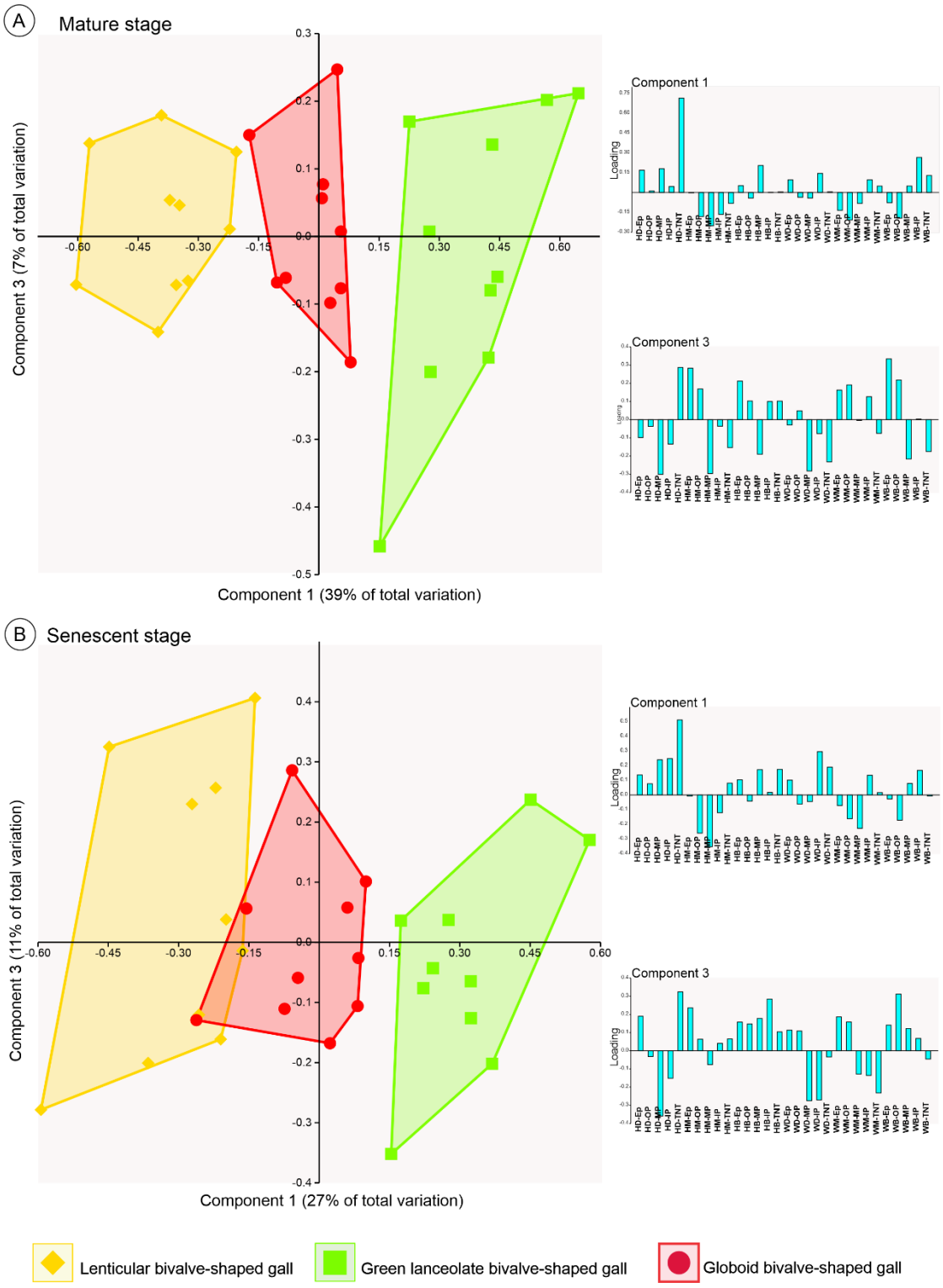

Supplementary fig. 2. Representation of the scores of the Principal component 1 (PC1) and 3 (PC3) in the developmental stages of the three *Lopesia* galls (Diptera: Cecidomyiidae) on *Mimosa gemmulata* Barneby (Fabaceae) pinna-rachis. (*a*) Mature stage. (*b*) Senescent stage. Ep, Epidermis; B, Basal zone; D, Distal zone; H, Height of the cells; IP, Inner parenchyma; MP, Median parenchyma; OP, Outer parenchyma; TNT, Typical nutritive tissue; W, Width of the cells.

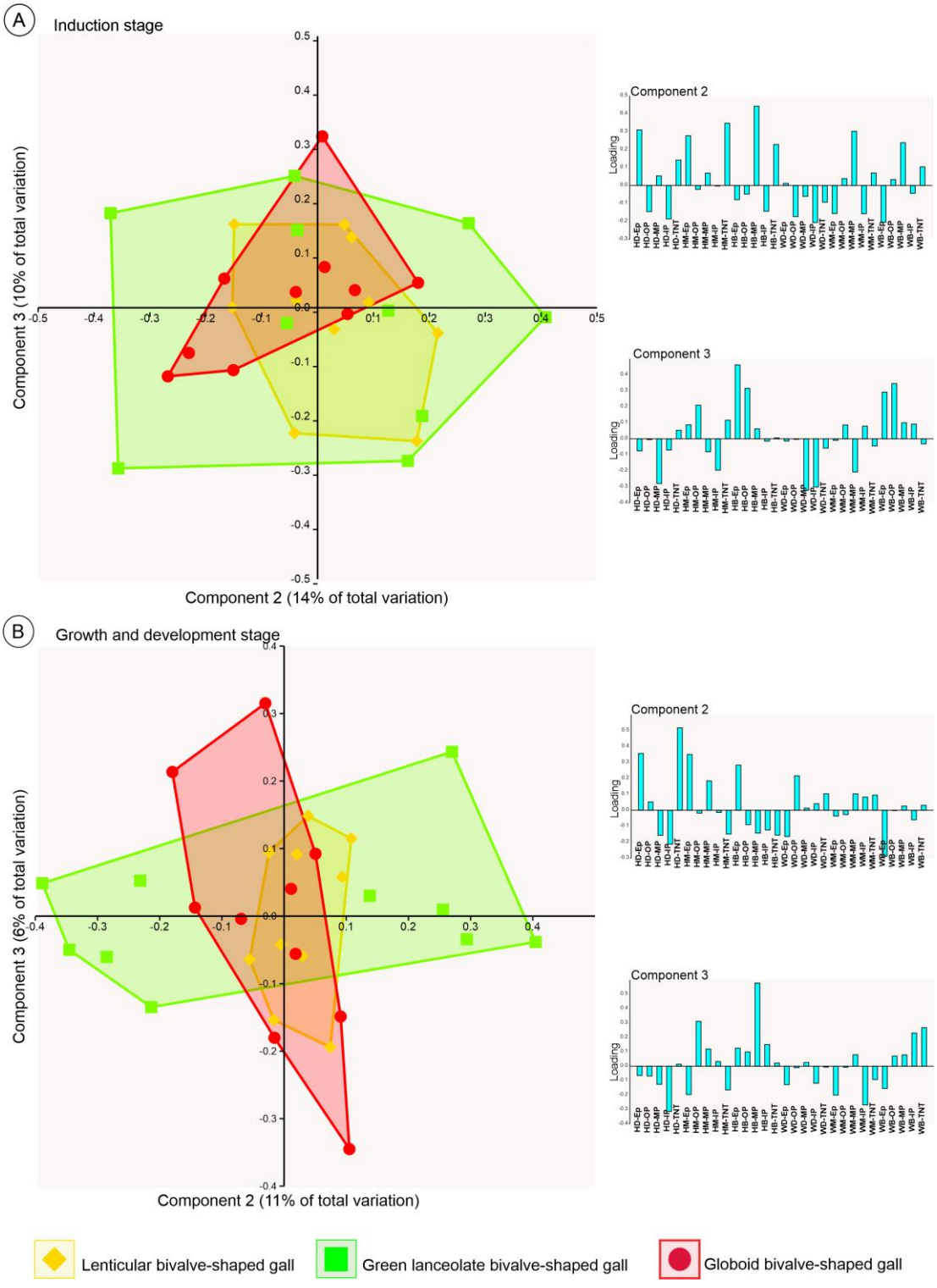

Supplementary fig. 3. Representation of the scores of the Principal component 2 (PC2) and 3 (PC3) in the developmental stages of the three *Lopesia* galls (Diptera: Cecidomyiidae) on *Mimosa gemmulata* Barneby (Fabaceae) pinna-rachis. (*a*) Induction stage. (*b*) Growth and development stage. Ep, Epidermis; B, Basal zone; D, Distal zone; H, Height of the cells; IP, Inner parenchyma; MP, Median parenchyma; OP, Outer parenchyma; TNT, Typical nutritive tissue; W, Width of the cells.

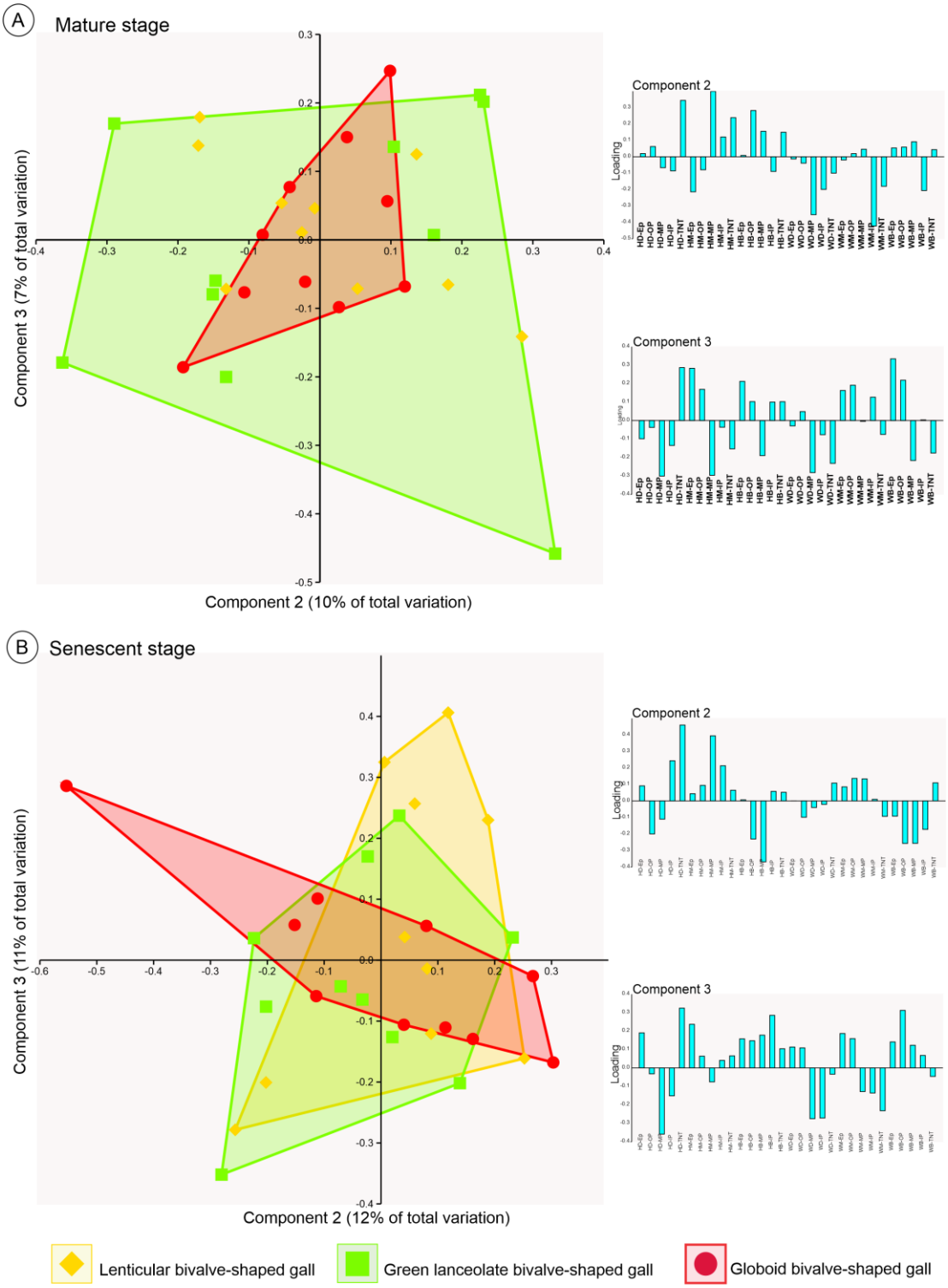

Supplementary fig. 4. Representation of the scores of the Principal component 2 (PC2) and 3 (PC3) in the developmental stages of the three *Lopesia* galls (Diptera: Cecidomyiidae) on *Mimosa gemmulata* Barneby (Fabaceae) pinna-rachis. (*a*) Mature stage. (*b*) Senescent stage. Ep, Epidermis; B, Basal zone; D, Distal zone; H, Height of the cells; IP, Inner parenchyma; MP, Median parenchyma; OP, Outer parenchyma; TNT, Typical nutritive tissue; W, Width of the cells.

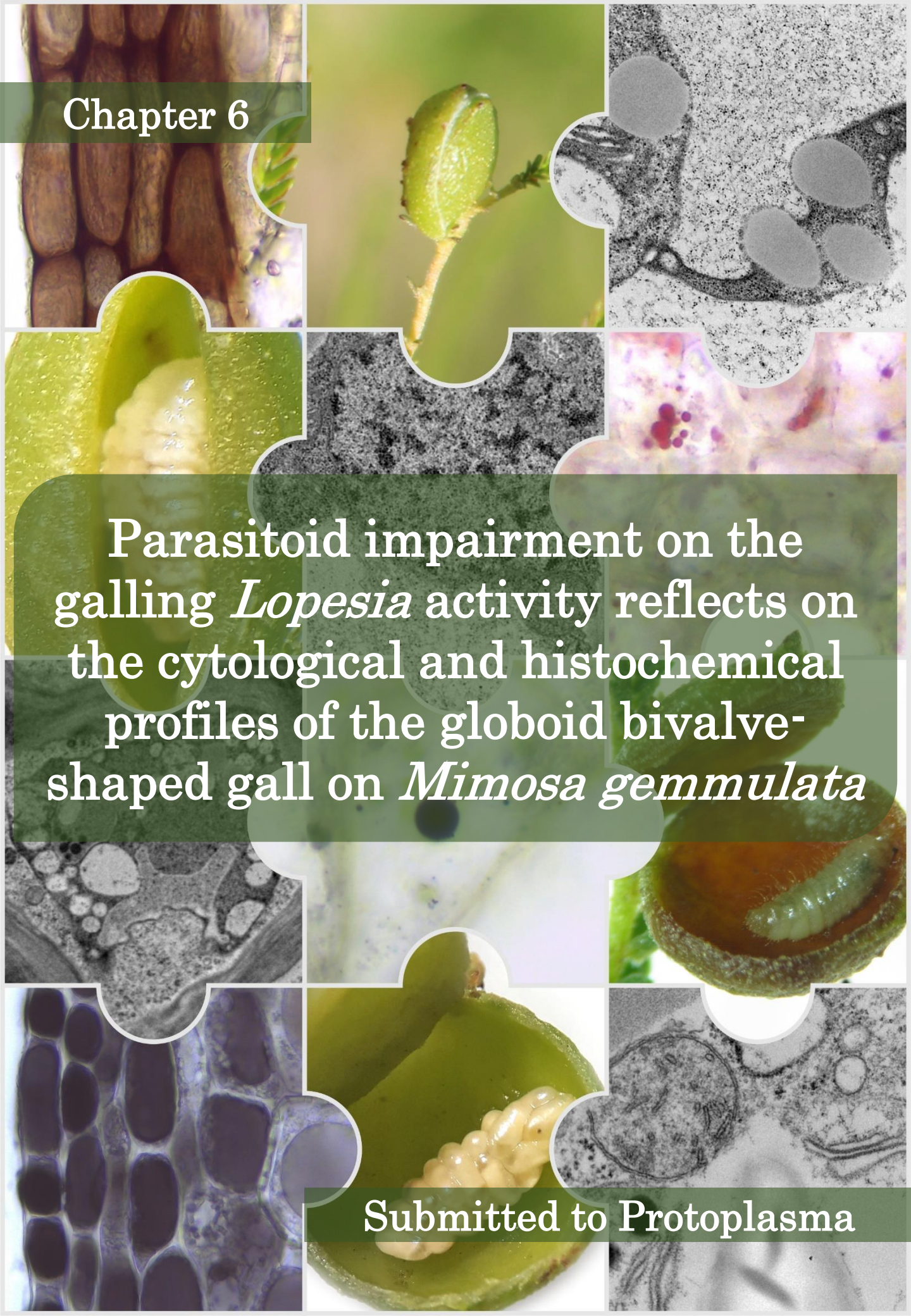

Chapter 6

Parasitoid impairment on the galling *Lopesia* activity reflects on the cytological and histochemical profiles of the globoid bivalve-shaped gall on *Mimosa gemmulata*

Submitted to Protoplasma

Parasitoid impairment on the galling *Lopesia* activity reflects on the cytological and histochemical profiles of the globoid bivalve-shaped gall on *Mimosa gemmulata*

Elaine C. Costa[1], Denis C. Oliveira[2], Rosy M.S. Isaias[1, *]

[1] Laboratório de Anatomia Vegetal, Departamento de Botânica, Instituto de Ciências Biológicas, Universidade Federal de Minas Gerais, Avenida Antônio Carlos, 6627, Pampulha, Belo Horizonte, Minas Gerais Zip code: 31270-901, Brazil

[2] Laboratório de Anatomia, Desenvolvimento Vegetal e Interações, Instituto de Biologia, Universidade Federal de Uberlândia, Campus Umuarama, Rua Ceará s/n, Uberlândia, Minas Gerais, Zip code: 38402-018, Brazil

[*]Corresponding author: rosy@icb.ufmg.br

ORCID: 0000-0001-8500-3320

Abstract: Gall cytological and histochemical features established by the constant feeding behavior of the associated gall-inducer may be changed due to the attack of parasitoids. We accessed two tri-trophic systems involving the globoid bivalve-shaped gall on *Mimosa gemmulata* Barneby (Fabaceae) and its gall-inducing *Lopesia* sp. (Diptera: Cecidomyiidae), which may be ectoparasitized by *Torymus* sp. (Hymenoptera: Torymidae) or endoparasitized by a polyembryonic Platygastridae (Hymenoptera), as models of study. The ectoparasitoid kill the *Lopesia* larva, and stop the feeding stimuli, while the endoparasitoid larvae feed in the *Lopesia* larva body and keep it alive for a certain time. Our hypothesis is that the time lapse of *Lopesia* feeding impairment by the two parasitoids will cause distinct cytological and histochemical responses in the ecto- and endoparasitized galls compared to the non-parasitized condition. In both parasitoidism cases, the impairment of the feeding behavior of the galling *Lopesia* directs the common storage and nutritive cells toward a similar process of induced cell death, involving cell collapse and loss of membrane integrity. The cell metabolism is maintained mainly by mitochondria, and by the translocation of lipids from the common storage tissue, via plasmodesmata, through the sclerenchyma cells toward the nutritive tissue of the ecto- and endoparasitized galls. Accordingly, the parasitoid impairment on the feeding behavior of the *Lopesia* larvae cause precocious senescence, but similar cytological alterations, and no impact over the histochemical profiles, regarding lipids, reactive oxygen species, and secondary metabolites, which support gall metabolism along the parasitoid cycles.

Keywords: ectoparasitism; endoparasitism; induced cell death; plant cell ultrastructure; plant-insect interaction; pycnotic nuclei.

Introduction

Galls are nutrient-rich and may be attacked by other trophic levels, such as inquilines, successors, predators, and mainly parasitoids (Askew 1975; Weis 1982; Luz et al. 2019; Rezende et al. 2021). Such organisms can affect the feeding behavior of the galling insect *taxa*, which reflects on the structural, cytological, and histochemical features of gall tissues (Bronner 1992; Oliveira et al. 2010, 2011; Ferreira et al. 2015, 2019; Rezende et al. 2019). The parasitoids represent the most common natural enemies of the galling insects in nature (Hawkins and Gagné 1989; Hawkins et al. 1997), and can be divided into ecto- and endoparasites (Godfray 1994; Hanson et al. 2014). The females of the ectoparasites inject a venom that normally paralyzes the host larva (Askew 1975; Hanson et al. 2014), while the females of the endoparasites oviposit inside the body of the host larva, but do not paralyze it (Askew 1975; Hanson et al. 2014). The first feeds on the host larva surface, and the latter feed inside the host larva body, which keeps its development at least for a while. In these two scenarios, the body of the gall inducers is eventually consumed (Godfray 1994; Hanson et al. 2014; Mayhew 2016), which impact gall metabolism.

Mimosa gemmulata Barneby (Fabaceae) is a super-host of four bivalve-shaped galls induced by undescribed species of *Lopesia* (Cecidomyiidae), two lanceolate galls, one lenticular gall, and one globoid gall. The highest investment in structural and nutritional metabolism has been demonstrated in the globoid bivalve-shaped galls (GG), which are related to the longest lifespan of the associated *Lopesia* sp. (Costa et al. 2021a, b). In the GG, the *Lopesia* larva can be ectoparasitized by a *Torymus* sp. (Hymenoptera: Torymidae) or endoparasitized by a Platygastridae (Hymenoptera) (Costa et al. 2021b). The Torymidae are generalist ectoparasitoids of galling insects (Askew 1975), which are commonly reported as causing the death of Cecidomyiidae larvae. The Platygastridae species have intimate relationships and are exclusive parasites of Cecidomyiidae larvae (Hanson et al. 2014). The peculiar two tri-trophic relationships involving the GG, the galling *Lopesia* sp., and the two Hymenoptera parasitoids constitute our models of study.

We hypothesize that the ecto- and the endoparasitoids have different impacts on the feeding behavior of the galling *Lopesia* sp., which will distinctly alter the GG cytological and histochemical profiles. To address this hypothesis, the cytological and histochemical features of the common storage and nutritive tissues of the galls with ecto- and endoparasitized larvae are compared to the non-parasitized condition. The following questions guided our discussion: (1) what is the impact of the parasitoidism over the GG cytological and histochemical profiles? And (2) will the impairment of the *Lopesia* larva feeding behavior by the ecto- and endoparasitoids imply in distinct cytological and histochemical profiles?

Materials and methods

Sample design

Samples of globoid bivalve-shaped (GG) mature galls (n = 50) were collected from individuals (n = 12) of *M. gemmulata* in a Cerrado area located at the Serra Geral, municipality of Caetité, State of Bahia, Brazil (14º04'36.8''S, 42°29'59''W). The galls were dissected, and the insects were analyzed with a stereomicroscope (ZEISS Stemi 508). The GG were separated in three categories: I - (control), with only the *Lopesia* larva; II - with the *Lopesia* larva ectoparasitized by the *Torymus* sp., and III - with the *Lopesia* larva endoparasitized by the Platygastridae.

Structural analyses

Samples of the control (non-parasitized GG) and of the two parasitized categories (n = 5 per each category) were fixed in Karnovsky's solution (Karnovsky 1965; modified to 0.1 mol L^{-1}, pH 7.2 phosphate buffer (PBS)), dehydrated in an *n*-butyl series (Kraus and Arduin 1997), and embedded in Paraplast (Sigma®, Leica Biosystems). Serial transverse sections (12 μm) were obtained with a rotatory microtome (Leica® 2035 Biocut), stained with 0.5% Astra blue and 0.5% safranin (9:1, v/v) (Bukatsch 1972), and mounted with colorless varnish Acrilex® (Paiva et al. 2006). A second set of the transverse sections were submitted to histochemical tests for the detection of phenolics and proanthocyanidins (Table 1). The histological sections were observed under a light microscope (Leica® DM500), and photographed with a coupled digital camera (Leica® ICC50 HD).

Cytological analyses

Fragments of the outer and inner tissue compartments of the GG (n = 3 per each category) fixed in Karnovsky`s solution were post-fixed in 1% osmium tetroxide (OsO_4) in 0.1 mol L^{-1} PBS, dehydrated in an ethanol series (O'Brien and McCully 1981), and embedded in Spurr® resin (Sigma-Aldrich) (Lufth 1961). The samples were sectioned (50–70 nm) in an Ultramicrotome Reichert-Jung-Ultracut (Leica, Wetzlar, Germany), contrasted in uranyl acetate and lead citrate (Reynolds 1963), and analyzed with a transmission electron microscope Tecnai™ G2-12 Spirit BioTwin (FEI, Hillsboro, USA; 120KV) at the Centro de Microscopia of the Universidade Federal de Minas Gerais (CM-UFMG).

Histochemical analyses

Gall fresh samples of the control (non-parasitized GG) and of the two parasitized categories (n = 5 per each category) were transversely sectioned with razor blades, and submitted to histochemical tests for the detection of primary and secondary metabolites, and reactive oxygen species (Table 1). Blank sections were used as controls. The sections were analyzed under a light microscope (Leica® DM500), and photographed with a coupled digital camera (Leica® ICC50 HD).

Results

Cytological profiles

Galls with non-parasitized Lopesia *larva* - The galls are extralaminar, green, and isolated; the larval chamber is central and shelters one *Lopesia* larva (Fig. 1a). Gall tissues are organized in outer (OC) and inner (IC) tissue compartments (Fig. 1a, b). In the OC, the common storage cells have polylamellated and thin walls with evident plasmodesmata, large vacuoles, and cytoplasm with peripheral-rich organelles (Fig. 1c). Several free ribosomes, oleosomes, and vesicles are observed; mitochondria are associated with chloroplasts, and the nucleus has parietal position (Fig. 1d-e). The chloroplasts have several plastoglobules, and starch grains (Fig. 1e). The sclerenchyma cells have polylamellated walls with dense cytoplasm in cell-to-cell communication area (Fig. 1f). The cytoplasm of the sclerenchyma cells has mitochondria, endoplasmic reticulum, free ribosomes, Golgi apparatus, and multivesicular bodies (Fig. 1f). In the IC, the nutritive cells have dense cytoplasm with free ribosomes, rough and smooth endoplasmic reticulum, Golgi apparatus, several mitochondria, chloroplasts with plastoglobules and starch grains (Fig. 1g, h), and prominent nucleus (Fig. 1i).

Galls with ectoparasitized Lopesia *larva* - The macroscopic aspects of the ectoparasitized galls and the organization of the OC and the IC is like that of the non-parasitized galls, but a *Torymus* sp. larva occupy the larval chamber (Fig. 2a, b). Cytological alterations are observed regarding the non-parasitized condition. The cells of the common storage tissue have sinuous walls (Fig. 2c) due to the collapse and loss of cellular integrity. The cytoplasm has polysomes, oleosomes, mitochondria, and chloroplasts with plastoglobules (Fig. 2d). Nevertheless, the organelles and membrane systems rupture occur, leading to their packaging process in the autophagic bodies (Fig. 2e, f). The sclerenchyma cells have live cytoplasm and the accumulation of lipids and proteins next to the cell-to-cell communication area (Fig. 2g). In the IC, the nutritive cells collapse (Fig. 2h). These cells have dense cytoplasm with free ribosomes, oleosomes,

mitochondria (Fig. 2i), several vesicles, few chloroplasts with plastoglobules and starch grains in disintegration process. The pyknotic nucleus have condensed chromatin (Fig. 2j).

Galls with endoparasitized Lopesia *larva* - The macroscopic aspects of the endoparasitized galls and the organization of the OC and the IC are like those of the non-parasitized galls, but the larval chamber shelters a *Lopesia* larva endoparasitized by several Platygastridae larvae (Fig. 3a-b). The changes in the cytological features of the endoparasitized galls differ from the non-parasitized condition, but are similar to those of the ectoparasitized galls. In the common storage cells, the walls are sinuous (Fig. 3c) evidencing symptoms of cell collapse. In the cytoplasm, the rupture of membrane systems and their packaging process in the autophagic bodies occur (Figs. 3d-e). The chloroplasts with plastoglobules and starch grains, polysomes, oleosomes, and mitochondria are also observed in the cytoplasm. In the IC, the cytoplasm has ribosomes, oleosomes, mitochondria, and chloroplasts with plastoglobules and starch grains in disintegration process (Fig. 3f-g). The pyknotic nucleus with condensed chromatin is observed (Fig. 3h).

Histochemical profiles

Galls with non-parasitized Lopesia *larva* - Histochemical gradients are established in mature galls. Starch grains, reducing sugars, reactive oxygen species (ROS), phenolic compounds, and proanthocyanidins have bidirectional gradients in gall tissues. Proteins and lipids have centrifugal gradients, and the terpenoids accumulate only in the OC (Fig. 4a). The starch grains (Figs. 4b-c), reducing sugars (Fig. 4d) and proteins (Figs.4e-f) accumulate in the protoplasm of the common storage, sclerenchyma, and nutritive cells. The lipids accumulate in the protoplasm of ordinary epidermal cells, glandular trichomes, common storage (Fig. 4g), and nutritive cells (Fig. 4h). Lignins are detected in the secondary walls of the sclerenchyma cells (Fig. 4i). The terpenoids are detected in the protoplasm of the glandular trichomes, and common storage cells (Fig. 4j). The ROS (Figs. 4k-l), phenolic compounds (Figs. 4m-n), and proanthocyanidins (Figs. 4o-p) accumulate in the cell walls and protoplasm of the ordinary epidermal, common storage, sclerenchyma, and nutritive cells.

Galls with ecto- and endoparasitized Lopesia *larvae* - In ecto- and endoparasitized gall tissues, the histochemical gradients are similar, but differ from that of the non-parasitized galls (Fig. 5a-b). Starch grains accumulate only in nutritive cells of the endoparasitized galls (Fig. 5b). The histochemical gradients

of proteins and lipids are altered similarly both in the ecto- and the endoparasitized gall tissues. In the nutritive cells, the accumulation of proteins is less intense (Fig. 5c), while the accumulation of lipids is more intense (Fig. 5d, e) compared to the non-parasitized galls. The gradients of ROS, phenolics, proanthocyanidins, terpenoids, and the detection de lignins in secondary cell walls in the ecto- and endoparasitized gall tissues (Fig. 5a-b) are like those of the non-parasitized galls.

Discussion

Cytological traits

The cytological features of the common storage and the nutritive tissues in galls is related to their structural-functional traits (Bronner 1992; Oliveira et al. 2010, 2011; Ferreira et al. 2015; Bragança et al. 2021), and develop in response to the constant stimulus of the *Lopesia* larva on the pinna-rachis tissues of *M. gemmulata*. In the common storage tissue, the large vacuole and the peripheral cytoplasm with few organelles relate to water storage (Shitan and Yazaki 2019) and cell hypertrophy, which are important for the structural development of the bivalve-shaped gall with the longest lifespan on *M. gemmulata* (Costa et al. 2021b). The large nucleus and dense cytoplasm rich in organelles of the nutritive cells (Bronner 1992) reveal intense metabolism for the synthesis of lipids and proteins involved in the feeding of the *Lopesia* larva (Costa et al. 2021b), and also in structural metabolism. The endoplasmic reticulum, Golgi apparatus, and vesicles indicate recycling and remodeling of cell wall components (Worden et al. 2012; Bragança et al. 2021), along gall development, in which the accumulation of xyloglucans works out as a carbohydrate source to the *Lopesia* larva (Costa et al. 2021b).

Despite the different parasitoidism strategies of the ecto- and the endoparasitoids on the feeding behavior of the *Lopesia* larvae, the cytological features are similarly impacted in the tissues of the GG. In the ecto- and the endoparasitized galls, the collapsed cell walls, the disintegration of the membrane systems and the packaging process are diagnostic cytological features of the common storage and of the nutritive cells, which also have pyknotic nuclei. The cytological features indicate clear symptoms of cell death as reported for the senescent process of leaves (Lim et al., 2007; Van Door et al. 2011), and of insect galls (Oliveira et al. 2010, 2011; Carneiro and Isaias 2015). Such cytological features may indicate a peculiar case of induced cell death due to the impairment of the feeding activity of the galling *Lopesia* larva by the attack of the ecto and the endoparasitoids.

The disintegration of the organelles and their packaging processes in the autophagic vacuoles are peculiar processes toward the remobilization of valuable resources to plant sinks (Wojciechowska et al., 2018). The packaging processes of chloroplasts with rupture of the membrane systems are notable cytological features of the parasitized galls. In contrast, the integrity of the mitochondria, which are essential for energy production along leaf development toward senescence (Chrobok et al. 2016), relates to the maintenance of the metabolism for effective mobilization of cellular materials, and progression of the precocious senescence in the cells of the common storage and of the nutritive tissues of parasitized galls. The oleosomes and polyribosomes indicate the synthesis of proteins and lipids (Crang et al. 2018; Ischebeck et al. 2020) in the tissues of the GG (Costa et al. 2021b). Such energetic molecules may be translocated by the numerous plasmodesmata that connect the cells of the common storage tissue to the cells of the nutritive tissue, passing by the sclerenchyma cells. Although the sclerenchyma is usually reported as a dead tissue at maturity (Crang et al. 2018), its cells have living protoplast, which is a peculiar cytological trait of the mechanical zone of the GG on *M. gemmulata*. Despite the precocious end of the gall life cycle by the parasitoidism, the mobilization of lipids is demonstrated by the histochemical gradients and opportunistically favor the *Torymus* sp. ectoparasitods and the Platygastridae endoparasitoids.

Histochemical traits

The gradients of carbohydrates, proteins, and lipids in the globoid bivalve-shaped galls are affected by the attack of the parasitoids on the *Lopesia* larvae, while the accumulation of ROS and secondary metabolites remains similar. The bidirectional gradient of reducing sugars used as food resource for the galling *Lopesia* (Costa et al. 2021b) is suppressed both in the ecto-and the endoparasitized galls, while the accumulation of proteins is reduced. In the ectoparasitized galls, the activity of *Torymus* sp. eventually kills the gall-inducing *Lopesia* and stops the stimuli for the maintenance of the nutritive cells. In the endoparasitized galls, the Platygastridae develop within the *Lopesia* body, and can stimulate the increasing and redirection of energetic resources through host manipulation (Askew 1975; Godfray 1994; Pennacchio and Strand 2006; Libersat et al. 2018). Despite the distinction in the attack of the parasitoids, the gradient of lipids is more intense both in the nutritive cells of the ecto- and the endoparasitized galls than in the non-parasitized galls.

The lipids have been reported as energetic source for gall maintenance, and food resource to several gall-inducing insects (Bronner 1992; Oliveira et al. 2010; Isaias et al. 2018; Rezende et al. 2019;

Bragança et al. 2021). Thus, the translocation and storage of lipids are important for the survival and future reproduction of the parasitoids (Visser and Ellers 2008; Mayhew 2016), as they have lost the capability of lipid synthesis along evolutive time and must exploit their host nutritional resources (Visser and Ellers 2008). The *Lopesia* larva hosts the Platygastridae, whose polyembryonic development (Hanson et al. 2014; Iwabuchi 2019) is indirectly supported by the lipids accumulated in the nutritive cells of the GG (Costa et al. 2021b).

The precocious senescence of the galls due to the parasitoidism has also been related to the accumulation of ROS and some secondary metabolites, both in the apoplast and in the symplast of the common storage and nutritive cells. The accumulation of ROS has been histochemically detected in galls and has also been related to the degradation of the membrane systems and plastids (Oliveira et al. 2010, 2011; Ferreira and Isaias 2015). The activity of the parasitoids seems to be inducing the cytological and metabolic processes responsible for ROS accumulation in parasitized gall tissues. Accordingly, the detection of phenolics, proanthocyanidins, and terpenoids in the protoplast, as well as the detection of lignins in cell walls may indicate metabolic responses of the cells toward scavenging the excess of ROS and balancing the REDOX homeostasis (Isaias et al. 2015) up to the emergence of the parasitoids and the end of the tri-trophic cycles.

Final considerations

The parasitoidism impacts the cytological and histochemical profiles of the tissues of the GG due to the impairment of the *Lopesia* larvae feeding behavior. However, the two different tri-trophic interactions resulted in similar cytological and histochemical profiles in the common storage and the nutritive cells, which partially corroborate our hypothesis. Even though the ectoparasitoid *Torymus* sp. larva eventually kills the gall-inducing *Lopesia*, which stop gall development, while the endoparasitoid Platygastridae keep the gall-inducing *Lopesia* larva alive for a longer time, host plant cell responses are similar. In both cases, the disintegration of membrane systems, plastids, and nuclei, and the similar histochemical profiles, regarding lipids, ROS, and secondary metabolites support gall metabolism along the two parasitoid cycles, and culminate in gall precocious senescence.

Funding: This study was financed by the *Coordenação de Aperfeiçoamento de Pessoal de Nível Superior* (CAPES) – Brazil– Finance Code 001 for E.C. Costa (888877.199702/2018-00) scholarship and by

Conselho Nacional de Desenvolvimento Científico e Tecnológico (CNPq) for the research scholarships to R.M.S. Isaias (304335/2019-2) and D.C. Oliveira (304981/2019-2).

Conflicts of interest/Competing interests: The authors declare no competing interest.

Ethics approval: Not applicable

Consent to participate: Not applicable

Consent for publication: Not applicable

Availability of data and material: The data and material can be made available as needed.

Code availability: Not applicable

Authors' contributions: ECC, RMSI, and DCO designed the experiments. ECC collected material and performed the experiments. All authors analyzed the results, discussed data, wrote, and reviewed the manuscript. RMSI coordinated the project.

Acknowledgments

We thank the Neotropical Gall Group for the reading and critical suggestions on the manuscript, and Professor Paul Hanson of the Universidad de Costa Rica for the identification of the parasitoids.

References

Askew R (1975) The organisation of chalcid-dominated parasitoid communities centred upon endophytic hosts. In Evolutionary Strategies of Parasitic Insects and Mites (Ed. Price PW), pp. 130–153. Springer, Boston, MA (US)

Bragança GP, Ferreira BG, Isaias RMS (2021) Distinct cytological mechanisms for food availability in three *Inga ingoides* (Fabaceae)—Cecidomyiidae gall systems. Protoplasma. https://doi.org/10.1007/s00709-021-01646-w

Bronner R (1992) The role of nutritive cells in the nutrition of Cynipids and Cecidomyiids. In: Shorthouse JD, Rohfritsch O (eds) Biology of insect-induced galls. Oxford University Press, New York, pp 118–140

Bukatsch F (1972) Bermerkungenzur Doppelfärbung Astrablau-Safranin. Mikrokosmos 61:255

Carneiro RG, Isaias RMS (2015) Cytological cycles and fates in *Psidium myrtoides* are altered towards new cell metabolism and functionalities by the galling activity of *Nothotrioza myrtoidis*. Protoplasma 252:637–646. https://doi.org/10.1007/s00709-014-0709-x

Costa EC, Martini VC, Souza-Silva A, Lemos-Filho JP, Oliveira DC, Isaias RMS (2021a) How galling herbivores share a single super-host plant during their phenological cycle: the case of *Mimosa gemmulata* Barneby (Fabaceae). Trop. Ecol.

Costa EC, Oliveira DC, Ferreira DKL, Isaias RMS (2021b) Structural and nutritional peculiarities related to lifespan differences on four *Lopesia* induced bivalve-shaped galls on the single super-host *Mimosa gemmulata*. Front. Plant Sci. 12:1–13. https://doi.org/10.3389/fpls.2021.660557

Chrobok D, Law SR, Brouwer B, Lindén P, Ziolkowska A, Liebsch D, Narsai R, Szal B, Moritz T, Rouhier N, Whelan J, Gardeström P, Keech O (2016) Dissecting the metabolic role of mitochondria during developmental leaf senescence. 172: 2132-2153. https://doi.org/10.1104/pp.16.01463

Crang R, Lyons-Sobaski S, Wise R. (2018) Plant Cell Structure and Ultrastructure. In: Plan Anatomy: A concept-Based Approach to the structure of Seed Plants. pp. 77-212 https://doi.org/10.1007/978-3-319-77315-5

David R, Carde JP. (1964) Coloration deffe´ rentielle des inclusions lipidiques et terpeniques des pseudophylles du Pin maritime au moyen du re´actif NADI. Comptes Rendus Hebdomadaires des Se´ances de l'Acade´mic des Sciences 258:1338–1340

Feucht W, Schmid PPS, Christ E (1986) Distribution of flavanols in meristematic and mature tissues of *Prunus avium* shoots. J. Plant Physiol. 125:1–8. https://doi.org/10.1016/S0176-1617(86)80237-1

Ferreira BG, Carneiro RGS, Isaias RMS (2015) Multivesicular bodies differentiate exclusively in nutritive fast-dividing cells in *Marcetia taxifolia* galls. Protoplasma 252:1275–1283. https://doi.org/10.1007/s00709-015-0759-8

Ferreira BG, Álvarez R, Bragança GP, Alvarenga DR, Pérez-Hidalgo N, Isaias RMS (2019) Feeding and other gall facets: patterns and determinants in gall structure Bot. Rev. 85:78–106. https://doi.org/10.1007/s12229-019-09207-w

Godfray HCJ (1994) Parasitoids. Behavioral and Evolutionary Ecology. Princeton University Press, 217 Princeton.

Hanson P, Nishida K (2014) Insect galls of Costa Rica and their parasitoids. In: Fernandes GW, Santos JC (eds) Neotropical insect galls. Springer, Dordrecht, pp 497–517

Hawkins BA, Gagné RJ (1989) Determinants of assemblage size for the parasitoids of Cecidomyiidae (Diptera). Oecologia 81:75–88. https://doi.org/10.1007/BF00377013

Hawkins BA, Cornell HV, Hochberg ME (1997) Predators, parasitoids, and pathogens as mortality agents in phytophagous insect populations. Ecology 78:2145–2152. https://doi.org/10.1890/0012-9658(1997)078[2145:PPAPAM]2.0.CO;2

Isaias RMS, Oliveira DC, Moreira ASFP, Soares GLG, Carneiro RGS (2015) The imbalance of redox homeostasis in arthropod-induced plant galls: mechanisms of stress generation and dissipation. Biochim. Biophys. Acta 1850:1509–1517. https://doi.org/10.1016/j.bbagen.2015.03.007

Isaias RMS, Ferreira BG, Alvarenga DR, Barbosa LR, Salminen J, Steinbauer MJ (2018) Functional compartmentalization of nutrients and phenolics in the tissues of galls induced by *Leptocybe invasa* (Hymenoptera: Eulophidae) on *Eucalyptus camaldulensis* (Myrtaceae). Aust Entomol 57:238–246. https://doi.org/10.1111/aen.12336

Ischebeck T, Krawczyk HE, Mullen RT, Dyer JM, Chapman KD (2020) Lipid droplets in plants and algae: Distribution, formation, turnover and function. Semin. Cell Dev. Biol. 108: 82–93. https://doi.org/10.1016/j.semcdb.2020.02.014

Iwabuchi K (2019) Polyembryonic Insects: An Extreme Clonal Reproductive Strategy. Springer Nature Singapore Pte Ltd., Tokyo University of Agriculture and Technology Fuchu, Tokyo, Japan 209p. https://doi.org/10.1007/978-981-15-0958-2

Johansen DA (1940) Plant microtechnique. McGraw-Hill, New York

Karnovsky MJ (1965) A formaldehyde-glutaraldehyde fixative of high osmolarity for use in electron microscopy. J Cell Biol 27:137–138.

Kraus JE, Arduin M (1997) Manual básico de métodos em Morfologia Vegetal. Editora da Universidade Federal Rural do Rio de Janeiro, Seropédica

Libersat F, Kaiser M, Emanuel S (2018) Mind Control: How Parasites Manipulate Cognitive Functions in Their Insect Hosts. Front. Psychol. 9:1–6. https://doi.org/10.3389/fpsyg.2018.00572

Lim PO, Kim HJ, Nam HG. 2007. Leaf senescence. Annu. Rev. Plant Biol. 58: 115–136. https://doi.org/10.1146/annurev.arplant.57.032905.105316

Luft JH (1961) Improvements in epoxy resin embedding methods. J Biophys Biochem Cytol 9:404–414. https://doi.org/10.1083/jcb.9.2.409

Luz FA, Mendonça Júnior MS (2019) Guilds in Insect Galls: Who is Who. BioOne (1):207–210. https://doi.org/10.1653/024.102.0133

Mazia D, Brewer PA, Alfert M (1953) The cytochemistry staining and measurement of protein with mercuric bromophenol blue. Biol Bull 104:57–67. https://doi.org/10.2307/1538691

Mayhew PJ (2016) Comparing parasitoid life histories. Entomol. Exp. Appl. 159(2):47-162. https://doi.org/10.1111/eea.12411

O'Brien TP, McCully ME (1981) The study of plant structure: principles and selected methods. Termacarphi Pty Ltd, Melbourne

Oliveira DC, Magalhaes TA, Carneiro RGS, Alvin MN, Isaias RMS (2010) Do Cecidomyiidae galls of *Aspidosperma spruceanum* (Apocynaceae) fit the pre-established cytological and histochemical patterns? Protoplasma 242:81–93. https://doi.org/10.1007/s00709-010-0128-6

Oliveira DC, Carneiro RGS, Magalhaes TA, Isaias RMS (2011) Cytological and histochemical gradients on two *Copaifera langsdorffii* Desf (Fabaceae) Cecidomyiidae gall systems. Protoplasma 248:829–837. https://doi.org/10.1007/s00709-010-0258-x

Paiva JGA, Fank-de-Carvalho SM, Magalhaes MP, Graciano-Ribeiro D (2006) Verniz vitral incolor 500®: uma alternativa de meio de montagem economicamente viavel. Acta Bot Bras 20:257–264. https://doi.org/10.1590/S0102-33062006000200002

Pennacchio F, Strand MR. (2006) Evolution of developmental strategies in parasitic hymenoptera. Annu Rev Entomol. 51:233–258. https://doi.org/10.1146/annurev.ento.51.110104.151029

Reynolds ES (1963) The use of lead citrate at high pH as an electronopaque stain in electron microscopy. J Cell Biol 17:208–212. https://doi.org/10.1083/jcb.17.1.208

Rezende UC, Custodio JF, Kuster VC, Goncalves LA, Oliveira DC (2019) How the activity of natural enemies changes the structure and metabolism of the nutritive tissue in galls? Evidence from the

Palaeomystella oligophaga (Lepidoptera)–*Macairea radula* (Metastomataceae) system. Protoplasma 256:669–667. https://doi.org/10.1007/s00709-018-1321-2

Rezende UC, Cardoso JCF, Hanson P, Oliveira DC (2021) Gall traits and galling insect survival in a multi-enemy context. Rev. Biol. Trop. 69:291–301. https://doi.org/10.15517/rbt.v69i1.42826

Rosseti S, Bonnatti PM (2001) In situ histochemical monitoring of ozone- and TMV-induced reactive oxygen species in tobacco leaves. Plant Physiol. Biochem. 39:433–442. https://doi:10.1016/S0981-9428(01)01250-5

Sass JE (1951) Botanical microtechnique. Iowa State College Press, Ames

Shitan N, Yazaki K (2019) Dynamism of vacuoles toward survival strategy in plants. Biochim Biophys Acta Biomembr. 11862: 183127 https://doi.org/10.1016/j.bbamem.2019.183127

Van Doorn W, Beers E, Dangl J, Franklin-Tong V, Gallois P, HaraNishimura I, Jones A, Kawai-Yamada M, Lam E, Mundy J (2011) Morphological classification of plant cell deaths. Cell Death Differ 18:1241–1246. https://doi.org/10.1038/cdd.2011.36

Visser B, Ellers J (2008) Lack of lipogenesis in parasitoids: A review of physiological mechanisms and evolutionary implications J. Insect Physiol. 54:1315–1322. https://doi.org/10.1016/j.jinsphys.2008.07.014

Weis AE (1982) Resource utilization patterns in a community of gallattacking parasitoids. Environ Entomol 11:809–815. https://doi.org/10.1093/ee/11.4.809

Wojciechowska N, Marzec-Schmidt K, Kalemba EM, Zarzyńska-Nowak A, Jagodziński AM, Bagniewska-Zadworna A (2018) Autophagy counteracts instantaneous cell death during seasonal senescence of the fine roots and leaves in *Populus trichocarpa.* BMC Plant Biol. 260:1–16. https://doi.org/10.1186/s12870-018-1439-6

Worden N, Park E, Drakaki G (2012) *Trans*-Golgi network – An intersection of trafficking cell wall components. 54:875–886. doi: 10.1111/j.1744-7909.2012.01179.x

Table 1. Histochemical tests applied to the globoid bivalve-shaped galls on *Mimosa gemmulata* Barneby (Fabaceae).

Histochemical Tests	Reagent - substance	Reaction mediums	Positive coloration	Reference
Lugol's reagent	Starch grains	1% potassium iodine–iodide solution for 5 min	Black grains	Johansen (1940)
Fehling's reagent	Reducing sugars	Solution "A" (6.93% II copper sulfate w:v) and "B" (34.6% sodium potassium tartrate and 12% sodium hydroxide w:v), with subsequent heating of the slide containing the samples to pre-boiling	Brown precipitates	Sass (1951)
Mercuric bromophenol blue	Proteins	Mercuric bromophenol blue solution for 15 min, wash in 5% Acetic Acid for 20 min and wash in distilled water for 15min	Blue precipitates	Mazia et al. (1953)
Sudan Red B (C.I. 26110)	Lipophilic substances	Saturated solution of Sudan Red B in 70°GL ethanol for 5 min	Red droplets	Johansen (1940)
Ferric chloride	Phenolics	10% ferric chloride solution for 5 min	Black or brown precipitates	Johansen (1940)
DMACA	Proanthocyanidins	p- dimethylaminocinnamaldehyde for up to 5 min	Magenta precipitates	Feucht et al. (1986)
Wiesner's reagent	Lignins	2% phloroglucinol in acidified solution for 5 min	Pink or red precipitates	Johansen (1940)
NADI	Terpenoids	1% α-naphthol, 1% dimethyl-p-phenylenediamine-NADI in 0.01 M phosphate buffer (pH 7.2)	Blue or purple droplets	David and Carde (1964)
DAB	Reactive Oxygen /species (ROS)	0.5% 3,3′-diaminobenzidine (DAB) (Sigma®) in the dark for 30–40 min	Brown precipitates	Rosseti and Bonnatti (2001)

Figures

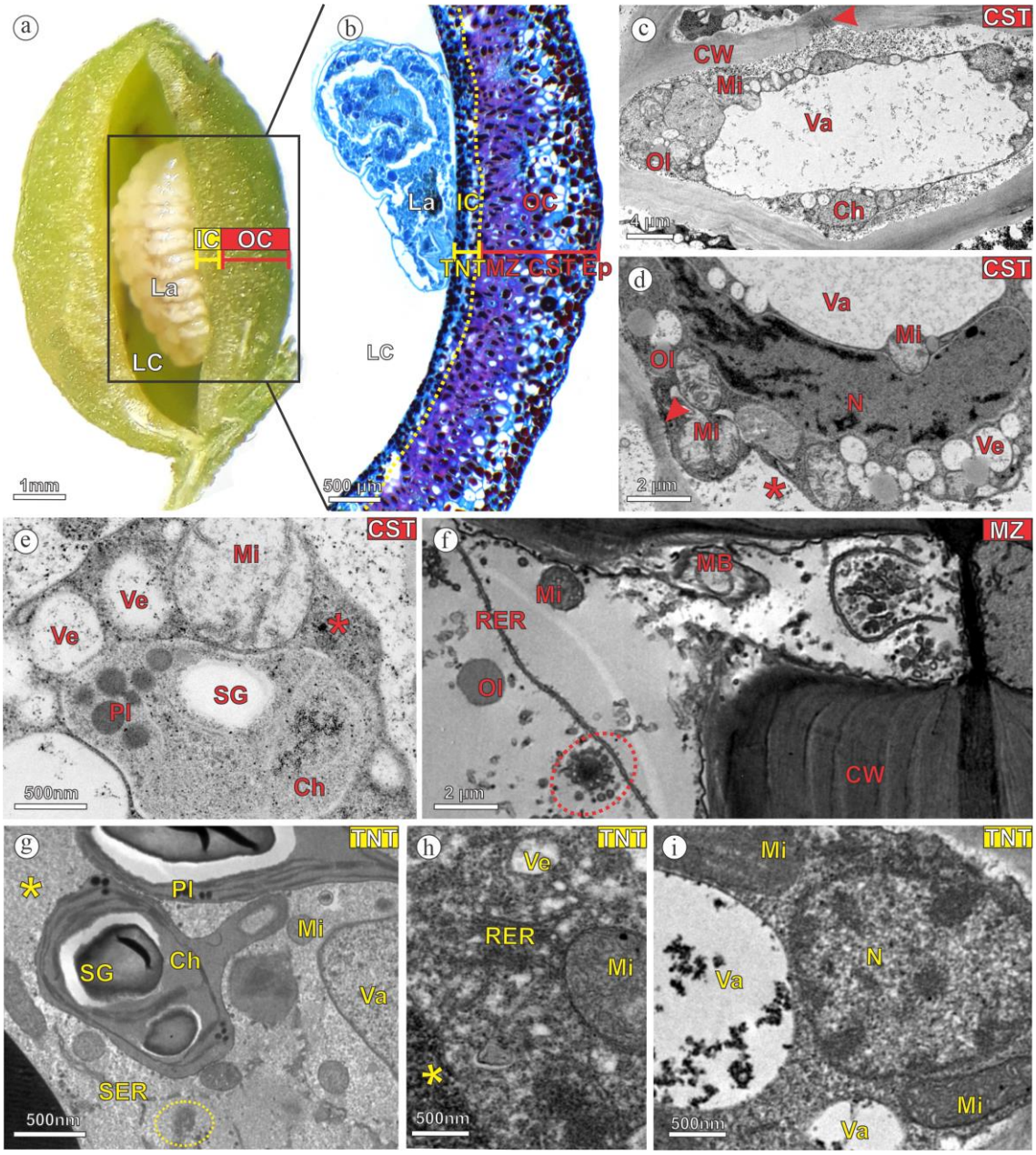
a
IC
OC
La
LC
1mm
b
La
IC
OC
TNT
MZ
CST
Ep
LC
500 µm
c
CST
CW
Mi
Va
Ol
Ch
4 µm
d
CST
Va
Mi
Ol
N
Mi
Ve
2 µm
e
CST
Mi
Ve
Ve
SG
Pl
Ch
500nm
f
MZ
MB
Mi
RER
Ol
CW
2 µm
g
TNT
Pl
Mi
SG
Ch
Va
SER
500nm
h
TNT
Ve
RER
Mi
500nm
i
TNT
Mi
N
Va
Mi
Va
500nm

Fig. 1 Globoid bivalve-shaped mature galls induced by *Lopesia* sp. (Diptera: Cecidomyiidae) on *Mimosa gemmulata* Barneby (Fabaceae). **(a)** Macroscopic aspect of a gall with *Lopesia* larva (La) inside the chamber. **(b)** Transverse section, evidencing gall histological organization. **(c-f)** Cytological features. **(c-e)** Common storage tissue. **(c)** A cell with thin walls (Cw) and plasmodesmata (red arrowhead), large vacuole (Va), and peripheral cytoplasm, where mitochondria (Mi), oleosomes (Ol), and a chloroplast (Ch) occur. **(d)** A cell with plasmodesmata (red arrowhead), evident nucleus (N), vacuole (Va), oleosomes (Ol), free ribosomes (red asterisk), vesicles (Ve), and mitochondria (Mi) associated with the nucleus. **(e)** Chloroplast (Ch) with plastoglobules (Pl) and starch grain (SG), vesicles (Ve), mitochondria (Mi), and free ribosomes (red asterisk). **(f)** Sclerenchyma evidencing secondary cell walls and cytoplasm with multivesicular bodies (MB), Golgi apparatus (red dotted circle), rough endoplasmic reticulum (RER), mitochondria (Mi), an oleosome (Ol), and cell-to-cell communication area. **(g-i)** Typical nutritive tissue. **(g)** Cell with smooth endoplasmic reticulum (SER), Golgi apparatus (yellow dotted circle), free ribosomes (yellow asterisk), mitochondria (Mi), chloroplast (Ch) with plastoglobules (Pl) and starch grain (SG). **(h)** Rough endoplasmic reticulum (RER), free ribosomes (yellow asterisk), and a vesicle. **(i)** Nucleus (N), mitochondria (Mi) and vacuoles (Va)

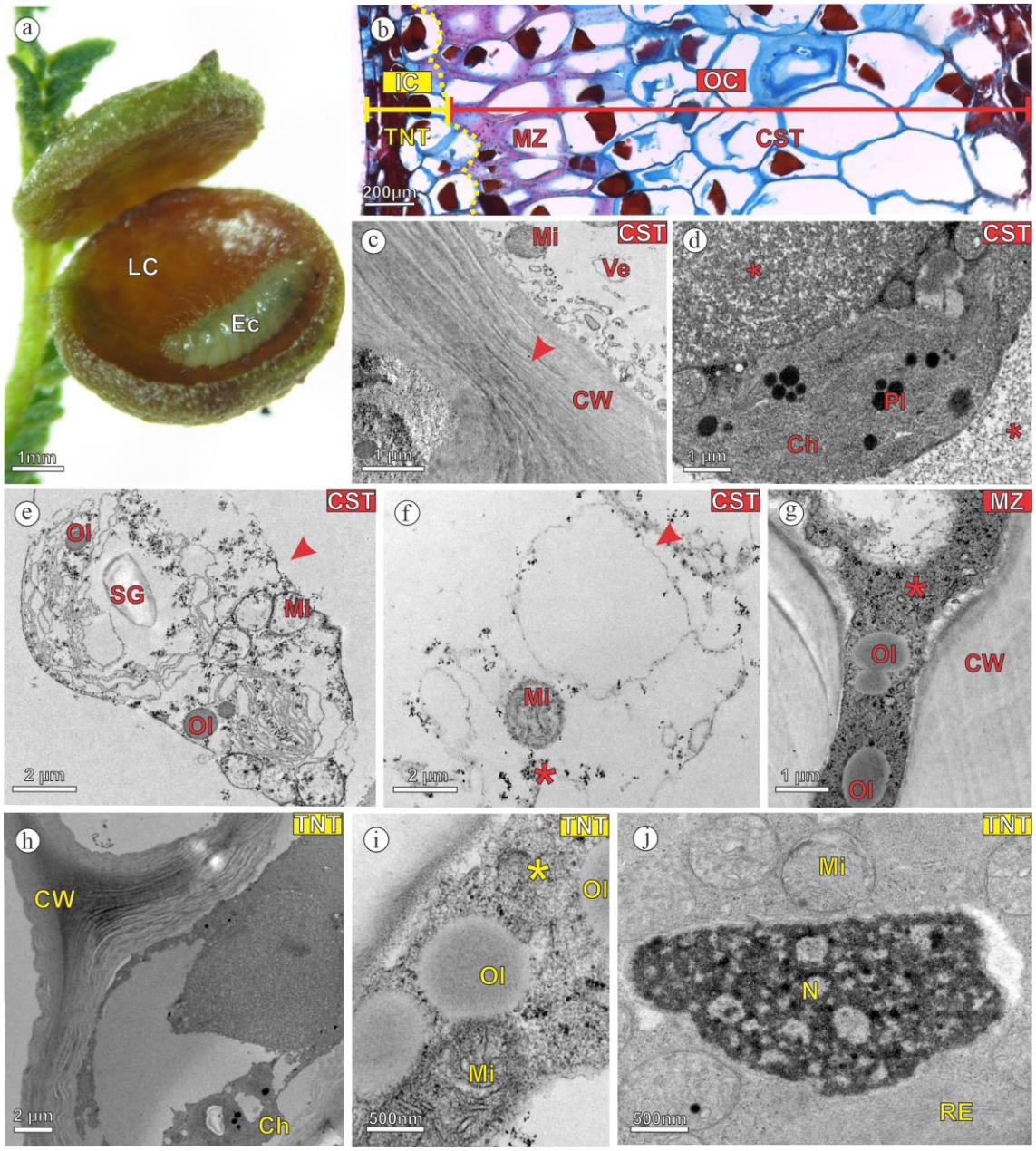
a
LC
Ec
1mm
b
IC
OC
TNT
MZ
CST
200µm
c
Mi
CST
Ve
CW
1 µm
d
CST
*
Pl
Ch
*
1 µm
e
CST
Ol
SG
Mi
Ol
2 µm
f
CST
Mi
*
2 µm
g
MZ
*
Ol
CW
Ol
1 µm
h
TNT
CW
Ch
2 µm
i
TNT
*
Ol
Ol
Mi
500nm
j
TNT
Mi
N
RE
500nm

Fig. 2 Globoid bivalve-shaped mature galls with *Lopesia* larva ectoparasitized by *Torymus* sp. (Hymenoptera: Torymidae). **(a)** Macroscopic aspect of a gall with *Torymus* sp. larva (Ec) inside the chamber (LC). **(b)** Transverse section, evidencing histological organization of an ectoparasitized gall. **(c-j)** Cytological features. **(c-f)** Common storage tissue. **(c)** Sinuous cell wall (red arrowhead), cytoplasm with vesicles (Ve), and mitochondria (Mi). **(d)** Detail of a chloroplast (Ch) with plastoglobules (Pl), mitochondria (Mi), and free ribosomes (red asterisk). (**e)** Packing process of organelles (red arrowhead), oleosomoes (Ol), mitochondria (Mi), and a remaining starch grain (SG). **(f)** Autophagic bodies (red arrowhead), mitochondria (Mi), and free ribosomes (red asterisk). **(g)** Detail of sclerenchyma cells with dense cytoplasm in cell-to-cell communication area, free ribosomes (red asterisk) and oleosomes (Ol). **(h-i)** Typical nutritive tissue. **(h)** Collaped cell walls (CW). **(i)** Free ribosomes (yellow asterisk), oleosomes (Ol) and a mitochondria (Mi). **(j)** Pyknotic nucleus (N), mitochondria (Mi), and endoplasmic reticulum (RE)

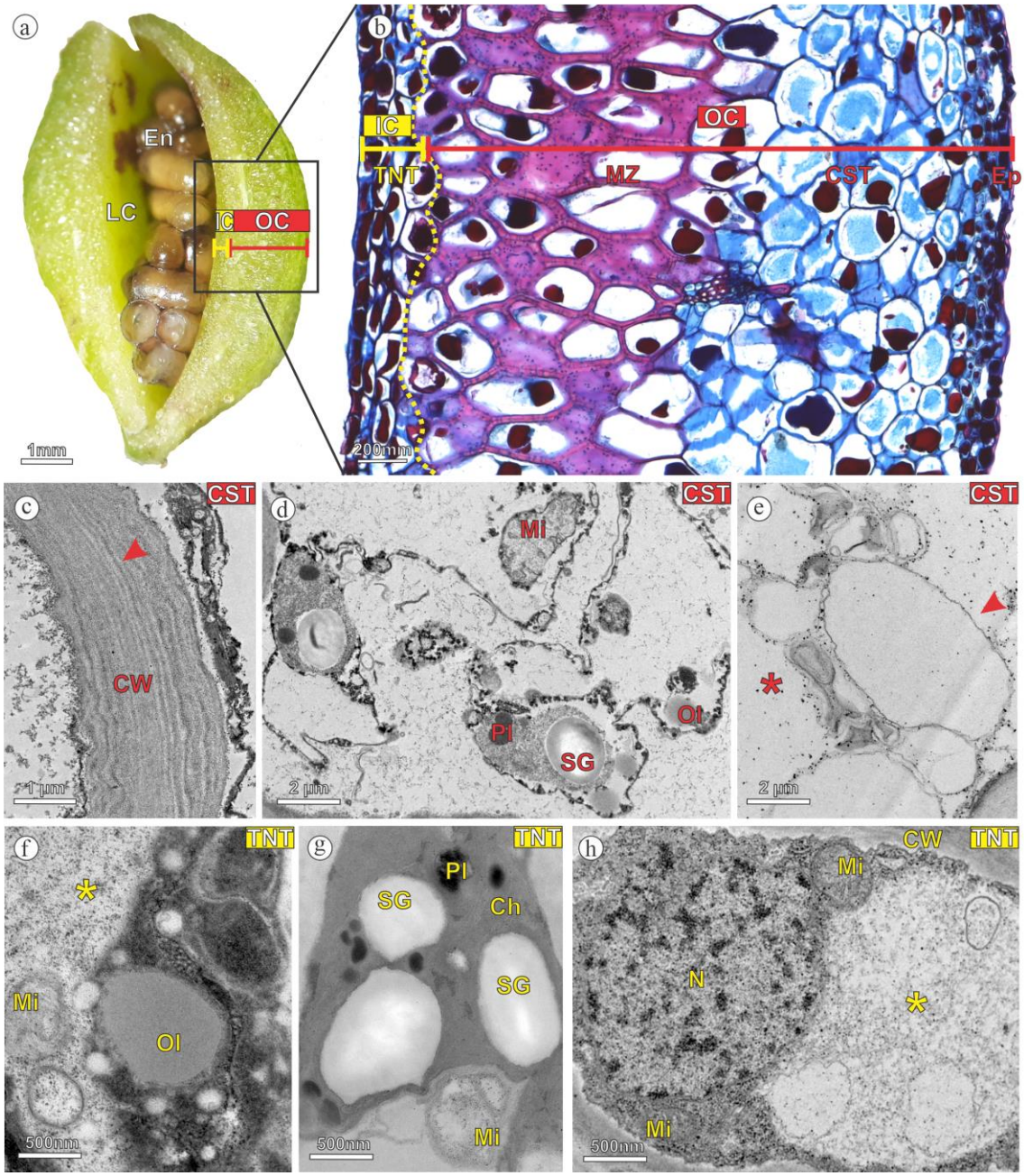

Fig. 3 Globoid mature bivalve-shaped galls with *Lopesia* larva endoparasitized by Platygastridae (Hymenoptera). **(a)** Macroscopic aspect of a gall with *Lopesia* larva the Platygastridae (En) inside the chamber (LC). **(b)** Transverse section, evidencing histotological organization of an endoparasitized gall. **(c-h)** Cytological features. **(c-e)** Common storage tissue. **(c**) Sinuous cell wall. **(d)** Detail of cytoplasm with chloroplasts (Ch) with starch grain (SG), mitochondria (Mi), oleosomes (Ol), free ribosomes and packing process. **(e)** Autophagic bodies (red arrowheads), and free ribosomes (red asterisk). **(f-h)** Typical nutritive tissue. **(f)** Detail of the cytoplasm with free ribosomes (yellow asterisk), oleosome (Ol) and mitochondria (Mi). **(g)** Chloroplast in disintegrating process with plastoglobules (Pl) and starch grains (SG). **(h)** Pyknotic nucleus (N), mitochondria (Mi), and free ribosomes (yellow asterisk)

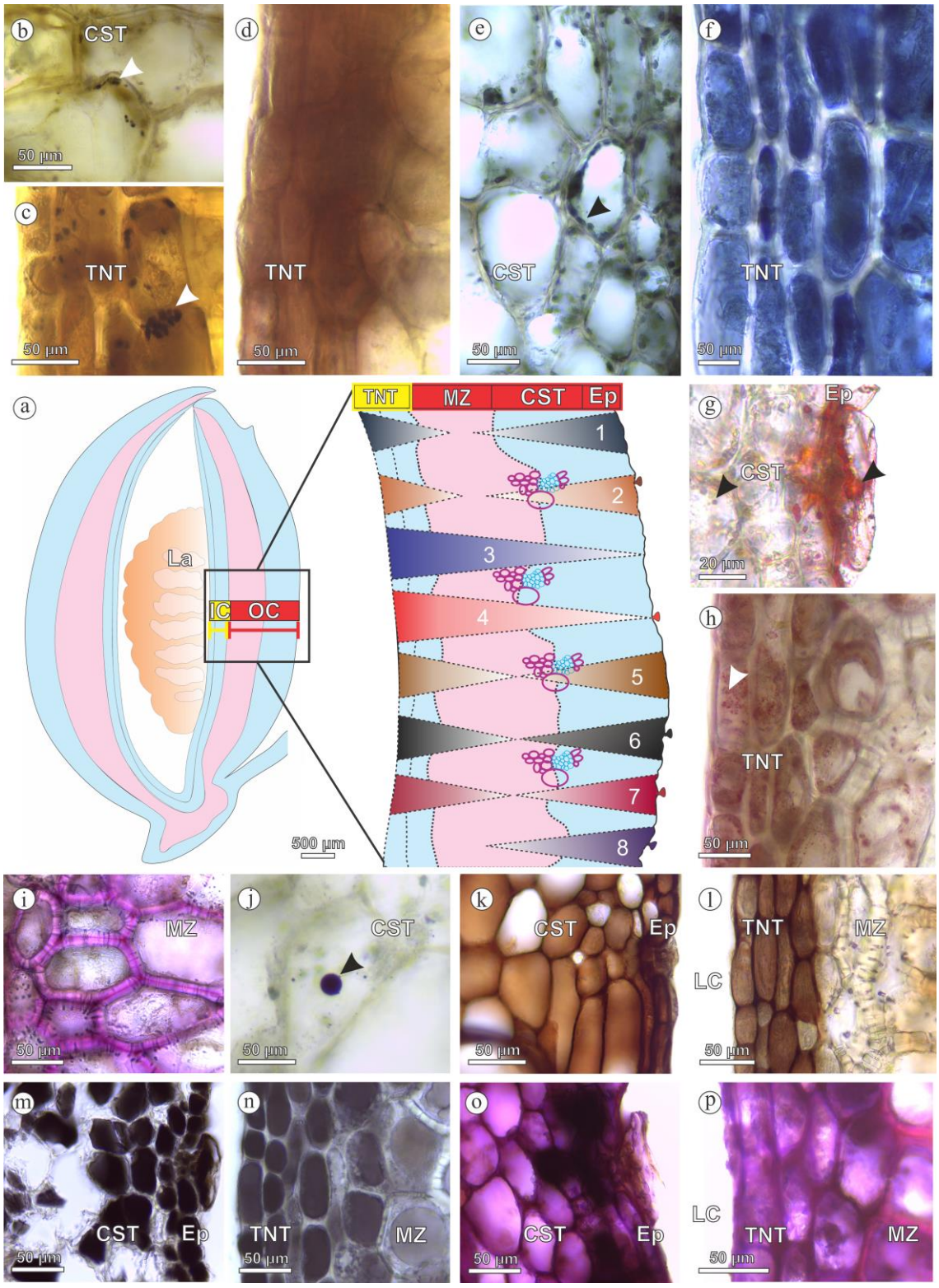
b
CST
50 µm
c
TNT
50 µm
d
TNT
50 µm
e
CST
50 µm
f
TNT
50 µm
a
La
IC
OC
500 µm
TNT
MZ
CST
Ep
1
2
3
4
5
6
7
8
g
Ep
CST
20 µm
h
TNT
50 µm
i
MZ
50 µm
j
CST
50 µm
k
CST
Ep
50 µm
l
TNT
MZ
LC
50 µm
m
CST
Ep
50 µm
n
TNT
MZ
50 µm
o
CST
Ep
50 µm
p
LC
TNT
MZ
50 µm

Fig. 4 Histochemical profile of mature globoid bivalve-shaped galls induced by *Lopesia* sp. (Diptera: Cecidomyiidae) on *Mimosa gemmulata* Barneby (Fabaceae). **(a)** Diagrams of the median region in transverse section, evidencing the organization of the outer (OC) and the inner (IC) tissue compartments, and the *Lopesia* larva (La) in the chamber (LC). The black square indicates the limits of the outer (OC - red square) and the inner (IC - yellow square) tissue compartments. The histochemical gradients are represented by colors and numbers, and the intensity of the colors indicates the direction of the gradients. Starch grains (1; bluish-black), reducing sugars (2, brownish-red); reactive oxygen species (5, brown); phenolics (6, black), and proanthocyanidins (7, magenta) form bidirectional gradients. Proteins (3, blue) and lipids (4, red) form centripetal gradients; and the terpenoids (8, purple) form a centrifugal gradient. **(b-p)** Histochemical reactions. **(b-c)** Starch grains (white arrowheads). **(d)** Reducing sugars. **(e-f)** Proteins (black arrowheads). **(g-h)** Lipids (black arrowheads). **(i)** Lignins. **(j)** Terpenoids (black arrowheads). **(k-l)** Reactive oxygen species. **(m-n)** Phenolics. **(o-p)** Proanthocyanidins

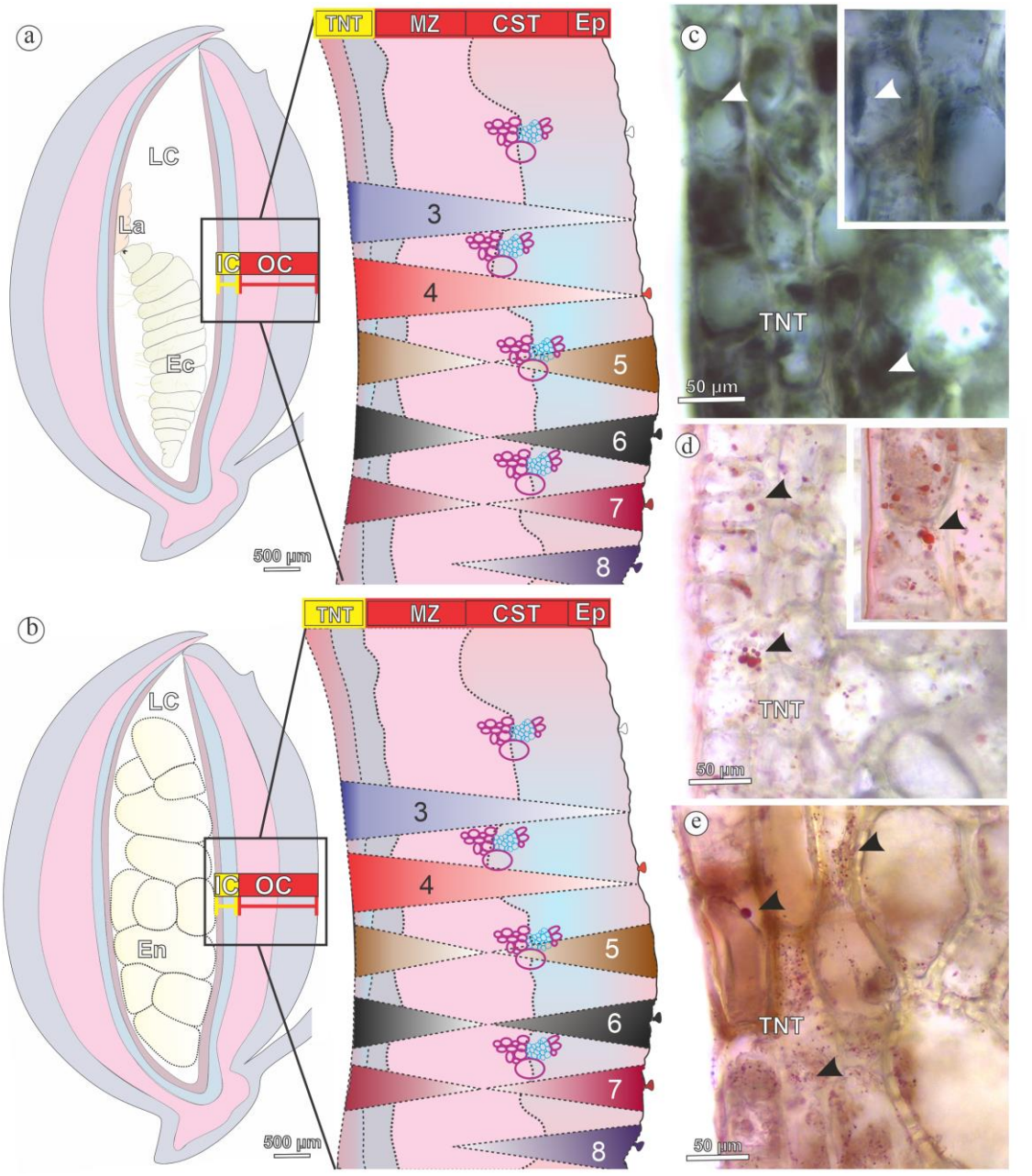
a
TNT
MZ
CST
Ep
LC
La
IC
OC
Ec
3
4
5
6
7
8
500 µm
b
LC
IC
OC
En
500 µm
c
TNT
50 µm
d
TNT
50 µm
e
TNT
50 µm

Fig. 5 Histochemical profiles of mature globoid bivalve-shaped galls induced by *Lopesia* sp. (Diptera: Cecidomyiidae) on *Mimosa gemmulata* Barneby (Fabaceae). **(a-b)** Diagrams in transverse section of the median region, evidencing the outer (OC- red squares) and the inner (IC- yellow squares) tissue compartments with **(a)** *Torymus* sp. larva (Hymenoptera: Torymidae) ectoparasitizing the galling *Lopesia*, and **(b)** *Lopesia* larva endoparasitized by Platygastridae (Hymenoptera) in the chamber (LC). The histochemical gradients are represented by colors and numbers, and the intensity of the colors indicates the direction of the gradients. Proteins (3, blue) and lipids (4, red) form centripetal gradients; reactive oxygen species (5, brown); phenolics (6, black), and proanthocyanidins (7, magenta) form bidirectional gradients; and the terpenoids (8, purple) form a centrifugal gradient. **(c-e)** Histochemical reactions. **(c)** Proteins in nutritive cells (white arrowheads) of ectoparasitized galls. **(d-e)** Lipids (black arrowheads) in the nutritive cells of **(d)** ecto- and **(e)** endoparasitized galls

CONSIDERAÇÕES FINAIS

A revisão bibliográfica das espécies de *Mimosa* hospedeiras de galhas aponta o endemismo de sistemas planta hospedeira-organismo galhador nos ambientes de Caatinga, Cerrado e Mata Atlântica e sugere modelos excelentes para estudos ecológicos, anatômicos e químicos, visando também a conservação ambiental. Além disso, destacam-se as espécies super-hospedeiras de organismos galhadores: *M. melanocarpa* e *M. incana* na Mata Atlântica, *M. tenuiflora* na Caatinga e *M. gemmulata* no Cerrado. Nos atributos anatômicos das *Mimosa,* os tipos, a superdiferenciação e as funções dos tricomas podem ser explorados nas galhas. Em *M. caesalpiniifolia,* a cutícula, os tricomas e as células mucilaginosas da epiderme estão associadas à absorção de água pelas folhas, temática que pode ser explorada tanto nos foliólulos de *Mimosa,* quanto nas suas galhas associadas em ambientes sazonalmente xéricos como a Caatinga e o Cerrado. A diversidade de metabólitos secundários em *Mimosa*, tais como terpenoides, flavonoides e alcaloides, e seu envolvimento no desenvolvimento e adaptação das galhas também merecem atenção. Ainda, as galhas vermelhas associadas à *M. ophthalmocentra* em ambientes de Caatinga são excelentes modelos para testar as hipóteses de proteção contra inimigos naturais e radiação solar envolvendo flavonoides (Figura 1).

Na super-hospedeira *M. gemmulata*, o hábito semidecíduo e o brotamento foliar contínuo suportam os ciclos de vida multivoltinos das quatro espécies de *Lopesia* que induzem as quatro galhas bivalvas. A abundância das galhas está relacionada à fenologia de *M. gemmulata*, que segue o padrão sazonal de disponibilidade hídrica no Cerrado. Os diferentes ciclos de vida dos insetos galhadores, bem como as suas estratégias de assincronismo entre os períodos de indução das galhas evitam à sua sobreposição. A duração do ciclo de vida de cada espécie de *Lopesia*, sendo 2 meses na lenticular, 3 meses nas lanceoladas verdes e marrons e 4 meses na globoide, influencia o desenvolvimento de cada galha, com maior aporte estrutural e nutricional direcionado à galha bivalva globoide, que tem maior longevidade (Figura 1).

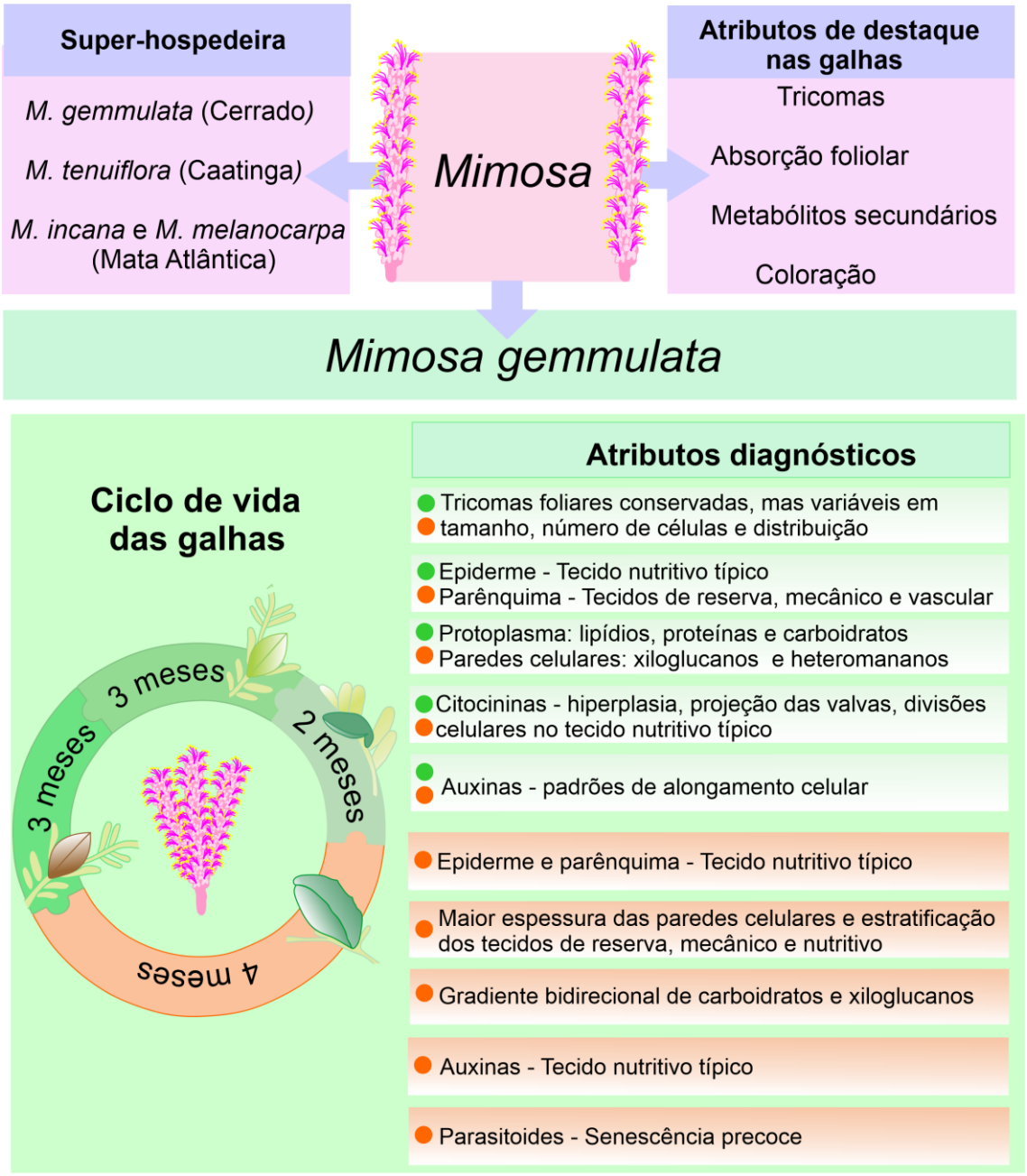

Figura 1: Síntese das considerações finais.

Os carboidratos no protoplasma de células de reserva e os heteromananos nas paredes de células nutritivas estão associados a funções estruturais nas galhas, enquanto os lipídios, proteínas e açúcares redutores no protoplasma, e os xiloglucanos nas paredes de células nutritivas estão envolvidos na alimentação do galhador como atributos comuns às quatro galhas bivalvas. A variação de 1 a 2 meses na longevidade de cada ciclo de vida tem influência direta no acúmulo de recursos estruturais e nutricionais nos tecidos das galhas bivalvas. De modo peculiar, um maior suporte estrutural e nutricional é

demonstrado no metabolismo da galha bivalva globoide comparado ao das outras galhas bivalvas, tanto na espessura das paredes celulares, quanto na estratificação dos tecidos de armazenamento, mecânico e nutritivo, bem como no gradiente bidirecional de carboidratos e nas reservas de xiloglucanos (Figura 1).

As diferenças estruturais-funcionais nas galhas bivalvas também são demonstradas na origem e nos destinos das linhagens celulares recrutadas na raquíola. Durante o desenvolvimento das galhas bivalvas, a manipulação dos tecidos epidérmicos e parenquimáticos da raquiola pelas quatro diferentes espécies de *Lopesia* resulta em fenótipos específicos. Os tipos de tricomas foliares não glandulares filiformes e glandulares peltados são conservados e envolvidos no fechamento das galhas, mas seu tamanho, número de células e distribuição é variável em cada galha. As células nutritivas típicas nas quatro galhas bivalvas são também originadas de células epidérmicas, mas, na bivalva globoide, têm origem mista, pois células parenquimáticas também se rediferenciam em nutritivas. As células parenquimáticas recrutadas na raquíola são também rediferenciadas em células dos tecidos de armazenamento, mecânico e vasculares. Essas mudanças estruturais e funcionais são relacionadas à nutrição, ao suporte hídrico e à proteção das quatro galhas bivalvas. Dentre os traços estruturais-funcionais, o maior potencial para respostas em todas as linhagens celulares da planta hospedeira é estimulado na galha globoide devido à sua maior longevidade (Figura 1).

As diferenças estruturais das galhas bivalvas são resultado da dinâmica temporal e espacial de citocininas e auxinas que determinam os padrões de divisões e alongamento nas linhagens celulares de cada galha. As citocininas estão relacionadas aos sítios de hiperplasia na fase de indução, marcada pela projeção das valvas, e na manutenção dos ciclos das células nutritivas ao longo do desenvolvimento das galhas. Por outro lado, o acúmulo de auxinas está relacionado, principalmente, à dinâmica de expansão no eixo anticlinal ou periclinal no estágio de crescimento e desenvolvimento da galha bivalva lenticular, na maturação das galhas lanceoladas verdes, e nestes dois estágios de desenvolvimento da galha globoide. Além disso, o alongamento anticlinal das células esclerenquimáticas e a detecção das auxinas nas células nutritivas são peculiaridades da galha bivalva globoide (Figura 1). Assim, as maiores dinâmicas celulares temporais, mediadas por citocininas e auxinas, também são associadas a maior longevidade das galhas bivalvas globoides.

Nas galhas bivalvas globoides, demonstramos que a entrada do ectoparasitoide *Torymus* sp. e do endoparasitoide Platygastridae no sistema *M. gemmulata-Lopesia* sp. impacta no comportamento alimentar da larva indutora, resultando em um processo precoce de senescência da galha (Figura 1). Nas duas relações tri-tróficas, as células das galhas bivalvas são caracterizadas pela desintegração dos sistemas de membranas, bem como pela condensação dos núcleos em células nutritivas. Apesar das alterações citológicas, a manutenção dos gradientes de lipídios, flavonoides, fenólicos e terpenoides parece suportar o metabolismo da galha ao longo dos ciclos dos dois parasitoides.

As diferenças durante o desenvolvimento das galhas bivalvas induzidas na raquíola de *M. gemmulata* são determinadas pelo tempo de estímulo no qual cada espécie de *Lopesia* manipula os tecidos de sua galha bivalva específica, por isso um maior mosaico de respostas celulares ocorre na galha bivalva globoide que tem maior longevidade.